Ems-Dollard primary production research Full data report

AG Brinkman, R Riegman, P Jacobs, S Kühn &
A. Meijboom

Report C160/14

IMARES Wageningen UR

Institute for Marine Resources & Ecosystem Studies

Client: Rijkswaterstaat / WVL
Postbus 17
8200 AA Lelystad

Publication date: 2015-06-28

IMARES vision:

- 'To explore the potential of marine nature to improve the quality of life'.

IMARES mission:

- To conduct research with the aim of acquiring knowledge and offering advice on the management and sustainable use of marine and coastal areas.

IMARES is:

- An independent, leading scientific research institute.

Recommended report citation:

Brinkman AG, Riegman R, Jacobs P, Kühn S & Meijboom A. 2014. Ems-Dollard primary production research, full data report. IMARES Report C160/14

P.O. Box 68
1970 AB IJmuiden
Phone: +31 (0)317 48 09 00
Fax: +31 (0)317 48 73 26
E-Mail: imares@wur.nl
www.imares.wur.nl

P.O. Box 77
4400 AB Yerseke
Phone: +31 (0)317 48 09 00
Fax: +31 (0)317 48 73 59
E-Mail: imares@wur.nl
www.imares.wur.nl

P.O. Box 57
1780 AB Den Helder
Phone: +31 (0)317 48 09 00
Fax: +31 (0)223 63 06 87
E-Mail: imares@wur.nl
www.imares.wur.nl

P.O. Box 167
1790 AD Den Burg Texel
Phone: +31 (0)317 48 09 00
Fax: +31 (0)317 48 73 62
E-Mail: imares@wur.nl
www.imares.wur.nl

Contents

Summary

The Water Framework Directive (WFD) requires EU member states to achieve good ecological and chemical status of all designated water bodies (rivers, lakes, transitional and coastal waters) by 2015. Therefore Rijkswaterstaat Waterdienst has initiated the project 'Research mud dynamics Ems Estuary' (*Onderzoek slibhuishouding Eems-Dollard*). The aim of this project, carried out by Deltares and IMARES, is to (1) improve our knowledge on the mud dynamics in the Ems Estuary (Figure 1.1), (2) to identify the reasons for the increase in turbidity and (3) to quantify measures to improve the ecological status of the estuary.

The whole research consists of an analysis of available data, the collection of new data as well as the improvement and application of numerical models.

The IMARES task, reported in this document, is to provide the numerical models with ecological data, and to answer a number of primary production related questions which are important for reaching aim (3).

The last detailed research on ecological characteristics of the Ems-Dollard estuary has been performed between 1976 and 1980. IMARES performed new research on phytoplankton presence and primary production in 2012 and 2103, and on phytobenthos presence and primary production in 2013. Beside this, concentrations of nutrients, suspended matter and a number of associated variables were measured.

This report provides a summary of the main findings. A detailed report containing an overview of the applied methods, the analytical procedures and the results is provided as 'Full data report' (Brinkman et al, 2014).

Rijkswaterstaat asked a number of research questions:

- *What is the pelagic primary production (PP) at present and are there differences between present primary production and primary production in the late seventies?*

Primary production values computed for the channels in 2012 and 2013 are of the same order of magnitude as for 1978, but much lower than those measured in 1979 and 1980. Largest absolute differences are found for the two outer stations (1 and 2), where present results are 60% of the values in 1979-1980. In the Dollard stations (5-6) we found no difference. In station 3 (in the OostFriese Gaatje) we found values of the same order as in the late seventies. Largest differences are found at station 4, where primary production found in 2012 is 40-50%, and in 2013 60-70% of the late seventies values.

System average primary production, including both the channels and the tidal flats for 2012 and 2013 was 120 and 125 g C m^{-2} y^{-1}, respectively. Colijn (1984) found an average value of 165 gC m^{-2} y^{-1}.

- *What is the benthic PP at present, and what are differences between now and the late seventies?*

We did not succeed in finding precise benthic primary production data. We computed a minimum benthic primary production of 11-14 g C m^{-2} y^{-1}, and a maximum of 80 g C m^{-2} y^{-1}. Based on a number of arguments, we believe that 40-80 g C m^{-2} y^{-1} is a most likely estimate. These values include the submersion period of the tidal flats.

The uncertainty thus is large and mainly determined by the benthic attenuation coefficient used and the assumptions on benthic diatom motility. Consequently, primary production values computed for 2013 can hardly be compared with the ones found for 1976-1978 by Colijn & De Jonge (1984) (93 g C m^{-2} y^{-1} for the tidal flats alone, including the submersion period).

- *What is the impact of suspended matter (SPM) on pelagic primary production?*

Assuming non-limiting nutrient concentrations, a 50% increase in light attenuation (corresponding to an increase in almost 50 % in suspended solids) would result in a 25% lower pelagic primary production at the inner stations (i.e. in the Dollard and nearby regions) according to our calculations. For the outermost stations (i.e. Huibertgat and Oude Westereems), a similar increase in light attenuation results in a 35-40% reduction of primary production. A 50% lower light attenuation coefficient (e.g. a 50% lower suspended solid concentration) would increase primary production about 40% in the Dollard and 60-65 % at the outermost stations. During times when nutrient availability rather than light is limiting primary production, the changes due to a decrease in suspended matter might not be as large as suggested. In the Ems-Dollard estuary, nutrient limitation might occur at the two outer stations in (late) spring. During that period, an increase in light penetration (less suspended matter) may not result in such an increase in primary production. Thus, at the outer stations changes probably will be smaller.

- *What is the impact of suspended matter (SPM) on benthic primary production?*

We did not study the relationship between suspended matter and benthic primary production. Since benthic primary production mainly takes place during emersion, we assume that a change in suspended matter content of the water column has a minor effect on benthic primary production.

- *What is the impact of suspended matter (SPM) on the start of the growing season?*

Light attenuation might also affect the start of the phytoplankton growing season. Although we did not specifically investigated this, it can be argued that especially at the beginning of the phytoplankton growing season, light is the most important limiting component, more than temperature and nutrients. Especially then, changes in light conditions will have the largest effect on algal biomass development.

- *Are there factors, other than SPM, that have affected the water column irradiances in the last decades?*

Next to suspended solids, also coloured organic carbon (CDOM) cq Yellow Substance (mostly consisting of humic-like organic matter) contribute to the light attenuation. This is especially the case in the more inner stations, where, next to high concentrations of suspended solids occur, also high

concentrations of Yellow Substance/CDOM can be found. In those areas, these components account for about 40% of the light attenuation.

- *What is the relationship between the light attenuation coefficient K_d and suspended matter now and in the late seventies*

The relationship found here between K_d and suspended matter (without regarding the role of coloured organic carbon (CDOM) or yellow Substances) is similar to the relationship reported by Colijn (1982) (Colijn did not distinguish CDOM or Yellow Substance).

- *To what extent is primary production by planktonic or benthic algae limited by nutrients or light?*

Pelagic primary production in both outer stations (1 and 2) is possibly limited in spring time by low phosphorus and silicate concentrations, but we could not prove this. Nitrate concentrations do not seem to have an impact on primary production. The three most inner stations (4 - 6) most likely did not suffer from nutrient deficiency.

There was no indication that nutrients play an important production limiting role for phytobenthos.

- *What is the effect of declining nutrient concentrations since the late seventies*

Primary production in 2012 and 2013 for both outer stations was about 10-20% below the 1978-values, and almost half of the 1979-1980 values. This could not be attributed to solar radiation conditions: applying 1978-1980 radiation conditions to the present setting revealed roughly the same results.

Alternative explanations for the lower pelagic production in 2012 and 2013 compared to the late seventies might be the lower nutrient concentration at present, an increased turbidity, a changed phytoplankton species composition and lower phytoplankton concentrations.

Nutrient concentrations, especially ortho-phosphate, dropped down to about 50% of the concentrations in the late seventies resulting in a lower primary production. Since we found a better water column light climate at the outer stations and still a lower production, a nutrient effect remains a plausible explanation. But, as said before, we could not prove nutrient limitation.

At the inner stations, light is limiting algal growth rates and also, we did not find a primary production decrease.

What we did find were lower chlorophyll-a concentrations in the outer parts of the estuary and a much lower presence of highly productive *Phaeocystis* algae as compared to the late seventies. Since this genus is commonly associated with a bad eutrophication status, a de-eutrophication effect is likely.

- *Are there geographical variations and/or temporal variations in the limitation of the growth of algae within the estuary?*

Nutrient limitations are most likely at both outer stations at the end of spring, beginning of summer while for the inner stations, nutrient limitation is less likely. With regard to light limitation, this occurs throughout the estuary. However, at the outer stations it is most prominent at the beginning

of the phytoplankton growing season and in late summer/autumn, while at the inner stations, light limitations occurs throughout the year.

- *What is the contribution of the phytobenthos to the total volume of pelagic phytoplankton?*

At the outer stations, benthic algae make up 15 (summer)-40 (winter) % of the total algae volumes; in the inner area this fraction is around 50%.

The report concludes with a couple of recommendations for improving procedures for sampling and analyses and for additional measurements.

Personnel and acknowledgements

Many persons contributed to the research. Basically Roel Riegman was the principal scientist, assisted by Catherine Beauchemin, Pascalle Jacobs, Susanne Kühn, André Meijboom, Hans Verdaat, Marjan Boone, Erika Koelemij, Robbert Jak, Mascha Dedert, Pepijn de Vries, Joël Cuperus, Babeth van der Weide, Lilian de Vos, Simon de Vries & Piet-Wim van Leeuwen. After Roels illness in summer 2013, Bert Brinkman took over the data elaboration; he is the first responsible for the data analysis presented in this report and corresponding author.

Furthermore, we are grateful to Rijkswaterstaat for their cooperation: the crew of the vessels Asterias and Kennemer (Bram, Jeroen, Herman, Theo, Max, Pieter, John) and of the vessel Eemshörn (Peter and Bert de Winter, and additional crew Johan and Klaas); the monitoring staff members Sander Cuperus (DNN-RWS), Magiel Hansen (RWS) and Fred Koopman (RWS) and the RWS nutrient lab (Ronald van der Vliet and others) and Marcel van der Weijden (RWS) who performed the vertical water column profile measurements.

Finally, the Koeman & Bijkerk consultancy, and especially Gersjon Wolters for his late night drives collecting our phytoplankton samples, and the HPLC-lab crew of DHI (Denmark).

1. Introduction

1.1 Water Framework Directive

The Water Framework Directive (WFD) obliges the EU member states to achieve good status of all water bodies (rivers, lakes, transitional and coastal waters) by 2015. It also introduces the principle of preventing any further deterioration of the status and maintaining good status through a number of measures. This forms the basis of the River Basin Management Plans (RBMP) set up by the Member States for each identified river basin.

The management plan for the implementation of the WFD (and Natura 2000) in the Netherlands is described in the "Bijlage Programma Rijkswateren 2010-2015" (Rijkswaterstaat, 2009). Herein, the context, perspectives, targets and measures for each designated water body (also including the Ems-Dollard) were laid out. The measures and targets necessary for improving the chemical and ecological quality, as requested by the WFD, are grouped under 3 main themes: Clean water ("Schoon water"), Biotope ("Leefgebied") and Connections ("Verbindingen").

Under the theme Clean water, three goals (and corresponding measures) have been defined:

1) reduction in chemical loads
2) reduction of eutrophication
3) improvement of the water transparency/reduction of water turbidity

As part of goal 3), the WFD obliges to improve our knowledge on the mud dynamics in the Ems-Dollard; before 2015 the reasons for the apparent increase in turbidity must be established. Therefore Rijkswaterstaat Waterdienst has initiated the project "Onderzoek slibhuishouding Eems-Dollard" ("Silt dynamics Ems-Dollard estuary"). This project should answer the following questions:

- What are the effects of the current dredging and dumping strategies on the mud dynamics in the Ems-Dollard?
- What are the effects of mud dynamics on ecology and the water quality elements of the WFD?
- Which solutions and measures exist to improve or restore the ecological quality?

Both the two latter answers are the core of this present report, thus focussing on turbidity and primary production of the system.

Reflection on the various ecological targets as defined by European and National statements by law urgently needs an updated input of data on the present role of the primary producers in the estuary.

1.2 Hypotheses for the whole research

In the literature review of phase 1 of this project (Spiteri et al, 2011), a number of hypotheses were formulated on the functioning and the changes in the Ems-Dollard estuary.

Table 1 Overview of research hypotheses for primary production (from Van Maren et al., 2011)

	Hypotheses	Model type	Data type
1	Pelagic primary production is controlled by turbidity in the Estuary.	3D WAQ-Eco model	Limiting factor determination, in situ light attenuation
2	Benthic primary production is mainly controlled by nutrients and resuspension.	3D WAQ-Eco model	Benthic primary production, and abundance of suspended benthic diatoms
3	Measures to reduce turbidity in the estuary will increase the risk for phytoplankton blooms and therefore deteriorate the ecological status.	3D WAQ-Eco model	
4	Measures to reduce turbidity in the estuary will have an effect on the BQE “phytoplankton”, currently classified as “good” within the context of WFD.	3D WAQ-Eco model	
5	The effect of decreased nutrient loads from land will reduce the benthic production, counteracting the effect of decreased turbidity in the estuary.	3D WAQ-Eco model	
6	Changes in turbidity and nutrient availability will change algal composition.	3D WAQ-Eco model	
7	The carrying capacity for higher trophic levels in the ecosystem, reflecting in the primary production, has been reduced since the late seventies as a consequence of increased turbidity		Historical data (MWTL)
8	The three MWTL stations in the Ems-Dollard are sufficiently representative in order to estimate the ecological status with regard to phytoplankton abundance.	3D WAQ-Eco model	Phytoplankton abundance and primary production

In order to test these hypotheses adequately, a combined modelling and measuring campaign was carried out in 2012 and 2013.

Hypotheses 1, 2 will be tested by analysing a combination of existing and new field observations. During the field campaign, phytoplankton pigment ratios will give an indication about whether light or nutrients are limiting for primary production. This can be further tested using the calibrated Delwaq-ECO model where all phytoplankton and microphytobenthos groups are represented by types that are either acclimated to light- nitrogen- or phosphorus limitation. The ratio of the different types in a specific area will give an indication of the limiting factor.

Hypotheses 3, 4, 5 and 6 will be tested by running different scenarios with the calibrated water quality/ecology model that is developed during the project. Of course, measurements are essential in order to calibrate and validate the model. The scenarios will be based on the proposed measures by the WFD.

Hypotheses 7 will be tested by analysing existing field observations. If possible, measured chlorophyll-a will be used as a proxy for primary production.

Hypothesis 8 will be tested by comparing the MWTL field observations with the proposed measurement and the results of Delwaq-ECO model.

Thus, most of the hypotheses tests will be performed with physical and ecological model runs.

Based on these hypotheses, several activities (Van Maren et al., 2011) were defined for modelling (are all Deltares tasks) and field measurements (IMARES tasks concerning primary production and related topics; Deltares tasks concerning silt dynamics and sediment characteristics).

The primary IMARES-task thus was to measure primary production and associated variables and deliver data to the Deltares modelling part. A number of related questions to be answered, just based on the results of the measurements, is listed in the next section.

1.3 Questions addressed in this research

This present field and laboratory research first addresses a couple of questions derived from the main questions mentioned above, and secondly, it is meant to deliver necessary field data to the models. The questions are

1. What is the pelagic primary production at present? Linked to Table 1, hypotheses 1, 6 & 7
2. What is the benthic primary production at present? Linked to Table 1, hypotheses 2, 6 & 7
3. What is the impact of suspended matter (SPM) on pelagic and benthic primary production? Linked to Table 1, hypotheses 1, 3, 4, 6 & 7
4. Have there been any changes in algal biomass and production compared to the late seventies? Linked to Table 1, hypotheses 7
5. Are there factors, other than SPM, that have affected the water column irradiances in the last decades? Linked to Table 1, hypotheses 1, 3, 4, 5,6 & 7
6. To what extent is pelagic and benthic primary production limited by nutrients or light? Linked to Table 1, hypotheses 1, 2, 5, 6 & 7
7. Are there geographical variations and/or temporal variations in the limitation of the growth of algae within the estuary? Linked to Table 1, hypotheses 8

Primary production measurements in the Ems-Dollard stem from over 30 years ago (see Spiteri et al, 2011). Since the mid-1970s, a decrease in nutrient concentrations has been observed and also other controlling factors, such as underwater light conditions, have also changed in the last decades due to changes in suspended matter concentrations. Therefore, the former primary production measurements are no longer representative of the current situation. In absence of primary production measurements, chlorophyll-a concentrations are often used as a proxy for algal biomass and even for primary production. However, chlorophyll-a concentration is merely an indicator of multiple processes and does not represent a production process in itself. In Table 2 and Table 3, an overview is presented on the topics and questions asked, and what analyses or variable collections consequently were performed.

Table 2 List of questions asked and what pelagic measurements were performed to answer these questions.

Topic / theme	Variable	Remarks
Supply to Deltares ecosystem model	Temperature	Continuous measurements
	Salinity & conductivity	Continuous measurements
	Oxygen concentration	Oxygen electrode. Continuous measurements
	Oxygen saturation	
	SPM	Several methods, local and continuous measurements, find relationship extinction coefficient, turbidity and suspended matter concentration (SPM)
	Turbidity	
	CDOM (Coloured dissolved organic matter)	Gives an idea of dissolved organic matter
	Yellow substances	Gives an idea of yellow substances (dissolved humic and fulvic acids)
Supply to Deltares ecosystem model / computation primary production	Light extinction	Needed to compute primary production in the field
Supply to Deltares ecosystem model / computation primary production	Chlorophyll	Compare to end '70-'s results. Several methods
Supply to Deltares ecosystem model / computation primary production	Primary production	Compare to end '70-'s results. ^{14}C incubations
Computation primary production	Inorganic C	Needed to interpret ^{14}C-measurements
Are nutrients or is light growth phytoplankton limiting?	[P], [NO3], [NH4], [Si]	Concentrations
	Growth limitation	Pigment absorption ratios
Algae species distribution / Supply to Deltares ecosystem model	Diatoms	Continuous measurements, and some algal cell counts
	Cryptophytes	
	Blue-greens	
	Green algae	

Table 3 List of questions asked and what benthic measurements were performed to answer these questions.

Topic / theme	Variable	Remarks
Supply to Deltares ecosystem model	Sediment temperature	Only at sampling site
Supply to Deltares ecosystem model / computation primary production	Sediment chlorophyll-a	Only at sampling site
Supply to Deltares ecosystem model / computation primary production	Benthic Primary production	Only at sampling site

1.4 The research

In 2012 and 2013, a number cruises were performed in the Ems-Dollard estuary to take water samples for further analyses and measure variables related to phytoplankton production in the water column. At six fixed stations, samples were taken to analyse chlorophyll-a, suspended particulate matter (SPM) and to assess photosynthetic parameters. The number of cruises in 2012 was 20, in 2013 19. Some work has been done in 2011 to test the methods, and this is not included in the present report. Continuous measurements of many parameters were performed with a PocketBox while sailing along the transect from Borkum to the centre of the Dollard, i.e. along the full axis of the estuary.

In 2013, also benthic samples were taken for further analysis of benthic primary production. Almost all samples, on twelve days total, were taken on a day prior to the pelagic sampling.

Pelagic primary production measurements were performed with the same methods as were used by Colijn (1983) to enable comparison of recent data with those obtained from the 1970s; benthic primary production data were obtained following a method different from the one applied by Colijn, but on similar sites.

1.5 General

The report on the primary production research performed by IMARES has been split in two: a concise report with an overview and of the work plus discussions and conclusions, and this report: an extended version containing lots of details on methods, analysis, results, discussion and conclusions.

1.6 This full-data report

This report contains a full description of the measurements and analyses performed, and the results. The report is divided into a couple of sections:

Chapter 2: characteristics of the area. It includes a description of the Ems-Dollard estuary, and a short overview of ecological processes in the system. Areas and average depths of compartments and tidal flats are listed.

Chapter 3: description of the measurements: where, when and how. This is meant as a complete overview of the logistic operations (sampling cruises) and coordinates of sampling sites. It gives the variables that were measured at the sampling sites only, and those that were continuously monitored during the cruises. Also the way the samples were taken and processes (stored, filtered, etc.) is described here.

Chapter 4-6: the analytical and mathematical methods used to analyse the data. The analytical methods used are described in a general way, not down to the smallest details of handling samples. Mathematical methods are described in such a way that it is completely clear how the data computations were performed. Chapter 4 contains all the analyses on pelagic and benthic data

collected at the sampling sites. Chapter 5 explains in detail how the pocket box data were checked. Chapter 6 explains all the regression analyses that were performed.

Chapter 7-10: the results. Chapter 7 contains results of the correlation analyses, and how these results were mutually used to correct other observations, e.g. salinity and conductivity, and turbidity, light attenuation and suspended solid concentration in the water column.

Chapter 11: discussions plus conclusions

Next to final conclusions and comparison with results of previous researches, also recommendations are part of this last chapter.

All chapters also have a 'what have we learnt'-section, including recommendations for future research.

2 Characteristics of the area

2.1 What is in this chapter

First an overview is given of the Ems-Dollard estuary based on previous research (section 2.2-2.5). In the second part of this chapter, morphological data and maps are presented.

2.2 General

On the basis of differences in morphology, current patterns, and the availability of nutrients and light, and biological properties, the area of the estuary (Figure 1) is usually subdivided in three sections (Fairbridge, 1980).

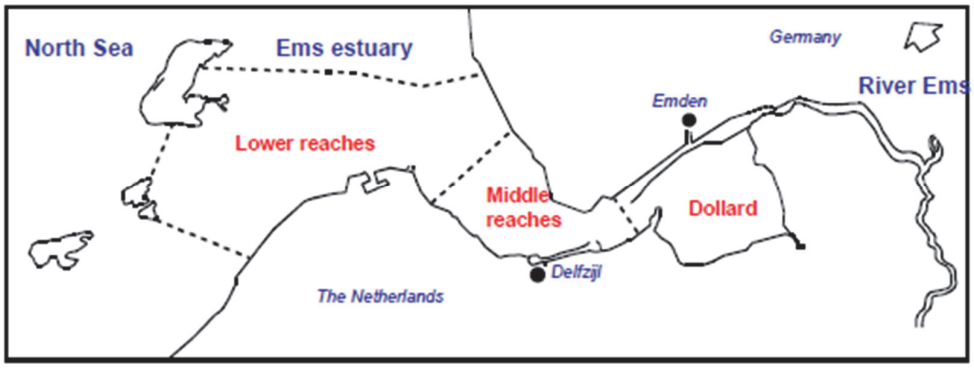

Figure 1 Division of estuary in three areas (figure from de Jonge & Brauer, 2007). Note that Colijn (1983) and also De Jonge (1992) also use different divisions (see chapter 3, Figure 14 and more)

The lower reaches are strongly influenced by the Wadden Sea and coastal North Sea. The middle section is subject to strong salt and fresh water mixing, and the upper section is heavily affected by freshwater input and tidal action.

The Ems-Dollard estuary is characterised by the presence of strong gradients (Figure 2). Seawards there is a strong increase in salinity (from 5 to 28 ‰). Summer suspended matter concentrations vary between 20 and more than 200 mg/L. Consequently, the shallow waters of the Dollard (mean depth of channels is 1.2 m) are very turbid (attenuation coefficients up to 6 m^{-2}). In the outer regions the average depth of the channels is 5.8 m and the light absorbance is much less (attenuation coefficients up to 1.2 m^{-2}) (Colijn 1983; de Jonge & Brauer, 2007).

The mean water column irradiance during the growing season of algae decreases with approximately 25%, going from the lower regions into the Dollard (calculated according to Riley 1957, based on measurements by Colijn 1983).

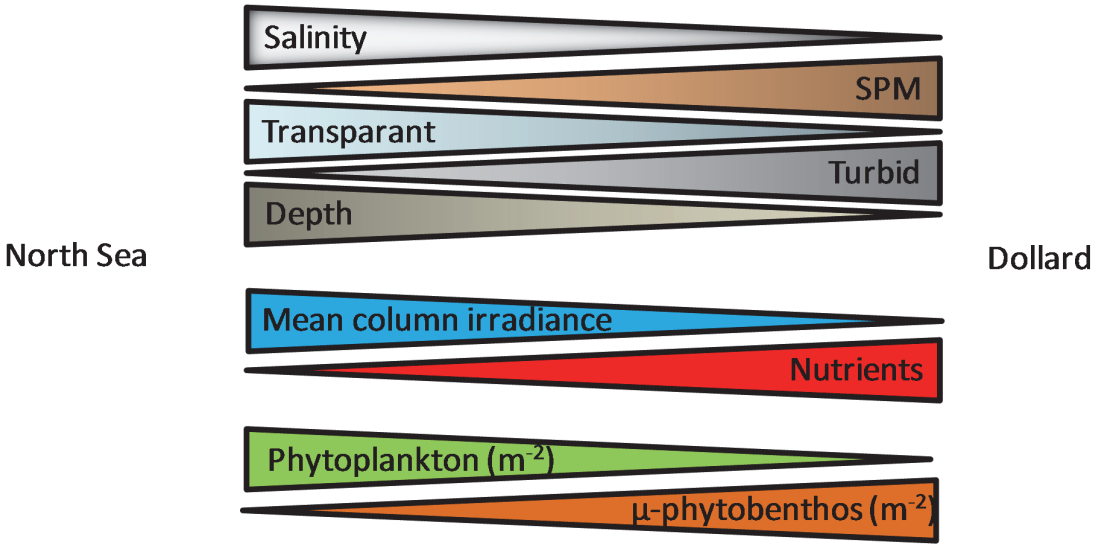

Figure 2 Gradients in properties of the estuary. Vertical cross section of each symbol symbolises the magnitude of the parameter, dependent of the location in the estuary.

Dissolved nutrient concentrations show the opposite gradient, showing higher values close to the discharge location of the rivers Ems and Westerwoldse Aa (Van Beusekom & De Jonge, 1998). The observed gradients in nitrogen indicate that the distribution of this nutrient is mainly determined by dilution of freshwater with sea water. With respect to phosphorus, there is an additional effect of interaction with the sediments (Van Beusekom & De Jonge 1998). During the past decades, a correlation between the annual average biomass of algae (i.e. chlorophyll-a) in the estuary and the annual N- and P-load from the river Ems has been observed (De Jonge & Brauer, 2007). In the higher region (The Dollard) the annual primary production of phytoplankton is not closely related to the input of phosphorus or nitrogen (De Jonge & Essink, 1991). In the lower region, a correlation between river discharge and summer primary production is observed (De Jonge & Essink 1991). The underwater light climate is considered to be limiting the algal primary production in the water column of the Dollard (de Jonge & Brauer, 2007) during the growing season. At the lower reaches, where the suspended matter is much lower than in the Dollard, nutrients are considered to be limiting the primary production. However, measurements on the physiological state of the algal cells (e.g. Riegman & Rowe, 1994) do not support this. More recently, indirect evidence for the growth limiting factor of phytoplankton in the Wadden Sea and coherent areas reveals light, silicate and phosphate the most controlling factors (Loebl et al., 2009). The same authors conclude that the control of phytoplankton biomass in turbid areas of the Wadden Sea seem to be more closely related to light and nitrogen. Direct measurements on the growth limiting factor by means of nutrient uptake experiments (e.g. Riegman et al, 1990) have not been carried out in the Ems-Dollard estuary.

A very extensive overview of the physical, chemical and biological properties of the three areas of the estuary is presented by de Jonge and Brauer (2007). One of the conclusions of these authors is that many environmental factors such as nutrient load, organic matter load, and suspended matter concentrations (SPM) have altered dramatically during the last 4 decades. Evaluation of the possible impacts of these changes with respect to the carrying capacity of the system is unfortunately restricted by the lack of data on the primary production by pelagic and benthic algae.

The last measuring campaign on phytoplankton and microphytobenthos originates from the late seventies (BOEDE, 1985). Unfortunately, this period was characterised by an extreme load of organic matter, as a consequence of untreated waste water discharge from strawboard and potato flour factories in the southeast of the province Groningen (The Netherlands) (for detailed information: see De Jonge & Brauer 2007). The maximum of these discharges was reached in 1977. This caused large parts of the Dollard estuary to suffer from anoxia. In the early nineties, oxygen levels had been restored to normal, as a consequence of large scale waste water treatment of industrial plants.

The occurrence of extreme high external loads of organic matter has some noteworthy consequences for the interpretation of the data that were collected by the BOEDE group in the late seventies. First of all, the participating scientists recognized the functioning of the microbial loop in terms of carbon transfer to higher trophic levels as an alternative route for the classical food-chain concept (algae-copepods-fish). This microbial loop concept was completely new. In fact, it took another four years before exactly the same concept was published in the international literature, at the time being a spin-off from a discussion session during a scientific symposium (Azam et al. 1983).

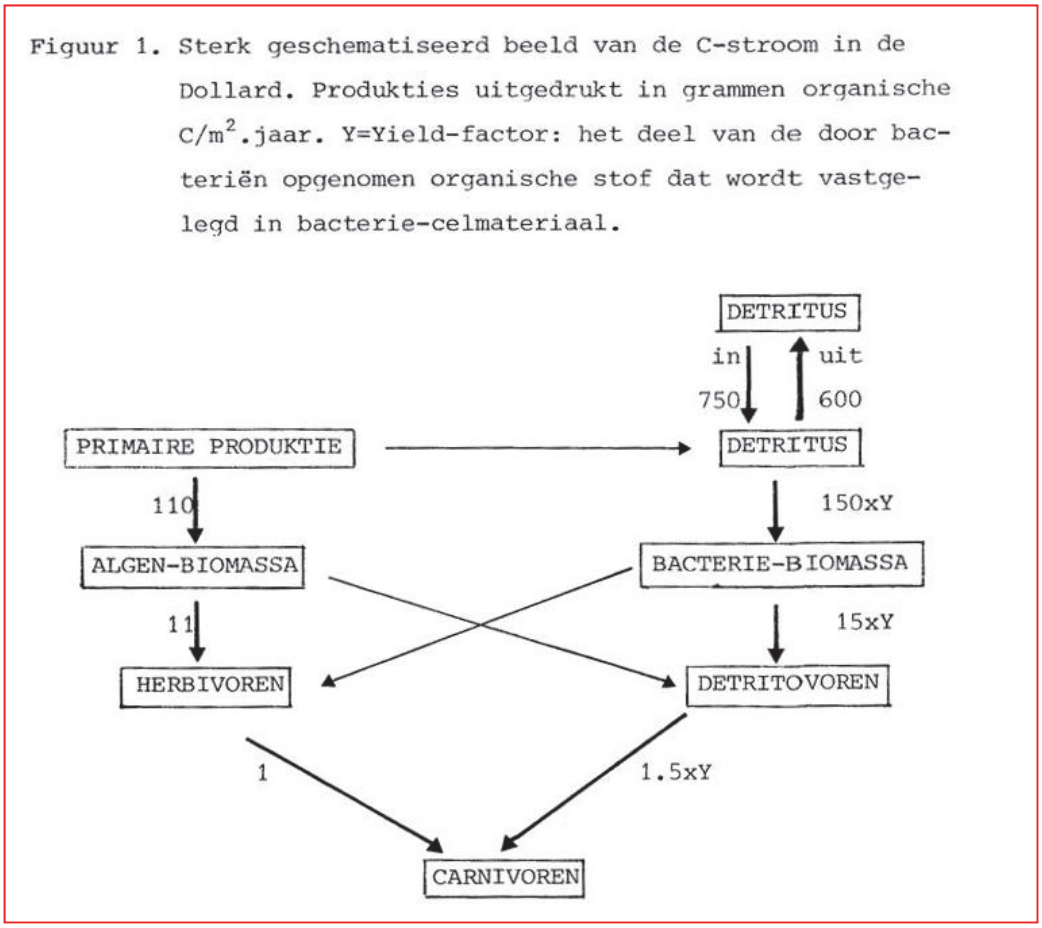

Figure 3 Conceptual carbon flow diagram (in g $C.m^{-2}.yr^{-1}$) in the Dollard, constructed in the late seventies on the basis of measurements by the BOEDE group (Picture from van Es, published in Wolf et al. 1979)

If the biomass of ciliates and copepods (Baretta & Malschaert, 1988) indeed was enhanced by additional food sources, originating from an enhanced bacterial production, it is be expected that the grazing pressure on pelagic and benthic algae must have been much higher during the period of waste water discharge. One indication of this phenomenon is given by Baretta &Ruardij (1988), who conclude on the basis of their modelling activities that the microzooplankton grazing on phytoplankton must play a very important role in the estuary. Another indication is given by the measured growth rate of phytoplankton. Colijn (1983) recorded maximum (gross) specific growth rates of phytoplankton in the order of 1-2.5 d^{-1}; the lower values at temperatures just above 0 ^{o}C, the highest values at 15 ^{o}C. At all temperatures, (much) lower values also occurred. In coastal waters that are not under the pressure of high organic matter loads, phytoplankton shows a daily and depth averaged specific growth rate in the order of approximately 0.2 to 0.3 d^{-1} (Riegman et al, 1998). Although not recognized in the present literature concerning the Ems Dollard, the possibility of an enhanced grazing pressure on algae must have had its impact on the species composition and biomass of this basic trophic level. This makes the extrapolation of quantitative biological data on biomasses and processes that were collected in the early seventies towards the present situation in the estuary not very useful.

In addition, there exist various well-documented records indicating that the turbidity in the estuary has increased in the last four decades (de Jonge 1995 a,b; de Jonge 2000). Statistical analysis reveals an average annual increase of suspended matter of 2 mg/l (Merkelbach & Eysink 2001). One of the possible causes might be the enhanced dredging activity and accompanying dumping of dredging material (De Jonge and Brouwer, 2007). In combination with the observed decrease in nitrogen and phosphorus concentration during the past two decades, it is to be expected that the species composition and consequently the photosynthetic properties of the phytoplankton and the microphytobenthos must have been altered since the seventies.

2.3 Phytoplankton

Phytoplankton biomass (measured as chl.-a) distribution is only known from data collected in the late seventies (Colijn 1983; De Jonge & Brauer 2006). Annual average chlorophyll-a varied in the period 1976-1980 between 4 and 12 µg.L^{-1}. Generally, higher values were observed in the outer region (9.49 µg.L^{-1}) than in the inner region (7.5 µg.L^{-1}). Long term monitoring at three locations (Huibertgat, Oost Friesche Gaatje and Groote Gat Noord) during the period 1976 – 1997 did not reveal any remarkable trend (De Jonge & Brauer, 2006) although these authors noticed a correlation between annual averaged values for dissolved inorganic phosphorus and chlorophyll-a.

Brinkman (2008) published a trend analysis study on Rijkswaterstaat monthly monitoring data for chlorophyll-a concentrations, available for the period 1976-2005 (Figure 4). Summer values (April-September) were log-transformed and the relationship was analysed using a generalized additive model (gam). Next to the analysis, also the 95% confidence interval for each estimate has been computed following a bootstrap procedure. The confidence intervals are shown by the bars in the same figures.

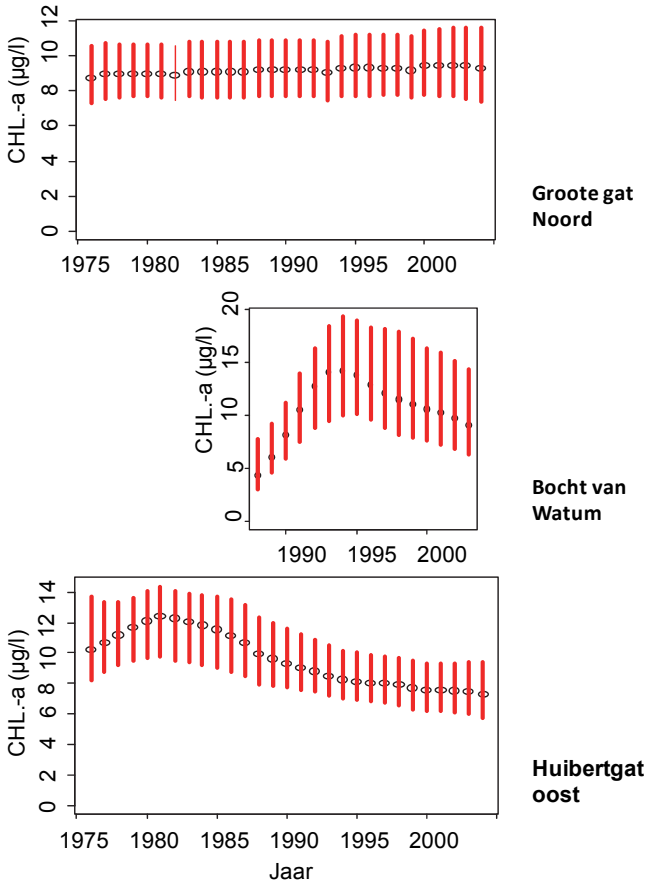

Figure 4. Long term trends in summer averaged chlorophyll-a with 95% confidence intervals in the water column at three sites in the estuary: Groote Gat Noord (Dollard), Bocht van Watum (middle region) and Huibertgat Oost (lower region). Source: Brinkman, 2008.

In the Dollard (at Groote Gat Noord) there is hardly any interannual variation in summer chl-a values. This may imply that the phytoplankton in this area is mainly acting as if it is in a turbidostat. Variations in incidental inputs of chlorophyll-a from the microphytobenthos are probably buffered by light control of the biomass of the pelagic algae.

At the middle region (Bocht van Watum) less data were collected in the past. Within the period from 1998 to 2003 there has been an optimum in the middle nineties. In the regions closest to the Wadden Sea and coastal area of the North Sea (Huibertgat Oost) maximum summer chlorophyll-a concentrations were present in the early eighties. From then on a gradual reduction in algal biomass (reflecting the reduction in nutrient discharges from the European continent) can be observed. It is unclear why the middle region shows a pattern that deviates from the other regions. An explanation might be that especially the middle region has been subject to morphological changes due to dredging activities. If water masses have altered their major flow patterns in the middle region, chlorophyll variations at one particular site, such as the Bocht van Watum, are to be expected.

Since from 1997 onward there has been a further reduction in nutrients in Dutch coastal waters (Brinkman, 2008), it is likely that also chlorophyll-a may have been reduced during the past decade, especially in the outer compartment where nutrients are limiting for algal growth rates during summer. This trend has been observed in the Wadden Sea (Phillipart et al. 2007).

Species composition of phytoplankton is recorded from scattered data collections (Van der Werff 1960; Van de Hoek et al., 1979). De Jonge (1985) presents information on resuspended benthic diatoms (mainly pennate species). This phenomenon of resuspension of microphytobenthos was originally demonstrated elsewhere (Bailly & Welsch 1980) and recognized as an important issue for the Dollard (Admiraal 1984). Most informative are the calculations showing that that micro-algae do resuspend into the water column after heavy wind periods (De Jonge 1992, De Jonge & van Beusekom 1992, 1995). This process dominates the species biomass and composition of phytoplankton in the channels of the Dollard. De Jonge & Brauer (2007) make a distinction between three groups of micro-algae in the estuary: 'real phytoplankton', resuspended microphytobenthic algae, and the microphytobenthos. In datasets where chlorophyll-a samples in the water column of the channels were collected, there are always micro-algae present that originate from the surrounding banks. Occasionally, this contribution of microphytobenthos to the plankton community may reach values up to 50% or more (Figure 8, from De Jonge & van Beusekom, 1992).

2.4 Primary production

The most recent data on primary production in the estuary originate from the late seventies in the previous century (Colijn 1983, Colijn & De Jonge 1984, Colijn & Admiraal 1987). Colijn used an incubator method where the photosynthetic properties of phytoplankton sample were measured by ^{14}C uptake. Combined with measurements on daily photosynthetic irradiation (PAR) and underwater light attenuation (Kd), a daily (or annual) primary production was calculated. Comparison with another method demonstrated that results from the incubator method deviate less than 10% from the more classical *in situ* method (Colijn 1983; Riegman and Colijn 1991). The observed annual primary production is presented in Table 4 (data from Colijn, 1983).

Table 4 Regional differences in the primary production and chlorophyll-a in the estuary. Data calculated as annual averages in the period 1976-1980. Data from Colijn (1983).

Annual average (1976-1980)		Region		
	unit	Outer	Middle	Dollard
Chlorophyll-a	mg/m2	55	27	9
Phytoplankton biomass	gC/m2	1.4	0.7	0.2
Primary production	C/m2/y	263	85	49

With respect to the extrapolation of this information to more recent years, at least two different serious drawbacks have to be mentioned. For the primary production calculations, Colijn used an empirically established relationship between suspended matter and light attenuation coefficient which revealed a "background" attenuation of 0.4 m^{-1}. This is due to the light absorption by dissolved

components. The observed value of 0.4 m^{-1} is very high, compared to the usual value of 0.1 that is observed in for example the Wadden Sea (Riegman, unpubl. results). The high background, indicating additional light absorbance by dissolved matter, probably was related to the extended discharge of untreated sewage water, being rich in refractory humic acids. It is very likely that the background attenuation has improved significantly after sewage treatment was applied on a large scale in the eighties.

The second drawback concerns the measured photosynthetic parameters. Extraction of these parameters from the data presented by Colijn (1983) shows a typical seasonal pattern (Figure 5).

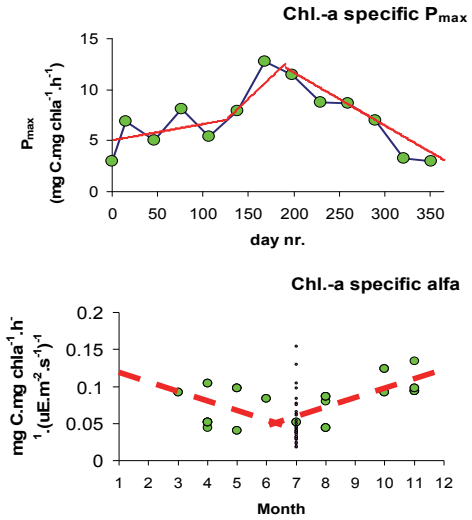

Figure 5 Seasonal pattern of the chlorophyll-a specific photosynthetic parameters Pmax and alfa, extracted from the data presented by Colijn (1983).

Alfa, a measure for the affinity of photosynthesis for light, shows a slight decrease during summer. This parameter is relatively more sensitive to the availability of light in the growth environment than to temperature. For P_{max}, here defined as the chlorophyll-a specific maximum photosynthetic rate, a reverse pattern is observed. This photosynthetic parameter is mainly determined by chemical processes, rather than physical processes in the algal cells. Higher in situ water temperatures explain why especially during summer high P_{max} values are found. Comparison with data from the Oosterschelde estuary (Malkin et al., in prep.) shows that the observed P_{max} values of the Ems-Dollard phytoplankton anno the late seventies were about 20% higher than the values that were measured the last decennium in the Oosterschelde. A possible explanation may be a difference in species composition between the different regions. It is known that photosynthetic performance of algal communities is not only regulated by external factors such as nutrients or light, but is also related to the species composition of the community since photosynthetic parameters are species specific properties. The lack of recent data on background light absorption, algal species composition, biomass and productivity, makes a quantitative extrapolation of the findings of Colijn on primary production in the Ems Dollard estuary towards more recent years by definition inadequate.

Additionally, several environmental factors have altered since the late seventies. Changes in human activities such as wastewater treatment, dredging, dumping of dredgings or the use of water for cooling purposes all will have their impact on the primary producers in the ecosystem. Here, the major impacts are generally recognized to be mediated by changes in nutrients, organic- and suspended matter, and processes that trigger the resuspension of microphytobenthos in the estuary.

2.5 Microphytobenthos

2.5.1 General

A general introduction is included in appendix A3.

2.5.2 Spatial distribution in the Ems-Dollard area

The microphytobenthos mainly constitutes of diatom species that live on the intertidal flats in the boundary level between the sediment and the water. Since the Ems-Dollard area is covered for 53% covered by tidal flats (Table 6), a substantial part of the primary production takes place on the sediment. During periods of high wind speed, up to 50% of the total chlorophyll-a in the water column can be made up by resuspended microphytobenthos species (Figure 8). Most of the microphytobenthos data in the Ems-Dollard were collected at six stations (Figure 6), sampled for biomass (de Jonge & Colijn, 1994; de Boer, 2000) and primary production (Colijn & de Jonge, 1984).

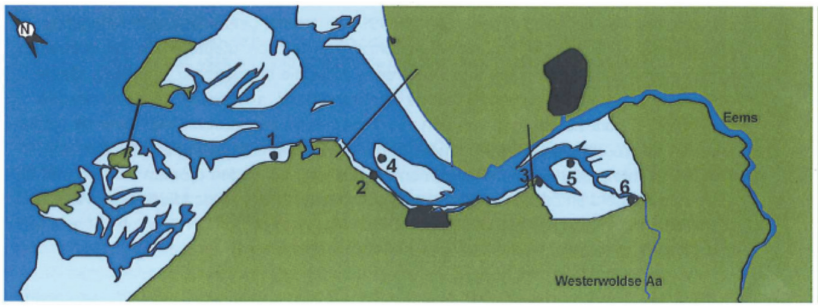

Figure 6. Locations sampled for microphytobenthos in the periods between 1976 and 1978, and between 1992 and 1999 (from de Boer, 2010).

Microphytobenthos is a descriptive term for the diverse assemblages of photosynthetic diatoms, cyanobacteria, flagellates, and green algae that inhabit the surface layer of sediments in marine systems (Underwood, 2001). Algal species living on a muddy substrate are called epipelic. Main species of phototrophs in the epipelic community belong to the group of Diatoms (Bacillariophyta) with genera such as *Navicula*, *Gyrosigma*, *Diploneis* and *Nitzschia* (Underwood, 2001). These algae live at the boundary layer between the sediment and the water column, and are able to actively move upward and downward through the sediment.

In the Dollard, close to the outlet of the Westerwoldse Aa, the species composition of the microphytobenthos has been studied by Peletier (1996) in 1976-1977, 1987 and 1993. Data were also used from Admiraal & Peltier (1980), Admiraal et al (1982), and Admiraal et al (1984). During the period covered in the study by Peletier (1996), organic waste inputs from the Westerwoldse Aa, resulting from the regional potato flour and cardboard industries (Essink, 2003), declined from high levels (observed before 1980) to reduced levels (1987-1993). The epipelic community was dominated by only a few species and changed during the course of the study period. Under high organic loads, *Navicula salinarium* and *N. pygmaea* were dominating, but these were replaced by *N. phyllepta* and *N. flanatica* when organic loads were reduced. The latter species showed lower tolerance to high ammonium and sulphide concentrations.

The dynamics of microphytobenthos biomass at six stations in the Ems estuary (Figure 6) was studied by de Jonge & Colijn (1994) in the period 1976-1978 and de Boer (2000) between 1992 and 1999. Peletier studied the microphytobenthos in the Dollard in 1987 and 1993 close to the discharge point of the river Westerwoldse Aa. Furthermore, Staats (2001) sampled four transects on the Heringsplaat in the Dollard 1995 an 1996.

In general, the seasonal trend shows higher concentrations of chlorophyll during summer than during winter (de Jonge & Colijn; de Boer, 2000). During summer, irradiance, photoperiod and temperature are higher, and also lower wind speed may result in higher chlorophyll concentrations in the sediment. Mean chlorophyll concentrations (acetone extraction) range from about 30 to 400 $mg.m^{-2}$ (de Jonge & Colijn; de Boer, 2000). A seasonal trend was also observed by Staats et al (2001) at the Heringsplaat in the Dollard, with high chlorophyll-a concentrations (in top 5 mm of sediment) of up to 90 $mg.kg^{-1}$ sediment in June, and low values of less than 10 $mg.kg^{-1}$ sediment in March, October and December. When averaged, the Dollard sediment contains about 70 mg chla m^{-2}, the mid reaches (Hond & Paap) about 15-20 mg chla m^{-2} and the lower reaches (that is including the tidal flats of Borkum and Zuid-OostLauwers) about 40 mg chla m^{-2}). Since the latter tidal flats cover a large area, microphytobenthos (and phytobenthic production) is this area important for the whole system.

Staats et al (2001) found that chlorophyll-a in the sediment did not show a clear depth distribution, except in the zone of high chlorophyll-a concentrations in the peak period (June) when almost all chlorophyll was restricted to the top 5 mm of the sediment. De Jonge & Colijn (1994) also conclude that most of the vital chlorophyll-a is present in the upper 0.5 cm of the sediment, however vital cells can be found down to 3 cm in the sediment. The ratio between the 0.5-2cm sediment layer and the 0 to 2 cm layer was fairly constant, and between 0.40 and 0.47, suggesting a fairly constant depth profile. Next to vital algae, chlorophyll-a can also be present in detrital material (dead cells) that may be buried deeper in the sediment. De Jonge & Colijn (1994) report mean total chlorophyll-a concentrations down to at least 12 cm depth. In contrast to the findings of Staats et al (2001) de Boer found a clear extinction curve of chlorophyll-a, and constructed curves for the six stations sampled between 1992 and 1999 (Figure 7).

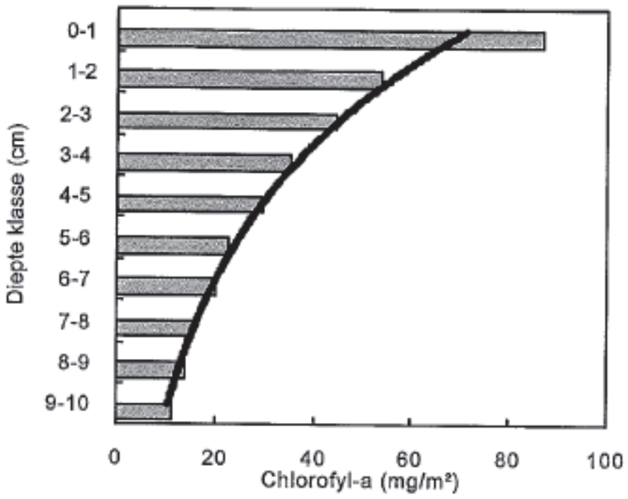

Figure 7. Mean chlorophyll-a concentrations related to depth in the sediment, on the basis of samples from six stations during different times of the year (from de Boer, 2000).

In relation to the depth distribution, it is worth mentioning that the euphotic layer in the sediment is at most 3 mm thick (Colijn, 1982). Only vital cells in the top few mm, i.e. only a small fraction of the total chlorophyll-a in the sediment, contributes to the primary production.

2.5.3 Factors controlling biomass

Factors influencing microphytobenthos biomass include irradiance, resuspension, nutrients, grazing, exposure, desiccation and others (Underwood, 2001). De Boer (2000) found significant relationships between the chlorophyll concentration with sediment composition, emersion period, climate variables and water quality parameters.

In the Ems estuary, the microphytobenthos is mainly present on the tidal flats. The period of emersion is most important for algal growth on the sediment, and is determined by the level of elevation of the flats and the tidal range. During submersion, the turbid water above the tidal flats limits growth at the sediment surface, and is usually assumed to be zero.

In case wind speed exceeds a certain level, microphytobenthos is resuspended simultaneously with mud from tidal flats in the estuary (de Jonge & van Beusekom, 2005). The extent of resuspension and deposition of mud is closely related to wind velocity (De Jonge & Van Beusekom, 2005). Highest densities of diatoms are also found on the margins of mudflats (Staats et al, 2001), and seem to follow mud content. During periods of higher wind speeds (> 6 m/s), the highest values for suspended matter in the lower reaches are found above the tidal flats, rather than in the main channel (de Jonge & Beusekom, 2005). Since maximum chlorophyll-a levels in the sediment are of the order of hundreds milligram chla m^{-2} (see below) against about 10 mg m^{-3} in the water column, it is obvious that resuspension will strongly affect the content of phytobenthos in the water column,

and that on the other hand the microphytobenthos content in the sediment will only be slightly affected.

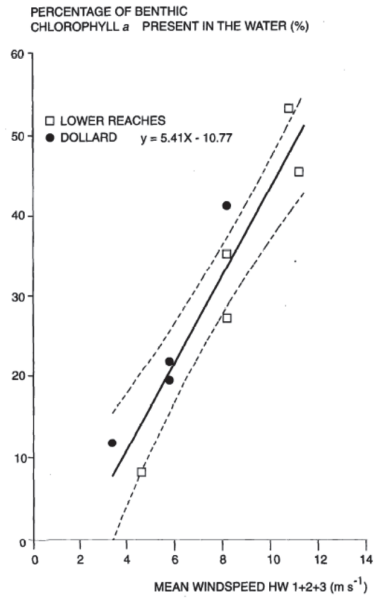

Figure 8. Relation between the fraction of resuspended chlorophyll-a and mean wind speed during the three preceding high water periods in the lower reaches and the Dollard (De Jonge & Van Beusekom, 2005).

It is generally assumed (e.g. Colijn & de Jonge, 1984) that nutrients are not limiting microphytobenthos growth at the water-sediment interface, since nutrients are probably taken up from the pore water of the sediment and not from the water column. However, no data on sediment nutrient concentrations are available for the Ems-Dollard (de Boer, 2000).

De Boer (2000) performed a limited study of the impact of macrofaunal grazing, by comparing chlorophyll biomass at Heringplaat with the average biomass and density of five diatom consuming species (*Hydrobia ulvae*, *H. ventrosa*, *Corophium volutator*, *Macoma balthica* and *Scobicularia plana*). No impact of grazing pressure on chlorophyll could be detected, however. In fact, there was a positive relationship between the density of *Macoma balthica* and chlorophyll biomass, showing a bottom up rather than a top down control.

The biomass (in the upper 5 mm of the sediment) close to the outlet of the Westerwoldse A showed a decreasing trend during the period of decreasing loads of organic material (Peletier, 1996). Chlorophyll-a levels reached highest levels in May-June with peak levels of ca 400 mg.m^{-2} in 1976, ca 200 mg.m^{-2} in 1977 and 1987, and ca 70 mg.m^{-2} in 1993. The difference in the development of microphytobenthos biomass was probably caused by the increasing numerical densities of the macrofaunal diatom grazers *Nereis diversicolor* and *Corophium volutator*, caused by the reduction of the organic waste. However, de Boer (200) could not detect a relationship between the macrofaunal grazing pressure and the chlorophyll concentration.

Whereas the temporal and seasonal biomass levels appear to be affected by a range of factors, variation between years appears to be closely correlated with the average temperature (de Boer, 2000; Figure 9).

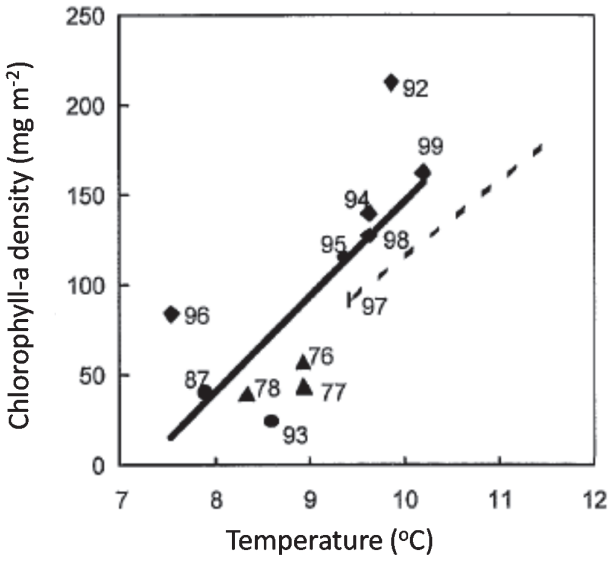

Figure 9. Relationship between yearly averaged microphytobenthic chlorophyll-a density (on the basis HPLC corrected values) and average temperature, based on data from Colijn & de Jonge (1984) for 1976-1978 (triangles), Peletier (1996) for 1987 and 1993 (circles), and de Boer (2000) for 1992, 1994-1999 (diamonds). The solid line represents the equation for the Ems-Dollard, the broken line the relationship found in the Oosterschelde (see de Boer, 2000).

2.5.4 Benthic primary production

The primary production of the microphytobenthos in the Ems estuary has been measured at six stations (Figure 6) from 1976 through 1978 (Colijn & de Jonge, 1984). During the period about 16 measurements were performed at each station, and measurement included the chlorophyll-a concentration, primary production (by ^{14}C carbon fixation), environmental parameters and sediment characteristics. De Boer (2000) calculated primary production rates for the period between 1992 and 1999 on the basis of chlorophyll-a concentrations and an empirical relationship established by De Jong & De Jonge (1995). It should be noted, however, that there may be a high variability between the production rates at a certain chlorophyll-a concentration (Colijn & De Jonge, 1984).

The time series of primary production measurements (Figure 10) published by Colijn & de Jonge (1984) form the basic data set (collected in the late seventies) that has been used for several succeeding publications by de Jonge c.s. An assessment of the total primary production of both phytoplankton and microphytobenthos was made by de Jonge (1995). It shows that the microphytobenthos production is relatively most important in the Dollard region, but in absolute values is more important in the lower reaches of the estuary (Figure 12). In the lower reaches, production by microphytobenthos takes place in the water column rather than on the tidal flats,

whereas in the Dollard production it is more important on the tidal flats. Microphytobenthos biomass makes up a considerable part of the total algal biomass in the estuary (Figure 11). The biomass of the microphytobenthos is both present on the tidal flats and in the water column of the estuary. Therefore, also production in the water column by microphytobenthos contributes substantially to the overall primary production in the estuary. Overall, the microphytobenthos production makes up about a quarter of the total primary production in the estuary (Figure 13), and in the shallow Dollard almost 70 %.

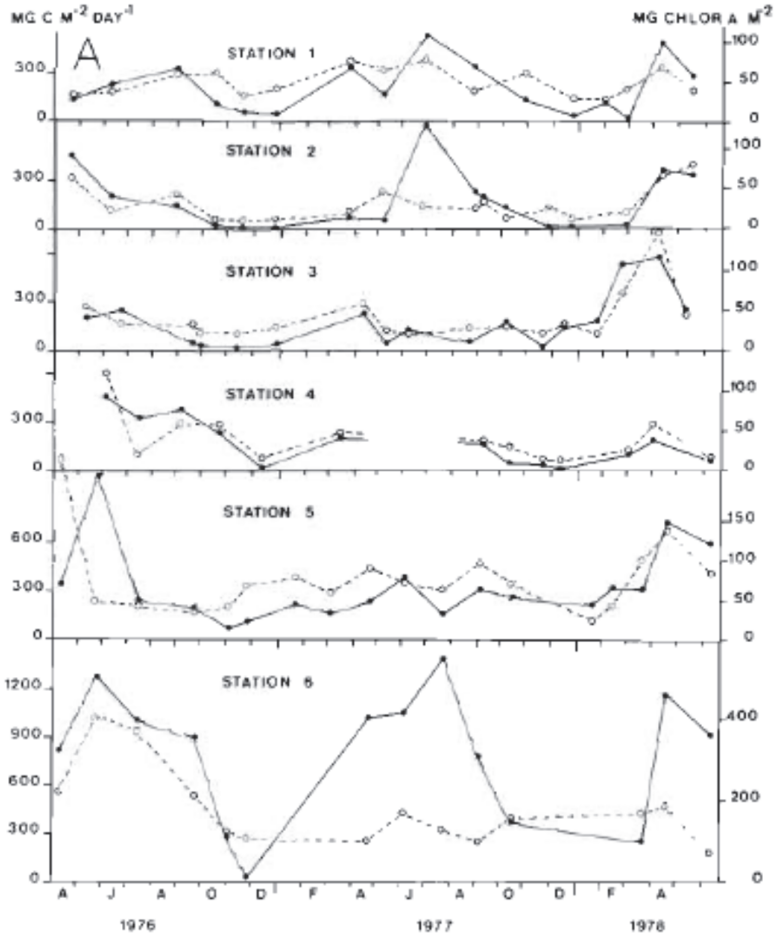

Figure 10. Daily primary production rates (solid circles) and chlorophyll-a (open circles) at the six stations as presented in Figure 6 (Source: Colijn & de Jonge, 1984).

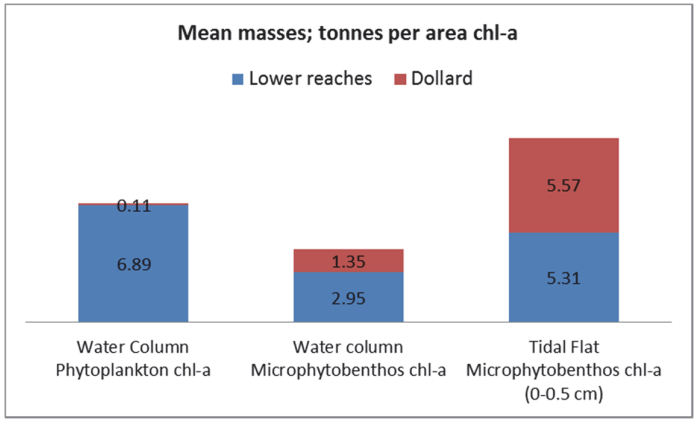

Figure 11. Chlorophyll-a (biomass) of phytoplankton and microphytobenthos in the Lower reaches and Dollard in the year 1977 (based on de Jonge, 1980). The values given have a considerable uncertainty, because they are based on measurements on just a few sites.

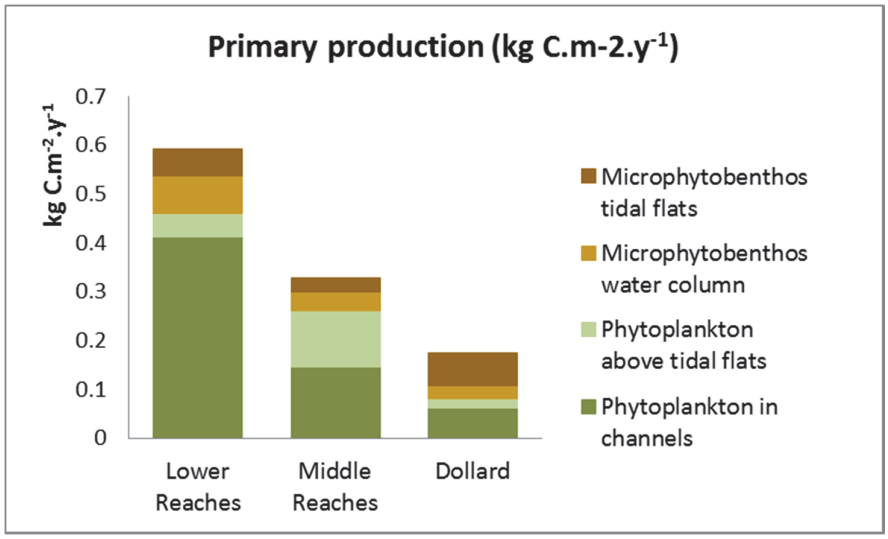

Figure 12. Mean annual primary production figures for different reaches of the Ems-Dollard estuary over the period 1976-1980 for phytoplankton (excluding excretion) and microphytobenthos (after de Jonge, 1995).

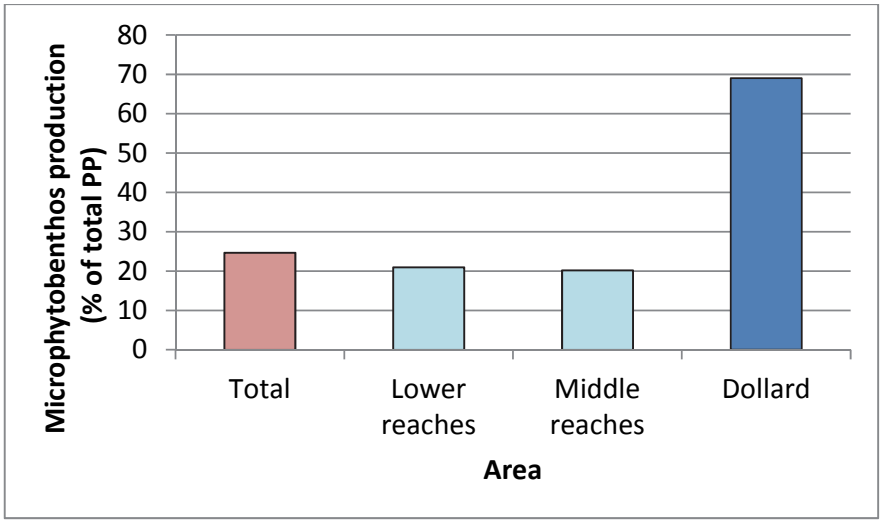

Figure 13. Contribution of microphytobenthos production to the total production in the total estuary and for the distinguished zones within the estuary (based on data by de Jonge, 1995).

2.6 System data and compartments

Hydromorphological characteristics of the area (Figure 14) are listed in Table 5 and Table 6. These values are needed to compute total primary production in the system, taking into account the depth of the system varying with the tides. Also, tidal flats run dry partly, and this is also accounted for.

The compartment numbering used in the different studies is somewhat confusing; Colijn (1983) uses two divisions: one in three compartments (Outer Reaches, Middle Reaches and Dollard), and one in 11 compartments (0..10) (Figure 14 - Figure 16). De Jonge (1994) also uses Colijns division, but De Jonge & Brauer (2007) again use the three compartments. The present study has a number of sampling stations; these stations are assigned to six compartments (Figure 16). Later on in this report when the whole system primary production and other characteristics are computed, the six and the 11-compartment set-up both are used.

Table 5 Main and sub-compartments, numbering and levels. 'Main'-compartments: 1= Outer reaches, 2= Middle reaches, 3= Dollard

City/Site	Compartments				
	Main	Sub	Colijn_nr	Reference plane MHW 2013 (m)	Amplitude 2013 (m)
Borkum	1		0	1.03	2.4
	1	1	I	1.03	2.4
Eemshaven	1	2	II	1.09	2.49
	2	3	III	1.25	2.65
Delfzijl	2	4	IV	1.32	2.7
Knock	2	5	V	1.31	2.99
	2	6	VI	1.36	3
	3			1.38	3
	3	7	VII	1.38	3
Emden	3	8	VIII	1.44	3
	3	9	IX	1.45	3.05

Table 6 Sub-compartments and their characteristics in the 70's and in 2013. % Emersion of tidal flats in periods 1997-2002 and 2003-2005. Sub-compartments 0 and 10 (Borkum and Shipping channel Emden) have not been considered further in the present study. TF is tidal flat, CH is channel. See

City/Site	Compartments			Area 1970 Km^2		Volume 1970 10^6 m^3		Volume 1970	Volume 2013 10^6 m^3		Volume 2013	% emersion tidal flat	
	Sub (Figure 14)	Colijn-_nr	ED-proj.	TF	CH	total MHW	Total MLW	% shoal to total	Total MHW	Total MLW	% shoal to total	97-02	03-05
Borkum*)	0		1						233.2	188.5	3.0	16.7	15.4
Oude Wester-Eems	1	I	1	80	62	575	370	9.7	590.4	434.9	3.5	8.3	7.3
Eems-haven	2	II	1	20	53	425	265	6.5	298.4	208.7	3.1	16.7	12.9
Hond	3	III	2	21	38	300	150	16.3	215.2	130.6	2.9	15.8	14.3
Delfzijl/ Oost-Fr. Gaatje	4	IV	3	22	20	215	125	16.7	104.9	68.0	4.5	25.2	25.2
Paap	5	V	3	16	14	120	50	26.3	102.7	59.4	7.5	13.4	12.2
Dollard-Mond	6	VI	4	4.1	14.4	115	70	3.5	84.0	44.8	2.4	17.8	17.9
Vaar-water Emden									39.7	19.8	6.4	20.0	18.4
GrGat-Noord	7	VII	5	21	8	72	25	31.9	41.2	15.6	12.6	20.3	19.5
Geise-Hoogzand	8	VIII	6	13.6	2.9	32	8	47.8	9.3	0.9	17.2	43.3	43.5
Hooge-Plaat	9	IX	6	40	3	47	405	71	0.2	0.0	84.1	37.0	39.2
Emden shipping channel *)	10												

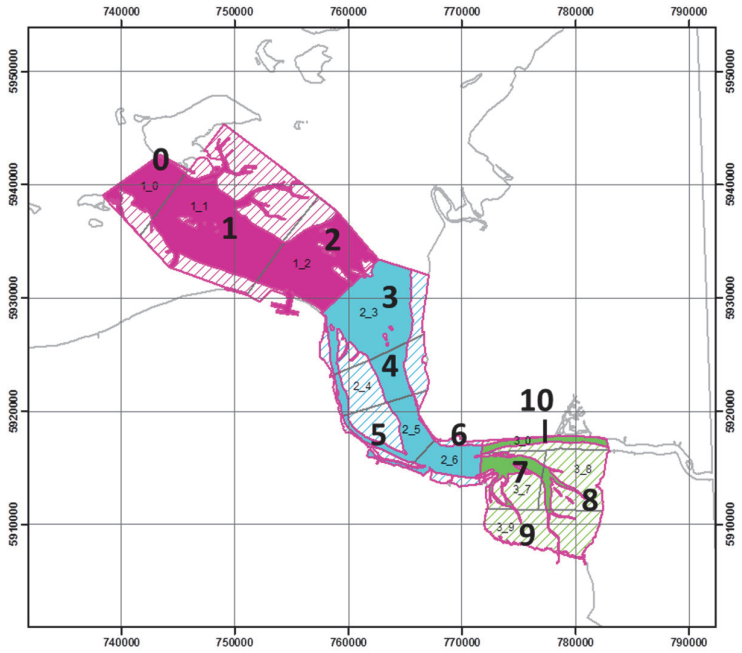

Figure 14 Compartments distinguished in the Ems-Dollard estuary; according to Colijn (1983). Characteristics are listed in Table 6. Compartment numbers 0-10 are referred to in Table 6, second column ("sub-compartments"). Compartments 0 and 10 were left out of the present study.

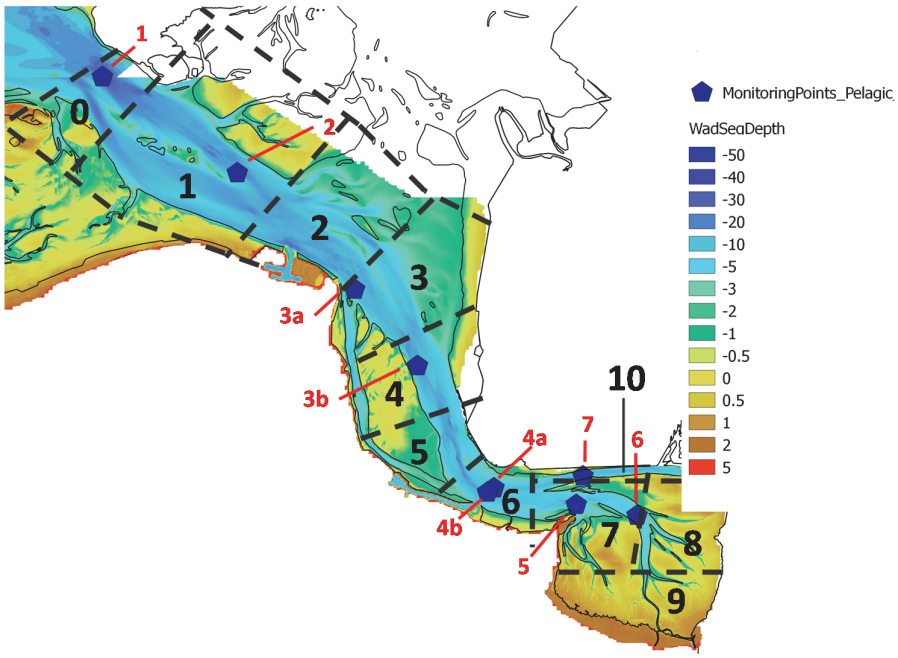

Figure 15 Compartments distinguished in the Ems-Dollard estuary; according to Colijn (1983). As Figure 14, but now drawn on a depth map. Characteristics are listed in Table 3. Compartment numbers 0-10 are referred to in Table 3, second column ("sub-compartments"). Sampling stations (1-6) used in the present study are mentioned; stations 3a and 4a were changed to 3b and 4b during the study.

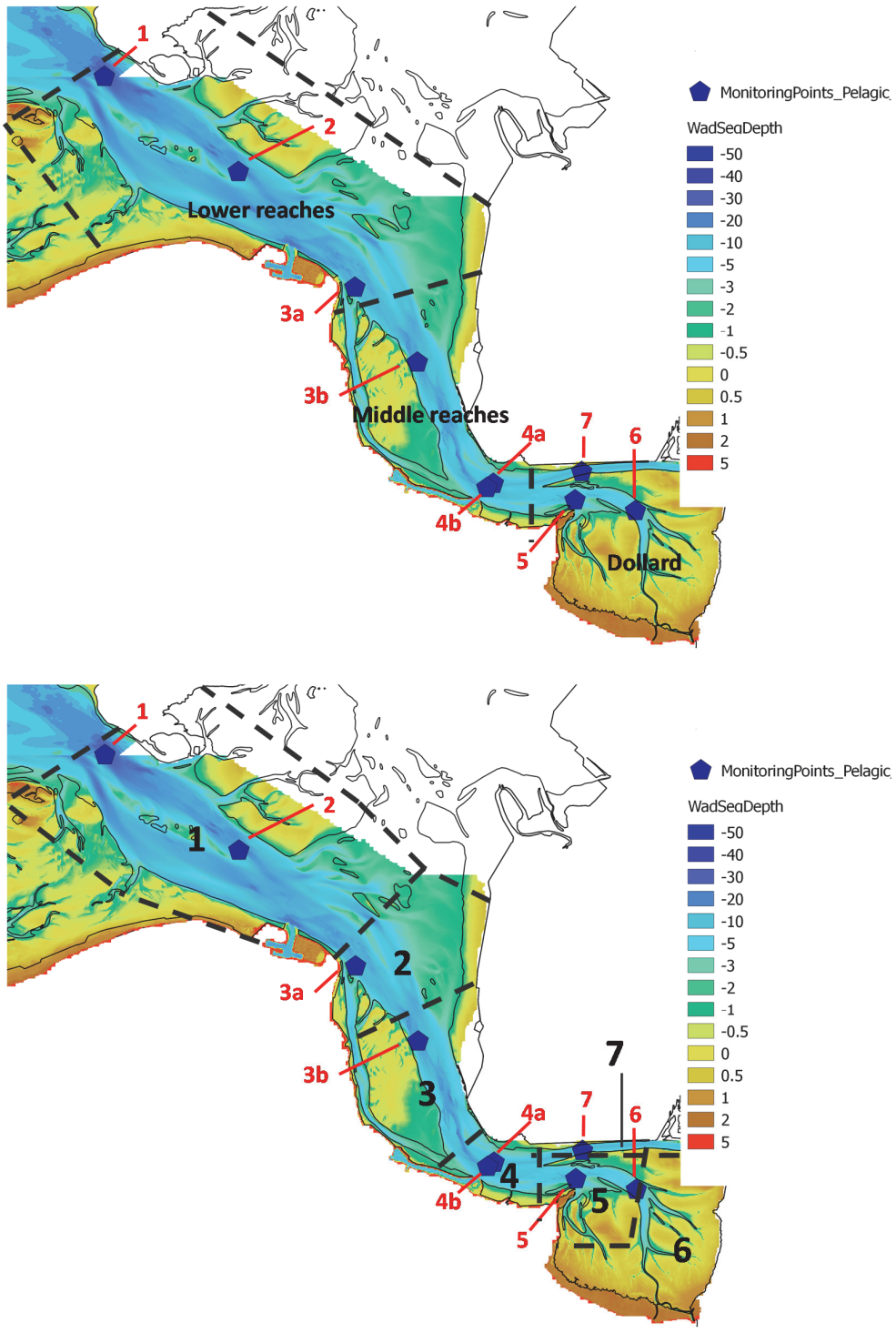

Figure 16 Compartments distinguished in the Ems-Dollard estuary. Upper: division into three main sections, as done by De Jonge & Brauer (2007). Lower: 6 compartments as used in the present study. Boundaries are the same as in Colijns study, but some Colijn compartments were merged. Table 5 and Table 6 give the numbering as well. Sampling stations (1-6) used in the present study are mentioned; stations 3a and 4a were changed to 3b and 4b during the study.

3 Methods-1: cruises, sampling sites, dates, procedures, variables measured

3.1 What is in this chapter

In this chapter all cruises are described, where the sampling sites were, what the sampling procedures were and what variables were measured. Sample analyses procedures are described in chapter 4.

3.2 Pelagic cruises

Cruises took place on the “Asterias” (Figure 17), a monitoring vessel of Rijkswaterstaat, based in Delfzijl (Groningen). Cruises were planned such, that the last sampling station, located upstream in the Dollard, was reached around low-tide. The sampling and measurements started downstream near Borkum, and the ship sailed against the tidal current to end up at the last station in the centre of the Dollard.

Figure 17 Vessel Asterias.

3.3 Benthic sampling trips

Sampling trips were performed using a smaller vessel, the Eemshörn, located at the Eemshaven (Figure 18). For transport to the tidal flats, a small boat was used (Figure 19).

Figure 18 The vessel Eemshörn, used for the benthic sampling program. In the background some researcher trails are visible.

Figure 19 The "Hurricane", used for transport between the "Eemshörn" and the tidal flats.

Figure 20 Sampling took place under very different conditions. Left: 2013, January 22nd, below: 2013, August, 15th

3.4 Sampled variables

Variables sampled during the research are listed in Table 7 and Table 8. In chapters 4 and further, methods of sampling and analyses are explained further.

Table 7 List of pelagic measurements. Pocket Box (see sections 3.6 and 4.5) measurements were done continuously. At each sampling site Pocket Box values were recorded by hand, next to other data.

Variable	Frequency	Method
Temperature	Continuous	Pocket Box
Temperature	Sampling site	HQ40D sensor
Salinity	Continuous	Pocket Box
Salinity	Sampling site	HQ40D sensor
Conductivity	Continuous	Pocket Box
Oxygen concentration	Continuous	Pocket Box
Oxygen concentration	Sampling site	HQ40D sensor
Oxygen saturation	Continuous	Pocket Box
Light extinction	Continuous	Pocket Box
Light extinction	Sampling site	LICOR sensor
SPM	Sampling site	Sampling/filtration/weighting
Chlorophyll	Continuous	Pocket Box
Chlorophyll	Sampling site	Sampling/ Acetone extraction GF/F filters / Fluorometry
CDOM (Coloured dissolved organic matter)	Continuous	Pocket Box
Turbidity	Continuous	Pocket Box
Diatoms	Continuous	Pocket Box
Cryptophytes	Continuous	Pocket Box
Blue-greens	Continuous	Pocket Box
Green algae	Continuous	Pocket Box
Yellow substances	Continuous	Pocket Box
Nutrients	Discrete	Sampling/filtration/ analysis by RWS
Primary production	Discrete	^{14}C incubation at different light intensities
Inorganic C	Discrete	Titration
Growth limitation	Discrete	Pigment ratio

Table 8 List of benthic measurements.

Variable	Frequency	Method
Temperature	Sampling site	Thermometer
Chlorophyll-a	Sampling site	Sampling, dilution, filtration, spectrophotometric analysis
Primary production	Discrete	^{14}C incubation at different light intensities

3.5 Sampling sites and sampling dates

3.5.1 Pelagic sampling sites and cruises

Pelagic sampling in 2012 and 2013 took place at six sites in the Ems-Dollard estuary, from the North Sea side to the gullies of the Dollard (Figure 21 & Figure 21). The sampling locations were adjusted

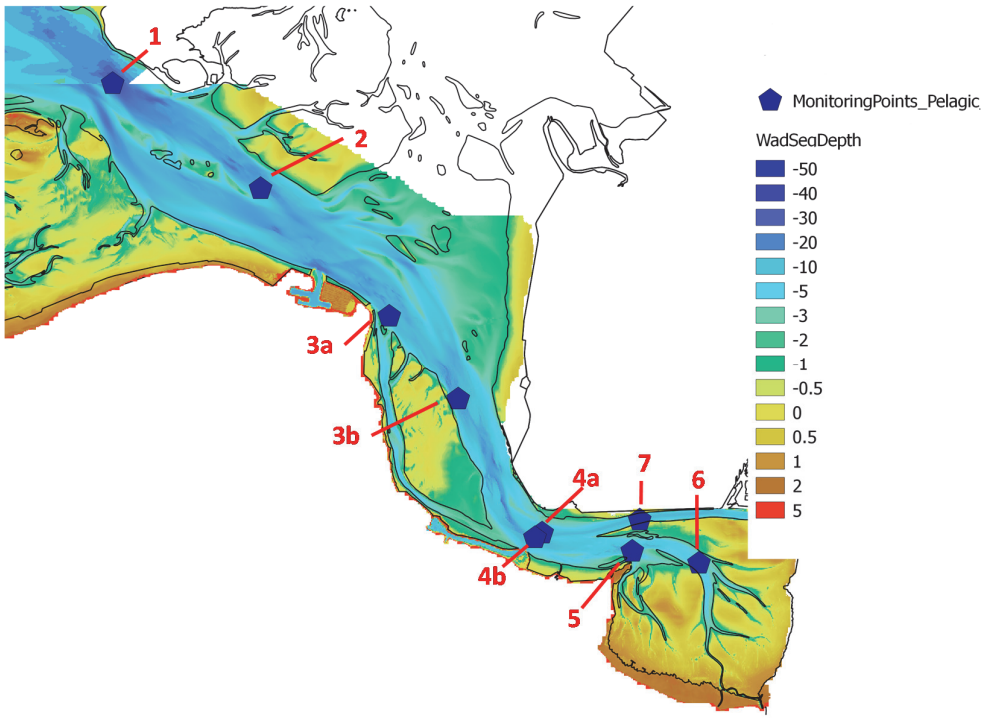

Figure 21 Pelagic sampling sites in the Ems-Dollard. Sites 3 and 4 changed position in the course of the year (Table 9). Water depth in mtrs. Same as Figure 16, but without compartment boundaries

during the programme (Table 9). Station 3 was repositioned because of interference with cooling water released from power plants, station 4 was repositioned from the side to more central in the shipping lane. Station 7, located up in the Ems river, was only sampled once. A number of 20 cruises was planned for 2012 (Table 10). Originally, the first cruise was planned at February 7, but was postponed by RWS to February 16 due to floating ice. In 2013, 19 cruises were done.

The position of the sampling stations and the vessel during the cruises has continuously been recorded by the PocketBox-GPS.

Some data were recorded continuously by the PocketBox (see section 4.5) *and* by hand (during the stops at each sampling site); this offers an opportunity to compare these results. It appeared that some data had to be corrected and sometimes even rejected. This is further elaborated in the "results"-sections (chapter 6-8).

Table 9 Sampling stations in 2012 and 2013. Positions after GPS measurements. RD-X and RD-Y are the 'Rijksdriehoekscoordinaten" of each monitoring site.

Station	Latitude	Longitude	RD-Y	RD-X	Cruise 2012	Cruise-2013
1	53.5595	6.6634135	620023	239571	2 – 21	22-40
2	53.5043	6.7887996	614031	247999	2 - 21	22-40
3a	53.4376	6.8969810	606753	255332	2 – 7	
3b	53.3940	6.9545404	601983	263634	8 - 21	22-40
4a	53.3245	7.0237790	594360	264044	3	
4b	53.3222	7.0175359	594090	263634	4 – 21	22-40
5	53.3141	7.1004698	593322	269180	2 – 21	22-40
6	53.3072	7.1572541	593322	269180	2 - 21	22-40
7	53.3300	7.1074281			6	

Table 10 Cruise numbers and corresponding dates and Julian day number. Note that the first cruise was in 2011, and served as a try-out. Results of that particular cruise are not part of this report. Light blue shaded 2013-data were combined with benthic measurements (Table 12)

Cruise	Code	Date	Daynr		Cruise	Code	Date	Daynr
1	101	2011-11-22	326		22	122	2013-01-22	22
2	102	2012-02-16	47		23	123	2013-02-21	52
3	103	2012-03-06	66		24	124	2013-03-07	66
4	104	2012-03-20	80		25	125	2013-03-25	84
5	105	2012-04-03	94		26	126	2013-04-04	94
6	106	2012-04-17	108		27	127	2013-04-18	108
7	107	2012-05-03	124		28	128	2013-05-02	122
8	108	2012-05-15	136		29	129	2013-05-22	142
9	109	2012-06-01	153		30	130	2013-06-04	155
10	110	2012-06-14	166		31	131	2013-06-19	170
11	111	2012-07-02	184		32	132	2013-07-03	184
12	112	2012-07-16	198		33	133	2013-07-18	199
13	113	2012-07-31	213		34	134	2013-08-01	213
14	114	2012-08-13	226		35	135	2013-08-15	227
15	115	2012-08-28	241		36	136	2013-08-29	241
16	116	2012-09-12	256		37	137	2013-09-16	259
17	117	2012-09-26	270		38	138	2013-10-15	288
18	118	2012-10-11	285		39	139	2013-11-14	318
19	119	2012-10-25	299		40	140	2013-12-12	346
20	120	2012-11-29	334					
21	121	2012-12-11	346					

3.5.2 Benthic sampling sites

Originally six sites were chosen to do all the benthic measurements. However, one site appeared to be a bad choice because of logistic reasons. The remaining five sites (coordinates in Table 11) are shown Figure 22. The sites were visited eleven times in 2013, from February 20th until December 11th (Table 12). A first visit in January had to be cancelled because of the heavy ice in the system (Figure 20 & Figure 24).

Table 11 benthic sampling stations in 2013. Positions after GPS measurements. RD-X and RD-Y are the 'Rijksdriehoekscoordinaten" of each monitoring site. Station "2" is missing, see text above.

Name	Number	Latitude	Longitude	RD_Y	RD-X
EDB01	1	53.46742	6.78829	609930.4	248045.3
EDB03	3	53.39422	6.94832	602003.6	258848.6
EDB04	4	53.313	7.08396	593170.4	268083.6
EDB05	5	53.29703	7.15154	591501.7	272630.6
EDB06	6	53.2566	7.17066	587034.5	274016.6

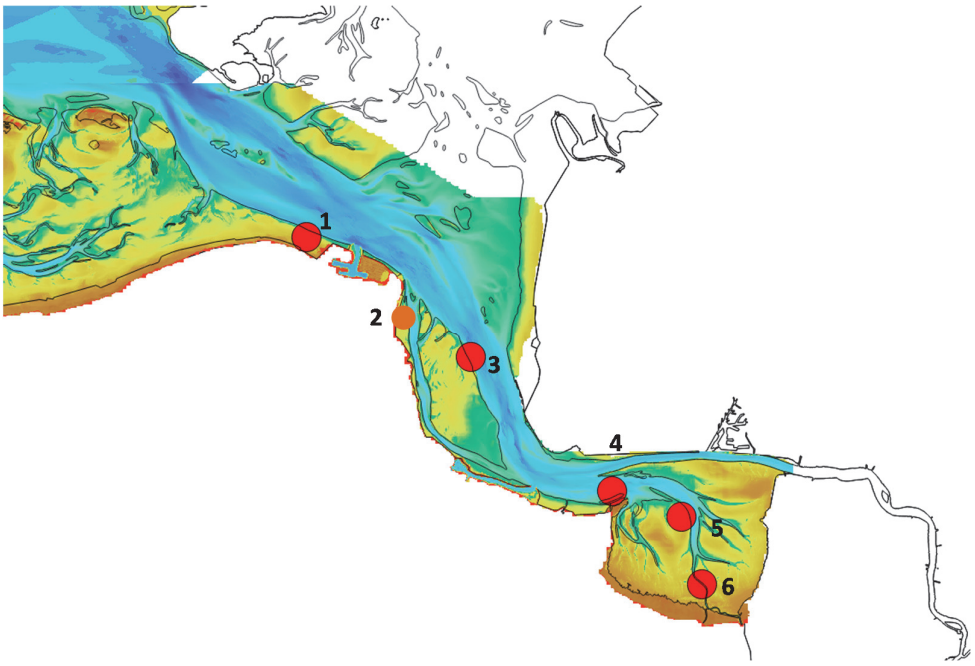

Figure 22 Benthic sampling sites in the Ems-Dollard projected on a depth-map of the area (same as Figure 21). Site number 2 (orange dot) was only visited once.

Table 12 Benthic sampling dates in 2013. Note that cruise nr 1 had to be cancelled due to ice. All sampling dates are on the day before the pelagic cruises, except for cruises 3 and 9. For coordinates see Table 6

Cruise	Code	Date	Daynr
1	1001	2013-01-21	21
2	1002	2013-02-20	51
3	1003	2013-03-21	80
4	1004	2013-04-17	107
5	1005	2013-05-21	141
6	1006	2013-06-18	169
7	1007	2013-07-17	198
8	1008	2013-08-14	226
9	1009	2013-09-11	254
10	1010	2013-10-14	287
11	1011	2013-11-13	317
12	1012	2013-12-11	345

3.5.3 Rijkswaterstaat sampling sites

Next to our own data, Rijkswaterstaat has its monthly monitoring program (MWTL, data in: Waterbase, 2014). When discussing our monitoring results, those of Rijkswaterstaat are mentioned as well, including their sites. Therefore, present and former monitoring sites are plotted in Figure 23.

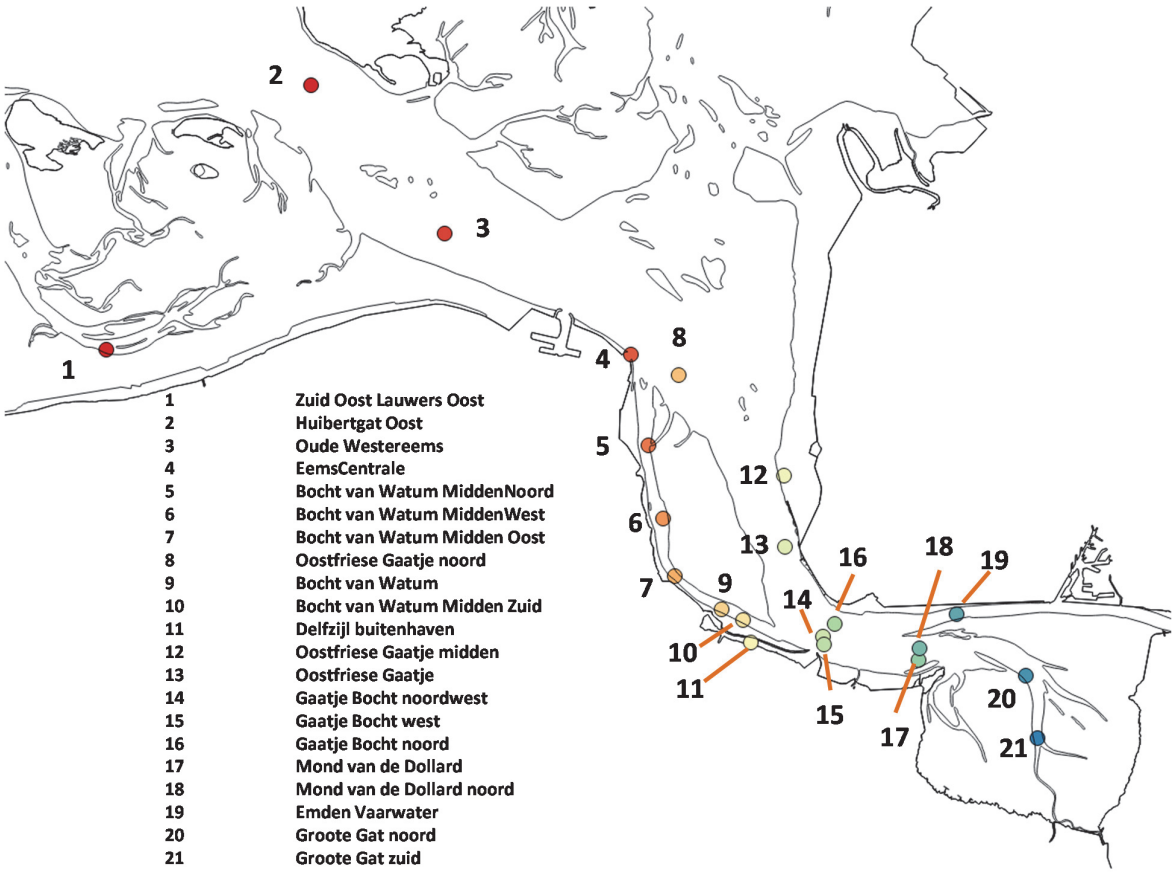

Figure 23 All present and former monitoring sites of Rijkswaterstaat in the Ems-Dollard area, plus the Zuid-OostLauwers Oost as the most nearby rest-of-the Wadden Sea site. Most monitoring sites are not samples anymore, only sites 1,2, 13 and 20 are still visited. Some of the site have only been sampled a few years.

Figure 24 Ice and snow conditions on January 23rd, 2013. After an attempt to reach the site from the dike.

3.6 Taking pelagic samples

3.6.1 Continuous Pocket Box measurements

During the cruises, a pressure pump pumped water through the pocket box (4h PocketBox, Jena Engineering) (Figure 25). The pocket box contained 23 sensors continuously measuring 17 variables (see below). During each cruise, the vessel stopped at each of the sampling sites (Figure 21), and PocketBox-data were stored, and used as a first indication of the local values. Better values were obtained later (at the data elaboration); based on the sailing velocities it was later decided when the vessel stopped, and the data for that period were averaged and used as definitive average PocketBox values at each sampling site. These average values were compared with data from a handheld multimeter (Hach HQ40d: Figure 28), data obtained in the laboratory (e.g. contents of suspended matter) and light extinction data obtained after analysis of light intensity measurements in the water column. This comparison results in a number of calibration factors. Finally, if necessary, PocketBox-data were re-processed using these calibration results.

3.6.2 Water samples at each monitoring site

Next to the continuous data assessment, water samples were collected at each of the six monitoring sites. Water was split from the pocket box and water samples were collected (Figure 26). These samples were processed on board and stored for further analysis (chlorophyll-a analyses and primary production measurements in the lab, phytoplankton counting by Koeman & Bijkerk and nutrient analyses in the RWS laboratory).

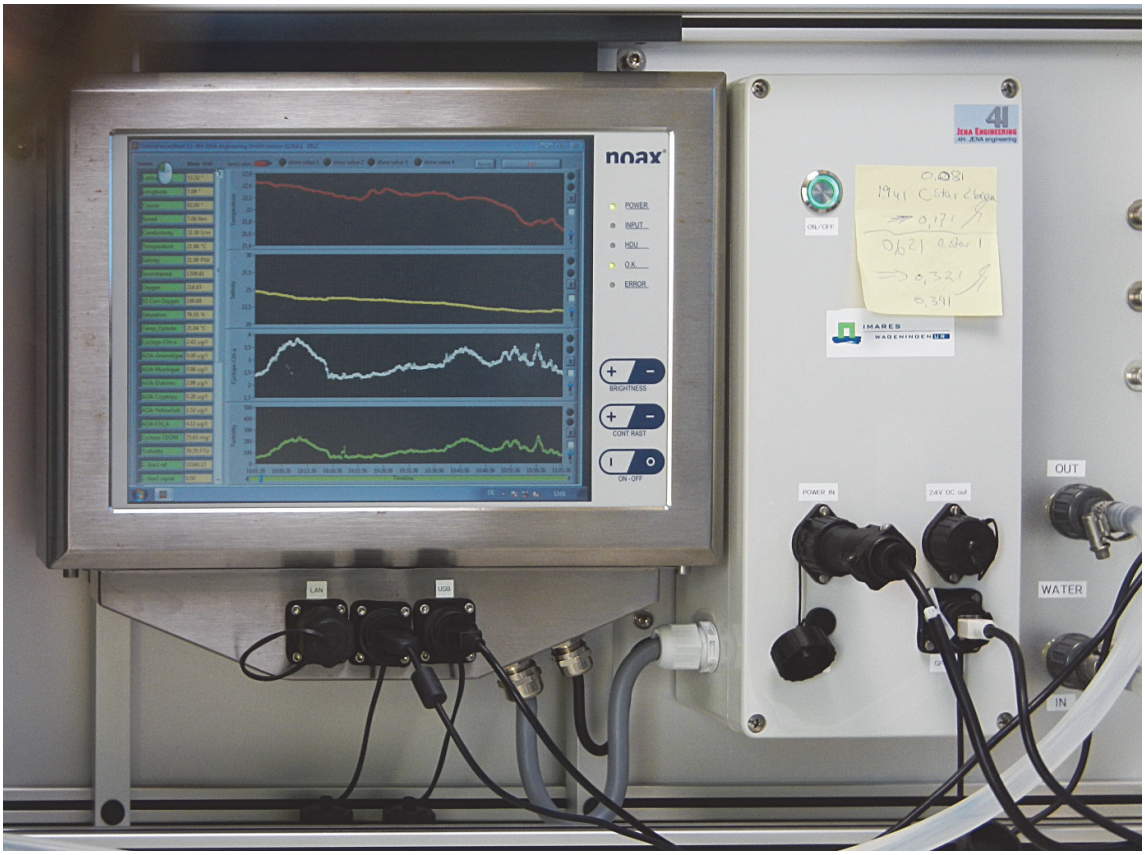

Figure 25 4H PocketferryBox (PocketBox) with output screen showing the some results of the continuous measurements along the transect of the estuary, from top to bottom: temperature, salinity, chlorophyll-a and yellow substance.

Figure 28 Hach HQ40d multimeter used for calibration/check of data from the PocketBox.

Figure 26 Collected samples waiting for further analysis on board. Mentioned on the bottles: date (May 15th, 2012), cruise number (8) and station number (1-6).

Figure 27 Sediment sampling. Above: the five 2.6 cm tubes, next to the 'Benthic Torch'. Middle: sampling on a sandy site (site 04). Lower: a muddy site in the Dollard (site 06)

3.7 Taking benthic samples

3.7.1 Sampling procedure primary production

Five sampling tubes (diameter 25.97 mm, area 530 mm^2) are filled each time with about 10 cm sediment and stored (Figure 27). In the lab, 2 mm was sliced off. Additional measurements revealed that the actual thickness of the slice was 2.11 mm, but the procedure followed probably implies that the accuracy of the slice thickness was about 0.1 mm (± 5%). The volume of each slice thus was 1059 mm^3 (± 53 mm^3).

3.7.2 Sample handling for primary production measurements

Five slices (in some cases this was less) together were dispersed in 1000 ml of filtered sea water; sometimes this volume was a bit different. The sea water has been collected in the Ems-Dollard at approximately the same location. After shaking the suspension, larger particles were allowed to settle and the dispersion was decanted. If needed, the dispersion was diluted, and next, divided into two parts (600 and 400 ml). The first was used for the ^{14}C-primary production measurements, the second was used for a fluorometric chlorophyll-a analysis. Of the dispersion (if needed, diluted; see the description for the ^{14}C-analyses), about 150 ml was filtered (over a GF/F glassfiber filter, effective pore diameter about 0.7 µm). This filter was extracted in 20 ml acetone. If needed, the acetone extract was also diluted. Finally, [chla] was determined by fluorometry-measurements. All measurements were corrected for the blanks (acetone).

3.7.3 Sampling procedure chlorophyll-a analysis

Within a 10 m circle around a marked spot, 5 samples were taken randomly using a cut-off syringe (diameter 24 mm). The syringe was pushed in the sediment and subsequently gently extracted. The sediment in the syringe was pushed upwards until 5mm (the top layer) remained. This core (5.56 cm^2) was placed in a centrifuge tube, carefully rinsing the syringe with filtered sea water. This procedure was repeated 4 times and resulted in one mixed sample per location. The sample was stored and transported in a cooler. Back at the IMARES lab tubes were stored at -80° C until further analysis.

Samples were freeze-dried, mixed and subsampled by weight. Chlorophyll-a in the subsamples (in duplicate) was extracted by homogenisation in 90% acetone with the addition of glass pearls. Samples were centrifuged and chlorophyll-a in the supernatant was determined spectrophotometrically. Correction for degradation products were made by reading after acidification (cf. De Jonge & Colijn, 1994). Finally, concentrations were converted from the subsample to m^{-2} (see section 4.6.1.5). All handling of the samples took place in the dark to prevent degradation of chlorophyll.

3.7.4 BenthoTorch

At each benthic sampling site 5 to 10 in situ chlorophyll-a measurements were performed fluorometrically using a so-called BenthoTorch (Figure 29) (bbe Moldaenke, Germany), see section 4.6.6. This is additional to the 5 samples taken for chlorophyll-a analysis in the lab.

The chlorophyll concentrations determined in the lab gave the total chlorophyll in 5 mm sediment, while BenthoTorch readings apply to the top-layer and thus are expected to give lower values. Extrapolation of these results to the top 5 mm cannot be made since it is expected that the attenuation of chlorophyll in the sediment is not constant in both space and time. Comparing the results from both methods however gave a validation for the chlorophyll concentrations.

Figure 29 BenthoTorch measurement of a stone surface on a river bank (picture copied from http://www.bbe-moldaenke.de/chlorophyll/benthotorch/)

4 Methods-2: analysis procedures

4.1 What is in this chapter.

All analysis methods are described, including the mathematics needed to come to the desired result.

4.2 Nutrients

Per station 250 ml of water was filter over 0.45µm Polydisc filters and stored at 4°C until further processing by RWS.

RWS-MWTL analysis procedures thus were applied. Results for 2012-2013 are available for dissolved inorganic phosphorus (ortho-P), ammonium (NH_4^+), nitrate (NO_3^-), nitrite (NO_2^-) and dissolved Si.

4.3 Suspended matter

The suspended matter content increases more or less from station 1 to 6 (see later). This has consequences for the amount of water that can be filtered per station. Depending on the station, between 400 and 50 ml of water was filtrated over a GF/C pre-weighted filter (effective pore size 1.2µm). Samples were taken in duplicate. Filters were placed in petri discs and stored at 4°C until further processing. Back in the laboratory on Texel the filters were dried (50°C, min 16 h) and weighted. As control two filters with reference material were also part of the analysis. The described procedure is in accordance with the MWTL analysis procedure (RWS).

4.4 Hach HQ40 multimeter

4.4.1 Temperature

Temperature is measured simultaneously with oxygen and conductivity.

4.4.2 Oxygen

Oxygen measurements are done with an IntelliCAL™ LDO101 Rugged Luminescent/Optical Dissolved Oxygen (LDO) meter with a Lumiphore sensor. Sensitivity range 0.05 to 20.00 mg/l. See http://www.hach.com/intellical-ldo101-rugged-luminescent-optical-dissolved-oxygen-ldo-probe-5-meter-cable/product-details?id=7640489865

4.4.3 Conductivity/salinity

Measured with an “Intellical”-probe, see http://www.hach.com/hq40d-portable-ph-conductivity-optical-dissolved-oxygen-do-orp-and-ise-multi-parameter-meter/product-parameter-reagent?id=7640501639. Salinity is computed by the instrument from the conductivity data.

4.4.3.1 General: chlorinity, salinity and conductivity

These values are related, and can be used to convert the one into the other.

Chlorinity concerns, based on the method of analysis, the sum of chloride, bromide and iodide in water –expressed as gram per kilogram. But, the latter two are of minor importance, and thus is the measured value similar to the chloride content.

Salinity is the total of dissolved matter in water (g kg^{-1}); the relationship with chlorinity is (Wooster, Lee, and Dietrich, 1969):

$$S = 1.80655\,[Cl^{-}] \qquad (g\ kg^{-1}) \qquad (1a)$$

[Cl-] is expressed in g kg^{-1}.

The conductivity strongly depends on the content of conducting anions and cations, and thus on salinity.

There is a precise conversion (UNESCO-standard; Fofonoff & Millard, 1983), but for the present situation a more simple conversion as the one by Williams (1986) is satisfactory:

$$S = 0.4665\ cond(25)^{1.0878} \qquad (g\ kg^{-1}) \qquad (1b)$$

With

$$cond(25) = \frac{cond(T)}{1+ft\cdot(T-25)} \qquad (mS\ cm^{-1}) \qquad (1c)$$

S : Salinity, g kg^{-1},

Cond : conductivity, mS cm^{-1} (at 25 ^{0}C and at the ambient temperature T)

T : temperature, ^{o}C.

In many cases, salinity is expressed in µS cm^{-1}, thus a factor 1000 higher.

Williams gives ft =0.02, but he used salinity as g l^{-1} (not per unit of mass). At T=30 ^{o}C the values are more or less the same, but deviate for lower temperatures. By choosing ft=0.0185 these deviations disappear.

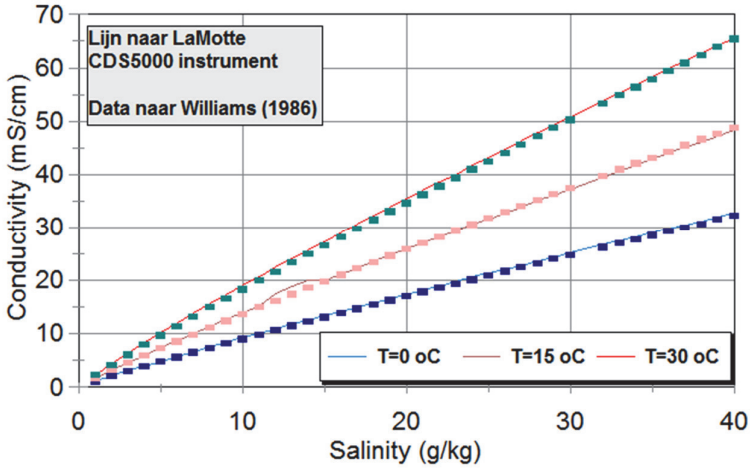

Figure 30 Conductivity and salinity after Williams (1986)

In the Netherlands 20 °C is used as standard temperature for the conductivity measurements.

The relationship between cond(20) and cond(T) is (Figure 30):

$$cond(T) = cond(20) \cdot \frac{1+ft\cdot(T-25)}{1+ft\cdot(20-25)} \qquad \text{(mS cm-1)} \qquad \text{(1d)}$$

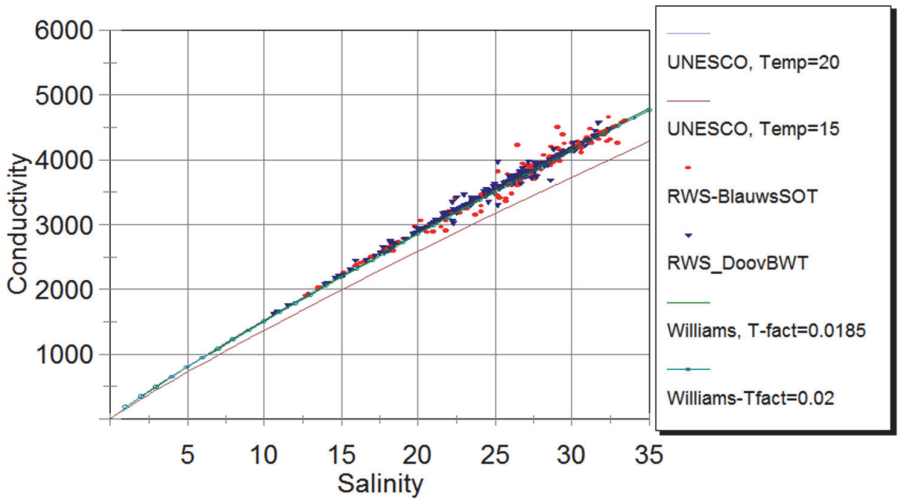

Figure 32 Salinity and conductivity according to UNESCO (Fofonoff & Millard1983), Williams (1986) and RWS-measurements in the western Dutch Wadden Sea (Blauwe Slenk-Oost and Doove Balg-West)

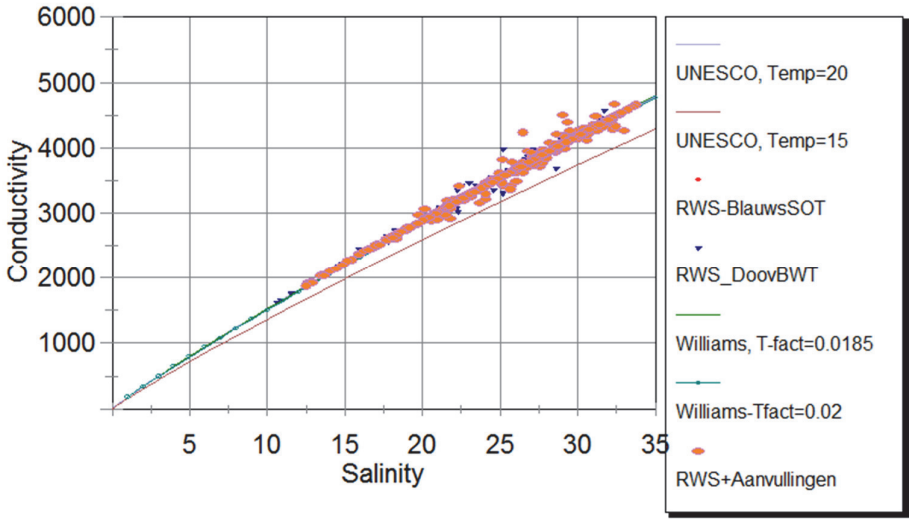

Figure 31 Conductivity and salinity, including the addition to the Rijkswaterstaat dataset.

4.4.3.2 Conclusions

Rijkswaterstaat uses in its tables conductivity at 20 °C. RWS uses the UNESCO-method (Fofonoff & Millard, 1983) as temperature relationship. The relationship is given in Figure 32.

Later on it has been checked whether the present data are consistent with these transformations from conductivity to salinity.

4.5 PocketBox-sensors

The PocketBox contains a couple of sensors, an overview of the variables recorded has already been presented in Table 7. Here, the several sensors are briefly explained.

4.5.1 Temperature

Temperature is measured by several sensors. One is separately mounted in the PocketBox, a second sensor is combined with the Optode-oxygen sensor. The type of sensors is not specified in the manual.

4.5.2 Conductivity

Conductivity is measured by an AADI 3919A 1W inductive conductivity sensor, ranging 0-75 mS cm^{-1} (AANDERAA, Norway; http://www.aadi.no). See also section 4.4.3.

4.5.3 Oxygen

Oxygen is measured through an AADI 3835 optode sensor (optical fluorescence quenching technique, see e.g. http://en.wikipedia.org/wiki/Optode), ranging from 0-500 µmol O2 l^{-1} ≈ 16 mg O_2 l^{-1}). Manufactured by AANDERAA, Norway (http://www.aadi.no).

The Hach-handheld (see above, section 4.4.2) meter delivers a value in mg O_2 l^{-1}. Since the molar mass of oxygen is 32, the relationship between optode values and Hach-handheld values should be:

$$O_2\ (\mu mol\ l^{-1}) = 31.25 * O_2\ (mg\ l^{-1}) \qquad (2a)$$

or

$$O_2\ (mg\ l^{-1}) = 3.20\ 10^{-2} * O_2(\mu mol\ l^{-1}) \qquad (2b)$$

The optode produces uncorrected values (O_2, µmol l^{-1}) and salinity & temperature-corrected values (ST Corr Oxygen, µmol l^{-1}). The optode contains its own temperature sensor. According to the manual[1], the correction is as follows:

$$\text{ST Corr Oxygen} = O2 * exp(salinity \cdot B + C_0 \cdot salinity^2) \qquad (2c)$$

with:

[1] The manual contains an error in equation 1d, where the whole right-hand term is multiplied with salinity; this product also appears in 1c.

$$B = b_0 + b_1 \cdot t_s + b_2 \cdot t_s^2 + b_3 \cdot t_s^3 \quad (2d)$$

and

$$t_s = ln(\frac{(298.15-T)}{(273.15+T)}) \quad (2e)$$

T = water temperature (°C), salinity= salinity (PSU).

The constants used are:
b_0 = -0.00624097
b_1 = -0.00693498
b_2 = -0.00690358
b_3 = -0.00429155
C_0 = -3.11680E-7

Data were stored in several ways (as for most PocketBox-data): reading values from the display/screen during each stop (done once every stop), and as average value based on the continuously stored values during the stop. The latter procedure has been explained above (section" Computing average values for each stop; detection of outliers"). Since it has been observed (previous section) that the temperature as measured by the optode was incorrect (especially at low values), it may be expected that the subsequently computed oxygen values are incorrect as well.

Note: it appeared that the temperature sensor of the optode give erroneous values (one or two degrees too low values). Consequently, one might expect incorrect final values for ST Corr Oxygen. This has been tested, but the error appeared to be minor. In Figure 33 it is explained why: the effect of temperature on the optode correction factor is relatively unimportant.

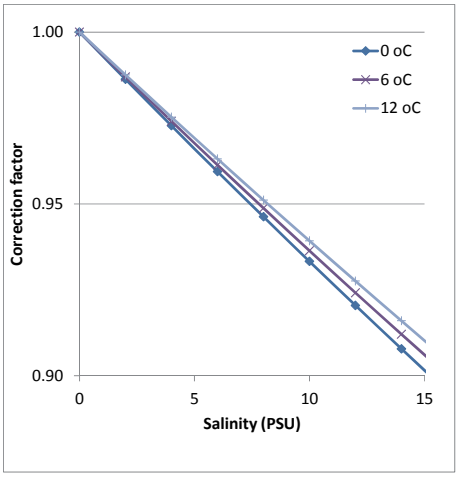

Figure 33 Optode signal correction factor as a fuctiob of salinity (PSU, X-axis) and temperature.

4.5.4 Coloured dissolved organic matter (CDOM) and Yellow Substances

CDOM

The PocketBox is equipped with a CYCLOPS-7 Submersible Fluorimeter (nr PN 21000-000), manufactured by Turner Designs California, USA. See http://www.turnerdesigns.com/applications/dom-fluorometer-application-notes.

Dissolved Organic Material (DOM) exists in many forms ranging from naturally occurring humic acids to by-products or secretions excreted from organisms. DOM is a highly abundant form of organic matter and represents a major reservoir of reactive carbon. It is also a dynamic substrate which can undergo reactions to become accessible to bacteria, plants, and animals as an energy source or it can photodegrade resulting in the production of volatile compounds that can have adverse effects on organisms and the environment. DOM typically contains chromophores that absorb UV and visible light, hence the term Chromophoric (or coloured) Dissolved Organic Materials (CDOM). CDOM will also fluoresce (hence the term FDOM) after light absorption allowing researchers a way to detect and quantify its abundance in water systems using fluorometry[2].

The CDOM-sensor has been calibrated by the manufacturer against Quinine Sulfate; values delivered in µg l^{-1}.

Yellow Substances

Yellow substances include humic and fulvic acid -like components. A Yellow Substance sensor is part of the AOA-equipment (= "Algae OnlineAnalyser", see below in section 4.5.8). It is also a fluorometric

[2] This coloured part of the text has been copied from the website

analysis and should cover more or less the same components as the CDOM-analyser does. Values also delivered in µg l^{-1}.

4.5.5 CYCLOPS-Chlorophyll-a

Next to coloured dissolved organic matter the CYCLOPS-7 Submersible Fluorometer also measures chlorophyll-a. It is a separate sensor in the PocketBox, measuring range 0-500 µg l^{-1}, lower detection limit 0.025 µg l^{-1}. *In vivo* calibrated using *Skeletonema costatum* monocultures. See also http://www.turnerdesigns.com/applications/dom-fluorometer-application-notes.

The Cyclops-sensor has been mounted as a back-up in case (one of the) the AOA-sensor(s) (section 4.5.8) failed.

4.5.6 C-Star light attenuation sensors

The PocketBox is equipped with two C-Star light attenuation sensors, manufactured by WETLabs, Oregon, USA (http://www.wetlabs.com). The basic principle is simple: a light source and a light detector at a certain distance; the light intensity loss depends on the light attenuation coefficient (see below, at equation 15). Initially a 25 cm light path sensor (C-Star-2) had been mounted, but soon it appeared that the water column, especially close to station 4-6, contained that much silt that the sensor's lower detection limit was reached. Next, a 10 cm light path sensor has been mounted (C-Star-1). The light source operates at 470, 530 and 650 nm wavelength.

Both sensors operate the same way.

The instruments deliver 'signal counts', where 'counts' is the digital equivalent to voltage output for analogue equipment. Data output is:

- Reference counts: signal strength in clean air
- Signal counts: signal strength of the captured light by the sensor
- Corrected signal raw counts:
- Calculated beam c (m^{-1}).

The instrument has some factory settings:

- A 'clean air output (CSC_{air})'. Comparing the corrected signal raw counts when the instrument is in clean air with this CSC_{air} is needed to check the instruments reliability.
- Signal counts for clean water: $CSC_{calibrated}$

The calibrated output of the instrument is an attenuation coefficient c (m^{-1}), which is computed following

$$c = -\frac{\ln(Tr)}{x} \qquad (m^{-1}) \qquad (3a)$$

with x as the length of the light path (m) and

$$Tr = \frac{CSC_{signal} - CSC_{dark}}{CSC_{calibrated} - CSC_{dark}} \qquad (-) \qquad (3b)$$

CSC_{dark} is the 'rest'-signal when the light pathway is blocked completely, CSC_{signal} is the actual signal, and $CSC_{calibrated}$ is the signal for clean water.

The actual signal (CSC_{sig}) is derived from the raw signal, corrected for temperature.

Thus, the c-value should be equal to the attenuation coefficient as measured with the light sensors during the stops at each monitoring site, but this appears not to be the case. The relationship between C and K_d has to be established, and used to compute K_d-values for all cruise positions from the C-values stored. This is evaluated in the next section.

4.5.7 Turbidity sensor

Turbidity is measured by a Seapoint sensor (Seapoint Sensors, Inc. Brentwood, New Hampshire, USA. http://www.seapoint.com), see http://www.seapoint.com/stm.htm.

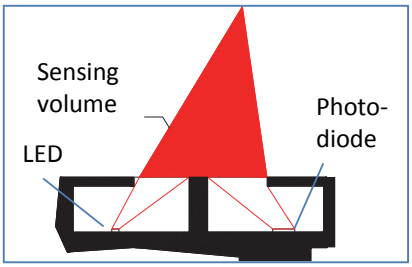

Figure 34 Seapoint FTU-sensor. Left is the LED-light source (880 nm), right the detector. The latter receives light scattered between 15-150 0. Drawing after Seapoint manual.

Operates with an 800 nm light source; the sensor is not placed opposite to the light source (as is the case with the C-Star attenuation sensors) but it receives scattered light (Figure 34). Output in FTU's (Formazin Turbidity Units, see http://en.wikipedia.org/wiki/Formazin_Turbidity_Unit#Measurement). Linear detection range 0-750 FTU, <5% deviation at 1600 FTU, maximum at 4000 FTU (with larger deviation from linearity).

4.5.8 The AOA-analyser (Algae Online Analyser)

The AOA-analyser (Algae Online Analyser) is provided by bbe Moldaenke, Germany (http://www.bbemoldaenke. de/chlorophyll/algaeonlineanalyser/). *These analyses are performed by measuring algae fluorescence via excitation by visible light. This excitation mainly depends on the chlorophyll-a, a common pigment in the plant world. The presence of other pigments indicates different algae classes. The interaction of these different pigments with chlorophyll-a results in a special excitation spectrum for taxonomic algae classes.*

The special patterns of this algal fluorescence - so-called fingerprints - are used in bbe fluorometers for the qualification of different algae classes. The light sources for the excitation are LEDs with selected wavelengths. The fingerprints of four algae classes and for yellow substances are predefined in the instrument. The physiological performance of the algae (algae activity) on photosynthesis is determined by excitation using additional background light. The resulting variable fluorescence allows the calculation of algae activity given as the Genty parameter. This Genty parameter represents the quantum yield and is also an expression of the vitality of the algae. [3]

Four algae types are distinguished: green algae, cyanobacteria (blue-greens), diatoms and cryptohycaea. All contents are expressed as µg chla l^{-1}; the sum is stored as total chla (µg chla l^{-1}).

[3] This coloured part of the text has been copied from the manual

4.6 Computation of phytoplankton carbon content from cell volume

4.6.1 General

The analyses by Koeman and Bijkerk on phytoplankton species (Wanink et al, 2014) composition also included biovolumes. These are given for each species, including the (average) volume for each species. For example, a large diatom like *Coscinodiscus radiates* is 200000 μm^3 cel^{-1}. A small species like *Delphineis minutissima* is only 27 μm^3 cel^{-1}. Supposed a spherical shape, 20 μm^3 cel^{-1} implies a 3.3 µm diameter, 200000 μm^3 cel^{-1} implies a 72 µm diameter. Smallest algae have not been identified on a species level, but were grouped ("Eukaryota < 3 µm", etc.).

4.6.2 From volume to organic-C content

Computing the C-content of an organism based on its volume can be done in two ways:

1- estimate the percentage of water, and use a standard formula to convert organic matter into organic-C
2- use standard formula that convert algal cell volumes into organic-C. This last implicitly contains an estimate of cell water content.

Both computations depend on the algae species. Diatoms have a silica skeleton, which is partly organic, but mostly SiO_2. Most important organic components in cell frustules are polysaccharides (Darley; in Werner, 1977). Thus, these frustules do not (-or hardly-) contribute to the organic C-content. Some of the *dinoflaggellates* have cellulose theca serving as armour.

For, all algae, the organic-C content can be computed following

$$Organic\_C = \alpha \cdot Plasma\ volume \qquad \text{(pg)} \qquad \text{(4a)}$$

With the plasma volume in μm^3; α=0.13 for thecate dinoflagellates and 0.11 for all other algae (comm R. Bijkerk).

For non-diatoms, the plasma volume is the same as the cell volume.

Diatoms have vacuoles, which mainly serve to regulate buoyancy since the specific mass of the silica frustules exceeds that of water. The plasma volume of diatoms follows from

$$Plasma\ volume = Cell\ volume - 0.9\ Vacuole\ volume$$

and the volume of the vacuoles has to be computed for each diatom species. This volume is estimated assuming a cytoplasm thickness of 1 µm. If the cell were spherical, with a volume V, the radius R would be

$$R = \left(\frac{3}{4\pi}\ V\right)^{1/3} \qquad \text{(µm)} \qquad \text{(4b)}$$

and the radius R_v of the vacuole

$$R_v = R - T_c \qquad \text{(µm)} \qquad \text{(4c)}$$

where T_c is the thickness of the cytoplasm, which is about 1.0 µm (pers comm R Bijkerk). That implies for the vacuole volume V_v

$$V_v = \frac{4}{3}\pi R_v^3 \qquad (\mu m^3) \qquad (4d)$$

and thus for the cytoplasm volume V_c

$$V_c = V - V_v \qquad (\mu m^3) \qquad (4e)$$

Diatoms appear in a large variety of shapes. They are either pennate (pen-like) or centric diatoms (disc-like). For a long, thin pennate diatom the result will be quite different than for a centric diatom. In both cases, the vacuole volume is relatively higher than for a spherical cell.

Also, according to these equations, the vacuole volume is relatively large for large cells, compared to small cells. This is also mentioned by Darley (1977) and (Werner, 1971).

The difficulty is that almost all shapes can be found in marine nature. Also, diatoms become smaller with each cell division (because the hypotheca ánd epitheca become both the new epitheca, and new hypotheca are formed) until they reach a minimum size and start to reproduce sexually.

The results of Koeman and Bijkerk mention the (mean individual) cell volume, and for a number of groups/species a distinction has been made between smaller and larger cells of the same species.

The shape of the cells were checked in a couple of databases:

http://nordicmicroalgae.org/

http://eol.org

http://www.algaebase.org

iatoms.lifedesks.org

Especially http://nordicmicroalgae.org/ comes with an estimate of the cell C-content, that depends on the diatom size and shape.

Thus, for all diatom species and groups mentioned by Koeman & Bijkerk, this information has been gathered, and implemented as good as possible in the equations 4a-4e. The information of C-content of diatoms as given by the databases and the results of the equations 4a-4e were compared, and in case deviations were considerable, an average value has been used.

Thus, individual organic-C content times the number of cells per unit of volume gives the total organic-C content of the water at each station and at each sampling day.

4.7 Chlorophyll-a, phytoplankton and microphytobenthos

4.7.1 Handling and analyses

Chlorophyll-determinations were performed in water samples (1), sediment samples (2), and sediment samples (3) that were used to measure the ^{14}C-uptake (determination of the primary production PI-curves). (2) was done by spectrophotometry, (1) and (3) by fluorometry.

Some of the samples were analysed using a HPLC-technique.

The PocketBox also measures chlorophyll, by an automated pigment analysis (AOA = “Algae OnlineAnalyser”, see above, section 4.5.8).

4.7.1.1 Handling water samples

Depending on the station, between 400 and 50 ml of the water samples taken (see above) was filtrated over a GF/F filter (effective pore size 0.7µm). Samples were taken in duplicate. Filters were wrapped in labelled aluminium foil and kept between -20 and -80°C until further processing.

Acetone (90%) was added to the filters to extract phytoplankton pigments. Phytoplankton cells on filters were destroyed (CO_2 cooled homogeniser with glass beads) to facilitate extraction. Samples were centrifuged and supernatant was analysed using a PAM (Pulse Amplitude Modulation) fluorescence meter.

4.7.1.2 Handling sediment samples for ^{14}C incubation experiments

In all samples used for the ^{14}C-incubation, also chlorophyll-a content has been determined, simply because it is necessary to know the amount of photoactive matter in the ^{14}C-analyses. The chlorophyll-a data in the ^{14}C-incubations and those measured in the field are needed to convert the ^{14}C-incubation results to field values for benthic primary production.

From the 1000 ml dispersion (if needed, diluted; see the description for the ^{14}C-analyses), about 150 ml is filtered (over a GF-F glassfiber filter, effective pore diameter about 0.7 µm). This filter is extracted in 20 ml acetone. If needed, the acetone extract is diluted. Finally, [chla] is determined. All fluorometric measurements are corrected for the blanks (acetone). Chlorophyll-a determinations in these “^{14}C-samples” were performed by fluorescence analysis; the analyses are always calibrated against dilution series of known chlorophyll-a stock solutions; these stock solutions are checked using a spectrophotometric analysis.

4.7.1.3 Handling sediment samples for determination chlorophyll-a content of the sediment

The sediment samples were taken, handled and filtered as described above. The freeze-dried filters are mixed with 20 ml 90% acetone and centrifuged for 15-30 min at 0 °C. Afterwards, the absorption of the supernatant (and a blank) is measured in a spectrophotometer at 480, 665 and 750 nm. After addition of 0.2 ml 1 N HCl absorption again is measured at 665 and 750 nm.

4.7.1.4 Fluorometric analysis

After handling (see above), the supernatant was analysed on a fluorescence meter to calculate chlorophyll-a concentration. Chlorophyll-a from spinach (Sigma) was used a reference. The method is described in more detail in Holm-Hansen (1965).

4.7.1.5 Spectrophotometric analysis

Sample preparation was similar to the one for the fluorometer analyses. However, the spectrophotometric procedure gives absorption values; the computation method is given in the next section.

4.7.1.6 Chlorophyll HPLC analysis

In order to check the analysis, a number of samples was analysed with a HPLC (High Performance Liquid Chromatography) by the Danish Water Quality Institute (WQI). With the HPLC-analysis, separate chlorophyll (a,b,c,..) are distinguished.

The filters[4] were transferred to vials with 6.00 mL 95% acetone with internal standard (vitamin E). The samples were mixed on a vortex mixer, sonicated on ice, extracted at 4°C for 20 h, and mixed again. The samples were then filtered through 0.2 µm Teflon syringe filter into HPLC vials, and placed in the cooling rack of the HPLC. 357 µl buffer and 143 µl extract were injected on the HPLC (Shimadzu LC-10A HPLC system with LC Solution software) using a pre-treatment program to mix in the loop before injection. The HPLC method used was the HPL method (Van Heukelem & Thomas, 2005 *in:* Hooker et al., 2005, NASA Technical Memorandum). Internal method No.: SF No.: 30/852:02.

In the analyses: α-carotene co-elutes partly with β-carotene and chlorophyll c1 co-elutes partly with chlorophyll c2, but the pigments were separated using the software of the HPLC. Chlorophyll c1 was calculated by the response factor of chlorophyll c2 (no standard for this pigment).

4.7.1.7 Chlorophyll standards

From a known, pure chlorophyll-a concentration (Sigma) a dilution series is prepared. As a blank, 90% acetone is used. For the dilution series the fluorescence is measured on the PAM and after measuring the fluorescence the series is acidified with an overdose of HCl (1-1.2N) and the fluorescence is measured again. All chlorophyll-a is transformed into pheophytin by this acidification.

Based on the fluorescence data a linear graph can be made for both the values before and after acidification. Regression coefficients for both of these lines are stored.

4.7.1.8 Phytoplankton counts

A couple of samples has been analysed on a species level by Koeman & Bijkerk (Groningen, http://www.koemanenbijkerk.nl/). Their results are reported separately (Wanink et al, 2014).

4.7.2 Spectrophotometric computation (determining benthic chlorophyll-a samples)

The absorption of a sample, (and a blank) is measured in a spectrophotometer at 480, 665 and 750 nm. After addition of 0.2 ml 1 N HCl absorption again is measured at 665 and 750 nm. Chlorophyll-a content in the acetone is computed after Lorenzen (1965):

[4] This paragraph originates from DHI, see appendix A2.

$$Chla = \frac{A \cdot K \cdot ((abs_{665} - abs_{750})_0 - (abs_{665} - abs_{750})_a)}{l} \quad (\mu g\ dm^{-3}) \quad (5a)$$

with

A	absorption coefficient of chlorophyll a = 11000 (mg m^{-3} cm)
K	factor to equate the reduction in absorbency to initial chlorophyll concentration (= 2.43). [Note: A*K= 267 (mg m^{-3} m)]
abs_{665}	absorbance at 665 nm
abs_{750}	absorbance at 750 nm
subscript 0	before acidification
subscript a	after acidification
l	cuvette length (m)

The difference between the absorbance at 665 and 760 nm is taken to correct for the contribution of pheophytin to the absorption. Note that Lorenzen gives a factor 11.0 for A, but without mentioning the units. There is a problem with many formula used in literature, when they deal with an absorption as result of the measurement, and translate it directly into an end value (mg chla m^{-3}). In most cases, the absorption coefficient used is not well recognized. For example, Lorenzen gives A=11.0, but this is only valid if l is in cm, and the ratio between extraction volume (in ml) and extracted volume (in l) is used as multiplier. Then the result is in mg chla m^{-3} of the original fluid. The absorption coefficient A thus has a strange unit (mg m^{-3} dm^3 ml^{-1} cm), which can be simplified to (mg m^{-3} dm^3 dm^{-3} cm = mg m^{-3} cm) if A is multiplied by 1000 and the volume of the extraction volume is in dm^3 instead of ml.

The amount of chlorophyll-a in the sample (20 ml acetone) is

$Amount_{chla}$ = 20 10^{-3} * [chla] (as measured in the cuvette, µg dm^{-3}) (µg chla) (5b)

Thus, the filters are supposed to contain all the chlorophyll-a that originally was in the five 0.5 cm thick and 530 mm^2 area samples, together 2650 mm^3 (or 2.65 10^{-3} dm^3). The density in the sediment thus is

$Density_{chla}$ = $Amount_{chla}$ / (530 10^{-6}) (mg m^{-2}) (5c)

The similar formula is used to compute the pheophytin content (Pheo, µg dm^{-3} in the cuvette), now with an extra constant R that gives the maximum ratio of $(abs_{665}\text{-}abs_{750})_0$ / $(abs_{665}\text{-}abs_{750})_a$

$$Pheo = \frac{A \cdot K \cdot (R \cdot (abs_{665} - abs_{750})_a - (abs_{665} - abs_{750})_0)}{l} \quad (\mu g\ dm^{-3}) \quad (5d)$$

Thus, the computation of pheophytin and chlorophyll-a is based on the same data. If e.g. the pheophytin-value is erroneously low, then the value for chlorophyll-a will be too high, and vice versa.

Finally some negative values for pheophytin remained, but these were close to zero, and had little effect on chlorophyll-a data.

4.7.3 Calculation of chlorophyll-a content in the sediment

The concentration of both chlorophyll-a and pheophytin in the sample is calculated in µg l^{-1} (acetone).

The amount of chla per extraction volume ($chla_{extr}$) now is

$$chla_{extr} = [chla] \cdot dilution \cdot extraction\ volume \quad (\mu g\ chla) \quad (6)$$

with *dilution* as the dilution factor of the acetone extract. The concentration of chla in the sample (chla_sample) is

$$chla_{sample} = \frac{chla_{extr}\ (\mu g)}{sampleVol\ (l)} \quad (\mu g\ chla\ l^{-1}\ (sample)\ ) \quad (7)$$

With sampleVol as the volume (l) of the sample that is filtered and extracted.

The amount of sediment that was dispersed in 1l seawater is known, as is the area of those samples. Thus, the quotient $chla_{sample}$ / (total area of sampled sediment , cm^2) gives the chla-content of the sediment in µg cm^{-2}; $*10^4/1000$ converts it to mg chla m^{-2} sediment.

4.7.4 Fluorescence computation (pelagic chlorophyll-a and all ^{14}C-samples)

The fluorescence of a sample comes from the concentration of chl-a and the concentration of pheophytin, [chla] and [pheo] respectively. The fluorescence of each concentration is described by the regression coefficients of the calibration graphs; with chla having a higher specific fluorescence compared to pheo. The regression slopes are rc_{chla} and rc_{pheo}, respectively.

The fluorescence of a sample can thus be described by equation (7a)

$$Fl = rc_{chla} \cdot [chla] + rc_{pheo} \cdot [pheo] \quad (8a)$$

which can be re-written to:

$$rc_{pheo} \cdot [pheo] = Fl - rc_{chla} \cdot [chla] \quad (8b)$$

After acidification with HCl, all chlorophyll is transformed into pheophytin. The fluorescence after acidification (Fl_{HCl}) depends on the fluorescence of the already present concentration of pheophytin (rc_{pheo} * [pheo]) as well the previous concentration of chlorophyll. Because 1 gram of pheophytin has a lower molecular mass than chlorophyll (the Mg-atom in chlorophyll-a is replaced by two protons), we need to correct for this loss in weight (RM, ratio molecular mass, RM=0.97). This gives a second equation:

$$Fl_{HCl} = rc_{pheo} \cdot ([pheo] + [chla] \cdot RM) \quad (8c)$$

or

$$Fl_{HCl} = rc_{pheo} \cdot [pheo] + rc_{pheo} \cdot [chla] \cdot RM) \quad (8d)$$

Substitute 7b into 8b:

$$\mathrm{Fl_{HCl}} = \mathrm{Fl} - \mathrm{rc}_{chla} \cdot [\mathrm{chla}] + \mathrm{rc_{pheo}} \cdot [\mathrm{chla}] \cdot \mathrm{RM}) \quad (9a)$$

$$\mathrm{Fl_{HCl}} - \mathrm{Fl} = [\mathrm{chla}] \cdot (\mathrm{rc_{pheo}} \cdot \mathrm{RM} - \mathrm{rc}_{chla} \cdot) \quad (9b)$$

and thus:

$$[\mathrm{chla}] = \frac{\mathrm{Fl} - \mathrm{Fl_{HCl}}}{\mathrm{rc}_{chla} - \mathrm{rc_{pheo}} \cdot \mathrm{RM}} \quad (\mu g\ chla/l\ acetone) \quad (9c)$$

Note that Fl and Fl_{HCl} are reversed to get positive values in nominator and denominator.

For [pheo] we can re-write equation 8a:

$$[\mathrm{pheo}] = \frac{\mathrm{Fl} - \mathrm{rc}_{chla} \cdot [\mathrm{chla}]}{\mathrm{rc_{pheo}}} \quad (\mu g\ pheo/l\ acetone) \quad (9d)$$

The equations above can now be used in determining the [chla] and [pheo] in each sample.

Both the rc_{chla} and the rc_{pheo} are determined every time that new standard chlorophyll-a was used (about once a year).

For the benthic samples in 2013: rc_{chla}= 44.26 (fluorescence units (µg chla $l^{-1})^{-1}$; rc_{pheo}= 14.88 (fluorescence units (µg pheo $l^{-1})^{-1}$). RM= molecular mass pheo/ molecular mass chla, which is 869.20 g mol^{-1} pheo/893.51g mol^{-1} chla = 0.97.

4.7.5 Chlorophyll computation from phytoplankton cell carbon and numbers

In section 4.5.2 is was explained how cell volumes give an estimate for organic C content of the cells. For diatoms, the vacuole volume is relevant, for non-diatoms the plasma volume equals the cell volume.

From this, chlorophyll-a content has been estimated using conversion factors from organic C-> chlorophyll-a content.

First, the ratio dry mass: plasma volume (δ) for most phytoplankton is about 0.27 (see section 4.6.2):

$$DM = \partial \cdot Plasma\ volume \quad (mg\ l^{-1}) \quad (10a)$$

with plasma volume in ml l^{-1}, dry mass (DM) in mg l^{-1} and δ =0.27 as an approximation. Next, organic C is about 38% of total organic matter (by mass, as a consequence of a general stoichiometric formula for phytoplankton organic matter $C_{150}H_{211}O_{70}N_{30}P$, as used in the EcoWasp-model (Brinkman, 2013)):

$$orgC = \gamma\ DM \quad (gC\ g^{-1}\ DM) \quad (10b)$$

with γ = 0.38 as C:DM-ratio used.

Then, chlorophyll can be computed for orgC with

$$Chla = \beta\ OrgC_{phyto} \quad (\mu g\ l^{-1}) \quad (10c)$$

with $OrgC_{phyto}$ is the organic C content of the water (mg orgC l^{-1}), and

β is the proportionality constant (µg chla mg^{-1} orgC).

C/Chl-a ratios reported are usually in the range of 20-60 (mg C mg^{-1} chla) (Eppley et al, 1977), although much wider ranges were reported (see e.g De Jonge, 1980). After Steele & Baird (1965), Kirk (1994) mentions a C:chla ratio of 20:1 in spring (when nutrients are not depleted) down to 100:1 in late summer. Riegman et al (1993) gave a ratio 20:1.

The dry mass: chla ratio always is a factor 2.6 higher (since about 38% (γ) of biomass is C). Thus, β may range from 16-50 µg chla mg^{-1} orgC. For γ*β the ranges becomes 6- 20. A rather common estimate is 10 µg chla mg^{-1} DM (1% of dry mass is chlorophyll, with β= 26.3 (µg chla mg^{-1} orgC)). Kirk (1994) mentions chlorophyll/dry biomass ratios varying from 0.09-1.5%.

Another approximation is one by R Bijkerk (pers. comm.):

$$log\ [Chla] = 0.825 + 0.679\ log\ [Cell\ volume] \qquad (-) \qquad (10d)$$

with Chla in µg l^{-1} and Cell volume in mm^3 l^{-1}.

Both approaches give different result for low and high biovolumes (Figure 35).

The difference is largest at very low and at very high biovolumes. Several argumentations may be valid:

- at high biomass levels, phytoplankton needs to increase its light capture capabilities , and thus: chlorophyll-a content will *increase* relatively with biomass
- at high biomass levels, phytoplankton may suffer from nutrient limitation (especially N), resulting in a *decrease* of chlorophyll-content.

For the present situation, the linear relationship is applied.

4.7.6 Measuring benthic algal groups

Benthic algal groups were measured by the so-called 'BenthoTorch'. The 'BenthoTorch' is also provided by bbe Moldaenke, Germany, and is based on the same principle as the AOA-chlorophyll-a analyser.

The bbe BenthoTorch uses the in vivo fluorescence of algal cells: the cell pigments are excited by LEDs of different colours (wavelengths) and emit red fluorescence light as a natural phenomenon with high sensitivity. The intensity of the chlorophyll fluorescence is used to calculate the different algae as chlorophyll-a, namely green algae, blue-green algae (cyanobacteria) and diatoms; plus total chlorophyll-a.

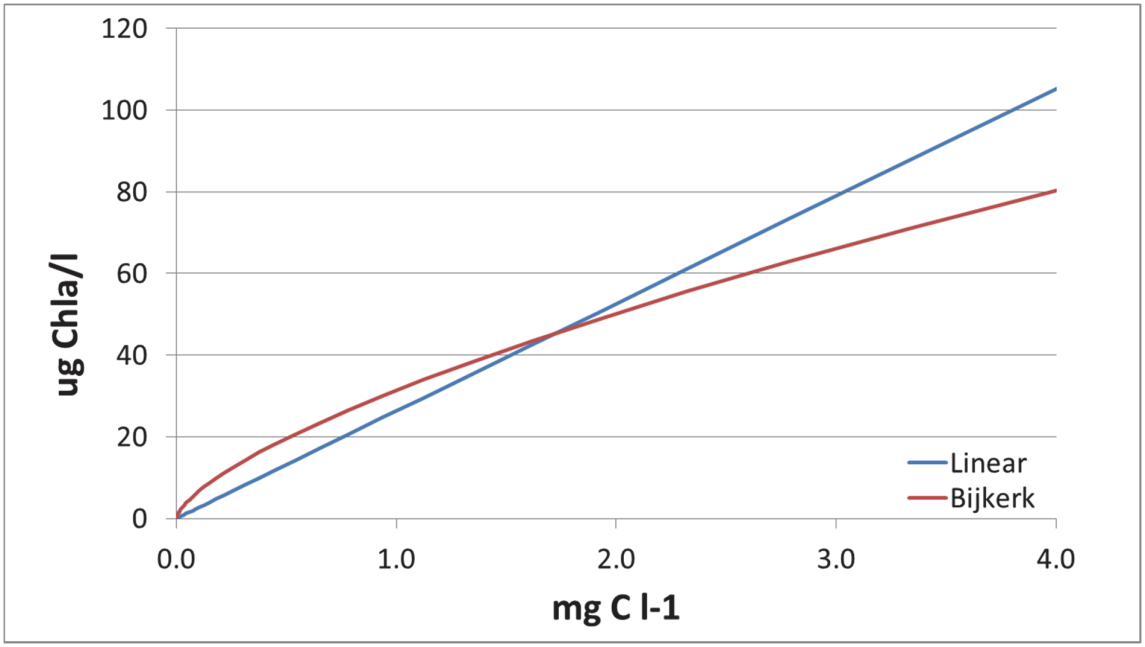

Figure 35 Estimates for chlorophyll-a content based on organic carbon concentration in the water, as computed following the equation by Bijkerk and according to a linear relationship as mentioned in this section.

First, the idea was that the Benthotorch data could be used after calibration against the chlorophyll-a data that become available from direct spectrophotometric measurements as described in the previous section. The instrument thus merely provides us with the distribution of algae, rather than exact concentrations or densities.

However, finally the spectrophotometric results were validated against these Benthotorch data. Details on algal composition have not been used.

4.8 Carotenoid-chlorophyll adsorption ratio: growth limitation

For every sample, the ratio of light absorption at 480 nm and at 665 nm has been measured. At 480 nm, typically the amount of phytoplankton carotenoid is measured, whilst absorption at 665 nm indicates the amount of chlorophyll-a (Riegman & Rowe, 1994). Carotenoids mainly serve as protection against radiation overdoses. Fucoxanthin for example is the most important carotenoid pigment in diatoms and dinoflagellates. Thus, a high value for this ration would indicate too much light, and a low value indicates that protection against high radiation values is not needed, and it thus can be expected that light may be limiting primary production. Riegman & Rowe found that this absorption ratio did not completely depend on fucoxanthin and chlorophyll-a alone, and they suggested that also the presence of chlorophyll-c3 (present in e.g. *Prymnsiophycaea*) affects this ratio. Absorptions at 480 and at 665 nm were corrected by the absorption at 750 nm, thus correcting for background absorption. Thus, the ratio found is calculated according to

$$\text{Absorption ratio} = \frac{\text{abs}_{480}\text{-abs}_{750}}{\text{abs}_{665}\text{-abs}_{750}} \quad (-) \qquad (11)$$

For a complete description of the analysis procedure, see Riegman & Rowe (1994).

4.9 Dissolved inorganic carbon concentration in the seawater

The amount of dissolved inorganic carbon in the filtered seawater is measured with an acid titration (Figure 36), until all charged carbonate is neutralized.

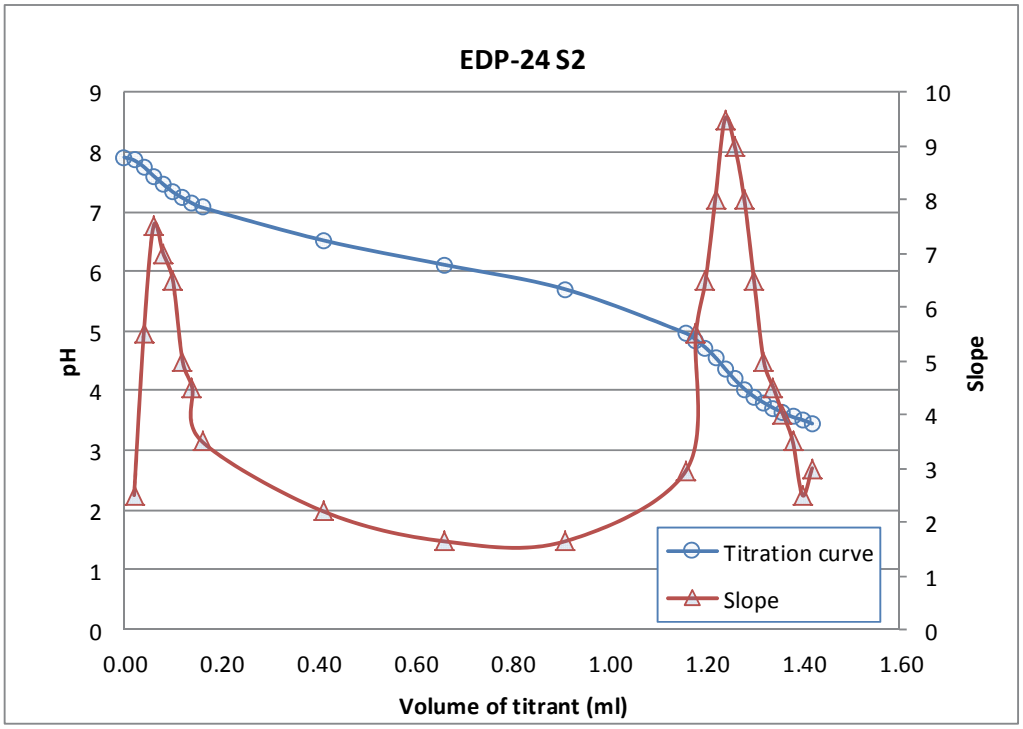

Figure 36 Example of an acid titration: the amount of acid needed to remove all HCO_3^- from the solution. Given the initial pH the total amount of dissolved inorganic carbon (= CO_3^{2-} + HCO_3^- + H_2CO_3) is known.

The initial pH is needed to compute the amount of H_2CO_3 in the solution; also the ionic strength is needed since the pH depends on the ration of the *activity* of HCO_3^- , H^+ and H_2CO_3, rather than the concentrations. The reaction is

$$HCO_3^- + H^+ = H_2CO_3 \qquad (12a)$$

And thus, pH (=- log $\{H^+\}$) follows from

$$\{H^+\} = \frac{\{H_2CO_3\}}{\{HCO_3^-\}} \qquad (13a)$$

or

$$[H^+] \cdot a_{H+} = \frac{[H_2CO_3]}{[HCO_3^-] \cdot a_{HCO_3^-}} \quad (13b)$$

With a_{H+} and a_{HCO32-} as the activity coefficients of the proton and of the bicarbonate ion (the one for H_2CO_3 = 1). These two values largely depend on the ionic strength of the solution.

However, at the normal pH-values, the amount of H^+ and of H_2CO_3 is minor (less the 0.1‰ of the bicarbonate concentration), and results therefore hardly depend on the ionic strength. The amount of dissolved carbon dioxide in the water (mol l^{-1}) is the same as the alkalinity (moleq l^{-1}). The pH is now only used to determine the endpoint of the titration.

4.10 Flow cytometer measurements

Phytoplankton cell counts were performed by means of flow cytometry (BD Accuri). Water subsamples (1 ml) were processed unfixed, immediately after collection. Fluorescence at wavelengths > 670 nm (FL3) was ascribed to chlorophyll. Forward scatter was used as an indication of cell size and based on the relative fluorescence to cell size, a distinction between phytoplankton and debris was made. Phytoplankton cell counts were further divided in two size classes (<3 µm: pico and >3-20 µm: nano) using 3 µm sized beads (spherotech, BD Accuri). Within the picophytoplankton, two distinct groups could be identified based on the presence ('picocyano') or absence ('other') of the pigment phycoerythrin (FL2: 585 nm).

For converting pico-and nanophytoplankton cells counts to carbon biomass spherical shapes were assumed. Conversion factors used were 1.07 x 10^{-7} µg C $µm^{-3}$ biovolume. Verity et al. (1992) give much higher values (up to 4.3 10^{-7} µg C $µm^{-3}$), but that must have been caused by water losses at algae cell preservation. The considerations from section 4.3.2 support a value of 1.03 x 10^{-7} µg C $µm^{-3}$ biovolume; Verity's value must be seen as unrealistic. To convert to chlorophyll-a content, a fixed conversion factor is used. See section 4.6.2 and 4.7.5.

Figure 37 BD Accuri flow cytometer

4.11 Measuring ^{14}C-uptake

Primary production was measured with the ^{14}C technique. Photosynthesis response curves were constructed from radioactive bicarbonate uptake during 2 hour incubations in a series of light intensities, ranging from 0 to 1400 µE m^{-2} s^{-1} (conform with Colijn 1983; Riegman et al. 1990; Riegman and Colijn 1991). This provides information on the maximum photosynthesis rate, light affinity and the photo-inhibition constant.

Notes:

In 2012 incubator light intensity was about 900 µE m^{-2} s^{-1}. Between two incubator flasks, a grey-filter was placed to reduce radiation from flask x to x+1. In the course of 2012, we have begun to measure light intensity inside each flask; these data were used to correct the computed values. This was continued in 2013.

From the water sample (benthic samples: from the 1 l diluted suspension) 50 ml is taken for each ^{14}C-tube; 8 tubes in total, to be incubated under varying light intensities; these vary from very high (> 1000 µE m^{-2} s^{-1}) to darkness. 80 µl ^{14}C-bicarbonate solution is added. The activity is measured as DPM (disintegrations per minute); this is known at the beginning of the incubation. Afterwards, the solution is filtered and the activity of the filtrate is measured. The ration gives the part of the labelled carbonate taken up by the algae. The original bicarbonate concentration is also known (see below), and thus, the amount of carbonate taken up (labelled plus not-labelled) during the experiment is known. The result is expressed as mg C l^{-1} h^{-1}. Since the chlorophyll-content is known, the activity as mg C (µg Chla)$^{-1}$ h^{-1} is known as well. These values are used to construct the PI (production vs irradiation)-curves. These curves are analysed as described in the next section.

4.12 Eilers-Peeters parameters

4.12.1 Computing the parameters

The primary production data in the water samples as a function of light intensity (the PI-curve) make it possible to find the a,b and c-parameters in the Eilers-Peeters primary production function (see separate appendix). This function describes primary production as a function of light intensity:

$$PP = \frac{I}{aI^2+bI+c} \qquad \text{(mg C (µg chla)}^{-1}\ \text{h}^{-1}\text{)} \qquad (14)$$

Data are available as tables as shown in Table 13, results are stored as table (a, b, and c-values, and as figures, e.g. Figure 38.

Thus, for each site and for each date, PI-curves (as a,b, and c-values) are available.

Fitting the curve to the data occurs using the NLS-routine (Non-linear least squares) from R, by Douglas Bates and Saikat De Roy (Bates & Chambers, 1992).

From the result, a maximum photosynthetic production rate P_{max} is computed (the maximum value in Figure 38, mg C mg^{-1} chla h^{-1}), and the slope α of the curve at I=0 (mg C mg^{-1} chla h^{-1} (µE m^{-2} s^{-1})$^{-1}$; α

equals 1/c) .Finally, the ratio P_{max} * α ((mg C mg^{-1} chla $h^{-1})^2$ (µE m^{-2} $s^{-1})^{-1}$) is used check the combination of a high possible production rate and an algae community growth sensitive to light.

Table 13 Production-Light data for station 2, the first sampling cruise (at day 47 in 2013)

Light uEm-2s-1	Production mgC.ug $chla^{-1}.h^{-1}$	Site and code	Date	Day number
720.3	0.6	521	2012-12-11	346
354.4	1.1	521	2012-12-11	346
102.7	1.1	521	2012-12-11	346
50.3	0.8	521	2012-12-11	346
25.7	0.5	521	2012-12-11	346
13.6	0.2	521	2012-12-11	346
7.4	0.1	521	2012-12-11	346
0.0	0.0	521	2012-12-11	346

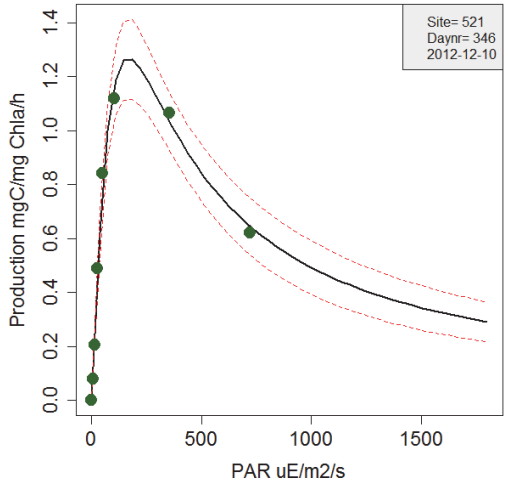

Figure 38 Production-Light curves for the data set from Table 13.

4.12.2 Further analysis of the Eilers-Peeters parameters

From these data, the maximum specific production rate (P_{max_spec}) has been found by multiplying Pmax (mg C mg^{-1} chla h^{-1}) with 24 (to convert to mg C mg^{-1} chla day^{-1}) and with the chlorophyll-a concentration found, and dividing this value by the phytoplankton C-concentration in the water. The best name for this variable is *first order gross ^{14}C uptake rate constant*, unit is d^{-1}.

The chlorophyll-a concentration may come from several sources (PocketBox (section 4.5.8), estimation after algae volume analyses (Koeman & Bijkerk, see section 4.6.1.8 and 4.6.5) and from fluorimeter analyses in the lab (section 4.6.1.4). Phytoplankton-C concentrations come from a conversion from the algae volumes (in 2013, see section 4.8) or from a simple conversion from chlorophyll-a to C (Figure 35).

Finally, since P_{max_spec} depends on temperature, a temperature correction is applied, using a rather commonly used formula by Eppley (1972):

$$P_{max\_spec(Tcorr)} = P_{max\_spec} / F(Temp) \quad (d^{-1}) \quad (14a)$$

with

$$F(Temp) = 0.59\, exp(0.0633 \cdot Temp) \quad (-) \quad (14b)$$

Bissinger et al (2008) came up with an 'improved' equation, but the sole difference was that their F(temp) was a factor 1.37 higher than the Eppley values.

4.12.3 The link with the primary production model

The parameters found here (the Eiler-Peeters parameters a, b and c) should go into the primary production model. In appendix A1.5 it is explained that any Monod-type equation fails to describe phytoplankton growth as a function of light intensity. An alternative might be a Smith-like equation, because of the quadratic terms in that equation; but then, as with a Monod-type equation, any light saturation effect cannot be covered.

4.13 Light penetration in the water column

At each sampling site, an underwater light profile was recorded. By slowly lowering a LICOR sensor

Figure 39 The LICOR light sensor that was lowered under water to construct a light attenuation profile under water at each sampling station. A similar sensor was kept on deck to store actual incident radiation.

under water, light at different depths has been measured (Figure 39), while an above water level sensor measures the actual light level just above the surface.

The global radiation (I_0, W m^{-2}) penetrates into the water column and intensities (I_z) decrease with depth (z) according to Lambert-Beer's equation

$$I_z = I_0 \exp(-k_d\, z) \qquad (W\ m^{-2}) \qquad (15)$$

From these measurements the light extinction coefficient (k_d, m^{-1}) was calculated.

There are two possible methods to estimate k_d. The first one is after logarithmic transformation of the data:

$$\ln\left(\frac{I_z}{I_0}\right) = -\,k_d\, z \qquad (16)$$

Such a transformation is valid if the *relative* error for the measurements (I_z) is constant for the whole z-range; in that case the absolute error in $\ln(I_z/I_0)$ is more or less constant for the whole z-range, and the minimum of LSQ

$$LSQ = \sum_{z=0}^{z=H}\left(\ln\left(\frac{I_z}{I_0}\right) - \ln\left(\frac{\hat{I}_z}{I_0}\right)\right)^2 \qquad (17)$$

has to be found. H is the depth of the water column. In eq.17 , $\hat{I}_z$ is the predicted value of the light intensity at each depth z, based on the estimated k_d-value, and I_z is the measured value.

However, it appeared that especially at larger z-values light intensities dropped below the sensors lower light sensitivity, and then the ratio I_z/I_0 becomes more or less constant. The advantage of fitting a linear model then disappears, and necessary conditions for applying a log-transformation are not valid anymore. This is illustrated in Figure 40.

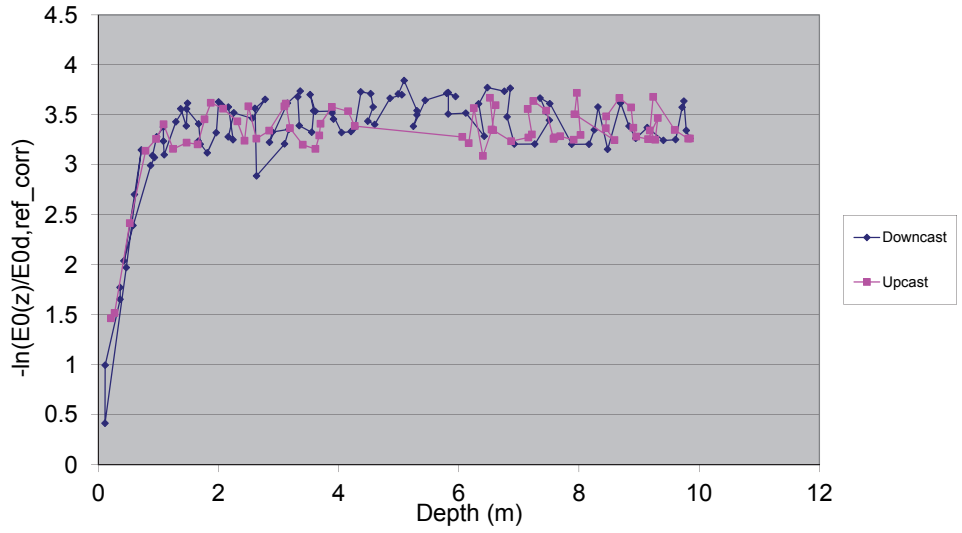

Figure 40 An extreme example (for station 1, at February 16th, 2012) of what happens after logarithmic transformation of the underwater light data. Downcast are data when lowering the sensor, upcast with decreasing depths. Only the very few data from the upper parts of the water column are useful.

A second possibility is to perform a non-linear analysis on the data (I_0 ~ z). In that case, the minimum of

$$LSQ = \sum_{z=0}^{z=H}\left(\hat{I}_z - I_z\right)^2 \quad (18)$$

has to be found. Again, $\hat{I}_z$ is the predicted light intensity value at each z, based on the estimate for k_d. Now, errors at high values of I_z (close to the surface) are crucial. Although the sensor values have the same absolute error (and thus, the necessary condition of normality of the residues for applying eq. 18 is met), large variations appear from time to time. These variations increase with increasing wave height: waves make that the sensor is not always at the same distance from the water surface, and also, light scattering affects the signal. In eq. 18 , the correct value of I_0 is important, more than it is in eq.17. Therefore, next to k_d, also β

$$I_z = (1-\beta)\cdot I_0 \exp(-k_d\, z) \quad (19)$$

is estimated. β accounts for (a) reflecting of solar radiation at the surface (usually about 5-10%, depending on the solar angle, or weather conditions (cloudy or clear sky, see e.g. Golterman, 1975) and (b) errors in the positioning of the water surface. If (b) is absent, β should have a value of about 0.1.

Estimation of k_d and β were performed using R (R 2013) and its NLS-routine (Bates & Chambers, 1992). Because of the sometimes large errors in the I_z-values for small z (close to the water surface), all analyses were performed including all measurements, but also after omitting the first 10 and 20 cm-values, respectively. Thus, for each data set, three values for k_d and β are obtained. If these values are not the same for all three data sets, an inspection 'by eye' was done and a 'best' value was selected. In that case mostly the shape of the curve or the characteristics of the measurements were taken into account. In Figure 41, an example is presented for the same site and day as in Figure 40.

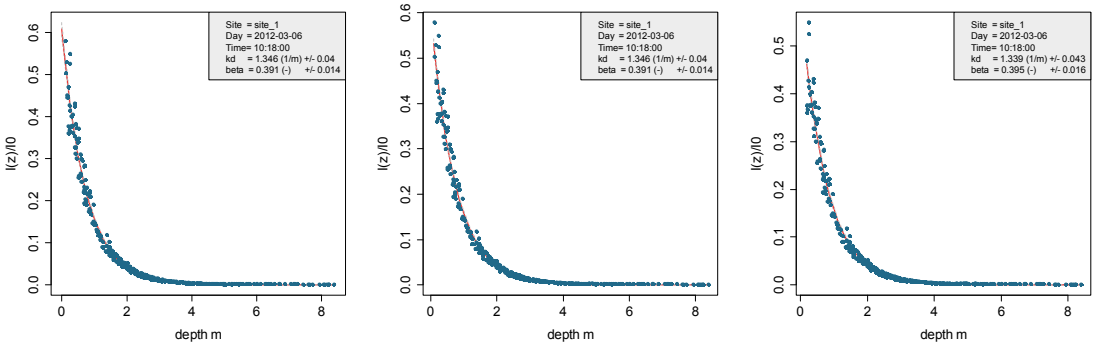

Figure 41 Data for the same station and sampling day as Figure 40, now results of the non-transformed analysis. Three possibilities were analysed: using al data (left figure), and omitting the above 10 resp. 20 cm of data (middle and right figures). Values for k_d here were 1.346 m^{-1} (left and middle) and 1.341 m^{-1} (right). A judgement 'by eye' one was not necessary. The β -value found was 0.395, indicating that the position of the sensors relative to the surface was not completely correct.

4.14 Light penetration in the sediment and sediment composition

4.14.1 General

The global radiation (I_0, W m^{-2}) penetrates into the sediment and intensities (I_z) decrease with depth (z) according to Lambert-Beer's equation

$$I_z = I_0 \exp(-k_d\, z) \qquad \text{(W m}^{-2}\text{)} \qquad (20)$$

The light attenuation coefficient (k_d, m^{-1}) is the crucial parameter here. In the water column, values of 1-10 are within the normal range, and are also measured during the two years Ems-Dollard research. Benthic values however have to be obtained from a) old values provided by Colijn (1983), b) literature, and c) extrapolations of pelagic values (k_d as a function of the silt content). In both cases, the local sediment composition (silt content, porosity) has to be taken into account.

As a first attempt, literature values can be used. Kühl et al (1994) give k_d=2.8-3.5 mm^{-1} (2800-3500 m^{-1}) for quartz sand particle sediment with grain size < 63 µm, and 1.6 mm^{-1} if grain size is about 125 µm. In their case, organic matter had been removed from the particles. They also showed that as a result of upwelling light (mainly scattering) radiation (named 'scalar' radiation) is up to 200% of the incident radiation. MacIntyre & Cullen (1995) give k_d=3.5-5.6 mm^{-1} for marine tidal sediments (in situ measurements), and Ihimi et al (2008) come up with values for tidal marine sediments of 8.1 mm^{-1} for 63-125 µm grain sizes (for grain sizes 63–125, 125–250, 250–500, 500–1000 µm respectively, k_d values were 8.10, 4.08, 2.92, 2.12 and 1.44 mm^{-1}). These Ihimi-values probably come closer to reality since the much lower Kühl-values concern cleaned quartz particles. Thus, values of 8 mm^{-1} for the inner Ems-Dollard stations, and 3-4 mm^{-1} for the outer stations probably are values to start with.

Colijn (1982) provided extinction coefficients (after unpublished data by Schröder), based on light extinction measurements on suspensions of solids. He came up with k_d-values varying between 5 to over 30 mm^{-1}.

Jorgensen & DesMarais (1986) describe k_d-measurements in silty sediments in San Francisco bay, and mention values from 2.3-20.3 mm^{-1}, depending on wavelength. Hopkins (1963) mentions 5-6 mm^{-1}. MacIntyre and Cullen (1995) mention much lower values of 0.9-1.3 mm^{-1}; their sediment concerned fine to medium sized sand (dominated by fractions 63-125 µm and 125-250 µm).

Unfortunately, there is hardly information found that couples sediment composition and k_d-values.

Later on, a separate approximation will be made based on the relationship found between k_d-values in the water column and the silt content measured. Sediment porosity and silt content then are also taken into account.

4.14.2 Wadden Sea silt data and silt conversion by Zwarts

In the period 1989–1997, Rijkswaterstaat had over 7000 sediment samples taken, covering the whole Dutch Wadden Sea (RIKZ, 1998), using a "Van Veen" sediment grab-sampler. The upper 10 cm was mixed, and from this, a wet sample was analysed with a Malvern 2600L laser particle sizer (GeoSea Consulting, UK). The samples were not treated in advance, that is, neither carbonates nor were organic particles removed, which is a standard procedure by adding acid and peroxide. This results in an erroneous estimation of the proportion of finer particles. Sampling density was 1 sample km^{-2}, up

to 2 km^{-2} in those areas where a higher variability was expected. The data were interpolated to a final 50*50 m grid size data set, using three points within a search distance of 1000 m. Such an interpolation implies that the 50*50 m data do not necessarily match the natural boundaries of the sediment types. Especially sediment composition in gullies between data points may deviate from the computed estimates.

The results for the silt content (the % of particles < 63 µm) appeared to be hard to interpret. Zwarts (2004) explained how the RIKZ-GeoSea data could be compiled into data that were assessed through standard sediment analyses methods.

In order to test the relationship between the GeoSea Malvern set and silt data analysed with a classical gravimetric method, Zwarts had 148 sediment samples analysed according to both methods. Zwarts et al (2004) wrote that the correlation was relatively weak: the Malvern % of particles < 16 µm appeared to be 2-3 times the gravimetrically determined silt content, with an R^2=0.67. A better correlation was found between the silt content and the Malvern-fraction < 63 µm (R^2 = .72). Therefore, the 63 µm-line was used to translate the Malvern-data to gravimetric silt content. The relationship is

$$Silt\ content\ (< 16\ \mu m) = 0.1879 * Silt\ content\ (< 63\ \mu m, Malvern) \qquad (20a)$$

4.14.3 Lake Veluwe data

From an existing study in Lake Veluwe (Brinkman & Van Raaphorst, 1986), a data set was available on sediment composition (silt%, H_2O%, elemental composition for P, Ca, Mg, Fe, Al, Si, CO_2, % organic matter and some other characteristics). Also the type of phosphate bond (divided into four fractions: weakly bound, incorporated into oxides, into carbonates and the rest) has been examined through a specific extraction method (Hieltjes, 1980). Silt content was analysed by a standard gravimetric method (see e.g. Zwarts, 1988; Zwarts et al, 2004).

The data from Lake Veluwe (Brinkman & Van Raaphorst, 1986) were still available, and were re-analysed. Unfortunately, none of the samples had been analysed on silt content *and* water content. Thus, the analyses had to be done by using one or more intermediate compounds.

Analyses were performed with a linear model (Chambers, 1992). The R-environment (R_Core Team 2013) was used to perform the analyses.

4.15 Global radiation & unit conversion

Hourly data are available from KNMI (KNMI,2015), for stations Lauwersoog and Nieuw-Beerta (Figure 42). Global radiation figures were weighted, see Table 14.

Table 14 Weighting of global radiation data for the six benthic sampling stations (radiation weighted, summed and divided by 6).

Station	Part Lauwersmeer	Part Nieuw-Beerta
1	5	1
2	4	2
3	3	3
4	2	4
5	1	5
6	0.5	5.5

Primary production measurements were performed with µE m^{-2} s^{-1} as unit, thus as photon flux. Global radiation is available from KNMI (KNMI, 2015) as heat flux J cm^{-2} h^{-1}, and by multiplying with (10^4/3600) this is converted to W m^{-2}. Since the energetic content of the radiation depends on the wavelength of the photons, conversion is only correctly possible for each wavelength separately; and for the whole spectrum if the spectral distribution is known. It can be very time-consuming to come to a proper conversion, since the spectral distribution heavily depends on e.g. the atmospheric conditions (humidity, cloud cover) and on the period of the day and of year. As a compromise, a fixed conversion factor is applied for all situations (this topic of what conversion factor to use has been discussed by many authors). The applied conversion is

$$\text{Photon flux } (\mu\text{E m}^{-2}\ \text{s}^{-1}) = \gamma_e \cdot \text{Photoactive radiation (PAR, W m}^{-2}) \qquad (21)$$

where PAR (photosynthetically active radiation) is that part of the global radiation that is captured by microphytobenthos pigments. PAR usually is taken at 45% of the global radiation; and the conversion factor γ_e = 2.515 (µE m^{-2} s^{-1}) (W m^{-2})$^{-1}$. Thus: from KNMI-data (W m^{-2}) to µE m^{-2} s^{-1}: multiply by 2.515.

Figure 42 Positioning of benthic sampling stations and both KNMI weather sites

4.16 Computing primary production in the water column

From the analyses above, the production per unit of chlorophyll-a is known (PP), and its light dependence. Light intensity in the water column is computed according to (eq.20), using the

estimated k_d-values, and light availability comes from the KNMI-data. Chlorophyll-a content is measured every sampling cruise.

Thus the production in the water column is (at each depth)

$$Prod = PP(eq.14) * chla \qquad \text{(mg C (µg chla)}^{-1}\text{ h}^{-1} * \text{(mg chla m}^{-1}\text{) = (mg C m}^{-3}\text{ h}^{-1}\text{)} \quad (22)$$

To compute the production per m^2, Prod is to be integrated over depth; this is done numerically.

4.17 Extrapolation and interpolation of results for a whole year

In order to estimate primary production for a whole year, the Eilers-Peeters parameters and the light extinction coefficient have to be inter- and extrapolated to the whole year. This is not needed for radiation data: these are available on an hourly basis. This elaboration of the Eilers-Peeters data needs extra attention first.

4.17.1 Extrapolation of Eilers-Peeters a, b and c-parameters for the whole year: rectangular, splines or moving-averages?

The EP-parameters were determined for each sampling date and position. They are assumed to be representative for the area, but have to be inter-/extrapolated to other days of the year.

A first attempt to apply splines as an interpolation method for a, b and c separately (Figure 43, right figures) had to be rejected as method since the three parameters cannot be considered independent. Especially a and b are correlated; the reliability of their values largely depends on how well the photo-inhibition appears in the incubation results. In case this is not very clear, a high value of a can be masked by a low value of b and vice versa. The c-parameter, that determines the initial slope of the PI-curve, is much more reliable, and less correlated with a or b.

A second method is a rectangular interpolation: values are assumed to be valid for the periods around the sampling day. The first values are also used for the whole initial period of the year, and the last values for the last period (Figure 43, left figures).

A third method applied concerned moving averages: the rectangular results were used to compute a moving average, and then this was repeated once more (Figure 43, middle graphs).

The spline-method gives some fancy results, like the one in the circle in Figure 43: the spline produces a value larger then both neighbour values. This example is just a 'low-key' example of what sometimes happens; splines sometimes came up with negative values.

Both the spline-method and the moving average method have to be considered as 'tricks' to produce interpolated results, without a sound basis for mathematical correctness; the correlation between the a and b-parameters is the main reason for this. The rectangular method is a trick as well, but the mathematical basis is sound.

Therefore, it was decided to basically use the a, b and c-values for the period around each sampling day (the rectangular method). To be complete, both other methods initially were applied in the

computations. However, the spline-method was skipped completely after a while, and only the moving averages are kept as an alternative interpolation method.

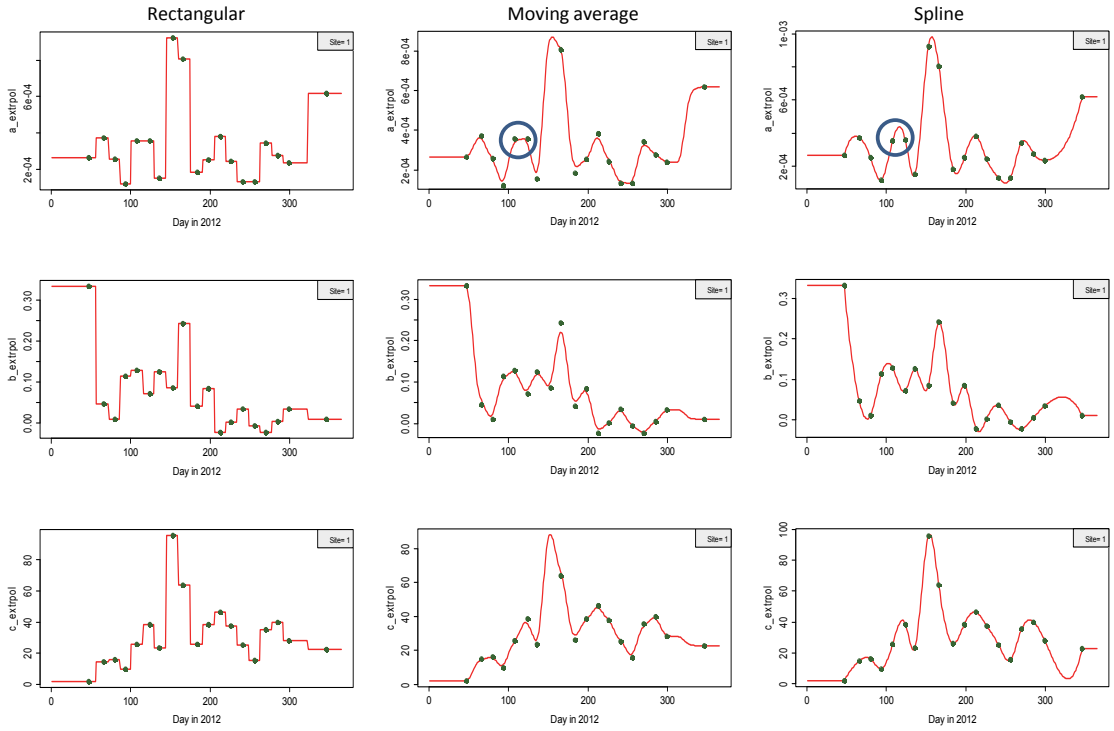

Figure 43 Extrapolation of available a, b and c-values to whole-year values. Site 1. Left: applying a rectangular method (assuming that each value is representative for the period around the sampling date), middle: moving average method, and right: after computing a spline

4.17.2 Extrapolation of the extinction coefficient for the whole year

The values found for the extinction coefficient K_d are extrapolated as well, using both the rectangular and the moving average method as described above. Here, the mathematical basis is correct for both methods, although it still is a trick to come to values for the whole year. The question however is how realistic the extrapolated results are, since the actual value of K_d depends on the tidal phase. At one site, K_d at low water may differ considerably from the value at high water.

4.18 Compute primary production at each pelagic station

The total production in the water column (in mg $C.m^{-2}.d^{-1}$) is calculated from the daily irradiation (Photosynthetic Active Radiation; PAR, measured in hourly intervals, from KNMI-global radiation data, KNMI, 2015), the vertical extinction coefficient (continuously), the vertical light profiles at the sampling stations), and the photosynthetic Eilers-Peeters parameters found.

Above it has been explained

- how the Eilers-Peeters parameters were obtained, and how they are extrapolated to the whole year,
- how the chlorophyll-a content in the water samples was analysed,
- how the incident radiation is obtained from the KNMI-data,
- how the light penetration in the water column is computed. Global radiation values are corrected a bit for reflection at the water surface.

Thus:

a) The ^{14}C-incubation provide the PI-curve (a,b, and c-parameters). These are extrapolated to the whole year. Production is in g C mg chla^{-1} d^{-1}.
b) The fluorometric analyses provide the chlorophyll-a content in the water column (mg chla l^{-1}).
c) The global radiation data (KNMI) give the energy influx at the water surface (expressed in µE m^{-2} s^{-1}).
d) (c), together with the estimates for the light attenuation coefficient (k_d, m^{-1}) gives the light intensity at each depth in the water column, at each hour of each day.
e) With (a, b and d) the primary production at each depth is computed for each hour at each day. This is done for 2000 thin layers (from 0.. water depth), summation over depth and for all 24 hours gives the daily production per m^{-2} (mg C m^{-2} d^{-1}).
f) (e) is done for channels at high and at low water, and for tidal flats at high and at low water.
g) Values for channels and tidal flats are computed as half the HW- plus half the LW-results
h) Since tidal flats are covered with water only part of the time (the relative emersion period), tidal flat values are multiplied by this emersion fraction to come to the correct estimate for daily tidal flat primary production.
i) All daily values are summed to get the yearly primary production (g C m^{-2} y^{-1}).
j) Each site is assumed to be representative for a certain area (compartment). These compartments were taken from Colijn (1984), see Table 6. Primary production times the area (m^2) of each compartment gives total primary production for this compartment (tonnes C y^{-1}).
k) Summing up all values from (i) gives total production in the system (tonnes C y^{-1}), and from that an average production per unit area is computed (g C m^{-2} y^{-1}).

Note that the primary production data all concern gross primary production values. Nett primary production (gross production - respiration losses) thus is not computed.

4.19 Vertical profiles of temperature, oxygen, salinity, turbidity and chlorophyll in the water column, or: is the water column well mixed?

In 2013, and extended into 2014, a number of water column profiles was assessed by Rijkswaterstaat at sampling site Groote Gat Noord (site nr 20 in Figure 23). Data for temperature, oxygen (occasionally), turbidity, chlorophyll-a, salinity and conductivity were measured during 35 visits in the local channel, having a depth of about 5 m. Chlorophyll-a was detected as fluorescence unit, and not really calibrated against laboratory chlorophyll-a measurements; salinity follows from conductivity (see section 4.4.3). For turbidity measurements see section 4.5.7.

5 Methods-3: pocket box cruises, position of sampling sites

5.1 What is in this chapter

The data obtained by the PocketBox have to be elaborated. Its positions are computed, a check is performed whether the vessel was just fast cruising, doing the survey or sampling at the sampling sites, and finally outliers in the data obtained have to be detected. In this chapter it is described how all these actions were performed.

5.2 Vessel position and coordinate transformation

The PocketBox stores its position as (Latitude, Longitude) values. First these are recomputed to 'Rijksdriehoekscoordinaten" following a simple transformation equation:

$$RD_X = -211509.2522 + 67695.30135 \cdot \text{Longitude}$$

$$RD_Y = -5235896.4770 + 109336.3555 \cdot \text{Latitude} \qquad (23)$$

These are simple locally valid equations, given a deviation of maximum 50 m. This is sufficient for the present data representation purpose.

5.3 Transformation of the position to a straight line-value

After transformation of the (Latitude, Longitude) values to 'Rijksdriehoekscoordinaten' (RD_x, RD_y), the position along the sailing trajectory is computed, as projected on the straight line between start and finish of the sampling trajectory. All values are presented in the final tables together with Latitude, Longitude, RD_x, RD_y and distance from the starting point of the trajectory near the island of Borkum (Figure 14, Figure 21).

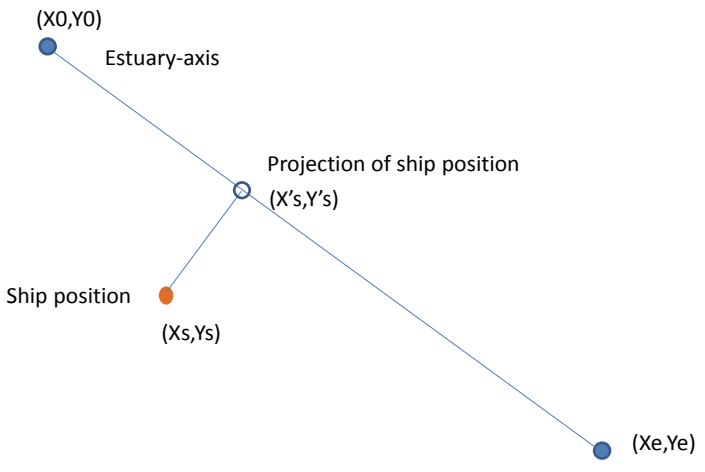

Figure 44 Projection of ship position on estuary axis

For computing the distance from the trajectory starting position, a straight line is drawn from the start to the finish of the sailing route, and all observation positions (X_s,Y_s) were projected on this axis line (Figure 44).

The goniometric equations needed for this projection are not given here, only a few computations of the type $c^2=a^2+b^2$ and a few similar-triangles transformations are needed. As a result, the (X'_s,Y'_s)-position is known, and the distance between (X's,Y's) and (X0,Y0).

5.4 Distinguishing between sailing, survey and sampling based on vessel speed

The behaviour of the ship was decided upon the vessel speed. An example is given in Figure 45. The six monitoring sites (Table 9) are clearly visible, since the vessel speed is much lower (and gets almost zero). Sailing in the beginning and at the end of the trip is also visible, since speed gets higher. After a few attempts, it was decided to make a distinction following:

Sailing : Cruise speed > 8.5 km h^{-1} (the ship is cruising fast)

Sampling : Cruise speed < 3.0 km h^{-1} (the ship almost stays at one position)

Survey : All other vessel speeds (the ship's cruising quietly, and doing serious PB-measurements)

The result for this same cruise (nr 36, at August 29th, 2013) is shown in Figure 46.

During sailing, the PocketBox was functioning (sometimes), but data are not reliable: the appearance of bubbles, foam (especially when weather conditions were rough) affected the probe signals. These data were removed from the final data set.

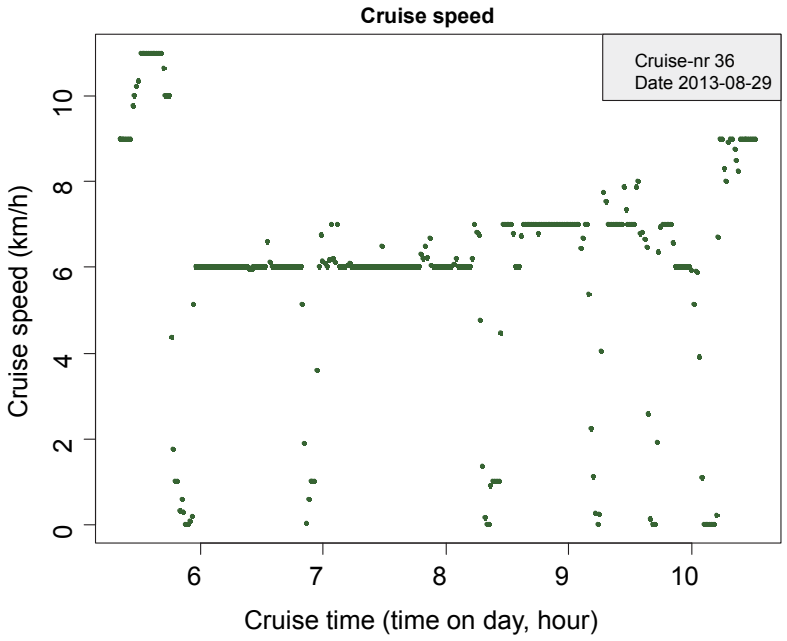

Figure 45 Vessel speed during a trip (this one: August 29th 2013). No distinction made between sailing, sampling and survey.

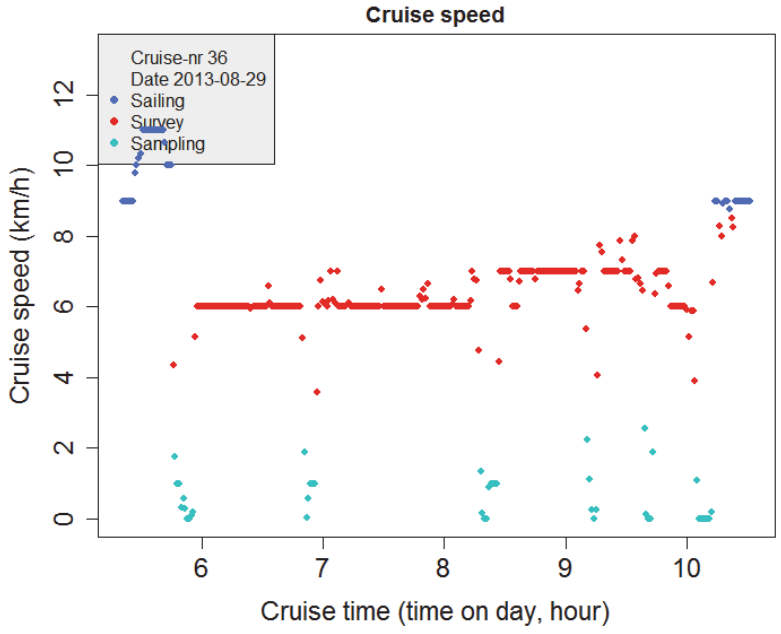

Figure 46 Similar to Figure 45, but now sailing, survey and sampling moments distinguished.

5.5 Vessel movements

Next to distinguishing between survey, sailing and sampling moments, the route of the vessel can be drawn. Two examples are given in Figure 47, showing that not always the whole trajectory was completed (always due to weather conditions) (upper figure), and that sometimes PocketBox sampling started far before the first sampling site was reached (lower figure).

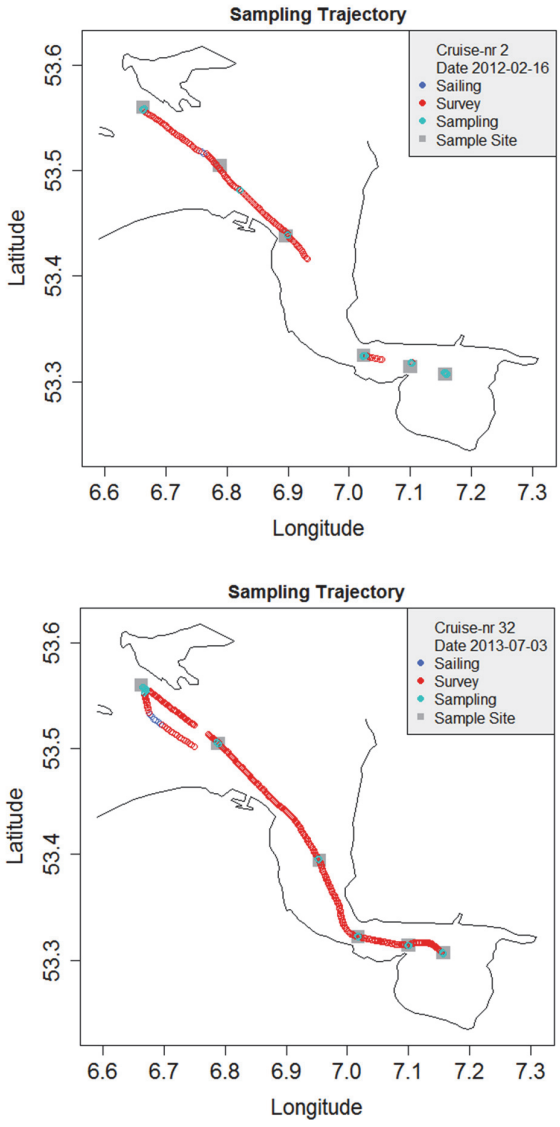

Figure 47. Sampling trajectory on Feb 16th 2012, and on July 3rd, 2013. It is clear that the trip in 2012 was not complete (which was due to ice), and also that sampling site 02 (the second outmost square in the upper figure) was not used; the real sampling site (grey-blue dots) is a few kilometres more inside the estuary. On 2013-07-03, PB-sampling already started before site 01 was reached.

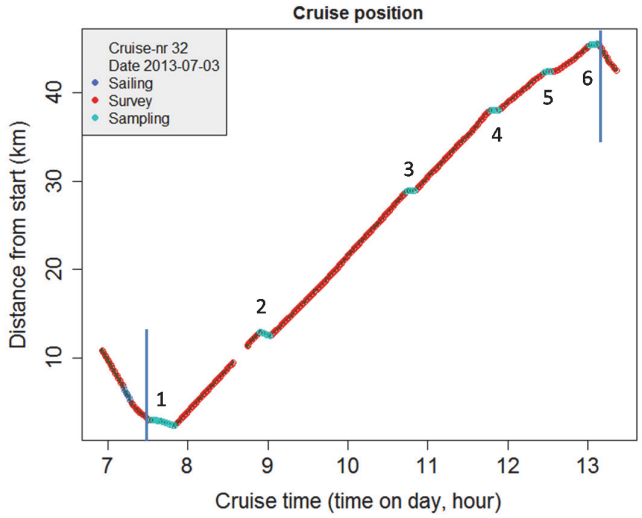

Figure 49 Position of the ship (distance to the first position of the trajectory) during cruise 31 on June 19th, 2013. Station numbers are mentioned. All data left of station 1 and right of station 6 are skipped.

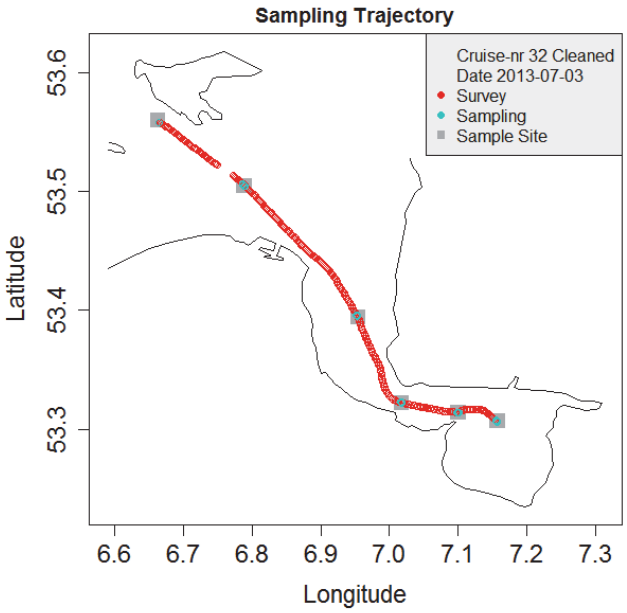

Figur **before the fi**

In Figure 49, the ships position during cruise nr 31 is shown; all data outside the trajectory (station 1 - station 6) are skipped, and the final vessel movement as stored in the final files is the one shown in Figure 48.

5.6 Computing average values for each stop; detection of outliers

The next question is how to find average values for the data recorded by the PocketBox at each sampling site.

Above it is explained how stops are identified (Figure 46). Simply averaging the data during the stops appeared not to be the correct method, since sometimes extreme values occurred in the data set.

These extreme values had to be recognized, and removed before further computation were performed. In Figure 50, average values are plotted based on *all* data at each sampling site (all the cyan dots). The few low values at these sites dominate the results.

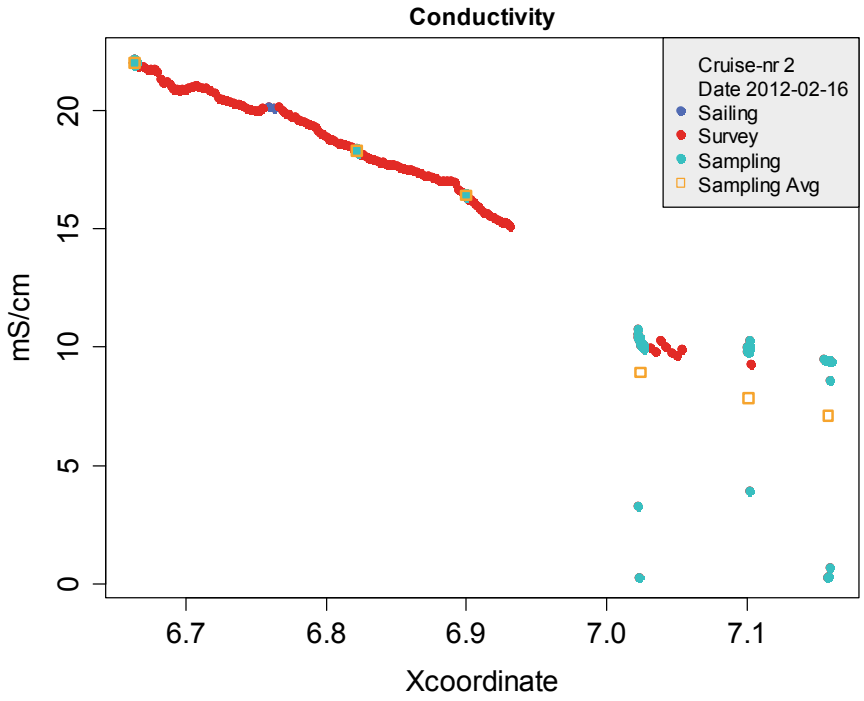

Figure 50 Conductivity as measured on Feb 16th, 2012. Saling (just a short moment between Xcoordinate 6.7 and 6.8),survey and sampling site values are clear (blue, red and cyan, respectively). Average values at the sampling sites are represented by the orange squares. These are averages of all cyan dots. Some low values at sites 4-6 largely affect the final average value.

In Figure 51, these extreme values were marked, and removed. This is done using the getOutliersI - function from R-library “extremevalues”. The procedure is not 100% perfect, but it is successful in most cases.

After removal of these outliers, averages for all variables were computed and stored. These values have to be compared (if possible) with the values following from the Hach–multimeter (e.g. conductivity) and the laboratory results (e.g. chlorophyll-content).

This comparison may lead to a calibration of the PocketBox-sensors, and last, the whole computation is repeated, now with calibrated values.

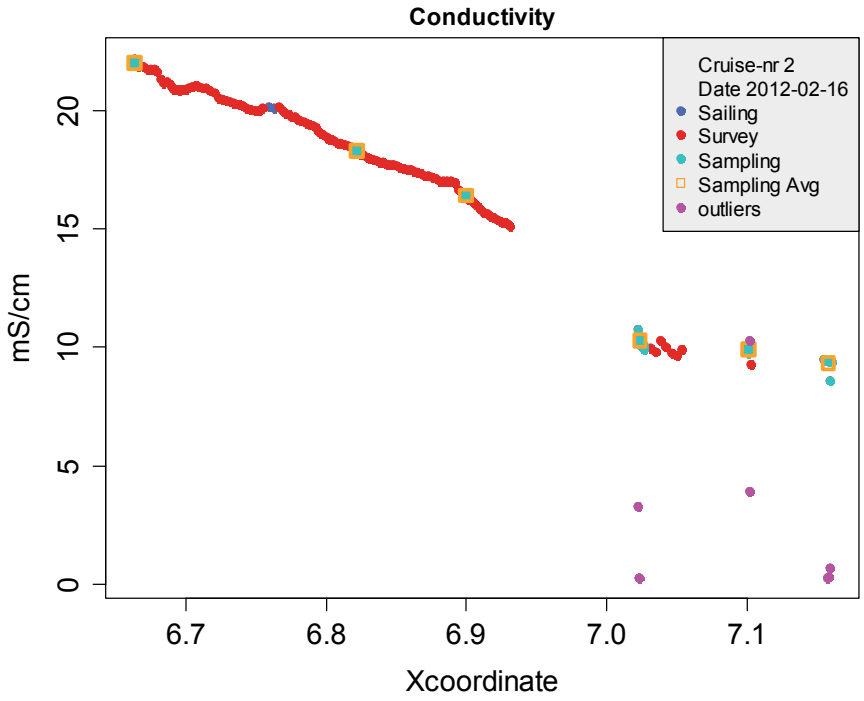

Figure 51 Conductivity as measured on Feb 16th, 2012. Similar to Figure 50, but now the outliers have been marked (purple dots), and removed from the computed average values.

The average values are stored separately, and used later on for regression analyses and comparison with data from the HACH-HQ handheld meter and data from the laboratory analyses.

6 Methods-4: regression analysis

6.1 What is in this chapter

There are two main reasons to perform a number of (linear) regression analysis:

- data exploration
- calibration

The first is a first attempt to find a particular behaviour of the data or relationships with other data; this related to further research. The second is needed since some data need to be adjusted. This acts as a possible calibration, and is needed to provide best data-series representing the 'system' and to deliver reliable data to the primary production model.

6.2 Regression

All relationships look like

$$\hat{Y} = a + \sum_i^N b_i \cdot X_i \qquad (24)$$

with the possibility to set a=0 in advance (no intercept).

Basically, two regression analyses were performed. The first concerns an investigation of the relationship between single variable data found at each sampling site. In that case, N in eq.24==1.

The second is an attempt trying to relate more than one independent variable to one response variable. For the latter exercise, a matrix has been used that defines the relationships to be investigated. Note that all the data used are values found at the monitoring sites: as averages from PocketBox data, or values that were simply recorded from the Hach-multimeter, or values found after analysis in the laboratory.

Table 15 Linear regression matrices. The relationships Y=a+bX1+cX2+ .. can be tested. The numbers of the variables (in the first row) are mentioned. On each row, a set is defined. What the dependent variable is, is written in the second column ("Y"). In the rest of the row, first the variable name is mentioned, and finally the variable(s) that is (are) included in the linear relationship. In the third row, the origin of the data is mentioned: PB=PocketBox, Lab=laboratory, Field=Field, Hach= Hach handheld meter, NUT=nutrient analysis, EP= ^{14}C-incubation and subsequent computation of Eilers-Peeters parameters. The column 'Doit' provides the possibility that only a few of the possible relationships (the rows) are executed.

Set	Y_Col	Name	DoIt	Susp Matter	Kd	CDOM	AOA_ Chla	AOA_ Yellow Subs	Salinity	Temp	DIN	DIP	Dsi	Pmax	Imax	Alfa
Data col	0	0	0	14	15	16	17	18	19	20	21	22	23	24	25	26
1	15	Kd	1	14	0	0	0	0	0	0	0	0	0	0	0	0
2	15	Kd	1	14	0	16	0	0	0	0	0	0	0	0	0	0
3	15	Kd	1	14	0	0	0	18	0	0	0	0	0	0	0	0
4	15	Kd	1	14	0	0	17	18	0	0	0	0	0	0	0	0
5	15	Kd	1	14	0	0	17	18	0	0	0	0	0	0	0	0
6	15	Kd	1	14	0	16	17	18	0	0	0	0	0	0	0	0
7	16	CDOM	1	0	0	0	0	18	0	0	0	0	0	0	0	0

8	16	CDOM	1	14	0	0	0	0	0	0	0	0	0	0	0	0
9	14	Susp Matter	1	0	0	0	0	0	19	0	0	0	0	0	0	0
10	14	Susp Matter	1	0	15	0	0	0	0	0	0	0	0	0	0	0
11	24	Pmax	1	0	0	0	0	0	0	20	0	0	0	0	0	0
12	25	Imax	1	0	0	0	0	0	0	20	0	0	0	0	0	0
13	26	Alfa	1	0	0	0	0	0	0	20	0	0	0	0	0	0
14	24	Pmax	1	0	0	0	0	0	0	0	21	0	0	0	0	0
15	25	Imax	1	0	0	0	0	0	0	0	21	0	0	0	0	0
16	26	Alfa	1	0	0	0	0	0	0	0	21	0	0	0	0	0
17	24	Pmax	1	0	0	0	0	0	0	0	0	22	0	0	0	0
18	25	Imax	1	0	0	0	0	0	0	0	0	22	0	0	0	0
19	26	Alfa	1	0	0	0	0	0	0	0	0	22	0	0	0	0
20	24	Pmax	1	0	0	0	0	0	0	0	0	0	23	0	0	0
21	25	Imax	1	0	0	0	0	0	0	0	0	0	23	0	0	0
22	26	Alfa	1	0	0	0	0	0	0	0	0	0	23	0	0	0
23	24	Pmax	1	0	0	0	0	0	0	0	0	0	0	0	25	0
26	30	Diatom_ AOA_ Chla	1	0	0	0	0	0	0	0	0	0	23	0	0	0
30	24	Pmax	1	0	0	0	17	0	0	0	0	0	0	0	0	0
31	33	CStar1	1	0	15	0	0	0	0	0	0	0	0	0	0	0
32	34	CStar2	1	0	15	0	0	0	0	0	0	0	0	0	0	0
34	33	CStar1	1	14	0	0	0	0	0	0	0	0	0	0	0	0
35	33	CStar1	1	14	0	16	0	0	0	0	0	0	0	0	0	0
36	33	CStar1	1	14	0	0	17	0	0	0	0	0	0	0	0	0
37	33	CStar1	1	14	0	0	0	18	0	0	0	0	0	0	0	0
38	33	CStar1	1	14	0	16	17	0	0	0	0	0	0	0	0	0
39	33	CStar1	1	14	0	0	17	18	0	0	0	0	0	0	0	0
40	33	CStar1	1	14	0	16	17	18	0	0	0	0	0	0	0	0
41	34	CStar2	1	14	0	0	0	0	0	0	0	0	0	0	0	0
42	34	CStar2	1	14	0	16	0	0	0	0	0	0	0	0	0	0
43	34	CStar2	1	14	0	0	17	0	0	0	0	0	0	0	0	0
44	34	CStar2	1	14	0	0	0	18	0	0	0	0	0	0	0	0
45	34	CStar2	1	14	0	16	17	0	0	0	0	0	0	0	0	0
46	34	CStar2	1	14	0	0	17	18	0	0	0	0	0	0	0	0
47	34	CStar2	1	14	0	16	17	18	0	0	0	0	0	0	0	0
48	26	Alfa	1	0	15	0	0	0	0	0	0	0	0	0	0	0
49	26	Alfa	1	0	0	0	17	0	0	0	0	0	0	0	0	0
50	26	Alfa	1	0	0	0	0	0	0	0	0	0	0	0	25	0
53	35	Chla_ Lab	1	0	0	0	17	0	0	0	0	0	0	0	0	0
57	33	CStar1	1	0	15	0	17	18	0	0	0	0	0	0	0	0
58	33	CStar1	1	0	15	16	17	18	0	0	0	0	0	0	0	0
59	38	Turbid	1	14	0	0	0	0	0	0	0	0	0	0	0	0
60	38	Turbid	1	14	0	16	0	0	0	0	0	0	0	0	0	0
61	38	Turbid	1	14	0	0	17	0	0	0	0	0	0	0	0	0

62	38	Turbid	1	14	0	0	0	18	0	0	0	0	0	0	0	0
63	38	Turbid	1	14	0	16	17	18	0	0	0	0	0	0	0	0

Table 15 (continued) This part is right of the previous part, the numbers in the first column denote to which row of the previous each row belongs.

Set	Y_Col	Name	Do It	CDOM	AOA_Chla	AOA_Yell Subs	Salin_Hach	Cond_Hach	Chla Cyclop	O2_umol_PB	C-Star1	C-Star2	ST Corr Oxyg	Turbidity
Data	0	0	0	16	17	18	27	28	29	32	33	34	37	38
24	27	Salin_Hach	1	0	0	0	0	28	0	0	0	0	0	0
25	19	Salinity	1	0	0	0	0	28	0	0	0	0	0	0
27	17	AOA_Chla	1	0	0	0	0	0	29	0	0	0	0	0
28	19	Salinity	1	0	0	0	27	0	0	0	0	0	0	0
29	31	O2_mg_Hach	1	0	0	0	0	0	0	32	0	0	0	0
33	33	CStar1	1	0	0	0	0	0	0	0	0	34	0	0
51	15	Kd	1	0	0	0	0	0	0	0	33	0	0	0
52	15	Kd	1	0	0	0	0	0	0	0	0	34	0	0
54	35	Chla_Lab	1	0	0	0	0	0	29	0	0	0	0	0
55	31	O2_mg_Hach	1	0	0	0	0	0	0	0	0	0	0	0
56	36	O2_ST Corr_new	1	0	0	0	0	0	0	0	0	0	37	0
64	14	SuspMatter	1	0	0	0	0	0	0	0	33	0	0	0
65	14	SuspMatter	1	16	0	0	0	0	0	0	33	0	0	0
66	14	SuspMatter	1	0	17	0	0	0	0	0	33	0	0	0
67	14	SuspMatter	1	0	0	18	0	0	0	0	33	0	0	0
68	14	SuspMatter	1	16	0	18	0	0	0	0	33	0	0	0
69	14	SuspMatter	1	16	17	18	0	0	0	0	33	0	0	0
70	14	SuspMatter	1	0	0	0	0	0	0	0	0	0	0	38
71	14	SuspMatter	1	0	0	18	0	0	0	0	0	0	0	38
72	14	SuspMatter	1	0	17	0	0	0	0	0	0	0	0	38
73	14	SuspMatter	1	16	0	0	0	0	0	0	0	0	0	38
74	14	SuspMatter	1	16	17	0	0	0	0	0	0	0	0	38
75	14	SuspMatter	1	16	0	18	0	0	0	0	0	0	0	38
76	14	SuspMatter	1	16	17	18	0	0	0	0	0	0	0	38
77	15	Kd	1	16	0	0	0	0	0	0	33	0	0	0
78	15	Kd	1	16	17	0	0	0	0	0	33	0	0	0
79	15	Kd	1	16	17	18	0	0	0	0	33	0	0	0
80	14	SuspMatter	1	0	0	0	0	0	0	0	0	34	0	0
81	14	SuspMatter	1	16	0	0	0	0	0	0	0	34	0	0
82	14	SuspMatter	1	0	17	0	0	0	0	0	0	34	0	0
83	14	SuspMatter	1	0	0	18	0	0	0	0	0	34	0	0
84	14	SuspMatter	1	16	0	18	0	0	0	0	0	34	0	0
85	14	SuspMatter	1	16	17	18	0	0	0	0	0	34	0	0

In R, all rows (with the parameter *DoIt* set to 1) are run; both for a situation with an intercept (a in eq. 24 =0), and one without intercept (any value for a is allowed).

So, a couple of equations like (eq.24) will result. Also here, it is necessary to identify possible outliers.

This is done by

- perform a first analysis
- compute the 95% confidence region for the regression line
- remove all those values that differ more than twice the difference between regression line and confidence value
- run the regression again, and store the results as final outcome.

In case there is just one independent variable X, the regression coefficients (a and b's) follow from

$$b = \Sigma [(xi - \overline{X})(yi - \overline{Y})] / \Sigma [(xi - \overline{X})^2] \quad (25a)$$

$$a = \overline{Y} - b \cdot \overline{X} \quad (25b)$$

with $\overline{Y}$ is the average value for Y, and $\overline{X}$ is the average value for X.

The (1-α)*100 % confidence region for the regression line is computed following

$$Y_c = \hat{Y} \pm t(M-1,1-\alpha) \cdot s_y \cdot \sqrt{\frac{1}{m} + \frac{(X-\bar{X})^2}{(m-1)\cdot s_x^2}} \quad (26)$$

where

m	degrees of freedom
Y_m	measured values
X	independent variable
$\hat{Y}$	estimated value
S_y	standard deviation of the residuals (Y-values): $s_y = \sqrt{\frac{\sum_{i=1}^{m}(Y_i - \hat{Y})^2}{(m-2)}}$
s_x	standard deviation of the X-values: $s_x = \sqrt{\frac{\sum_{i=1}^{m}(X_i - \bar{X})^2}{(m-1)}}$

The (1-α)*100 % confidence region for each data point is computed following

$$Y_c = \hat{Y} \pm t(M-1,1-\alpha) \cdot s_y \cdot \sqrt{1 + \frac{1}{m} + \frac{(X-\bar{X})^2}{(m-1)\cdot s_x^2}} \quad (27)$$

Eq's (26) and (27) are only effective in case of one independent variable (N=1 in eq. 24).

7 Results-1: Correlations and corrections

7.1 What is in this chapter

A first treatment of all data obtained is to check their validity, which is possible since some variables were measured in more than one way (e.g. temperature, chlorophyll-a, and more). Second, a number of observations is closely related, such as light attenuation and suspended solid content. Such relations are investigated in the next section. Third: continuous measurement by the PocketBox are screened and outliers are detected.

7.2 Temperature

Temperature was measured separately by the PocketBox, and also by the optode (measuring oxygen). Next, the handheld Hach-meter was used for temperature measurements, and during each sampling stop, a T-value was recorded by hand (from the PocketBox-T data).

It appears (see Figure 52) that the Hach40-handheld data are the same as the T-data from the PocketBox (those obtained as single values by reading the T-data, and those obtained as average of all T-values during each stop). The T-values as recorded by the optode differed considerably from the others, and had to be rejected.

It was not really necessary to recompute temperature (T), but only the 'correct' one had to be chosen.

Conclusions for temperature measurements

Hach40-handheld data and PocketBox temperature data are correct, optode temperature values are incorrect.

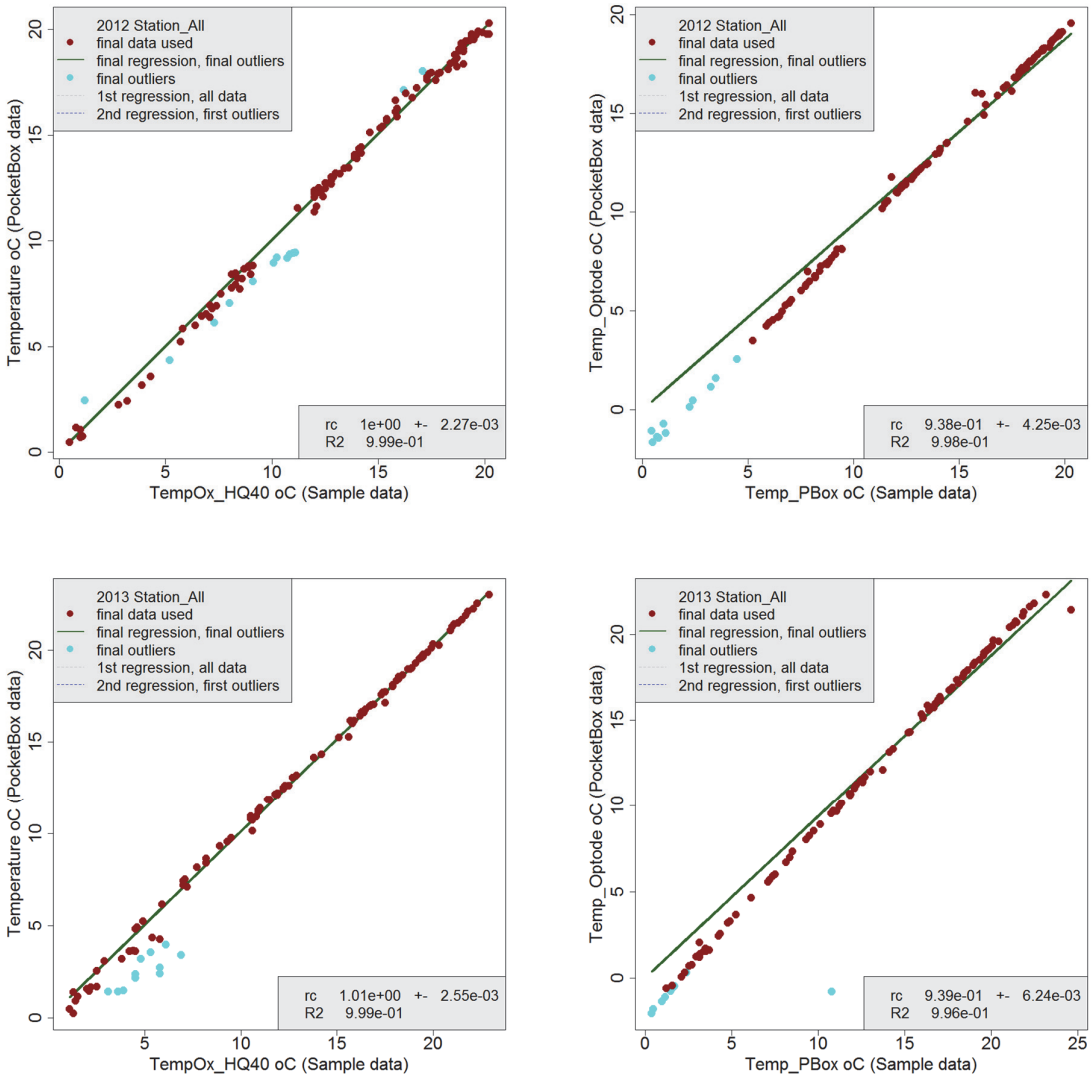

Figure 52 Temperature measurements. Left: T as measured by the PocketBox (Y-axis) vs T measured by the Hach40 handheld meter; right: T as measured by the optode-T-sensor vs T as assessed from the PocketBox at the sampling stops. Upper: 2012, lower: 2013. T during the sampling stops was also computed from *all* the T-observations during each stop; these were as good as the same as the one recorded by hand from the PocketBox-measurements.

7.3 Oxygen

7.3.1 Check on the corrected oxygen values from the Pocket-Box optode sensor

First a quick test is performed to check the results from the optode O_2-sensor. In section 7.2 it is shown that the optode temperature sensor gives erroneous results; in section 4.5.3 it has been explained that the effect of such a T-difference is minor. This has been checked first; from Figure 53 it can be concluded that there is no difference between both. Thus, the standard corrected values as delivered by the optode oxygen sensor are correct. There might be a difference between the optode results and those from the Hach-handheld meter; this is elaborated in the next section.

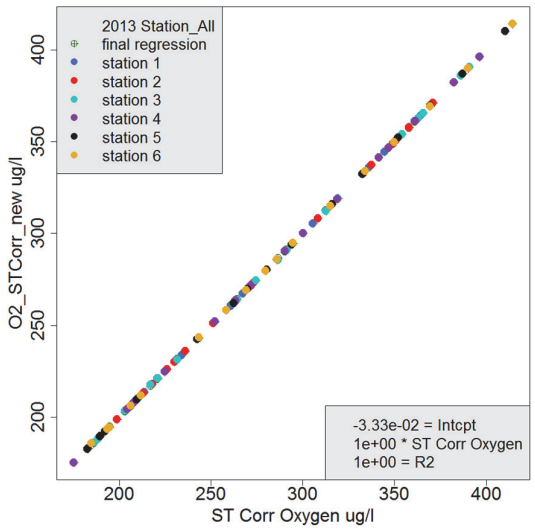

Figure 53 Standard corrected oxygen concentrations from the optode sensor (X-axis) and oxygen concentrations after an own corrections of the uncorrected optode values, using correct temperature values (T-axis). Dot colours denote monitoring stations.

7.3.2 Relationship between the Hach-oxygen sensor and the PocketBox-oxygen sensor

In Figure 54, oxygen data from the PocketBox (corrected for salinity and temperature) and data from the Hach-handheld meter are plotted. The slope should be 31.25 (eq. 2a), and the intercept 0, but it is obvious that this is not the case. Slopes and intercepts are given in Table 16. The relationship between both is much better in 2013 than in 2012; the slope of the non-intercept regression is also correct in 2013.

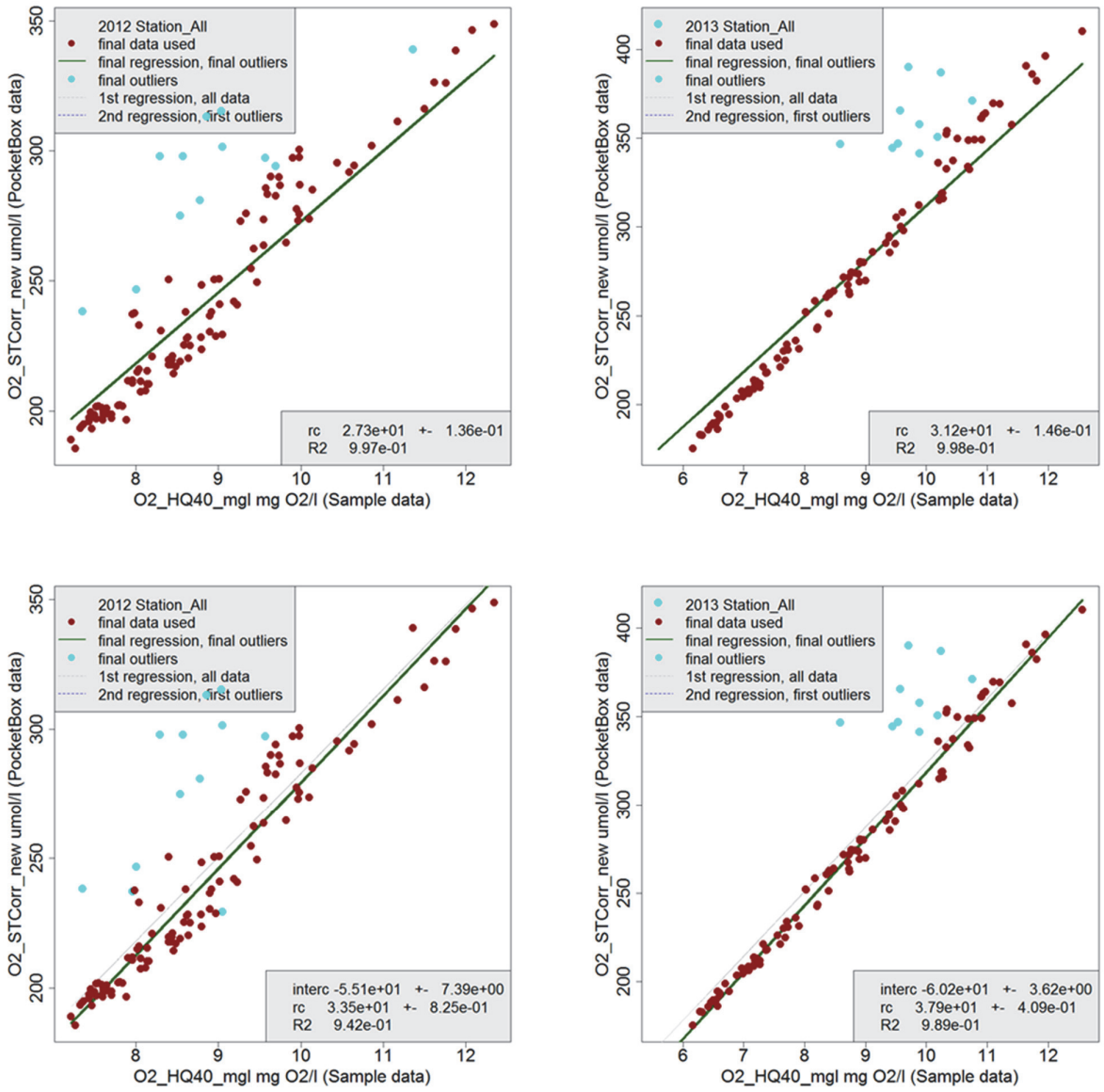

Figure 54 Oxygen data from the Hach HQ handheld meter and from the PocketBox (optode-measurements), corrected for salinity and temperature. upper: no intercept, lower: with intercepts. Left: 2012, right: 2013. Cyan dots were identified as outliers after the first regression.

Table 16 Regression results for PocketBox-oxygen values and Hach-HQ oxygen values. Light green values were applied to compute calibrated oxygen values from the PocketBox-data

Hach-values (mg/l) as function of PocketBox-values (µmol/l)				
PocketBox	Expected=0	Expected=3.20e-2		Remark
Hach HQ	a	b	R^2	
2012 intcpt	2.18	2.38e-2	0.90	After removal of outliers
2013 intcpt	2.18	2.07e-2	0.95	After removal of outliers
2012 no intcpt	0	3.18e-2	0.99	After removal of outliers
2013 no intcpt	0	2.78e-2	0.99	After removal of outliers
PocketBox-values (µmol/l) as function of Hach-values (mg/l)				
Hach HQ	Expected=0	Expected=31.25		
PocketBox-ST-corrected O2	a	b	R^2	
2012 intcpt	-54.3	33.4		After removal of outliers
2013 intcpt	-60.4	37.9		After removal of outliers
2012 no intcpt	0	27.3		After removal of outliers
2013 no intcpt	0	31.2		After removal of outliers

In Figure 55, saturation values from the Hach-handheld meter and from the PocketBox are presented. The 2012-data show a number of irregularities, the 2013 data are more consistent. The 2013-data show the same deviation from the 1:1-line as the concentration graphs do. At lower oxygen values the PocketBox-values are below the Hach-values.

The question arises what the cause of these differences is. The temperature correction has been removed as possible error source (section 7.3.1).

7.3.3 Conclusions for oxygen measurements

It can be concluded that

a) there are large individual deviations from the expected regression lines (eq. 2a) for the values obtained by the PocketBox and those obtained by the Hach-HQ handheld meter, especially in 2012. In 2013, the data are more consistent.
b) Regression results are best if an intercept is allowed, but consistency with eq. 2a is best in 2013, with zero intercept.

At this moment it is not clear what the cause of these differences is.

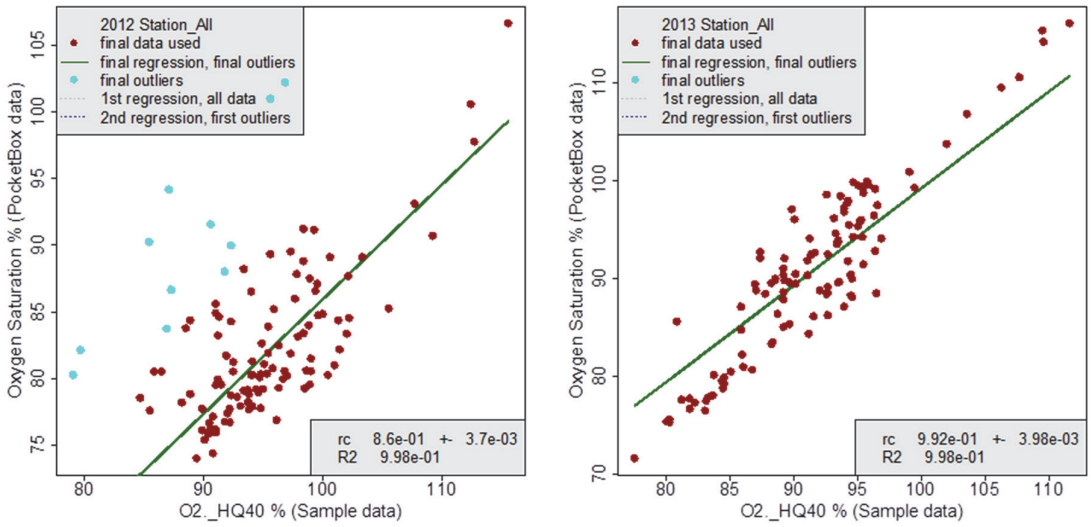

Figure 55 Oxygen saturation-% data from the Hach HQ handheld meter and from the PocketBox (optode-measurements), corrected for salinity and temperature. Intercept is set to 0. Left: 2012, right: 2013. Light blue dots were identified as outliers

7.4 Salinity and conductivity as measured by the Hach-handheld meter, and the PocketBox

Data obtained by the Hach-handheld meter and by the PocketBox

The PocketBox-sensor (a 'Type 4319' conductivity sensor by Aanderaa Instruments) delivers output as conductivity (in mS cm^{-1}) and as salinity (in PSU, see above). The Hach-HQ handheld meter output is recorded as salinity (PSU) only. Actually, both meters register the conductivity, and compute salinity from these values.

First, it is necessary to check what conversion is used by the PocketBox to compute salinity from conductivity. A comparison between computed salinity and measured salinity, according to a conductivity at 25 ^{o}C is done first (see section 4.4.3).

Two situations are shown in Figure 57, for both years 2012 and 2013: one using conductivity at 25 ^{o}C as basis, and one using conductivity at 20 ^{o}C as basis; it clearly shows that the PocketBox applies the 25 ^{o}C-relationship.

Next, it is necessary to check the results from the Hach-HQ handheld meter and those from the PocketBox. The Hach-meter is calibrated every once and a while, and is assumed to give the correct results in terms of salinity. In Figure 58, it is shown that in 2013 both data are exactly the same, but for 2012 a number of measurements deviate from that picture.

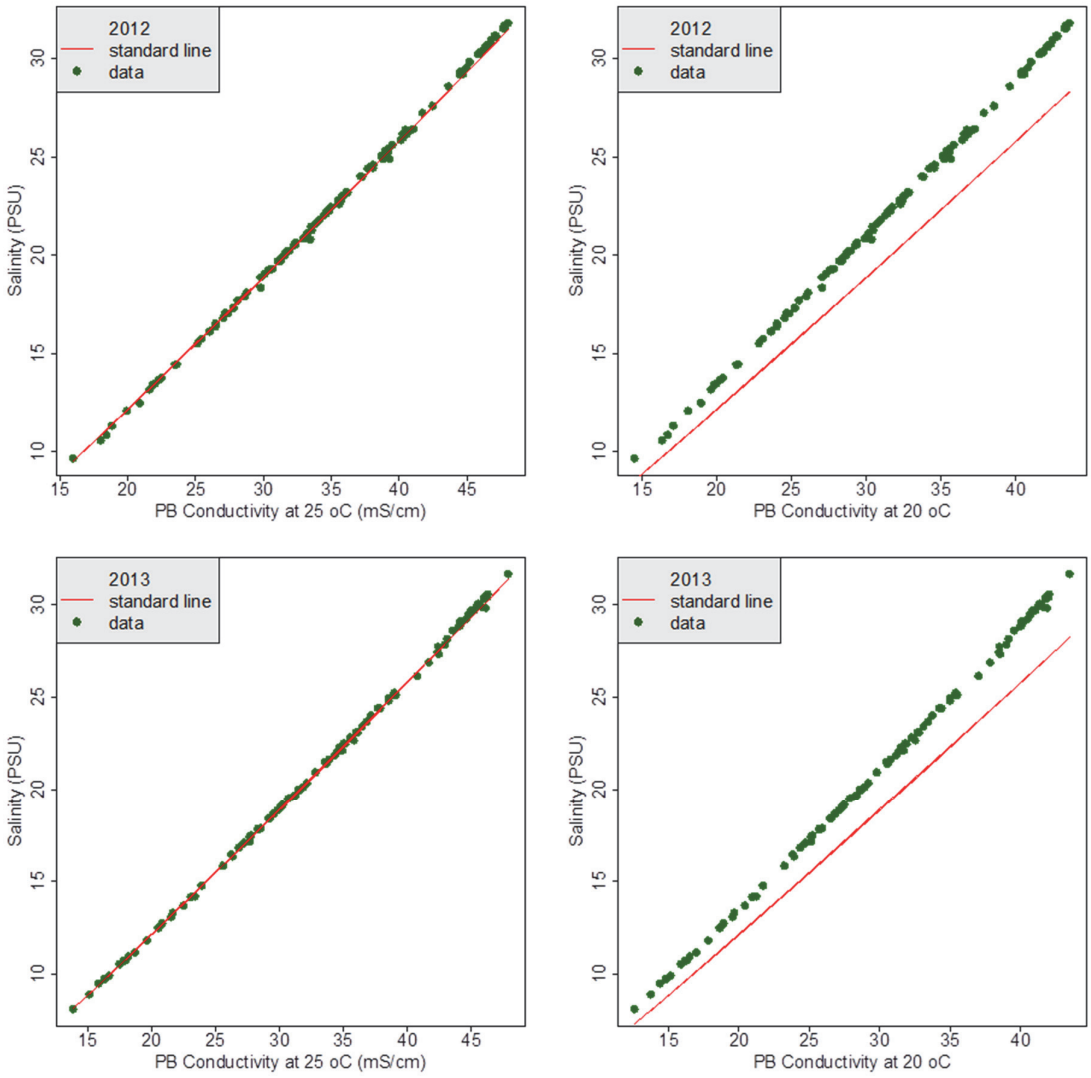

Figure 57 Conductivity and salinity according to the PocketBox for 2012 (upper) and 2013 (lower). Salinity is always computed from conductivity. Left: based on conductivity standardized at 25 °C and subsequent salinity computation, right dito, but based on conductivity standardized at 20 °C.

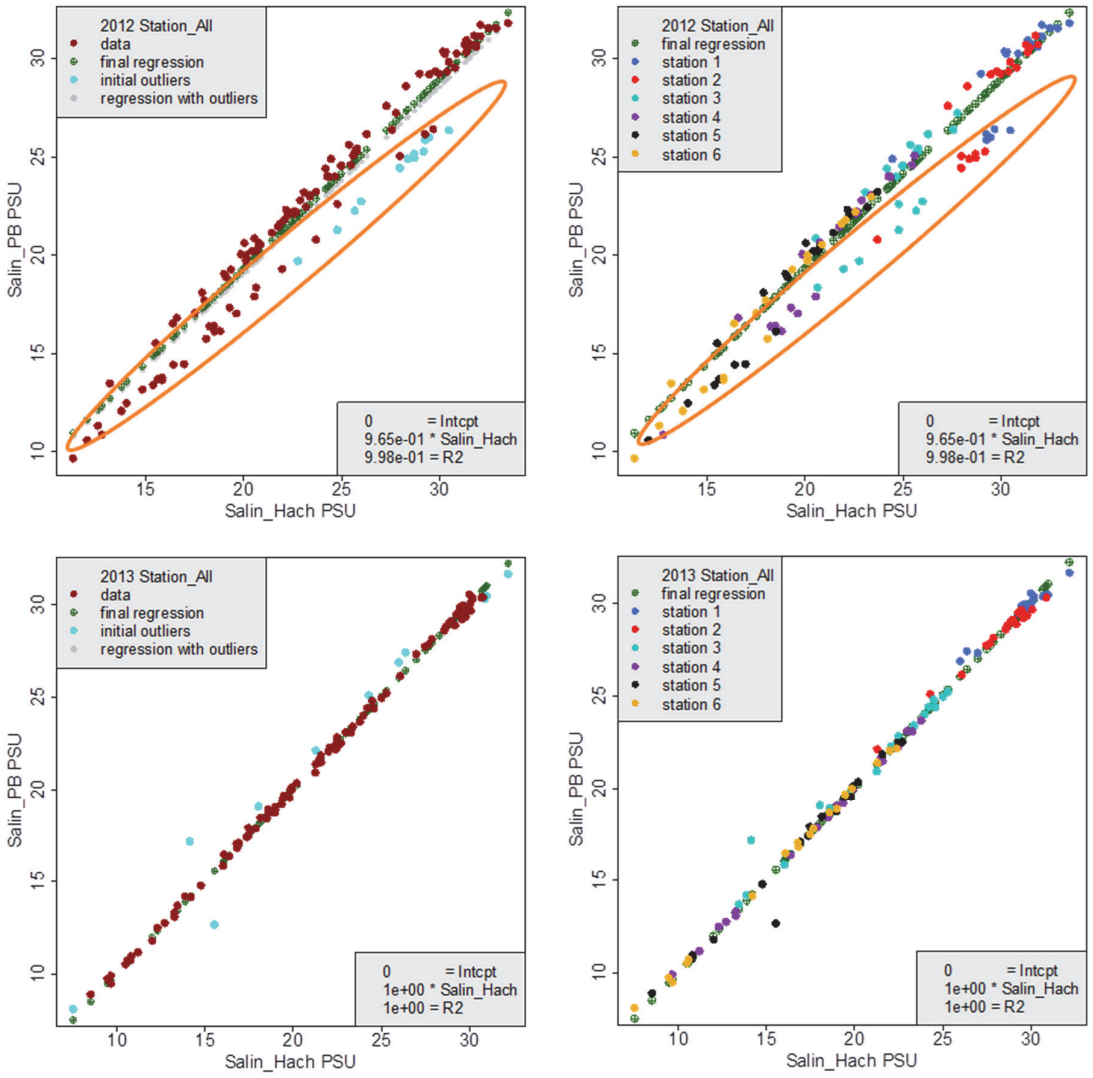

Figure 58 Salinity according to the PocketBox and the Hach-HQ handheld meter for 2012 (upper) and 2013 (lower). Salinity is always computed from conductivity. Left: all stations together, with outliers identified, right: each station is separately coloured.

The 2012-data that differ from the general picture concern the first seven cruises; deviations from the line similarly occur for all stations . From cruise 8 on, all PocketBox and Hach-HQ data are the same.

Conclusion for salinity measurements

The question now is whether the Hach-HQ data are the reliable ones or the PocketBox-values. Since the PocketBox calibration has been unaltered in the period 2012-2013, and the Hach-HQ meter is adjusted from time to time, it is more possible that something went wrong with the Hach-adjustments. *Thus, it is assumed that the PocketBox values represent the correct salinity data*.

7.5 C-Star1 and C-Star2 results

The C-Star1 and C-Star2 measurements give the light attenuation at each position; their unit according to the manual is m^{-1}. The C-Star1 sensor has a 10 cm light pathway, the C-Star2 sensor a 25 cm pathway. The latter therefore is more suitable in the most turbid areas of the system.

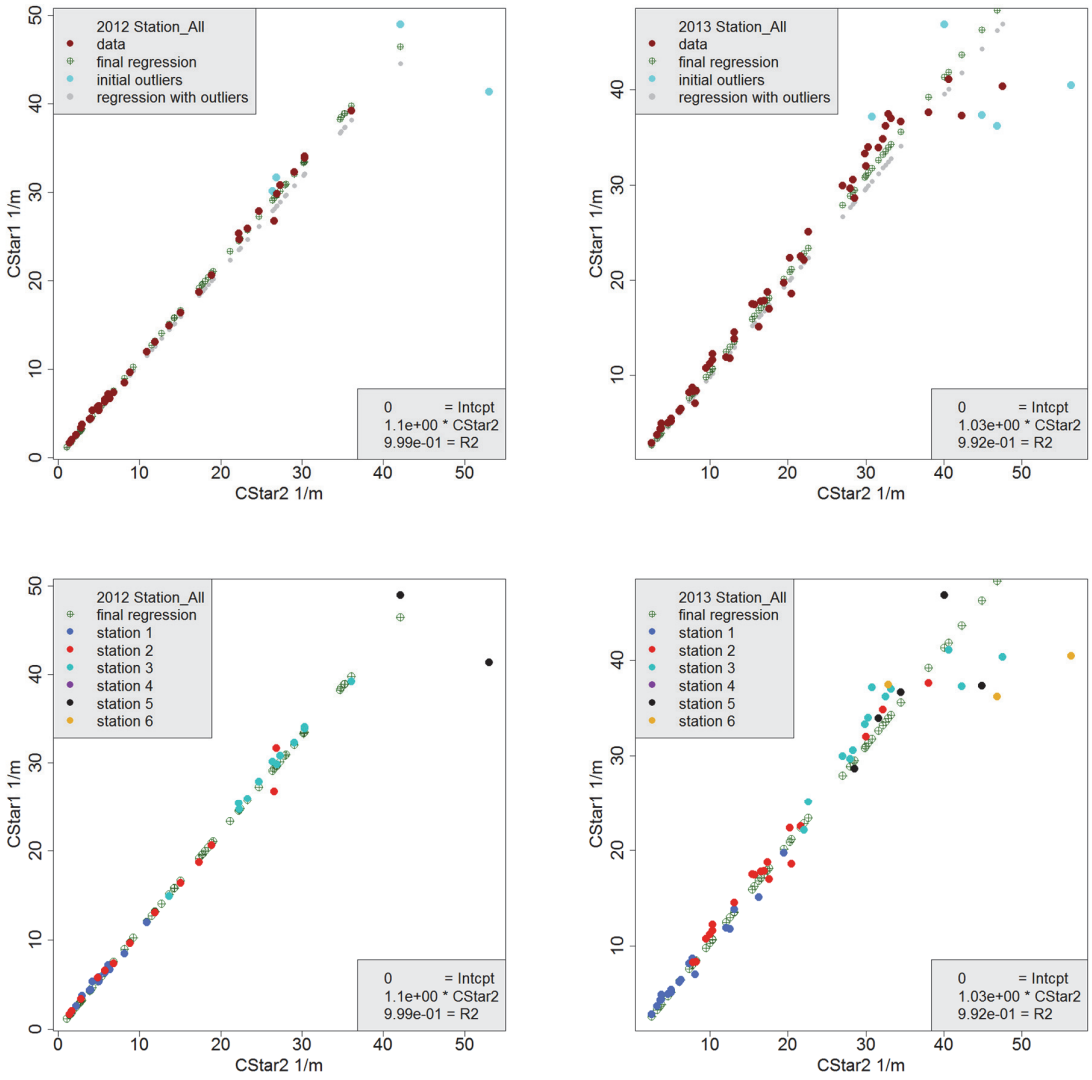

Figure 59 Results for the attenuation measurements with the C-Star1 and the C-Star2 sensors. Left: 2012, right: 2013. Upper all stations together, and outliers (with respect to the first regression) identified; lower: all data (including outliers), final regression line, and data coloured per monitoring site.

From Figure 59 it follows that both sensors differ only slightly. In 2012, the C-Star1 sensor gave a 10% higher output than the C-Star2 sensor; in 2013 this difference only was 3%. C-Star1 sensor values are preferably used further on, since the sensor is better suited for a turbid system like the Ems-Dollard.

7.6 C-Star transmittance values and the light attenuation coefficient K_d

The C-Star1 and C-Star2 measurements give the light attenuation at each position; their unit according to the manual is m^{-1}. The C-Star1 sensor has a 10 cm light pathway, the C-Star2 sensor a 25 cm pathway. The first therefore is more suitable in the most turbid areas of the system. Comparison with the K_d-measurements at each sampling point reveals large differences: whereas K_d-values range up to 10 à 20 m^{-1}, C-Star1 values reach their highest values possible (100). This is an indication that also the 10 cm sensor is not suitable to function in the most turbid areas of the system.

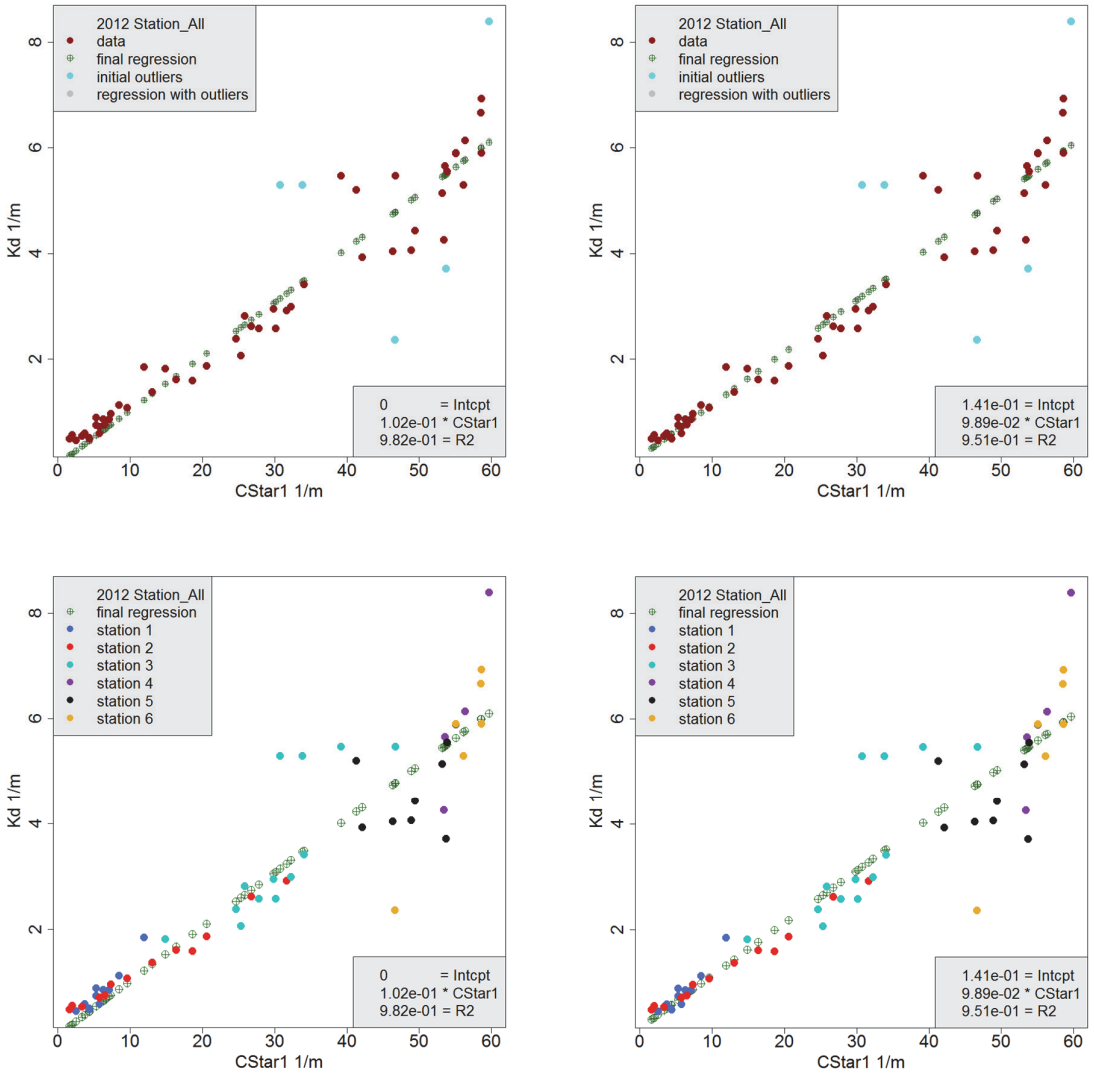

Figure 60 Relationship between C-Star1 measurements by the PocketBox, and the Kd-measurements performed at each sampling station in 2012. C-Star1 has a 10 cm light pathway. Left: without intercept, right: with intercept. In both upper graphs, the outliers were identified; in the lower graphs results for each sampling station are distinguished.

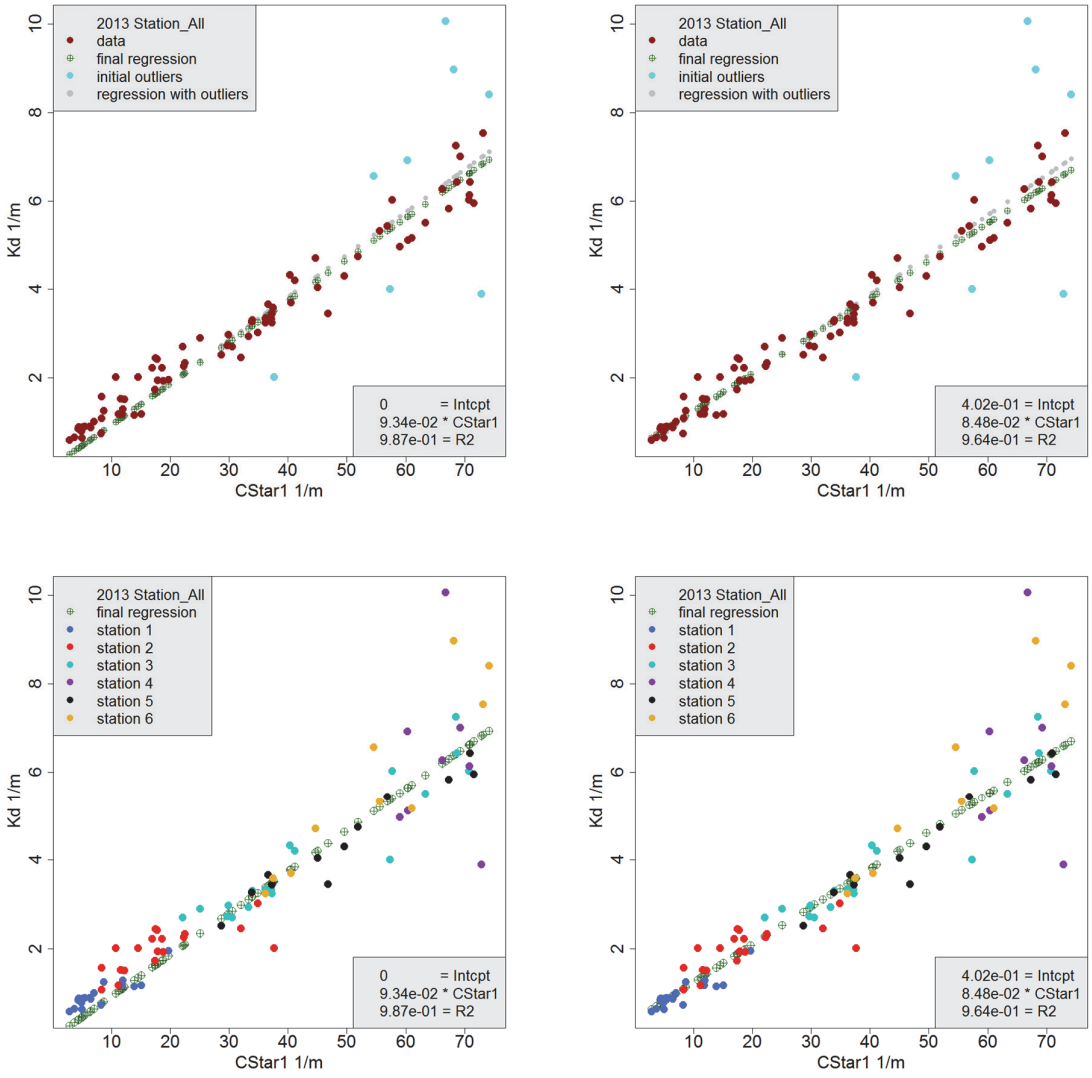

Figure 61 Relationship between C-Star1 measurements by the PocketBox, and the Kd-measurements performed at each sampling station in 2013. C-Star1 has a 10 cm light pathway. Left: without intercept, right: with intercept. In both upper graphs, the outliers were identified; in the lower graphs results for each sampling station are distinguished.

All values of k_d in 2012 and 2013 were related to the C-Star values, in Figure 60 and Figure 61 the relationship between k_d and C-Star1-values is depicted, for 2012 and 2103, respectively.

Regressions were performed for datasets were C-Star-values did not exceed a value of 60 (this should be m^{-1} but it isn't). For values close to 80 à 100, the sensor did not give a reliable result.

Values for the regression coefficient are a bit different in both years, as are the intercepts. In 2012 the intercept (0.14) comes close to zero (what would be expected), in 2013 the value found is 0.4. This might be an indication of not completely cleaned sensor surfaces.

A parameter overview including 95% reliability is given in Table 17 and Table 18. For the transformation of C-Star data to K_d-values, the C-Star1 data were used, with application of the coefficients 0.121 (2012) and 0.104 (2013).

Table 17 2012 regression coefficients, their 95% reliability and the R^2 of the regression line for K_d, C-Star1 and C-Star2 data. All regression lines are Y_Var = coeff * X_Var; the intercept was set to 0.0.

2012	Regression parameters			Std of regression parameters			
Y_Var	Kd	CStar1	CStar2	Kd_Std	CStar1_Std	CStar2_Std	R2
CStar1	9.60	-	-	0.179	-	-	0.982
CStar2	7.55	-	-	0.228	-	-	0.948
CStar1	-	-	1.103	-	-	0.005597	0.999
Kd	-	0.102	-	-	0.00191	-	0.982
Kd	-	-	0.121	-	-	0.003467	0.953

Table 18 2013 regression coefficients, their 95% reliability and the R^2 of the regression line for K_d, C-Star1 and C-Star2 data. All regression lines are Y_Var = coeff * X_Var; the intercept was set to 0.0.

2013	Regression parameters			Std of regression parameters			
Y_Var	Kd	CStar1	CStar2	Kd_Std	CStar1_Std	CStar2_Std	R2
CStar1	10.21	-	-	0.154	-	-	0.985
CStar2	9.38	-	-	0.192	-	-	0.978
CStar1	-	-	1.059	-	-	0.00707	0.997
Kd	-	0.095	-	-	0.00137	-	0.986
Kd	-	-	0.104	-	-	0.00213	0.978

7.7 Transformation of C-Star data into K_d-values: including dissolved substances

Next to the results from the previous section it is checked whether and, if yes, how the relationship between K_d-values and C-Star-data can be adjusted when including other data.

The relationship K_d= fie(C_Star1, CDOM, AOA-Chla, AOA_Yellow Substance) was checked. Results are summarized in Table 19. From Figure 62 it can be concluded that CDOM adds to the result in 2013, especially at low K_d values. There is little effect of Yellow Substance and/or chlorophyll-a. At the end, including all variables gives best results for 2013, but for 2012 extra variables next to C-Star1 do not contribute to a better result (graphs not shown here).

Concluding: K_d-values can be computed from PocketBox-data using the equation

$$K_d = a_1 \cdot CStar1 + b_1 \cdot CDOM \qquad (m^{-1}) \qquad (28)$$

With

a_1 = 0.098 (2012) and 0.082 (2013)

b_1 = 0.0038 (2012) and 0.0073 (2013)

C-Star1-data are in m^{-1}, and CDOM in µg l^{-1}.

Table 19 2012 and 2013 regression coefficients, their 95% reliability and the R^2 of the regression line for K_d as a linear function of C-Star1, CDOM, AOA-Chla and AOA_Yellow Substance. The intercept was set to 0.0. Final equation used is marked light green.

2012	Regression parameters						Std of regression parameters			
Y_Var	a	CDOM	AOA_ Chla	AOA_ Yellow Subs	CStar1	R2	CDOM	AOA_ Chla	AOA_ Yellow Subs	CStar1
Kd					0.103	0.96				0.003
Kd		0.0038			0.098	0.96	0.006			0.009
Kd		0.0014	0.016		0.098	0.96	0.006	0.044		0.009
Kd		0.0019	0.015	0.019	0.096	0.96	0.012	0.044	0.55	0.010
2013	Regression parameters						Std of regression parameters			
Y_Var	a	CDOM	AOA_ Chla	AOA_ Yellow Subs	CStar1	R2	CDOM	AOA_ Chla	AOA_ Yellow Subs	CStar1
Kd					0.098	0.98				0.002
Kd		0.0073			0.082	0.97	0.002			0.005
Kd		0.0049	0.018		0.084	0.98	0.002	0.008		0.004
Kd		-0.0027	0.025	0.413	0.083	0.98	0.004	0.008	0.19	0.004

Predicted values for k_d are plotted against observations in Figure 62, showing that the equations chosen gives reasonable results. But it is also clear that values for k_d>7 are not predicted; a consequence of the limited range of the C-Star1 values.

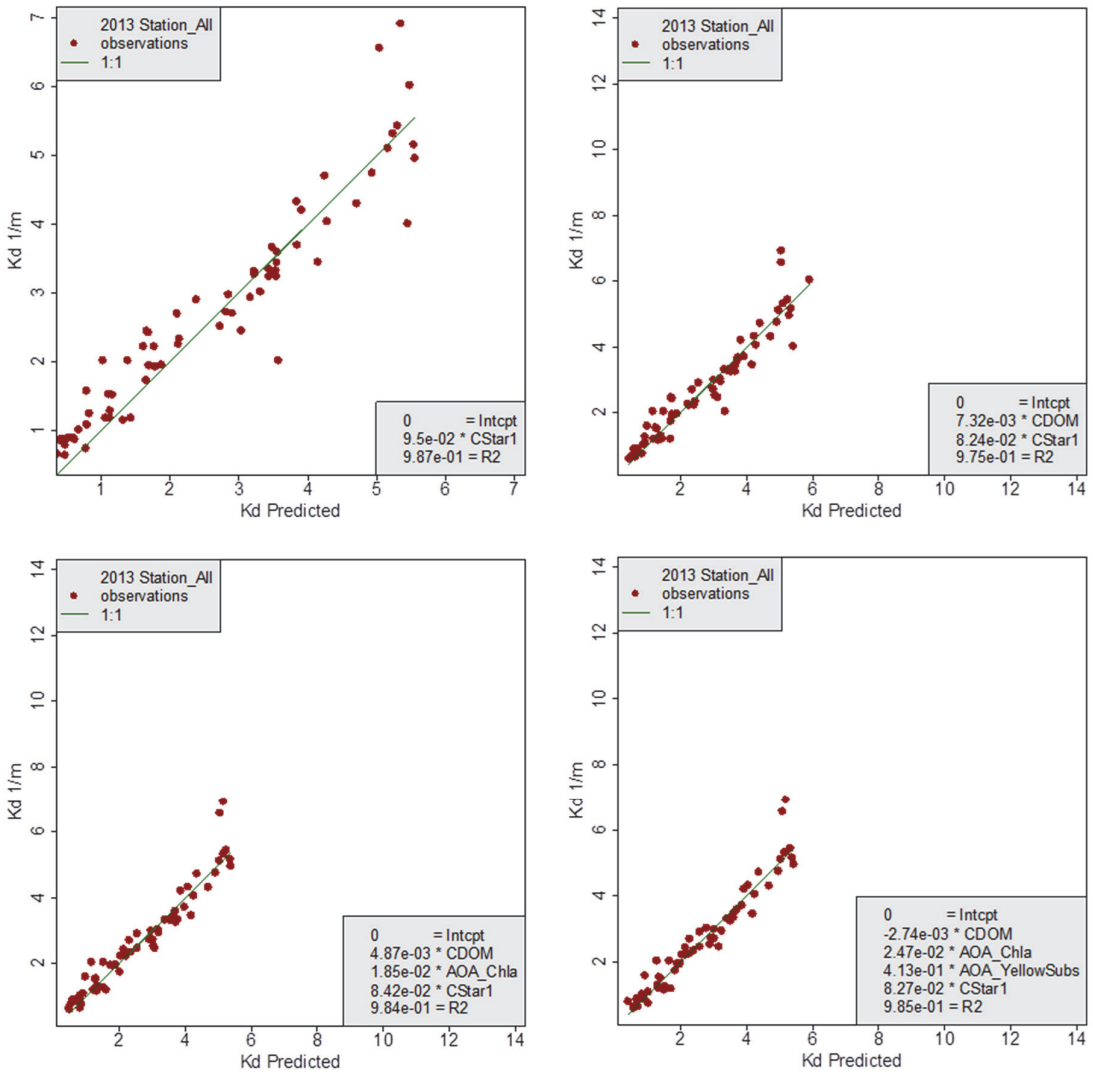

Figure 62 2013 Light attenuation coefficient K_d as a function of C-Star1-attenuation data, chlorophyll-a, CDOM and yellow Substances. X-axis: predicted K_d-values from the regression function found ; Y-axis: the measured values

7.8 Transformation of turbidity data into K_d-values

Turbidity data provide another possibility to estimate k_d-values in the more turbid areas of the system. It is shown in Figure 63 how well k_d can be explained by turbidity values alone and in combination with observations for CDOM, chlorophyll-a and yellow substances. The lower

Table 20 Light attenuation values k_d predicted from turbidity, CDOM, AOA-chlorophyll-a and AOA-yellow substances. Upper table: 2012, lower 2013. Upper halves: intercept allowed, lower halves, intercept=0. The green shades regression results are the final choice.

2012		Regression coefficients						Standard deviations of regression coefficients				
nr	Y_Var	Incpt	CDOM	AOA_Chla	AOA_ YellowSub	Turb idity	R2	Incpt	CDOM	AOA_ Chla	AOA_ YellowSu	Turbidit
86	Kd	0.11				0.065	0.71	0.28				0.0041
87	Kd	-0.79			1.40	0.050	0.79	0.32			0.27	0.0040
88	Kd	-0.57	0.025			0.053	0.79	0.30	0.005			0.0038
89	Kd	-0.76	0.003		1.15	0.054	0.72	0.41	0.009		0.52	0.0051
90	Kd	-0.89	0.007	0.12	0.88	0.052	0.66	0.57	0.013	0.091	0.75	0.0055
nr	Y_Var	Incpt	CDOM	AOA_Chla	AOA_ YellowSub	Turb idity	R2	Incpt	CDOM	AOA_ Chla	AOA_ YellowSu	Turbidit
86	Kd					0.066	0.91					0.0021
87	Kd				0.94	0.049	0.92				0.21	0.0041
88	Kd		0.019			0.051	0.92		0.004			0.0037
89	Kd		0.001		0.77	0.054	0.89		0.010		0.49	0.0051
90	Kd		0.003	0.05	0.75	0.052	0.87		0.013	0.087	0.74	0.0056

2013		Regression coefficients						Standard deviations of regression coefficients				
nr	Y_Var	Incpt	CDOM	AOA_Chl a	AOA_ YellowSubs	Turb idity	R2	Incpt	CDOM	AOA_ Chla	AOA_ YellowSu	Turbidit
86	Kd	0.29				0.053	0.80	0.22			0	0.0027
87	Kd	-0.44			1.21	0.039	0.87	0.21				0.0029
88	Kd	-0.62	0.02			0.042	0.86	0.22	0.003			0.0025
89	Kd	-0.34	0.00		1.58	0.034	0.77	0.33	0.010		0.52	0.0038
90	Kd	-0.77	-0.01	0.073	2.34	0.031	0.77	0.41	0.011	0.027	0.58	0.0040
nr	Y_Var	Incpt	CDOM	AOA_Chl a	AOA_ YellowSub	Turb idity	R2	Incpt	CDOM	AOA_ Chla	AOA_ YellowSu	Turbidit
86	Kd					0.055	0.94					0.0014
87	Kd				1.04	0.038	0.96				0.14	0.0029
88	Kd		0.019			0.040	0.96		0.003			0.0024
89	Kd		-0.005		1.55	0.033	0.93		0.010		0.52	0.0037
90	Kd		-0.016	0.047	2.12	0.030	0.93		0.011	0.023	0.58	0.004

graphs in Figure 63 give an idea of the quality of the prediction. However, there's only a minor improvement between the prediction based on turbidity alone, and the one with CDOM, chlorophyll-a and yellow substances added as independent variables; it is hardly visible when comparing the graphs. This also follows from Table 20; the reliability of the turbidity regression coefficients is in the order of 5-10% of the values, while this ratio is much higher for the other three

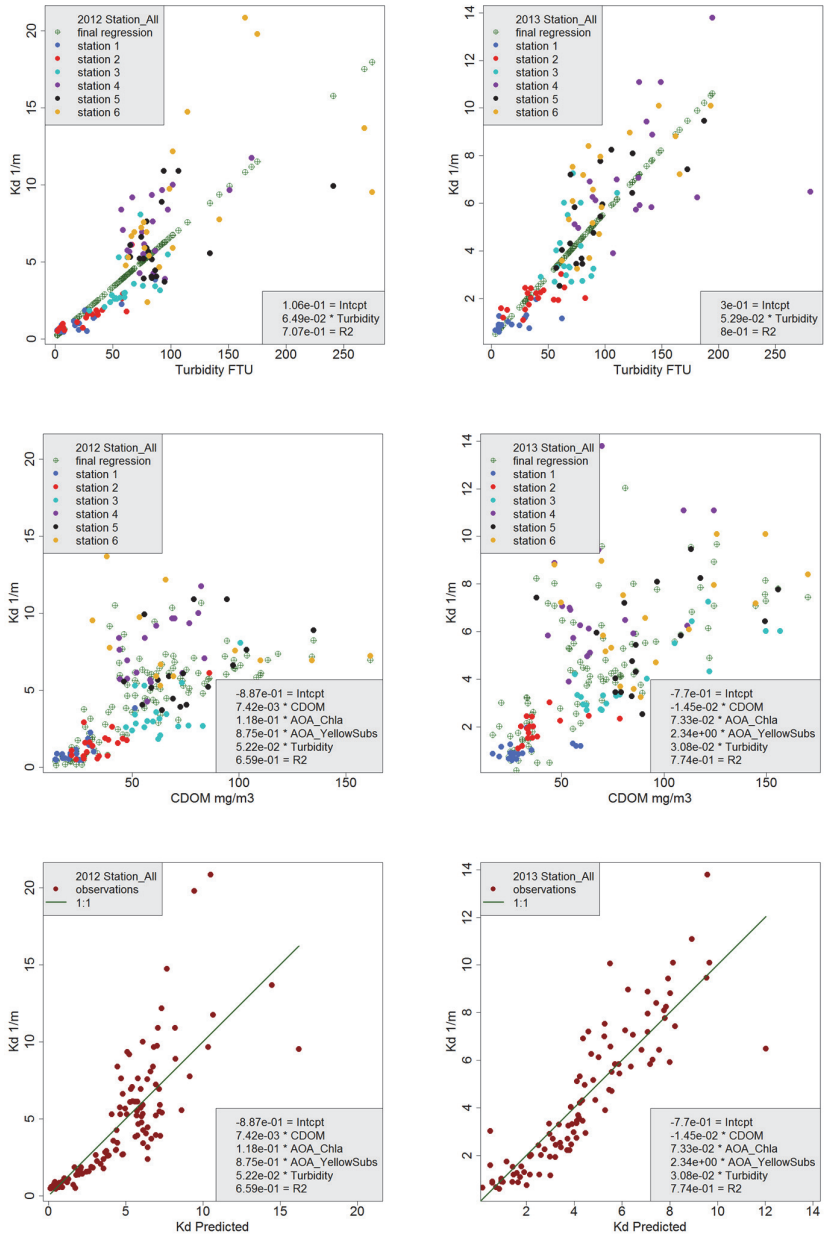

Figure 63 Light attenuation coefficient k_d. Upper: as a function of turbidity alone, mid: as a function of CDOM, Chlorophyll-a, YellowSubstances and turbidity. Lower: Same as the middle two, but now the predicted k_d-values (X-axis) against the observed values (Y-axis).

covariates. This is also the case for the intercept, and therefore, the equation k_d = a* turbidity, with a=0.066 in 2012, and 0.055, is the final choice.

7.9 Extinction coefficient k_d and suspended matter

The topic in the previous sections was how to find best values for the light attenuation coefficient from the PocketBox-data, since it is a crucial variable when computing primary production.

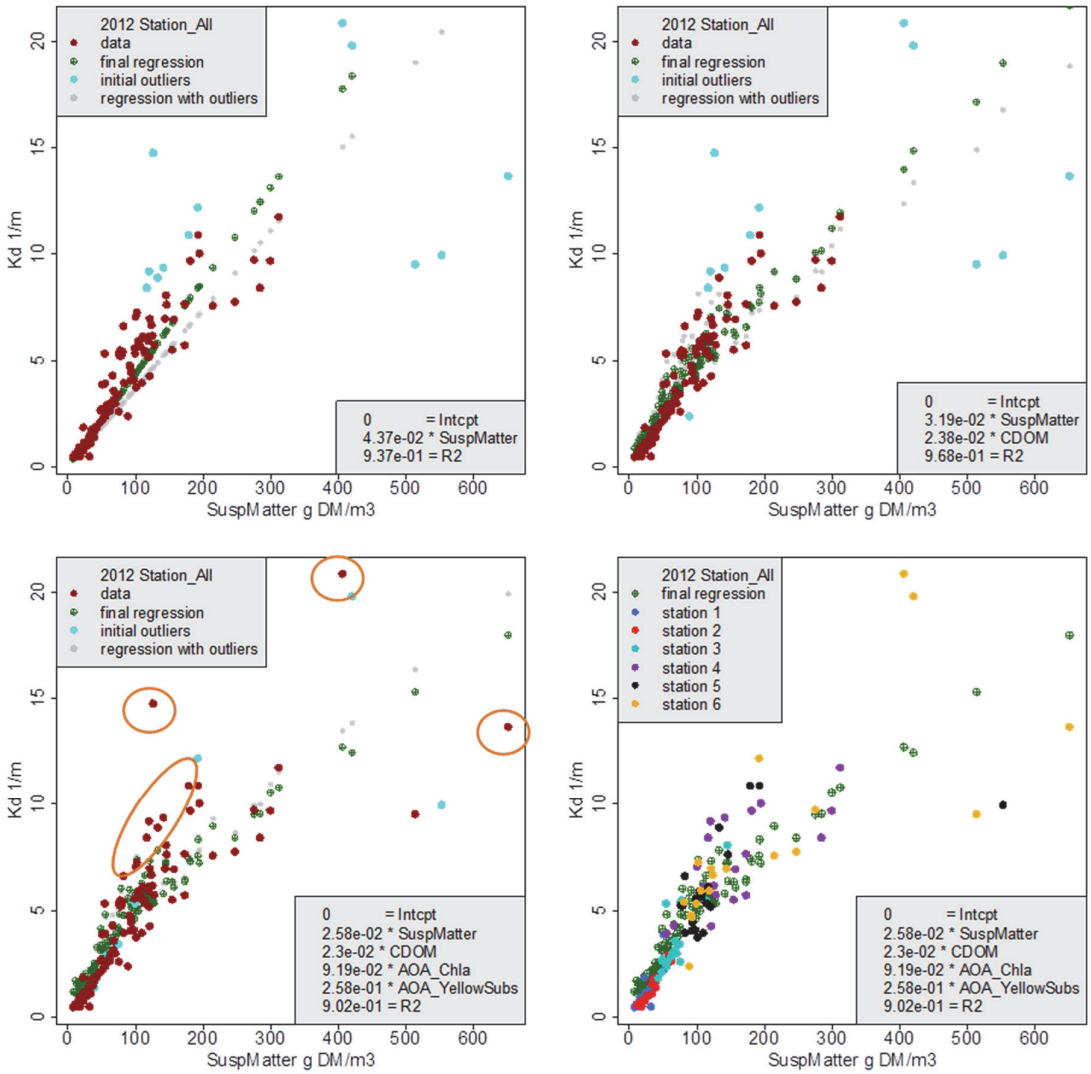

Figure 64 Relationship between Kd, suspended matter, CDOM, Chl-a and yellow substances in 2012. Upper left: only Suspended matter as independent variable; upper right: CDOM (coloured organic matter) is included; lower left: all variables included. Note that the R2-value gets lower in the lower left graph; this is because a number of data points that were identified as outliers in the upper right graph are now part of the R2-computation (in the orange circles/ellipse). Lower right: as lower left, but with all station separately coloured.

The question now is how the light attenuation coefficient depends on the suspended matter concentration in the water column: the relationship between extinction coefficient (K_d), suspended matter and coloured substances has been checked. K_d is available at every sampling station as is suspended matter. Other variables come from the PocketBox-dataset. Examples for the 2012 results are shown in Figure 64, for 2013 in Figure 65.

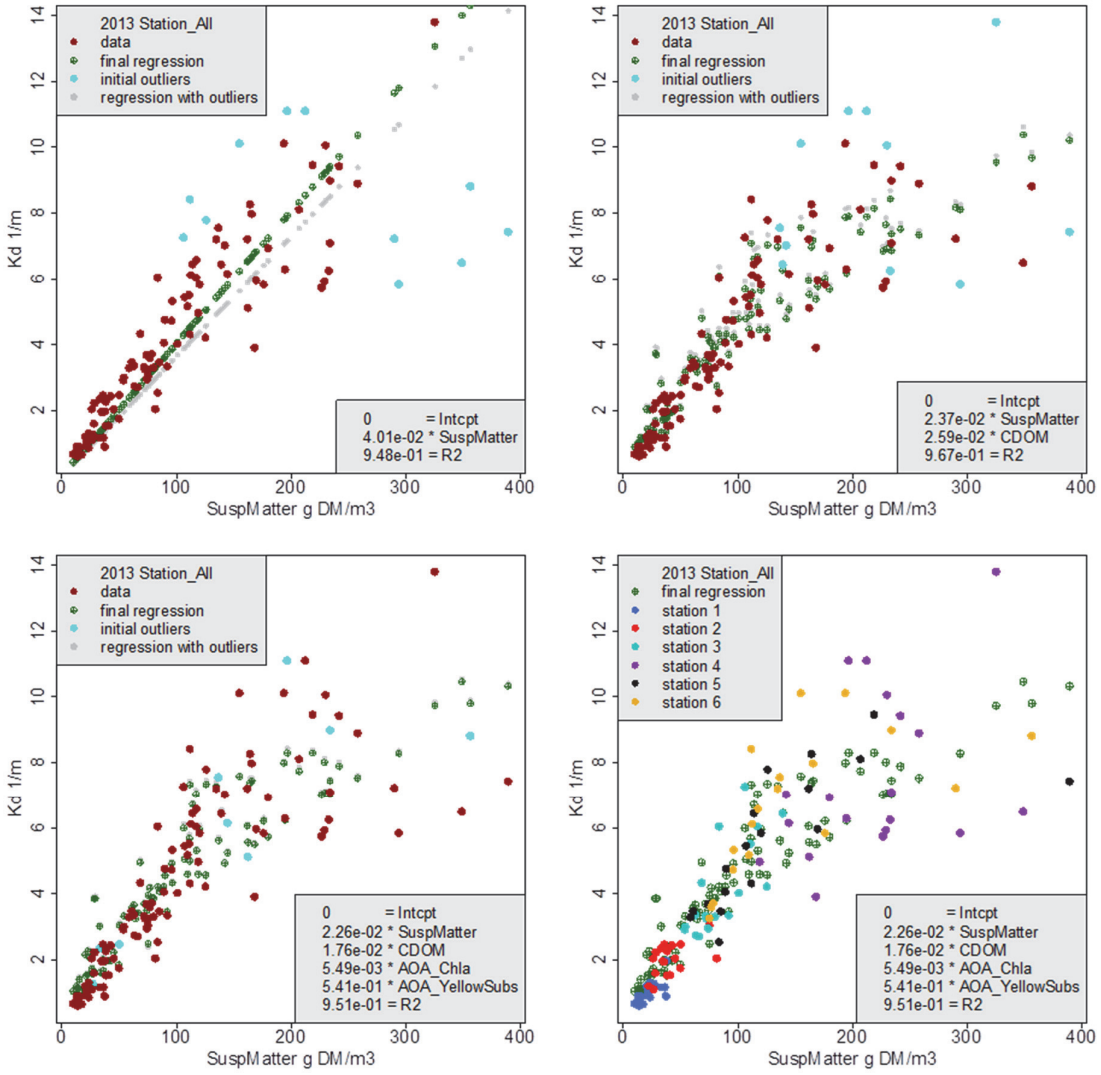

Figure 65 Relationship between Kd, suspended matter, CDOM, Chl-a and yellow substances in 2012. Upper left: only Suspended matter as independent variable; upper right: CDOM (coloured organic matter) is included; lower left: all variables included. Lower right: as lower left, but with all station separately coloured.

Coloured dissolved organic matter (CDOM) or Yellow Substance contributes significantly to K_d. It can be seen from both upper graphs in Figure 64 and Figure 65 that suspended matter alone (both the left graphs) does not produce good predictions when concentrations are high. This is accounted for by high values of CDOM and/or Yellow Substance.

Regression coefficients are mentioned in Table 21. The green shades values gave best results.

Table 21 2012 and 2013 Relationships between the light attenuation coefficient k_d and suspended matter plus a number of additional variables. K_d in m^{-1}, suspended matter in g DW l^{-1} and CDOM and both AOA-variables in µg l^{-1}. Light green cells denote the relationship applied for 2012 and 2013. CDOM originates from the Cyclops-sensor in the PocketBox (section 4.5.4).

2012	Regression parameters						Std of regression parameters			
Y_Var	a	Susp Matter	CDOM	AOA_ Chla	AOA_ Yellow Subs	R^2	Susp Matter	CDOM	AOA_ Chla	AOA_ Yellow Subs
Kd		0.044				0.94	1.1E-03			
Kd		0.032	0.024			0.97	1.4E-03	0.002		
Kd		0.030			1.30	0.90	2.4E-03			0.21
Kd		0.025		0.075	1.40	0.90	2.1E-03		0.074	0.29
Kd		0.025		0.075	1.40	0.90	2.1E-03		0.074	0.29
Kd		0.026	0.023	0.092	0.26	0.90	2.1E-03	0.011	0.073	0.62
2013	Regression parameters						Std of regression parameters			
Y_Var	a	Susp Matter	CDOM	AOA_ Chla	AOA_ Yellow Subs	R2	Susp Matter	CDOM	AOA_ Chla	AOA_ Yellow Subs
Kd		0.037				0.89	1.3E-03			
Kd		0.023	0.029			0.95	1.3E-03	0.002		
Kd		0.022			1.40	0.95	1.7E-03			0.14
Kd		0.022		0.025	1.37	0.95	1.7E-03		0.016	0.14
Kd		0.022		0.025	1.37	0.95	1.7E-03		0.016	0.14
Kd		0.023	0.016	0.007	0.56	0.95	2.0E-03	0.010	0.019	0.51

7.10 Turbidity and suspended plus dissolved matter

Next to both the C-Star1 & 2 light attenuation sensors, the turbidity sensor signal (FTU) depends on the amount of suspended solids in the water. The turbidity sensors measure a light reflection signal, and therefore depend in a way different from the C-Star sensors on the type of suspended matter. Regression coefficients are listed in Table 22. The 2012 graphs show that turbidity is best related with suspended matter combined with CDOM as a correction. With slightly different regression coefficients, the 2013 data give similar results: FTU is best explained by suspended matter plus CDOM.

Table 22 2012 and 2013 Relationships between turbidity and suspended matter plus a number of additional variables. Turbidity in FTU, suspended matter in g DW l^{-1} and CDOM and both AOA-variables in µg l^{-1}.

2012	Regression parameters						Std of regression parameters			
Y_Var	a	Susp Matter	CDOM	AOA_ Chla	AOA_ Yellow Subs	R2	Susp Matter	CDOM	AOA_ Chla	AOA_ Yellow Subs
Turbidity		0.58				0.93	0.02			
Turbidity		0.39	0.43			0.97	0.01	0.03		
Turbidity		0.42		3.79		0.94	0.02		0.53	
Turbidity		0.40			17.89	0.96	0.02			1.77
Turbidity		0.39	0.27	1.00	3.21	0.96	0.02	0.10	0.72	5.82
2013	Regression parameters						Std of regression parameters			
Y_Var	a	Susp Matter	CDOM	AOA_ Chla	AOA_ Yellow Subs	R2	Susp Matter	CDOM	AOA_ Chla	AOA_ Yellow Subs
Turbidity		0.63				0.92	0.02			
Turbidity		0.49	0.31			0.95	0.02	0.04		
Turbidity		0.62		0.48		0.92	0.02		0.35	
Turbidity		0.49			14.70	0.95	0.03			2.39
Turbidity		0.51	0.46	-0.22	-7.65	0.95	0.03	0.17	0.33	8.92

More interesting is the reverse relationship: estimation of suspended matter by turbidity. Relationships are mentioned in Table 23 and pictured in Figure 70. Suspended matter (mg l^{-1}) is best described by turbidity (FTU), corrected with CDOM-values (µg l^{-1}):

Suspended matter = a1 * Turbidity + a2 * CDOM (mg l^{-1})

With

a1= 1.78 (2012) and 1.65 (2013),

a2= -0.32 (2012) and -0.26 (2013).

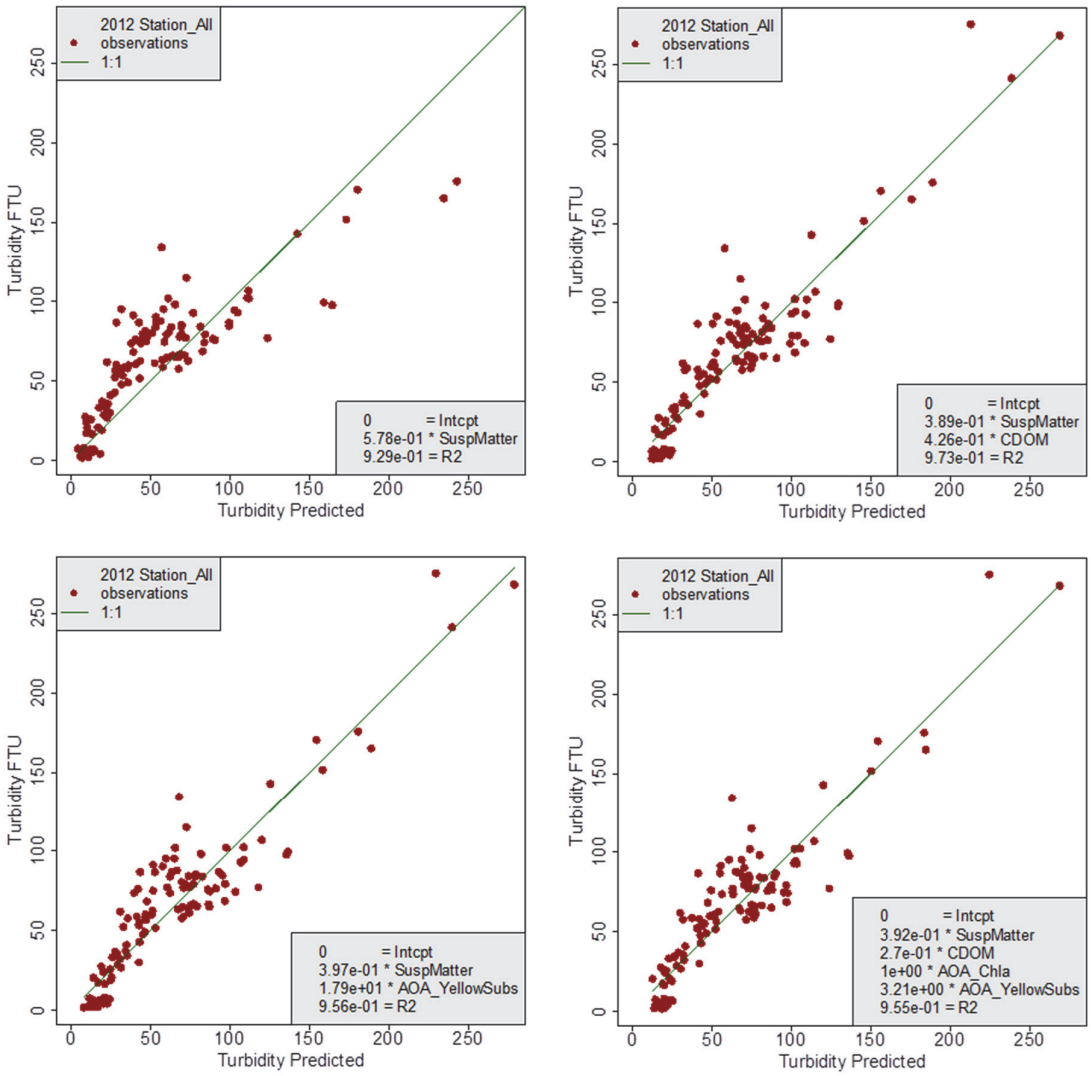

Figure 66 2012: Turbidity measured (Y-axis) and as predicted from suspended matter concentration and some more independent variables (X-axis).

Table 23 2012 and 2013 Regression parameters and reliability for relationships between suspended matter and turbidity and some additional variables. Independent variables are all recorded by the PocketBox. Regressions with intercept a=0. Light green cells denote the final regression equation choice.

2012	Regression parameters						Std of regression parameters			
Y_Var	a	CDOM	AOA_ Chla	AOA_ Yellow Subs	Turbidity	R2	CDOM	AOA_ Chla	AOA_ Yellow Subs	Turbidity
SuspMatter					1.53	0.94				0.038
SuspMatter				-20.14	1.99	0.94			4.24	0.079
SuspMatter			-0.750		1.59	0.94		0.97		0.072
SuspMatter		-0.32			1.78	0.94	0.080			0.073
SuspMatter		-0.52	-0.044		2.04	0.92	0.118	1.37		0.098
SuspMatter		-0.63		10.20	1.92	0.92	0.206		10.40	0.095
SuspMatter		-0.69	-0.971	11.02	2.02	0.92	0.229	1.67	13.56	0.103
2013	Regression parameters						Std of regression parameters			
Y_Var	a	CDOM	AOA_ Chla	AOA_ Yellow Subs	Turbidity	R2	CDOM	AOA_ Chla	AOA_ Yellow Subs	Turbidity
SuspMatter					1.43	0.94				0.035
SuspMatter				-6.64	1.56	0.94			4.42	0.094
SuspMatter			0.018		1.42	0.94		0.40		0.046
SuspMatter		-0.26			1.65	0.95	0.072			0.071
SuspMatter		-0.32	1.587		1.58	0.94	0.094	0.83		0.085
SuspMatter		-1.15		51.61	1.47	0.94	0.243		13.06	0.089
SuspMatter		-1.35	2.695	59.04	1.31	0.94	0.237	0.80	12.45	0.095

7.11 C-Star1 attenuation coefficients and suspended matter

Similar to the topic handled above for k_d-values, also C-Star1 attenuation coefficients can be related to suspended matter concentrations and CDOM, etc. In Figure 67 some results are shown for 2012; the relationship between C-Star1 attenuation coefficients and suspended matter with or without CDOM as covariate is much better than the one shown in the previous section for k_d. However, C-Star1 data are not available for the most turbid areas, and it is there where the relationship between suspended matter and k_d is worse than it is for the stations 1-3 (Figure 63). Results for 2013 (not shown) are a bit more scattered. A comparison for observations and predicted values for C-Star1 attenuation coefficients is presented in Figure 68. Regression results are summarized in Table 24.

Different from the figures for K_d, there is only little improvement in the C-Star1 <-> suspended solids relationship when adding CDOM, Yellow Substances or chlorophyll-a as covariate. This also is related to the fact that the most turbid areas are not part of the regression.

Thus, for the lower and middle regions of suspended matter values, the relationship also offers a good possibility to estimate suspended solid concentrations from the C-Star1 values. This and other

attempts to estimate suspended solids concentrations in the water column are presented in the next sections.

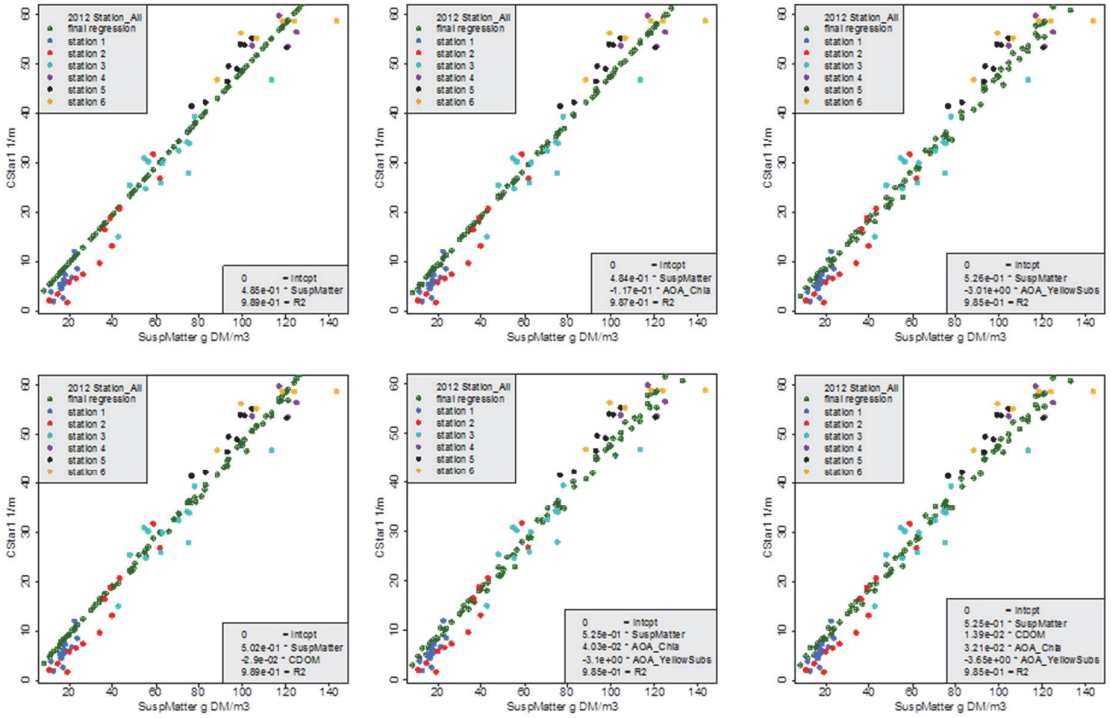

Figure 67 2012-Relationship between C-Star1-data (as extinction coefficient, m^{-1}), suspended matter, CDOM, Chl-a and yellow substances in 2012. Upper left: only Suspended matter as independent variable; both other two upper and lower left graph: AOA-Chla, AOA-Yellow Substance and CDOM added (respectively) as covariate. Lower middle: chl-a and yellow substance added; lower right: all variables added. All station separately coloured.

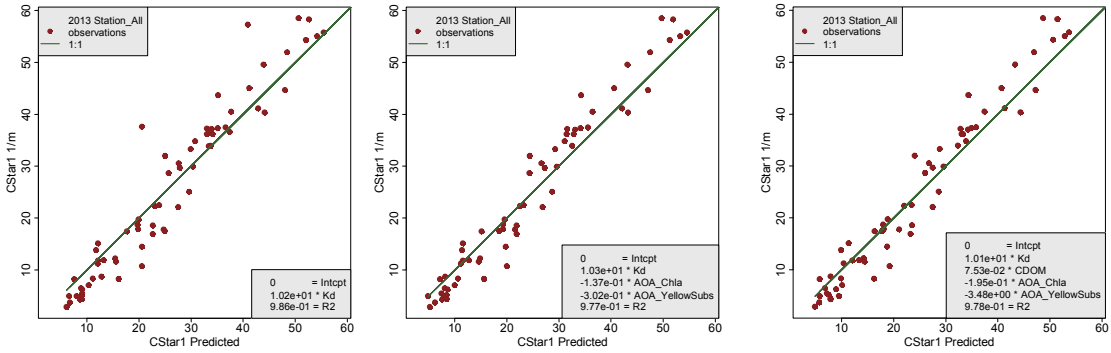

Figure 68 C-Star1 extinction coefficients, measured (Y-axis) and predicted (X-axis) from the mentioned independent variables. Left: K_d as only explaining variable; middle: Chlorophyll-a and yellow substances added; right: also CDOM added.

Table 24 Regression parameters and reliability for several relationships between C-Star1 and a number of explaining variables, Note that R^2-values are after removal of outliers. Green shaded is the preferred relationship.

2012		Regression coefficients						Standard dev regress. coefficients.				
nr	Y_Var	Intcpt	Susp Matter	CDOM	AOA_Chla	AOA_Yellow Subs	R2	Intcpt	Susp Matter	CDOM	AOA_Chla	AOA_Yellow Subs
34	CStar1	-3.02	0.51				0.96	1.02	0.014			
35	CStar1	-3.32	0.50	0.018			0.96	1.24	0.024	0.041		
36	CStar1	-5.13	0.49		0.703		0.97	1.28	0.016		0.28	
37	CStar1	-4.15	0.49			2.04	0.96	1.45	0.031			2.42
38	CStar1	-5.51	0.48	0.021	0.715		0.97	1.47	0.026	0.040	0.28	
39	CStar1	-7.46	0.44		0.888	3.90	0.97	1.97	0.035		0.30	2.52
40	CStar1	-8.67	0.43	-0.086	1.057	8.47	0.97	2.17	0.037	0.068	0.33	4.38
2013												
34	CStar1		0.44				0.94		0.013			
35	CStar1		0.31	0.198			0.97		0.016	0.020		
36	CStar1		0.44		0.022		0.94		0.016		0.15	
37	CStar1		0.32			9.65	0.97		0.019			1.17
38	CStar1		0.31	0.208	-0.170		0.97		0.018	0.023	0.11	
39	CStar1		0.30		0.027	10.29	0.97		0.020		0.11	1.20
40	CStar1		0.30	0.149	-0.102	3.37	0.97		0.019	0.069	0.12	3.48

7.12 Estimating suspended matter concentrations from C-Star1 data, data on turbidity, CDOM and Yellow Substance and k_d- measurements

In the previous sections it was investigated how to estimate the light attenuation parameter(s) from data on suspended solids, turbidity, yellow substances and CDOM. Next, the question is how to estimate suspended solid concentrations from continuous measurements and from k_d-measurements. Since most of these are reverse actions of what was elaborated above, a short overview will do.

7.12.1 Suspended matter and C-Star1-measurements

Regression coefficients for Suspended Matter=fie(CDOM, Yellow Substance, AOA-Chlorophyll-a, C-Star1) are given in Table 25 and Table 26. The best choice is marked green: the use of C-Star1 values alone will do. Note: C-Star1-values are not available in the most turbid areas of the system, and it is there that CDOM etc becomes important.

Table 25 2012: Regression parameters and reliability for relationships between suspended matter and some continuously recorded PocketBox-variables. Regressions with intercept a=0. Light green cells indicate the relationship applied to compute suspended matter concentrations from PocketBox-data

2012	Regression parameters						Std of regression parameters			
Y_Var	a	CDOM	AOA_ Chla	AOA_ Yellow Subs	CStar1	R2	CDOM	AOA_ Chla	AOA_ Yellow Subs	CStar1
SuspMatter					2.04	0.99				0.030
SuspMatter		0.241			1.73	0.99	0.058			0.086
SuspMatter			1.01		1.93	0.99		0.47		0.072
SuspMatter				13.04	1.62	0.99			2.61	0.094
SuspMatter		-0.045		15.33	1.62	0.99	0.123		5.55	0.094
SuspMatter		-0.051	0.16	15.13	1.61	0.99	0.125	0.44	5.62	0.097

Table 26 2013: Regression parameters and reliability for relationships between suspended matter and some continuously recorded PocketBox-variables. Regressions with intercept a=0. . Light green cells indicate the relationship applied to compute suspended matter concentrations from PocketBox-data

2013	Regression parameters						Std of regression parameters			
Y_Var	a	CDOM	AOA_ Chla	AOA_ Yellow Subs	CStar1	R2	CDOM	AOA_ Chla	AOA_ Yellow Subs	CStar1
SuspMatter					2.02	0.98				0.04
SuspMatter		-0.121			2.33	0.95	0.078			0.16
SuspMatter			0.58		2.07	0.95		0.30		0.08
SuspMatter				-5.06	2.35	0.95			3.73	0.15
SuspMatter		-0.001		-5.92	2.38	0.95	0.146		6.87	0.17
SuspMatter		-0.144	0.36	1.40	2.33	0.95	0.165	0.26	7.82	0.16

7.12.2 Suspended matter and k_d -measurements

Regression coefficients for Suspended Matter=fie(k_d, CDOM,Yellow Substance) are given in Table 27.

A short overview of the most important results is drawn in Figure 69. It is concluded that in 2012, suspended matter= 20.2 * k_d , in 2013 : suspended matter= 24.3 * k_d. Suspended matter in mg l^{-1}, k_d in m^{-1}.

Table 27 Regression parameters and reliability for relationships between suspended matter, k_d and continuously recorded PocketBox-variables CDOM and AOA_Yellow Substances. Regressions with and without intercept. Light green cells indicate 'best' relationship. Suspended matter in mg l^{-1}, k_d in m^{-1}, CDOM and Yellow Substances in µg l^{-1}.

2012		Regression parameters					Std.dev of regression parameters			
nr	Y_Var (mg/l)	Intcpt	Kd	CDOM	AOA_ Yellow Subs	R2	Intcpt	Kd	CDOM	AOA_ Yellow Subs
10	SuspMatter	3.35	19.7			0.91	3.22	0.59		
91	SuspMatter	16.82	21.9	-0.40		0.90	4.41	0.80	0.08	
92	SuspMatter	7.08	18.4		0.41	0.81	7.23	1.07		6.15
93	SuspMatter	7.99	18.6	-0.36	15.06	0.81	7.18	1.06	0.17	8.73
10	SuspMatter		20.2			0.96		0.38		
91	SuspMatter		22.6	-0.18		0.96		0.87	0.07	
92	SuspMatter		17.9		5.63	0.93		1.02		3.93
93	SuspMatter		18.6	-0.34	19.23	0.93		1.06	0.17	7.89

2013		Regression parameters					Std.dev of regression parameters			
nr	Y_Var (mg/l)	Intcpt	Kd	CDOM	AOA_ Yellow Subs	R2	Intcpt	Kd	CDOM	AOA_ Yellow Subs
10	SuspMatter	-1.84	24.3			0.71	8.31	1.55		
91	SuspMatter	20.46	27.6	-0.59		0.82	6.34	1.46	0.11	
92	SuspMatter	17.54	30.4		-30.85	0.75	9.70	2.27		8.64
93	SuspMatter	24.99	28.0	-1.27	31.28	0.79	9.09	2.14	0.28	15.78
10	SuspMatter		24.0			0.89		0.84		
91	SuspMatter		27.8	-0.35		0.94		1.32	0.08	
92	SuspMatter		30.6		-21.86	0.90		2.29		7.16
93	SuspMatter		28.4	-1.14	37.28	0.91		2.21	0.28	16.20

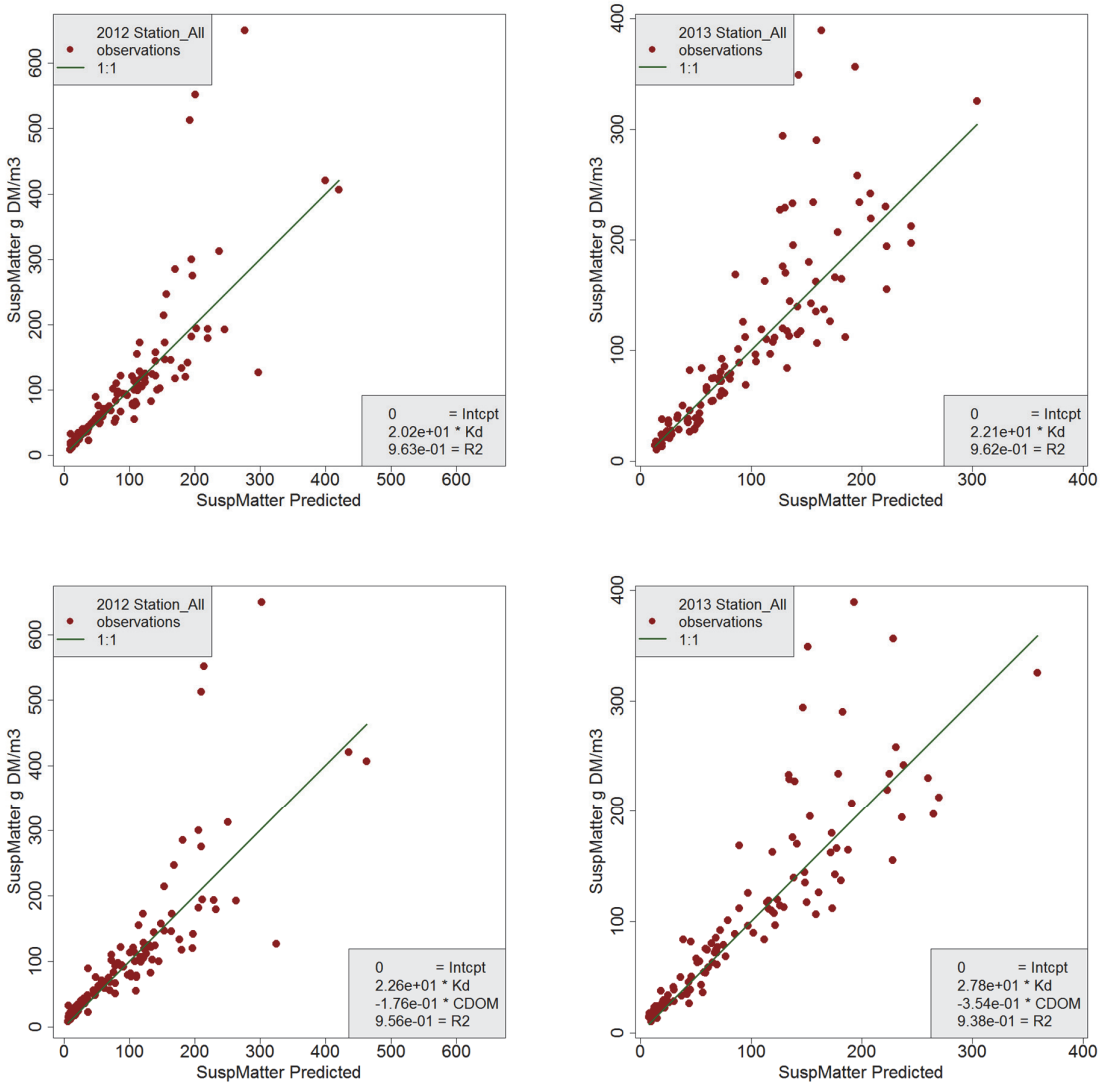

Figure 69 Predicted and observed suspended matter concentrations. Predictions based on the light attenuation coefficient k_d alone (upper graphs), and k_d plus CDOM (lower graphs). Left: 2012, right: 2013.

7.12.3 Suspended matter and turbidity

Regression coefficients for Suspended Matter=fie(Turbidity, CDOM, Chla, Yellow Substance) are given in Table 27.

A short overview of the most important results is drawn in Figure 70. It is concluded that in 2012, suspended matter= 1.53 * Turbidity, in 2013 : suspended matter= 1.46 * Turbidity. Suspended matter in mg l^{-1}, Turbidity in FTU. Note that regression results sometimes give a positive contribution of e.g. yellow substances to suspended matter. This is not what is expected: turbidity is expected to be a sum of all light reflecting particles and substances, including yellow substance, and thus, the

latter should have a negative regression coefficient when describing suspended matter concentration.

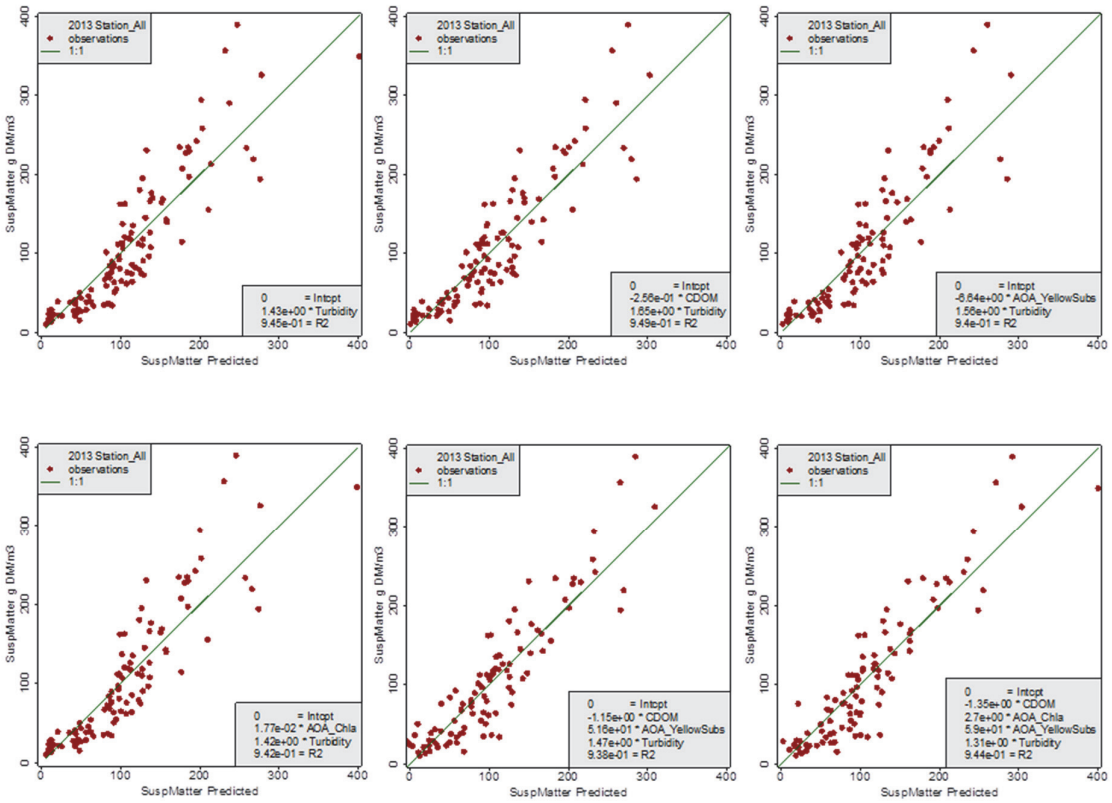

Figure 70 2013-relationships between suspended matter concentration and turbidity and some additional variables. Turbidity, corrected by CDOM gives the best result, although differences are small. Relationships for 2012 are similar; see also Table 28.

Table 28 Regression parameters and reliability for relationships between suspended matter, turbidity and continuously recorded PocketBox-variables CDOM, AOA-Chla and AOA_Yellow Substances. Regressions with and without intercept. Light green cells indicate 'best' relationship, light-light green denote second-best. Suspended matter in mg l^{-1}, turbidity in FTU, CDOM, Chla and Yellow Substances in µg l^{-1}.

2012		Regression parameters						Std.dev of regression parameters				
nr	Y_Var	Intcpt	CDOM	AOA_Chla	AOA_Yellow Subs	Turbid	R2	Intcpt	CDOM	AOA_Chla	AOA_Yellow Subs	Turbid
70	SuspMatter					1.53	0.94					0.04
71	SuspMatter				-20.47	1.98	0.94				4.23	0.08
72	SuspMatter			-2.82		1.84	0.90			1.33		0.09
73	SuspMatter		-0.32			1.78	0.94		0.08			0.07
74	SuspMatter		-0.53	0.01		2.04	0.92		0.12	1.36		0.10
75	SuspMatter		-0.56		7.22	1.89	0.94		0.16		8.04	0.08
76	SuspMatter		-0.70	-0.74	11.80	2.01	0.92		0.23	1.60	13.26	0.10
2013		Regression parameters						Std.dev of regression parameters				
nr	Y_Var	Intcpt	CDOM	AOA_Chla	AOA_Yellow Subs	Turbid	R2	Intcpt	CDOM	AOA_Chla	AOA_Yellow Subs	Turbid
70	SuspMatter					1.46	0.92					0.04
71	SuspMatter				-6.29	1.54	0.92				5.01	0.09
72	SuspMatter			0.31		1.42	0.92			0.53		0.05
73	SuspMatter		-0.26			1.64	0.93		0.09			0.08
74	SuspMatter		-0.30	0.66		1.63	0.93		0.10	0.52		0.09
75	SuspMatter		-1.03		46.11	1.45	0.94		0.23		12.41	0.09
76	SuspMatter		-1.40	1.70	61.57	1.40	0.94		0.25	0.52	13.50	0.10

7.12.4 Summary for suspended matter

Suspended matter content in the water column can be estimated based on turbidity data and on C-Star1 light attenuation data. Also k_d-values can be used, but these were measured at the same time suspended solid samples were taken. Thus, the latter is interesting, and the results may be used to estimate suspended solids contents in case solely light attenuation data are available. But for the present research the relationship

suspended solids = $f^{ie}(k_d,..)$

is of minor interest. On the other hand, the relationship

kd = f^{ie} (suspended solids,..)

(see section 7.9) may be useful when needed in an ecosystem model that computes suspended solid contents and primary production.

7.13 Chlorophyll in water column

7.13.1 General

Chlorophyll-data were obtained in several ways:

- The AOA-sensor in the PocketBox (section 4.5.8)
- The Cyclops-chlorophyll-sensor in the PocketBox, merely as a back-up in case of AOA-sensors failure (section 4.5.5)
- The fluorometer measurements in the laboratory (section 4.6.4)
- HPLC-analyses on a part of the water samples also used for the fluorometer measurements (done by DHI, Denmark)
- Estimations based on algal cell volume (section 4.7) (analyses performed by Koeman & Bijkerk (Wanink et al, 2014))

No spectrophotometric absorption measurements were performed on water column samples (these have only been applied to sediment samples).

Both the PocketBox sensor data are available from the single readings at each sampling stop, and as averages of the continuously stored values.

HPLC-analyses were performed to test the performance of the other procedures. Through HPLC (High Performance Liquid Chromotography), the separate chlorophyll types can be distinguished, where the results from the AOA-sensor and the fluorometer analyses merely give the sum of chlorophyll-a, b c1, c2, d and f. Chlorophyll-a is most occurring, but all other types together may be up to 50% of the total (depending on algae type, season, etc., see e.g. Kirk, 1994).

In the next sections it is investigated how well all chlorophyll-data mutually match.

7.13.2 Cyclops sensor and fluorometry measurements in the laboratory

In Figure 71, results from both analyses are illustrated. The regression coefficient is 1.48 in 2012 and 1.79 in 2013. In 2012, the correlation coefficient R^2 is 0.96 (after removal of outliers); in 2013 results are less consistent, R^2 is 0.85 with more outliers. Chlorophyll-a data (for both analyses) in 2012 are much lower than in 2013, but that cannot be an explanation.

Conclusions will be drawn in the last sub-section, after the other chlorophyll-a observations are analysed.

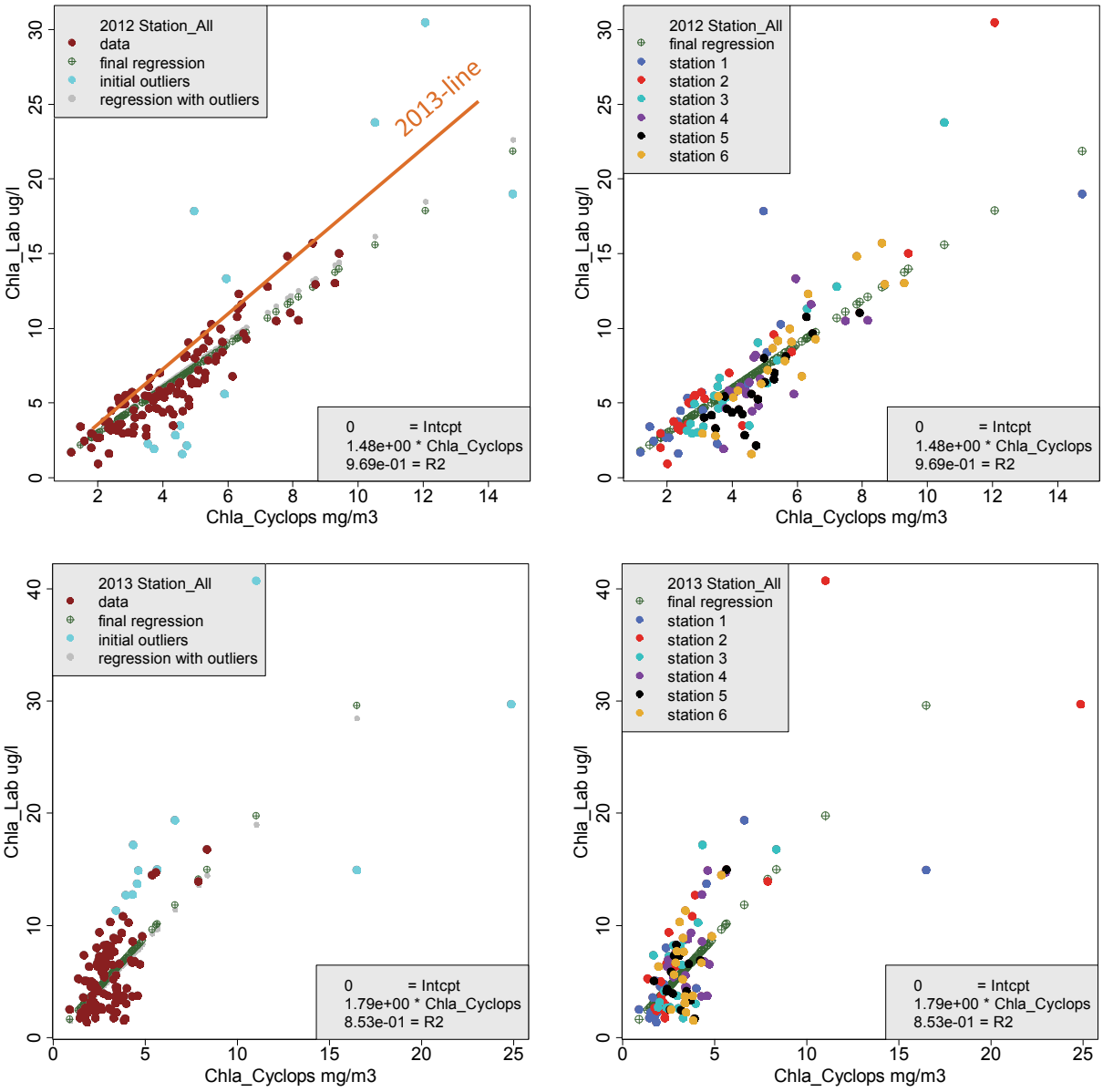

Figure 71 Chlorophyll-measurements, results from the Cyclops sensor, and from the analysis done in the laboratory using a fluorescence meter. Upper: 2012, lower: 2013. Left: all data, with outliers identified; right: all stations separately distinguished. Since the 2013 results differ from those in 2012, the 2013 line has been drawn (orange) in the 2012-graph.

7.13.3 AOA- sensor values and fluorometer measurements in the laboratory

AOA-chlorophyll-a is the sum of the four chlorophyll-a signals for diatoms, cryptophycaea, cyanobacteria (blue-greens) and green algae. In both years, chlorophyll-a according to the

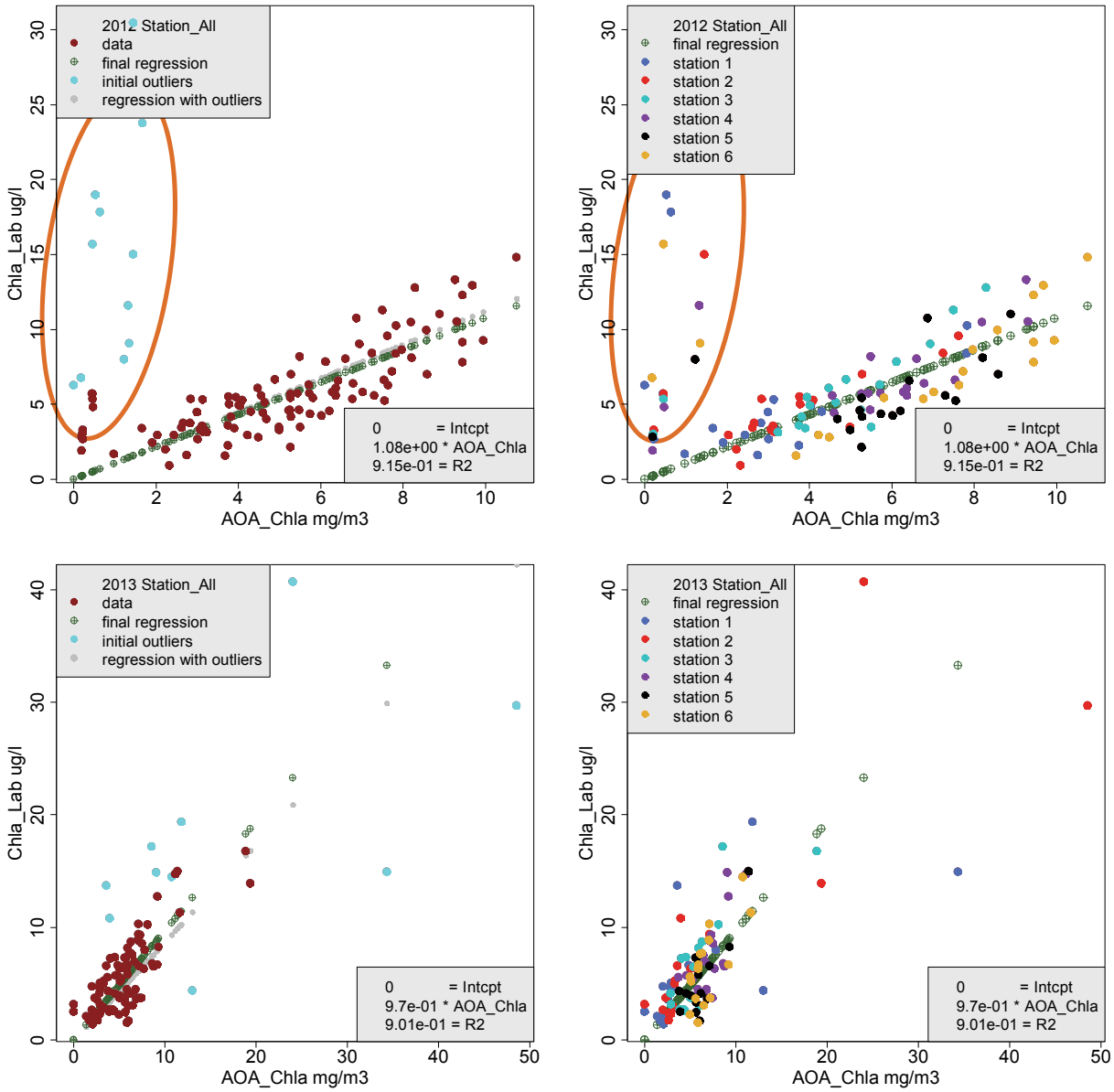

Figure 72 Chlorophyll-measurements, results from the AOA-sensor (X-axis) and the fluorometric analyses in the laboratory. Upper: 2012, lower: 2013. Left: all data, with outliers identified; right: all stations separately distinguished. The data within the orange

fluorometer measurements is –on average- equal to the AOA-data (Figure 72), except for a few exceptional data (within the orange ellipse in Figure 72). Individual observations, however, may sometimes show large deviations from this average picture. Examination of the early 2012-data reveals that during cruises 3 and 4 something went wrong with (one of the) AOA-sensors. Cruise 3: both sensors for diatom and green algae gave no signal. Cruise 4: sensors for blue-green, diatom and green algae gave no or hardly any signal. Next: cruise 5: green algae sensor gave no signal, but since this signal is small this period, it maybe (although not certain) hardly affected total chlorophyll-a values.

First conclusion for the use of the AOA-sensors is that results for cruises 3 and 4 are unreliable and have to be ignored; results for cruise 5 possibly are underestimating the real situation. A last check is performed in the next section (using Cyclops-chlorophyll-a- values).

It is also concluded that for all other observations (all from cruise 6 and later) AOA-chlorophyll-a values are reliable observations of chlorophyll-a in the field.

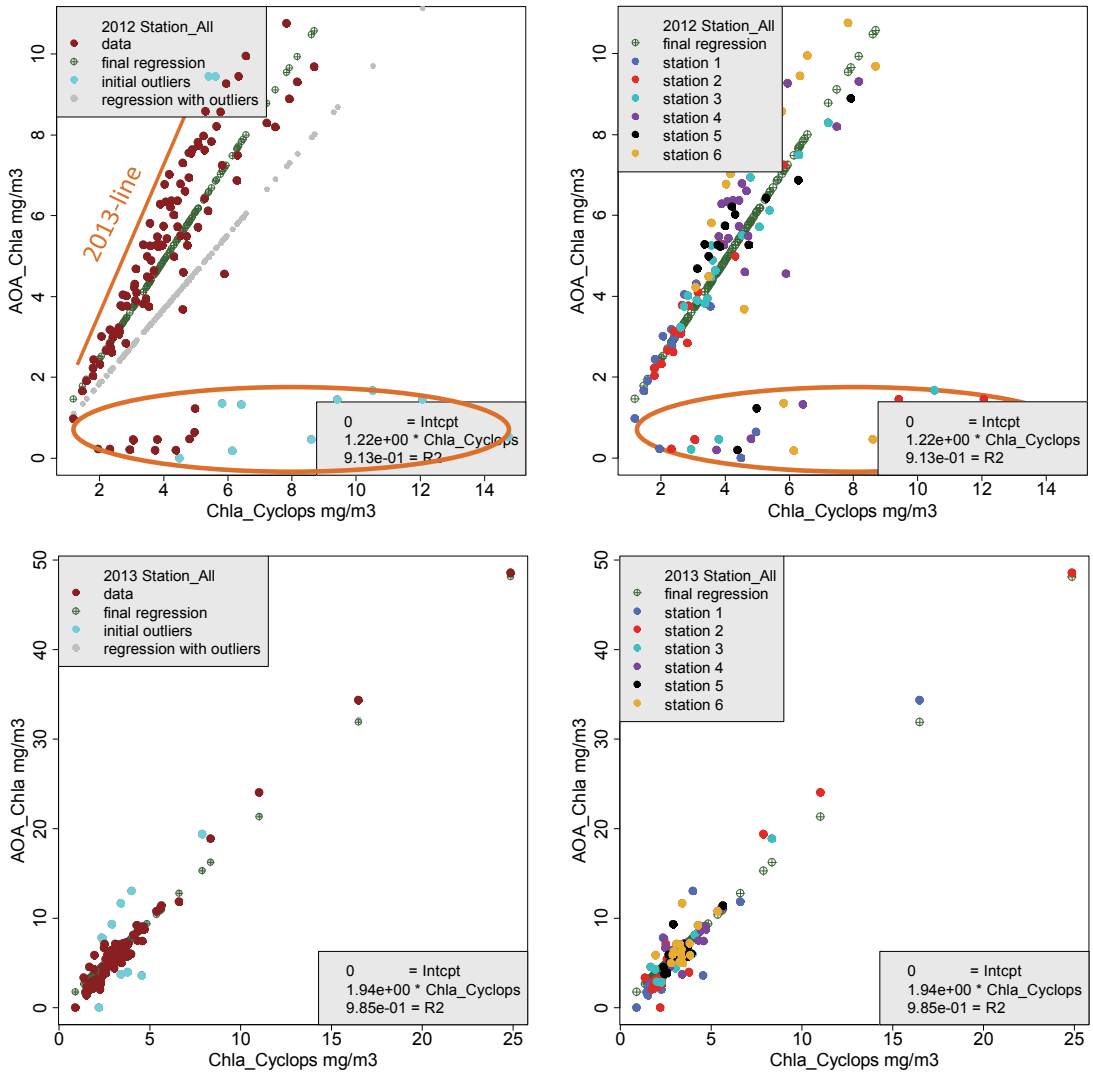

Figure 73 Chlorophyll-measurements, results from the Cyclops sensor (X-axis), and from the AOA-sensor (Y-axis). Upper: 2012, lower: 2013. Left: all data, with outliers identified; right: all stations separately distinguished.

7.13.4 AOA- and Cyclops-sensors

Finally, the responses from the Cyclops chlorophyll-a sensor and the AOA-sensors can be compared (Figure 73). It is noted again that the Cyclops-sensor has been mounted as a back-up in case (one of the) the AOA-sensor(s) failed.

The erroneous AOA-observations in the early cruises in 2012 (orange circle in the figure) have already been mentioned above. Obviously, the Cyclops-sensor gives a lower signal in 2013, compared to the 2012-values (2013: 73% of the 2012-signal).

7.13.5 HPLC-measurements

There is a strong correlation between the ^{10}log-transformed HPLC- and fluorometer values (R^2 = 0.989) with a regression coefficient that is exactly 1, see Table 29), an indication of good quality data. However, the intercept = 0.036, implying that the HPLC-values are almost 9% above the fluorometer values. This difference is significant. Since the fluorometer values are assumed to reflect all chlorophyll, and HPLC just chlorophyll-a, the intercept should be a negative value instead of a positive.

Table 29 Linear regression model y = a +bx, with y = log10(HPLC_Chla) and x = log10(PAM_Chl); R2 = 0.989.

	Value	Std error	t-value	Pr(>|t|)
a	0.036	0.016	2.3	0.033
b	1.000	0.023	44	$<2x10^{-16}$

Further, it is tested whether the ratio between HPLC-values and fluorometer values varies with time, but this appeared to be not the case.

For pheophytin (degradation product of chlorophyll) the correlation coefficient (fluorometer vs HPLC) is lower (R2 = 0.822). Also, pheophytin fluorometer values are considerably lower than HPLC-values.

The best explanation for both correlations (HPLC-chlorophyll-a higher than fluorometer chlorophyll, and HPLC-pheophytin values considerably lower than fluorometer pheophytin) comes from a remark made by the DHI. They write in their letter: “The samples were somehow affected by degradation, since the concentrations of pheophytin-a and pheophorbide-a were higher than usually seen for water samples”. Since the fluorometer pheophytin values differed even more from HPLC –values, (further) degradation of the fluorometer samples might be an explanation as well.

Table 30 Linear regression model y = a + b x, with y = ^{10}log(HPLC_Pheo) and x = ^{10}log (Fluorometer_Pheo); R^2 = 0.822.

	Value	Standard deviation	t-value	Pr(>|t|)
a	-0.848	0.076	-11.05	$1.9x10^{-10}$
b	1.17	0.12	10.11	$9.97x10^{-10}$

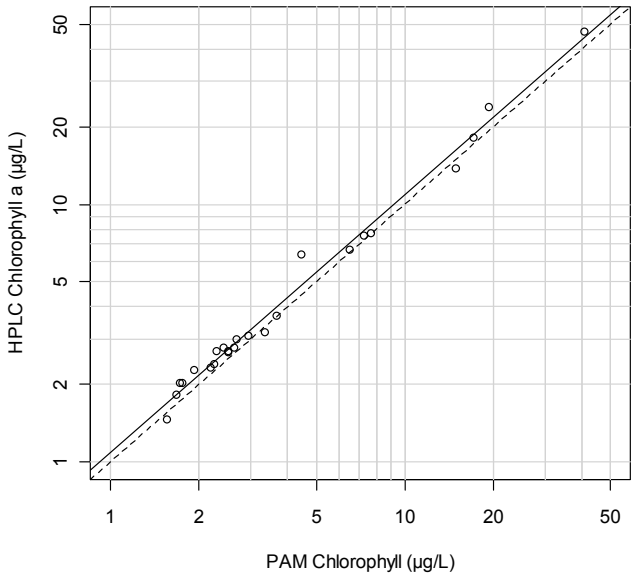

Figure 74 Chlorophyll-data: X-axis: fluorometer values, -axis: HPLC-values. Dashed: 1:1-line, solid line: regression (Table 1)

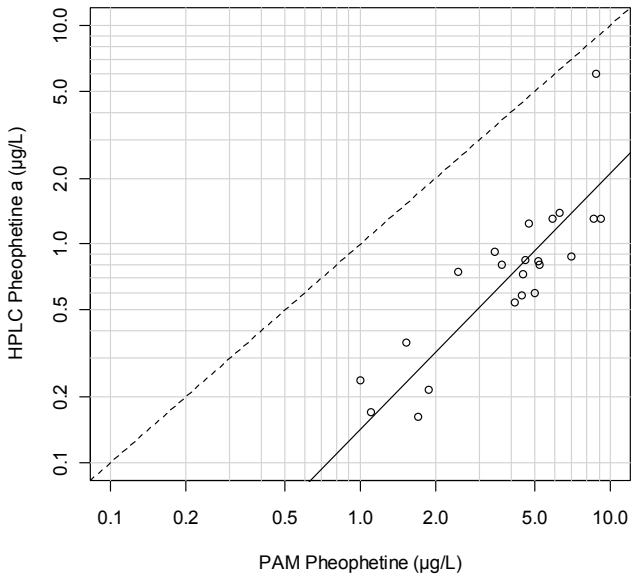

Figure 75 Fluorometer pheophytin values (x-axis) and HPLC-pheophytin values (y-axis). Dashed line = 1:1, solid line is linear regression result (Table 30).

7.13.6 Conclusions for chlorophyll measurements

AOA_chlorophyll-a data: these are supposed to be correct values for chlorophyll-a (excluding other chlorophyll-types); cruises 3-5 (in 2012) however are unreliable since some sensors did not function.

Cyclops-chlorophyll—values: these are structurally lower than AOA-chlorophyll-a and fluorometer chlorophyll-values. However, there's a good correlation with AOA-values, and thus, Cyclops-values can very well be used to add to the AOA-data (in case these are erroneous).

Fluorometer chlorophyll-a ("Chla-lab"): based on the HPLC-control it may be concluded that most fluorometer values are somewhat too low. This is in agreement with the observations that on average AOA-chlorophyll-a values are the same as the fluorometer values whereas one would expect somewhat higher fluorometer values.

The samples analysed by DHI showed an average chlorophyll-a: pheophytin-a ratio of 7. This ratio in all fluorometer analyses together was 1.7 in 2012 and 1.5 in 2013. If a 'proper' ratio would have been about 7 (or even a bit higher), fluorometer chlorophyll-values would have been 35% (ratio 7) to 40% (ratio 9) higher than the values given here.

As a comparison, the Rijkswaterstaat Waterbase data (these are based on HPLC-analyses) were checked as well, and those results are summarized in Table 31. These results support the suggestion that the pheophytin data obtained in the laboratory analyses are far too high, and thus, laboratory chlorophyll-a values probably are roughly 35% higher than reported.

Table 31 Rijkswaterstaat Waterbase-values for chlorophyll-a and pheophytin in the Ems-Dollard area; these are based on HPLC-analyses. A simple analysis has been performed: all chlorophyll-a and all pheophytin data available are simply averaged.

	Station number (approximately)	Chlorophyll-a (µg l^{-1})	Pheophytin (µg l^{-1})	ratio
Huibertgat	Station 1	8.25	0.23	35.9
Oostfriese Gaatje	Stations 3/4	7.86	0.83	9.5
Groote Gat Noord	Station 6	8.6	0.97	8.9

There are two possible explanations for such a difference:

a. It concerns a real degradation of chlorophyll -> pheophytin somewhere between sampling and analysing the samples.
b. The equation used to compute pheophytin and chlorophyll is not correct

If (a) is the case, the sampling handling needs revision, if (b) is the case, the formula parameters need revision. Both chlorophyll and pheophytin values are based on the same data, with parameters that account for the absorption characteristics of both pigments. That means that the result is rather sensitive to the parameters used. A too high value for pheophytin automatically results in a too low value for chlorophyll, and vice versa.

This question cannot be solved now.

7.14 Conclusions for this chapter: what have we learnt?

7.14.1 Chapter content?

The results of the measurements were checked. First it was checked how the same data obtained with different methods or instruments match; secondly the relationships between variables were analysed.

7.14.2 What went OK?

At the end one must conclude that it has been very wise to perform more than one chlorophyll analysis. It now is possible to identify some shortcomings in for example the data set obtained by the fluorometric laboratory analyses.

The several methods for measuring temperature, conductivity, oxygen were proven to be very useful.

The combination of direct measurement of the light attenuation, suspended matter content in the water column, the use of the C-Star sensors plus the turbidity measurements gives the possibility to relate the results with each other, and estimate suspended matter content during the cruises, next to the direct data on the sampling sites alone.

Phytoplankton cell counts plus assessment of cell volumes was found very useful.

All ^{14}C- pelagic primary production measurements were successful.

7.14.3 What needs improvement and what are main recommendations for future work?

A few improvements are definitely possible or even needed.

First: the fluorometric analysis (and subsequent computation) of chlorophyll-a and pheophytin. The method has been calibrated against chlorophyll-a standard solutions, but not against pheophytin-standards. The algorithm used is rather sensitive to errors: an error in the pheophytin measurements directly affects the chlorophyll-a result. It is recommended to use pheophytin standard as well.

Second: the carotenoid:chlorophyll adsorption ratio was supposed to give information whether phytoplankton growth was nutrient or light limited. Afterwards it appears that it had been better to test this method better; the results now can hardly be interpreted the way they were meant to.

Third: measuring benthic primary production is difficult; it would have been better to apply and the present method, and the one used by Colijn. Next to that, there are other methods to assess benthic primary production, and such methods need to be considered as well; not instead of, but additionally to the present method.

Fourth: the continuous measurement of light attenuation (C-Star1 & 2) was successful, but in the most turbid areas even the shortest light pathway sensor (C-Star1) appeared to be too long. An even shorter sensor (2-3 cm) is needed next time.

Fifth: the PocketBox was equipped with two sensors that measured Coloured Dissolved Organic Matter: the Cyclops CDOM-sensor and the AOA-Yellow Substance sensor. They both should gave similar results, but they did not. It is necessary to calibrate both sensors against the same standards.

Sixth: Flow cytometer analyses appear promising, but need much more time to come to reliable results; combination with algae cell counts probably is needed.

Seventh: despite the observation that the pelagic primary production incubations went OK, it is advised to include other methods as check, such as an oxygen optode detection and/or chlorophyll-activity detection with a pulse-amplitude modulation method (PAM).

Eight: computation of benthic primary production is rather sensitive to the estimated light penetration in (and attenuation of) the sediment top layer. More attention could have been paid to assess this sediment top layer light attenuation characteristics.

Ninth: to find out whether light or nutrient are phytoplankton growth limiting, incubations with different nutrient additions could have been performed. A second possibility is after the bacteria activity tests following Kuipers & Van Noort (2008).

8 Results-2: State variables in the Ems-Dollard

8.1 Introduction

In the previous chapter the quality of the observations was checked. In this chapter, final values for all state variables (from temperature to chlorophyll, and corrected if necessary, according to the findings in chapter 7) are presented. Due to the character of the data, a short comparison with older data plus a short discussion is –where relevant- included in each sub-section.

8.2 Temperature

Temperature as measured by the PocketBox (those data that are reliable, see section 7.1) is shown in Figure 76. Maximum values reach up to about 22 °C, in the shallow parts of the Dollard. There is a slight tendency from station 1 to 6 to higher values in summer, and lower in winter; also temperature rise in spring is earlier at station 6 than at station 1. Similarly, temperature drop at the end of the autumn goes faster at station 6. Spring temperatures in 2013 were considerably lower than in 2012 (especially between days 60-120), and summer temperatures in 2013 (up to 22 °C) were higher than in 2012 (about 20 °C max). Generally, compared to average values for the period 1971-1997 (Figure 77), there are no extraordinary values recorded.

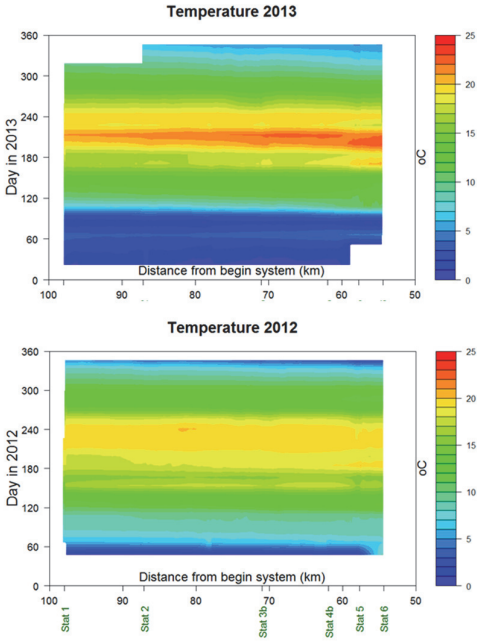

Figure 76 Temperature in the system, as recorded by the PocketBox (see section 4.4.1 & 7.2), left: 2012, right: 2013. Distances mentioned are from Herbrum (DE). Sampling stations 1-6 mentioned.

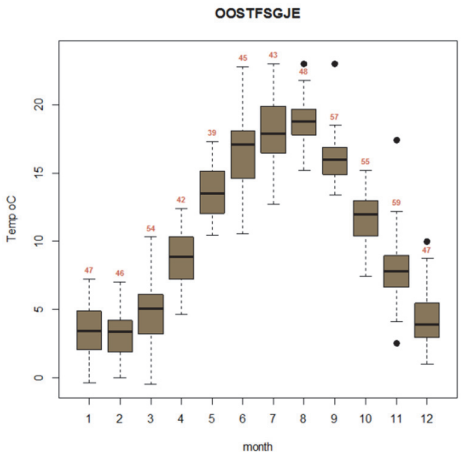

Figure 77 Monthly averaged water temperature at OostFriese Gaatje (roughly station 3; see Figure 23, nr 13), period 1971-1997. Source: Waterbase (2014).

8.3 Conductivity/salinity

Conductivity and salinity in the system in 2012 and 2013 are presented in Figure 78. Lowest values go down to below 10 mS cm^{-1} and 5 PSU in winter when fresh water discharge is highest; highest values reach about 44 mS cm^{-1} and 32 PSU in summer at low river run-off. As expected, Dollard-values show lowest salinities.

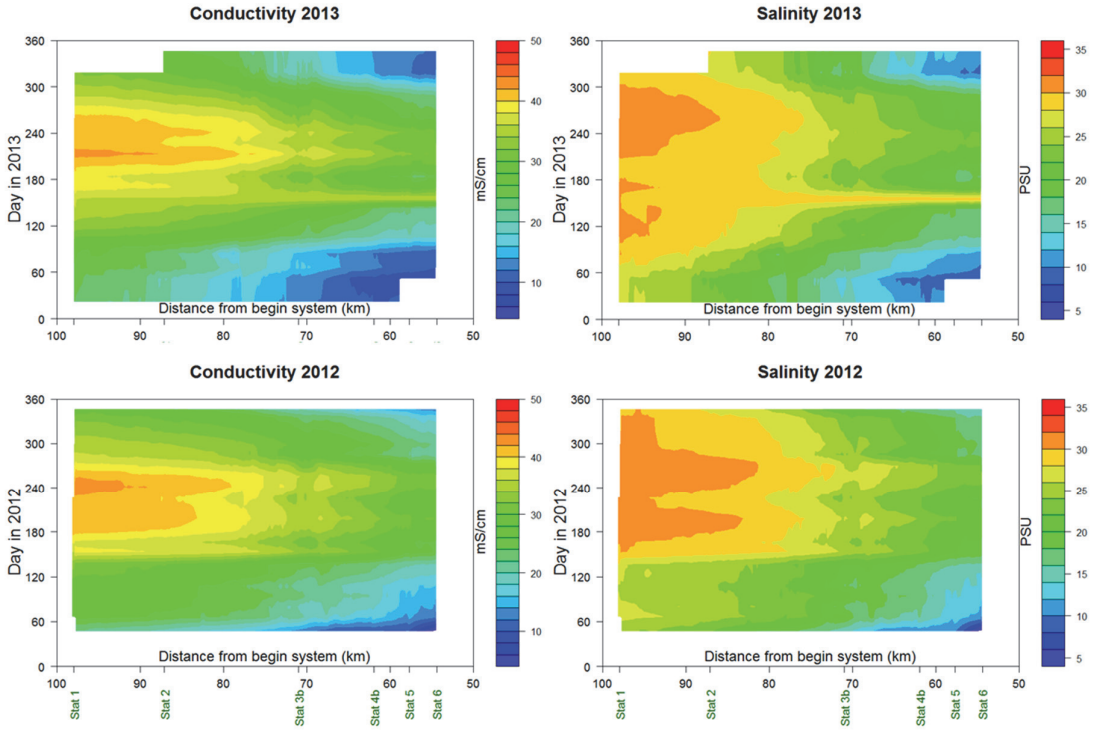

Figure 78 Conductivity (upper) and salinity (lower) in the system during 2012 (left) and 2013 (right), as recorded by the PocketBox (see section 4.3.3, 4.4.2 & 7.4). Distances mentioned are from Herbrum (DE). Sampling stations 1-6 mentioned.

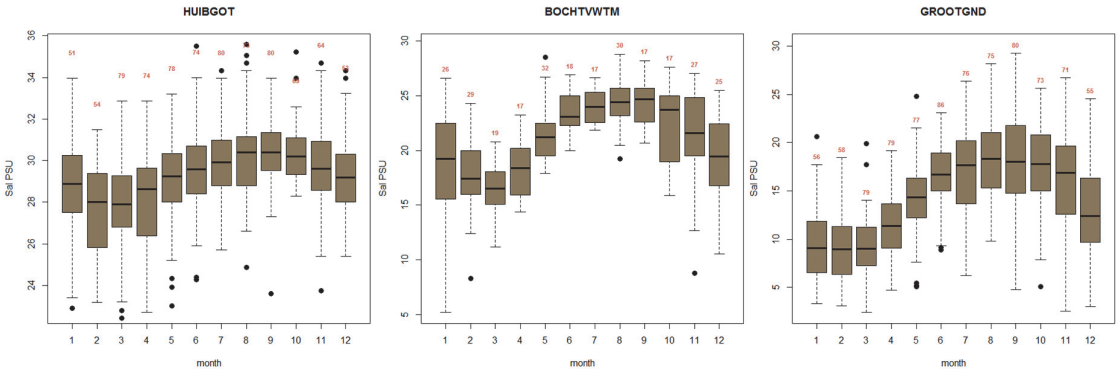

Figure 79 Salinity in the estuary, monthly averages as boxplots for the period 1975-2011 (Huibert gat Oost, left, site = station 1), 1988-2012 (Bocht van Watum, middle, site = between station 3 & 4), 1975-2011 (Groote Gat Noord, right, site = station 6). Mind the different Y-axis scales. Source: Waterbase (2014). Nrs give the nr of observations. Site nrs in Figure 23 are 2, 9 and 20, respectively.

Comparison with Waterbase-values (Waterbase, 2014; Figure 79) gives that lowest Waterbase data are roughly of the same order a the PocketBox results, for all three stations shown. This also is valid for the maximum values observed. There's one comment on the Waterbase data: some values are above 34 PSU, and such values are almost at or even above open ocean values (which is 35 PSU; Broecker, 1974), and not very likely in these areas.

8.4 Nutrients

8.4.1 Introduction

In this section, available nutrient data for the present cruises and the past (Water quality monitoring results (MWTL; Waterbase 2104)) are presented and compared.

8.4.2 Phosphate

Results for ortho-phosphate (o-P) are presented as level plots in Figure 80, and as pure measurements in Figure 81.

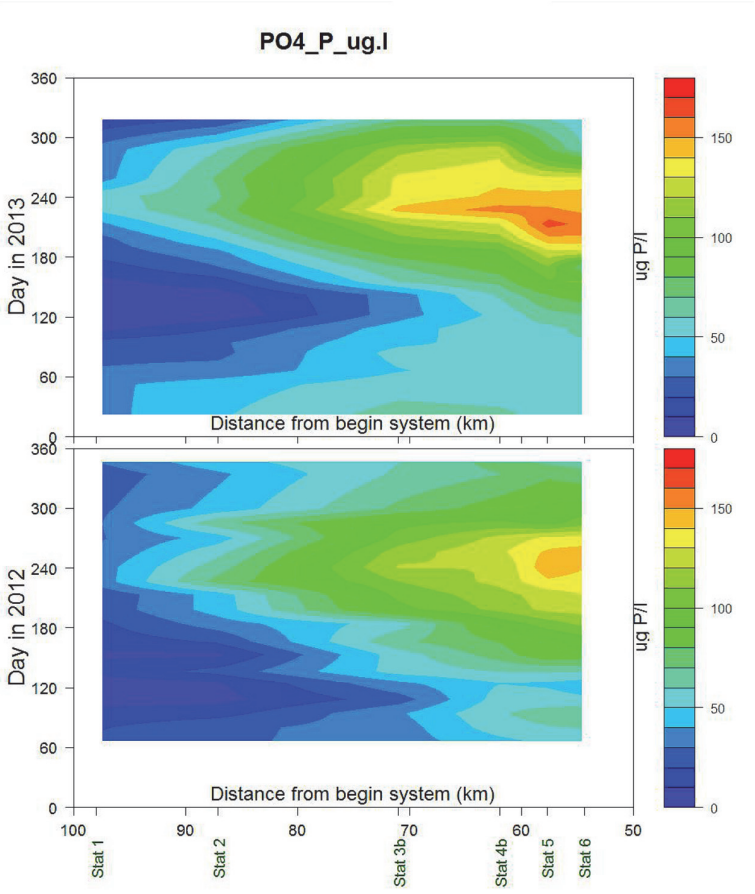

Figure 80 Level plots for ortho-phosphate for 2012 lower) and 2013 (upper). Distances mentioned are from Herbrum (DE). Sampling stations 1-6 mentioned.

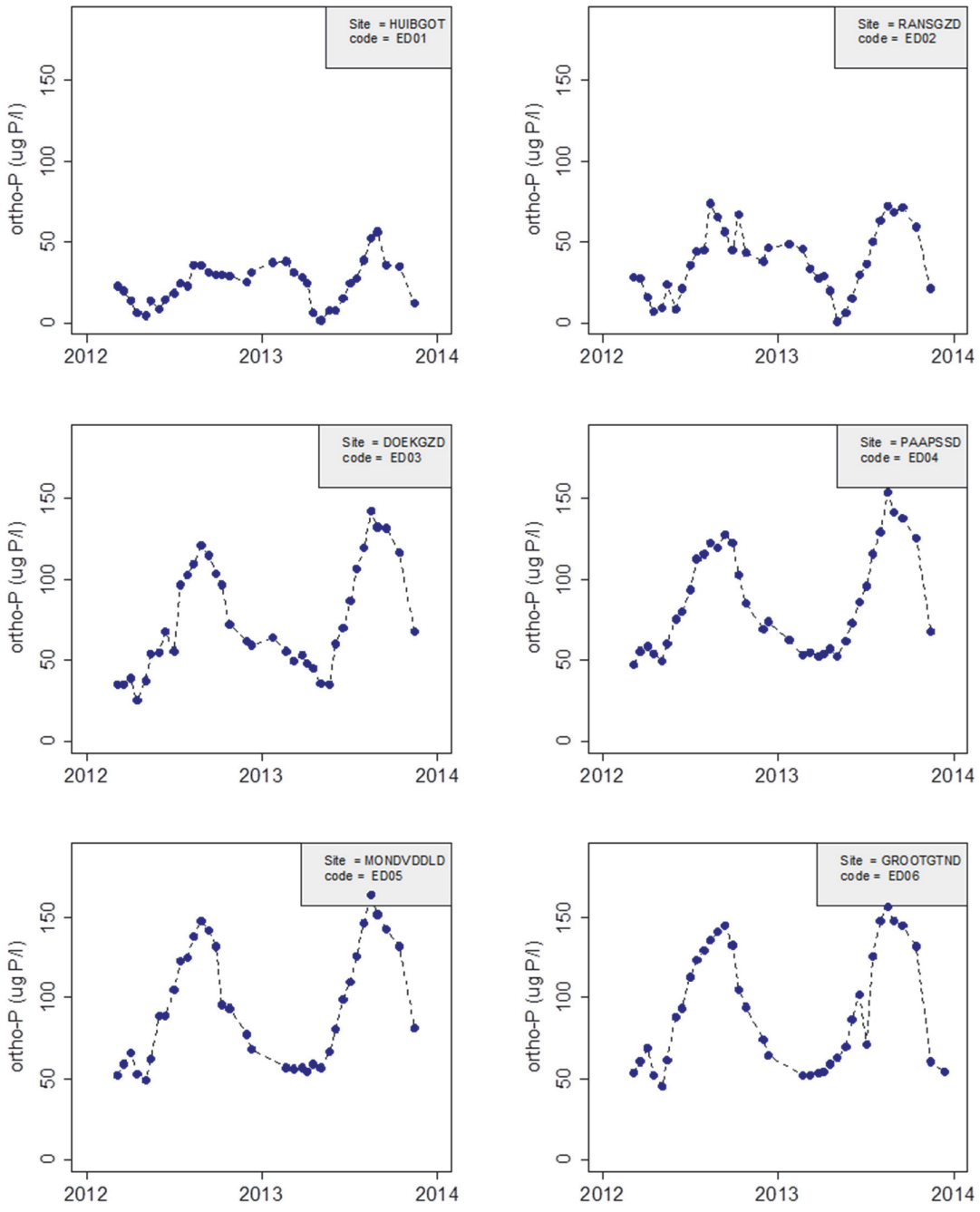

Figure 81 Water sample results for ortho-phosphate (dissolved inorganic phosphate) for all six stations, and both monitoring years. Code numbers ED01..ED06 give the station numbers according to Figure 16

Figure 82 Waterbase-data (Waterbase, 2014) for phosphate at HuibertGat Oost (site 1, upper) and Oostfriese Gaatje (between our sites 3 and 4, lower). See Figure 23 for position details. For both figures: total P (upper left), particulate P (upper middle), o-P (upper right), dissolved organic (lower left), a course estimate of inorganic solid bound P (lower middle) and lower right data on suspended solids (ZS). Own data for 2012 and 2013 (circles), and Colijn data for 1976-1980 (bars) added. At OostFriese Gaatje, two data are added, for our stations 3 and 4, and for Colijn stations 4 and 6 (because both positions do not cover the Waterbase-site).

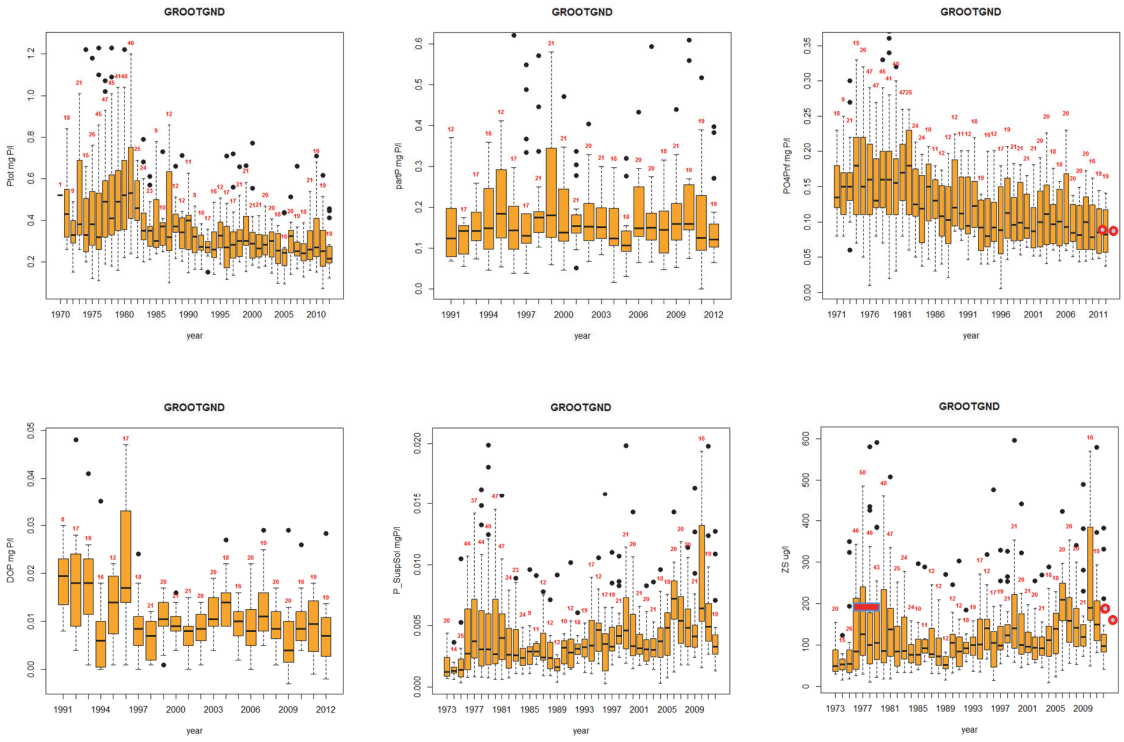

Figure 83 Waterbase-data (Waterbase, 2014) for phosphate at Groote Gat Noord Oost (site 6). See Figure 23 for position details. Total P (upper left), particulate P (upper middle), o-P (upper right), dissolved organic (lower left), a course estimate of inorganic solid bound P (lower middle) and lower right data on suspended solids (ZS). Our data for 2012 and 2013 (circles), and Colijn data for 1976-1980 suspended solids (bars) added.

MWTL-data as far as available are shown in Figure 82 - Figure 83, seasonal trends (for all years together) are presented in Figure 93.

It is obvious that at site 1 (Figure 82, upper) total and dissolved P dropped since 1980. At Huibertgat Oost (site 1) this is even more clear (down to about 30-40% of the 1980-values) than at Groote Gat Noord (site 6, down to about 50%), roughly. The time series at site 3-4 (Oostfriese Gaatje) is not long enough draw conclusions for the whole period. Levels for dissolved P (o-P) were lower in 1995 than in 1980, down to about 60%; total-P seems to be somewhat higher than in 1980 although this view is biased a bit by the two much higher values in 1988 and 1989.

Trends in the other parts of the Wadden Sea were analysed by Brinkman (2008), and these results are in line with the conclusions then. The large o-P concentration drop around 1990 is typical for most Wadden Sea sites, and therefore, the inner Dollard area and Ems in the vicinity of sites 3 and 4 behave a bit a-typically.

MWTL-data (Waterbase, 2014) give highest values in autumn (Figure 93), up to about 60 µg P l^{-1} at Huibertgat Oost (==station 1), 140 µg P l^{-1} at Bocht van Watum =station 3 à 4) and 200 µg P l^{-1} in the Dollard area (=station 6). Lowest values are 10 µg P l^{-1}, 50 µg P l^{-1} and about 70 µg P l^{-1} respectively at these same stations. Nowadays these maximum values are lower, as presented. The springtime

pattern now is different from the all-time average picture, especially for the inner stations. Whereas the late spring-rime minimum hardly appeared in the data in the '70's-'80's, these are present now, indicating a substantial P- consumption. These observations have consequences when interpreting the primary production measurements (chapter 9).

8.4.3 Silicate

Results for dissolved silicate are presented as level plots in Figure 84 and as pure measurements in **Figure 85**.

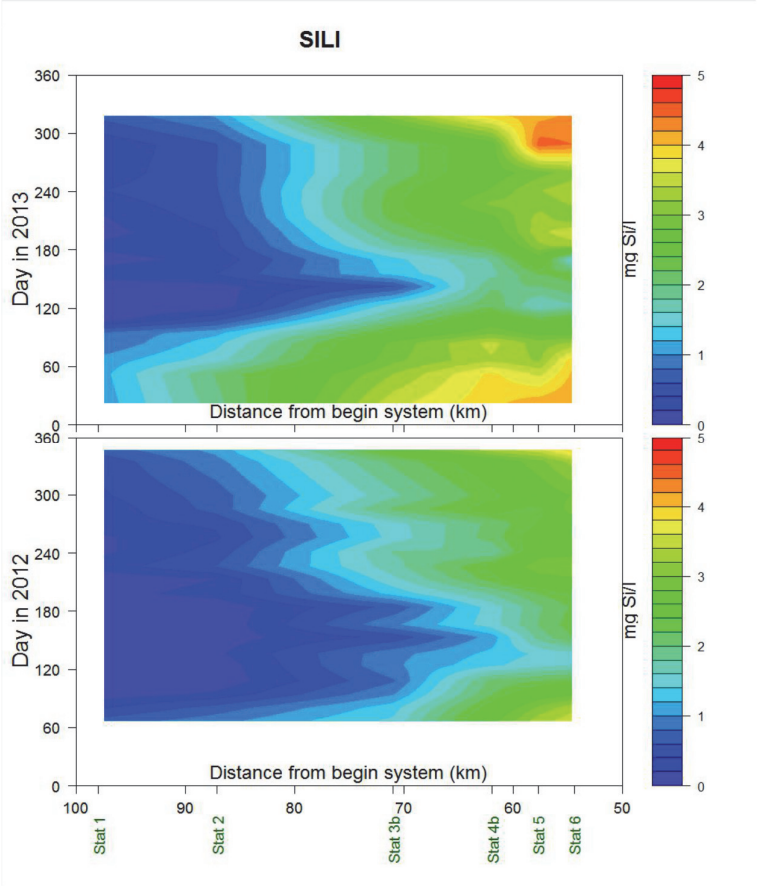

Figure 84 Level plots for dissolved silicate for 2012 lower) and 2013 (upper). Distances mentioned are from Herbrum DE). Sampling stations 1-6 mentioned.

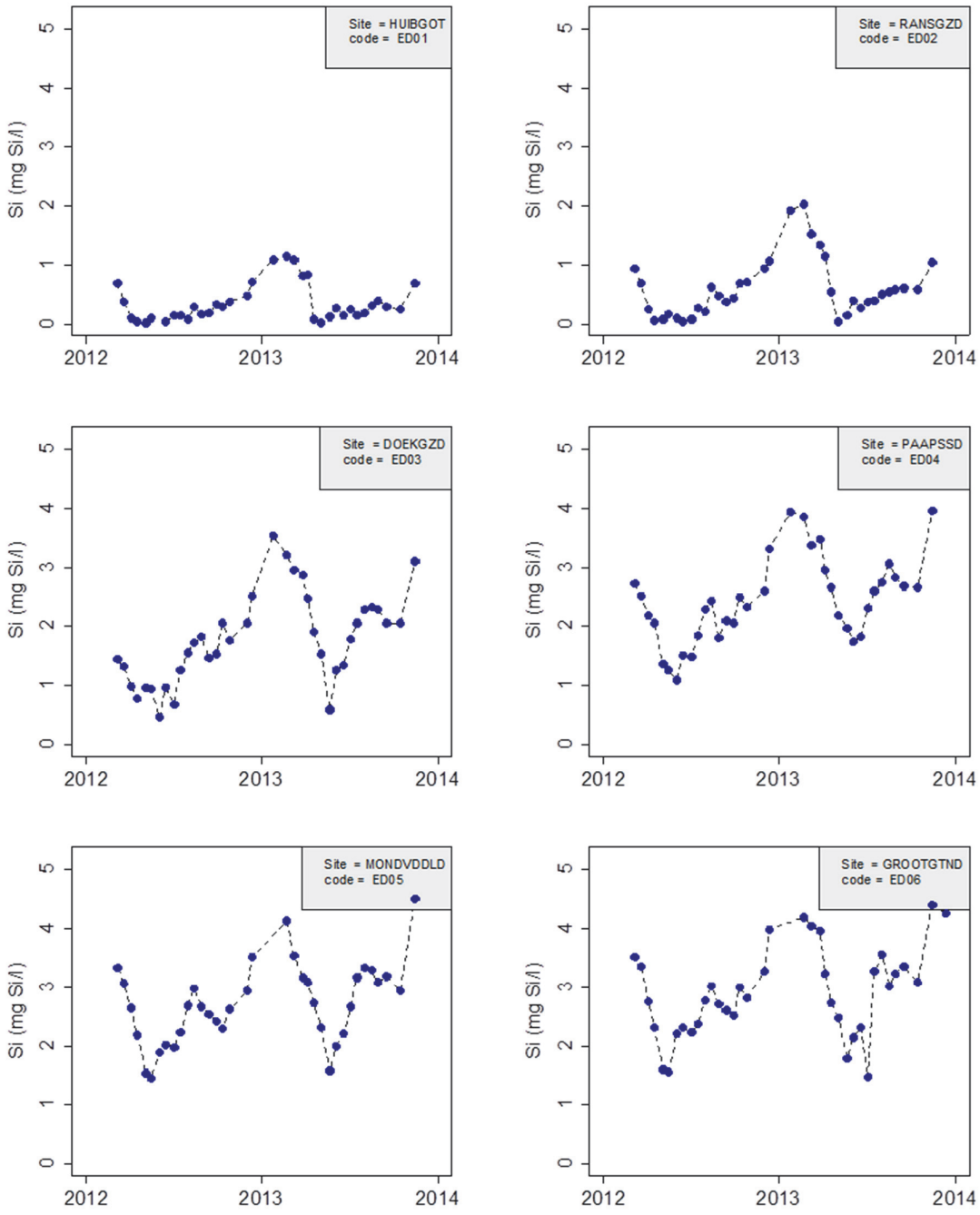

Figure 85 Water sample results for dissolved inorganic silicate for all six stations, and both monitoring years. Code numbers ED01..ED06 give the station numbers according to Figure 16

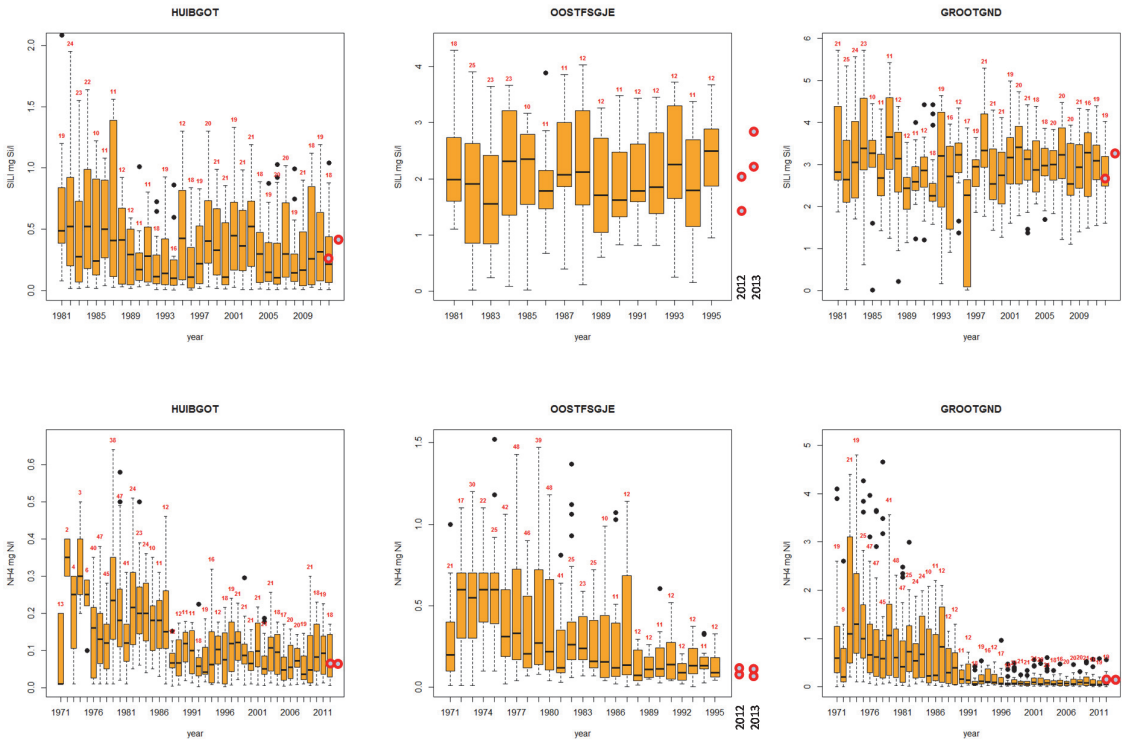

Figure 86 Waterbase-data (Waterbase, 2014) for silicate (upper) and ammonium (lower). Left: Huibert Gat Oost (site 1), middle: OostFriese Gaatje (between sites 3 and 4) an dright: Groote Gat Noord Oost (site 6). See Figure 23 for position details. Own data for 2

MWTL-data as far as available are shown in Figure 86, seasonal trends (for all years together) are presented in Figure 93.

It is obvious that silicate concentrations did not change substantially in the system since the beginning of the data series, except for silicate values at site 1 (Figure 86, upper). Here, a variation with years can be observed, with lower concentrations now than in the beginning of the '80-s. Generally, silicate concentrations in the outer areas are 15-25% of those in the innermost areas. Values found in the present research all are not different from the Waterbase-data.

Trends in the other parts of the Wadden Sea were analysed by Brinkman (2008), and these results are in line with the conclusions in that report.

MWTL-data (Waterbase, 2014) give highest values in winter, up to about 1 mg Si l^{-1} at Huibertgat Oost (==station 1), 2.5 mg Si l^{-1} at Bocht van Watum =station 3 à 4) and 4 mg Si l^{-1} in the Dollard area (=station 6). Lowest values are below 0.1 mg Si l^{-1}, 1 mg Si l^{-1} and about 1.5 mg Si l^{-1} respectively at these same stations.

Maximum and minimum values in the present research are more or less similar to these Waterbase data. However, the general picture is somewhat different, at least for 2012 when a true late spring minimum did not appear. In 2013, low late spring values appeared at all six stations.

8.4.4 Ammonium

Results for ammonium (NH_4^+) are presented as level plots in Figure 87 and as pure measurements in Figure 88. At all sites maximum values were recorded during winter.

Ammonium patterns are similar in the Waterbase data and in the present research, but values are much lower in the 2012-2013 dataset. Station 1: 0.02-0.3 mg N l^{-1} (Waterbase) and <0.02 – 0.2 mg N l^{-1} now. Station 3-4: 0.06 – 0.3 mg N l^{-1}, and 0.05 – 0.2 mg N l^{-1} now, and station 6: below 0.1 – 1.7 mg N l^{-1} and below 0.02 – 0.4 mg N l^{-1} now. Most distinct summer minima occur in the Dollard area. Thus, especially in the inner areas ammonium concentrations are much lower than they used to be. This is a general trend, see Brinkman (2008), but in the Dollard area this pattern is extreme which doubtlessly will be related to the changes in organic waste discharges that still took place since the end of the '70-s and beginning of the '80-s (see e.g. Essink & Esselink, 1998).

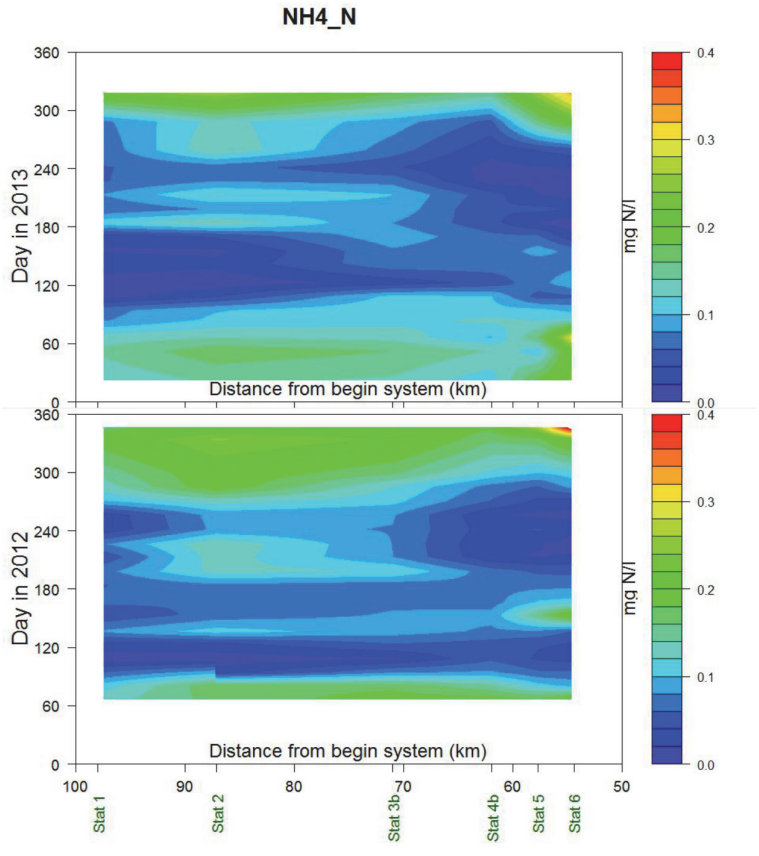

Figure 87 Level plots for ammonium NH_4^+ for 2012 lower) and 2013 (upper). Distances mentioned are from Herbrum (DE). Sampling stations 1-6 mentioned.

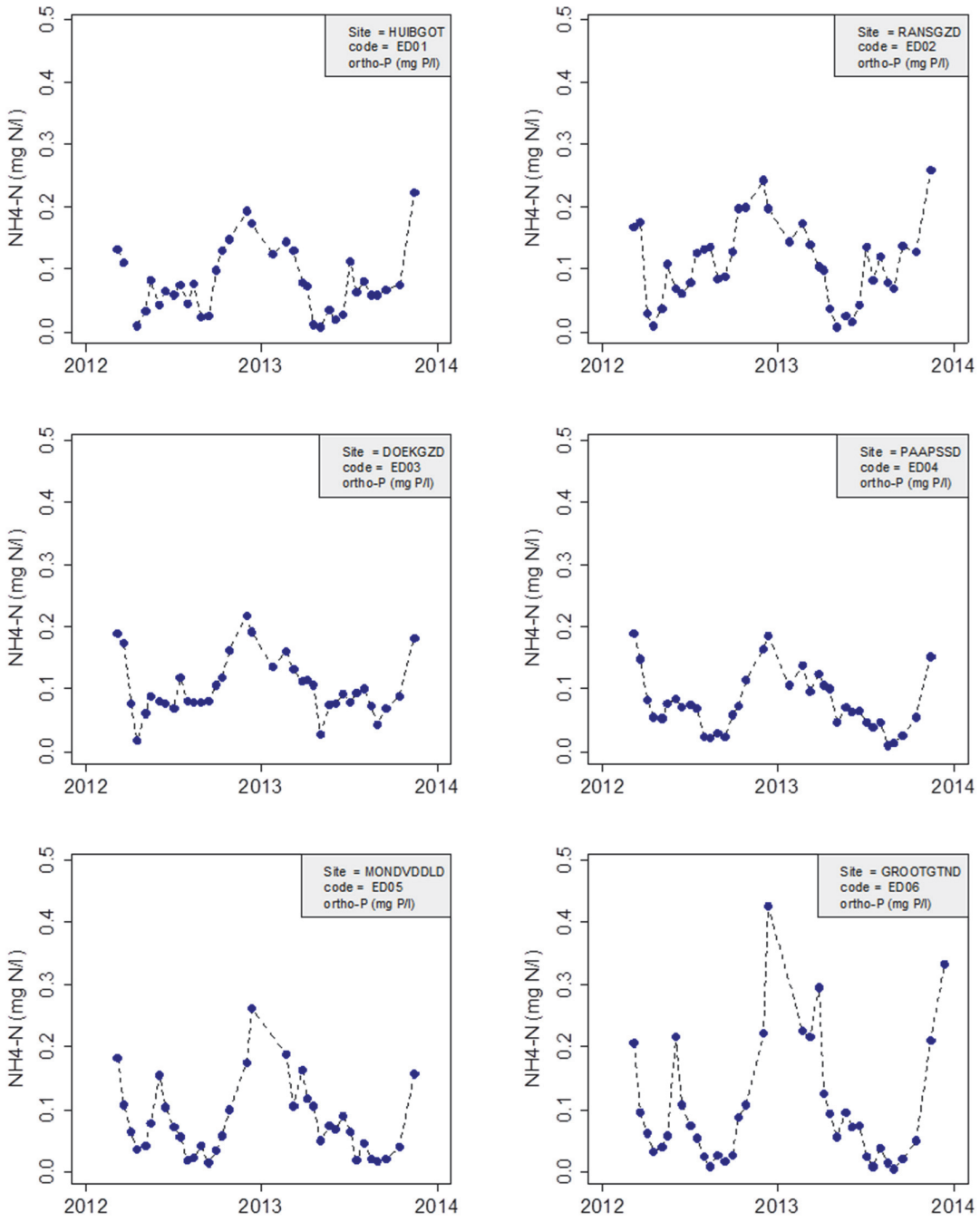

Figure 88 Water sample results for ammonium (NH4+) for all six stations, and both monitoring years. Code numbers ED01..ED06 give the station numbers according to Figure 16

8.4.5 Nitrate

Results for dissolved nitrate are presented as level plots in Figure 89 and as pure measurements in Figure 90. Maximum values are reached during winter, and minimum values during summer (mostly July); outer area values reach up to 1 mg N l^{-1}, in the Dollard area these reach almost 5 mg N l^{-1}.

MWTL-data (Waterbase, 2014) are confirm out results, and also give highest values in winter, up to about 1 mg N l^{-1} at Huibertgat Oost (==station 1), 2.5-3 mg N l^{-1} at Bocht van Watum =station 3 à 4) and 4 mg N l^{-1} in the Dollard area (=station 6). Lowest values are below 0.1, 0.5 and about 1 mg N l^{-1} respectively at these same stations.

The pattern in both datasets is similar, with lowest values in July-August.

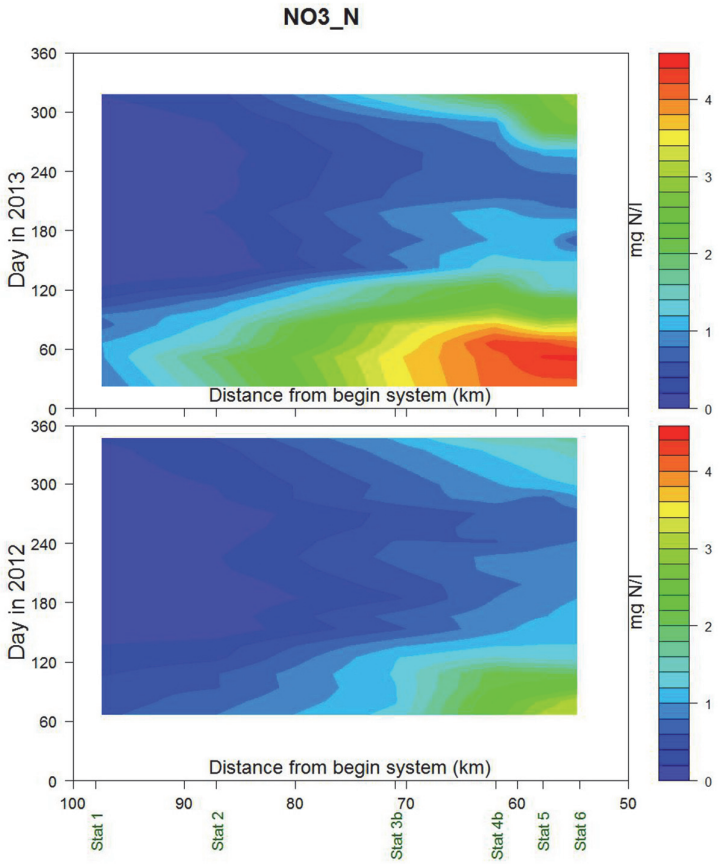

Figure 89 Level plots for nitrate NO_3^- for 2012 lower) and 2013 (upper). Distances mentioned are from Herbrum (DE). Sampling stations 1-6 mentioned.

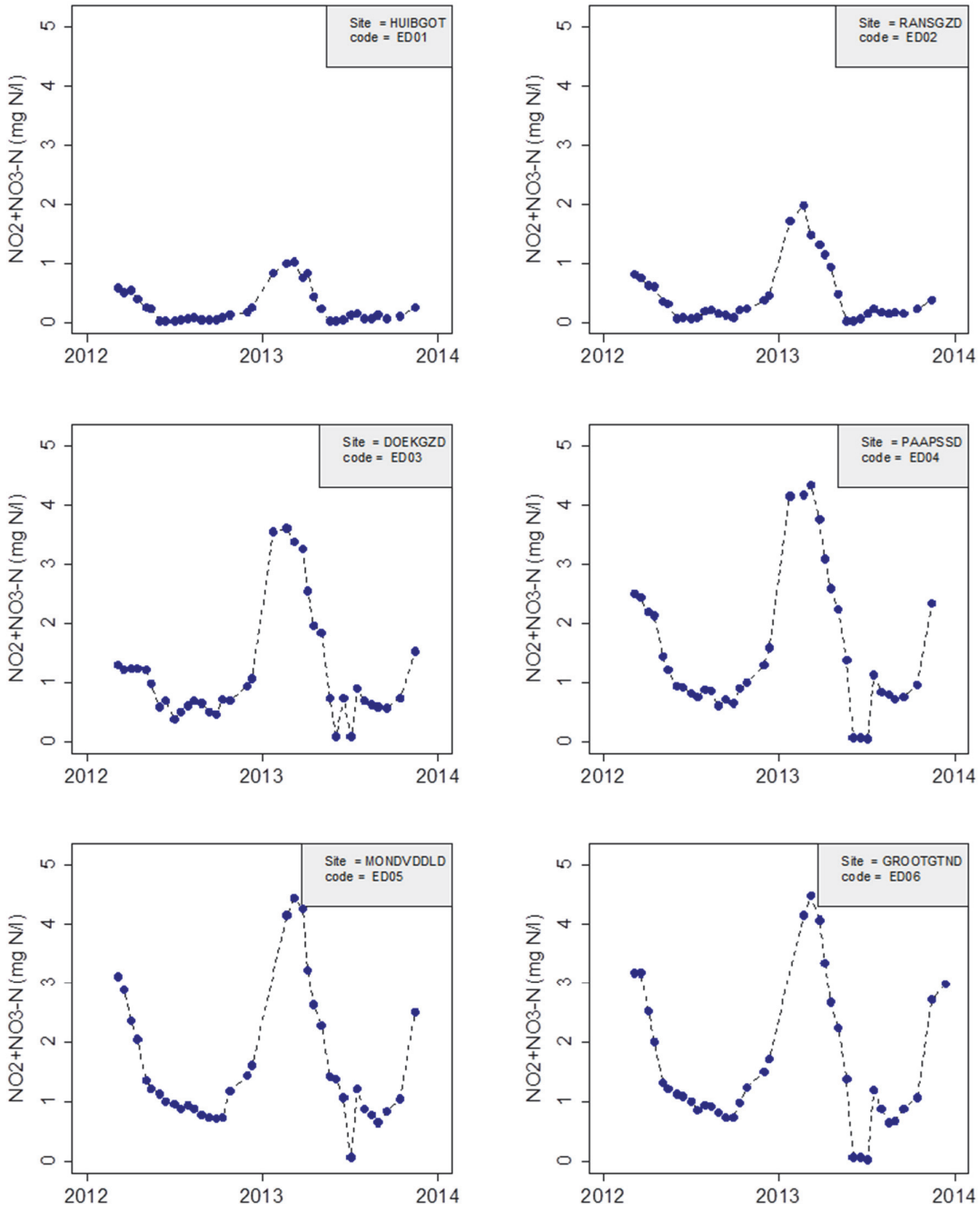

Figure 90 Water sample results for nitrate (NO3-) for all six stations, and both monitoring years. Code numbers ED01..ED06 give the station numbers according to Figure 16

8.4.6 Nitrite

Results for dissolved nitrite are presented as level plots in Figure 91 and as pure measurements in Figure 92. Maximum values are reached during winter, and minimum values during summer (mostly July). Maximum values are more or less the same for all stations: about 0.04-0.05 mg N l^{-1}.

Nitrite values are highest in winter, which is common since the oxidation from nitrite to nitrate is strongly temperature dependent. High concentrations nitrite are a health risk, but the values found in the system are one to two orders below the values considered as risky (1 mg NO_2-N l^{-1} is mentioned by EPA (http://www.water-research.net/index.php/nitrate). The Dutch legislation gives 0.1 mg NO_2-N l^{-1} as maximum for drinking water. WHO (1998) gives 3 mg NO_2-N l^{-1} as maximum for acute effects, and 0.2 mg NO_2-N l^{-1} for chronical effects. See https://www.dunea.nl/drinkwater/belangrijkste-stoffen/gezondheidkundige-normen#Nitraat).

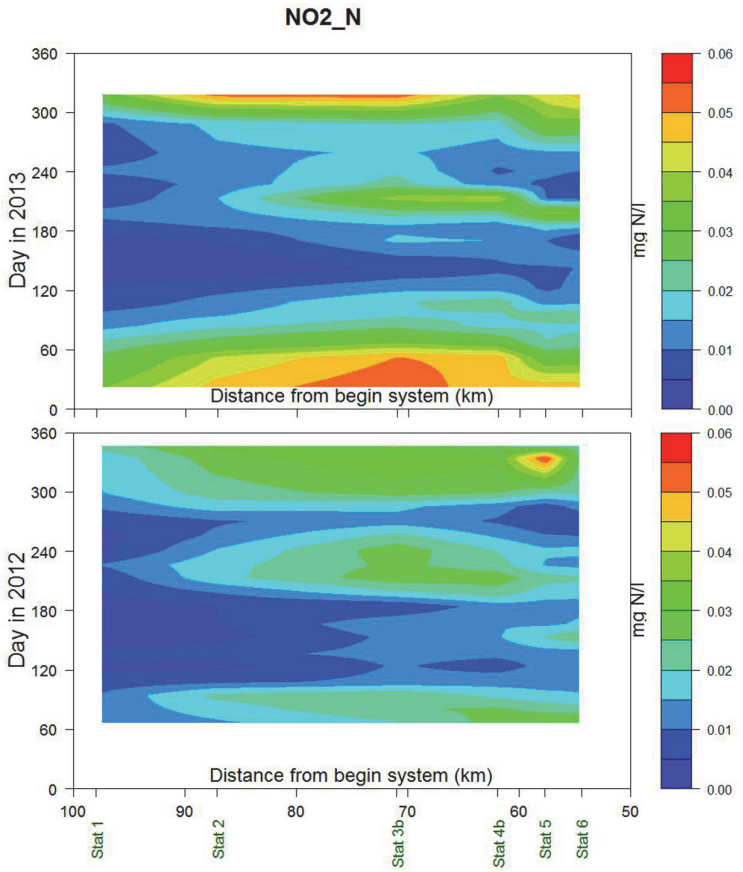

Figure 91 Level plots for nitrate NO_2^- for 2012 lower) and 2013 (upper). Distances mentioned are from Herbrum (DE). Sampling stations 1-6 mentioned.

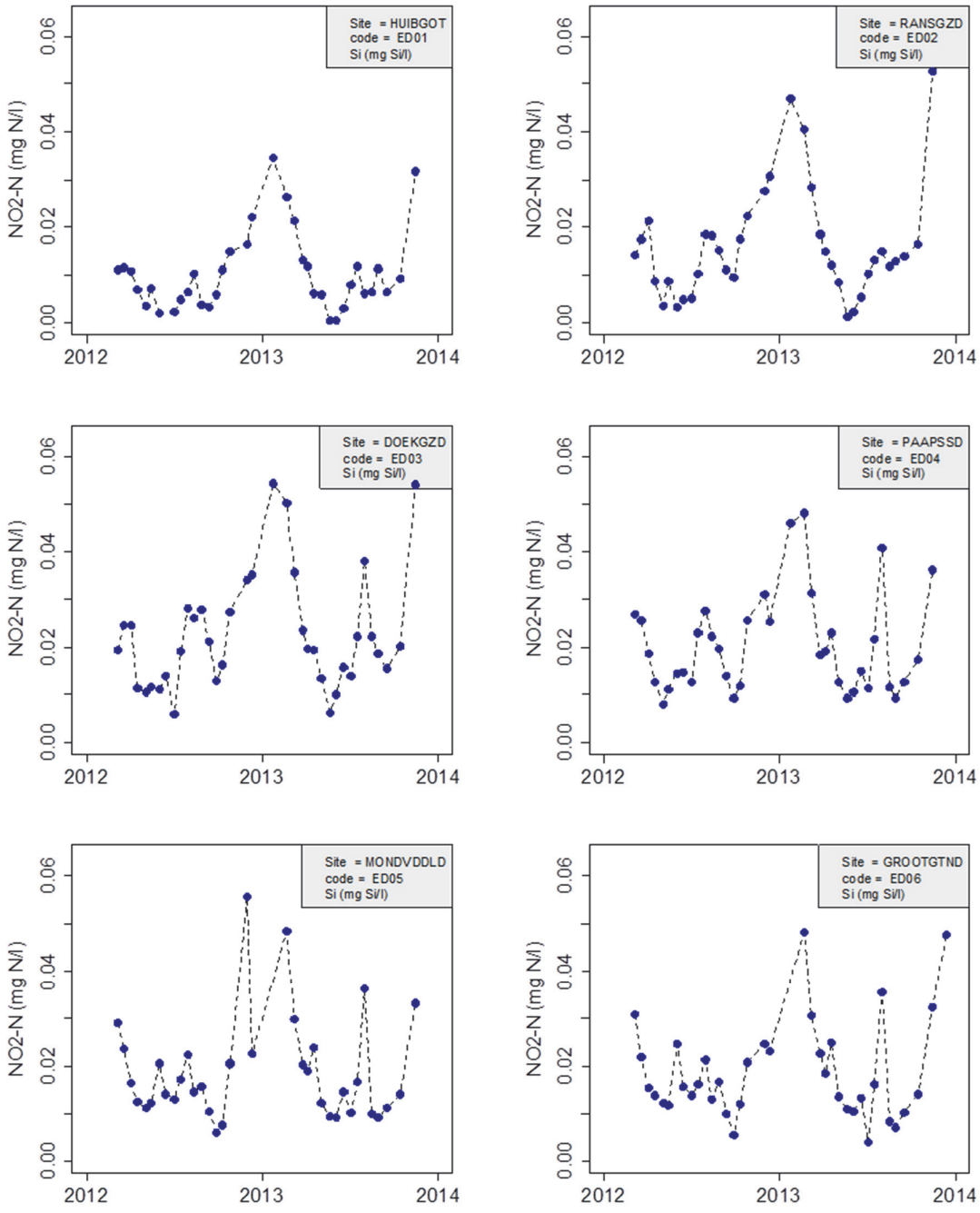

Figure 92 Water sample results for nitrite (NO2-) for all six stations, and both monitoring years. Code numbers ED01..ED06 give the station numbers according to Figure 16

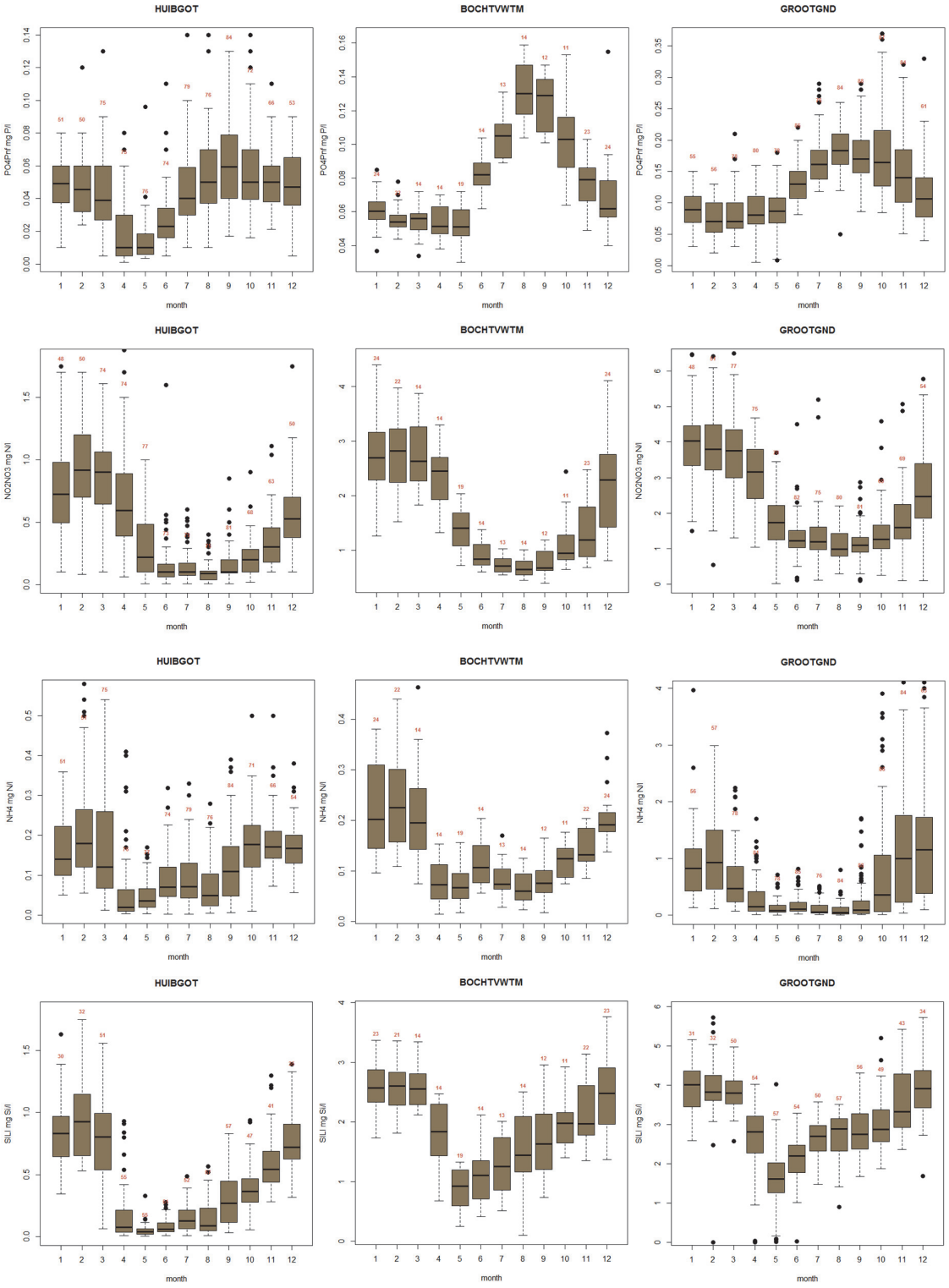

Figure 93 Nutrients in the estuary, monthly averages as boxplots for the period 1975-2011 (Huibert gat Oost, left, site = station 1), 1988-2012 (Bocht van Watum, middle, site = west of stations 3 & 4), 1975-2011 (Groote Gat Noord, right, site = station 6). Mind the different Y-axis scales. Source: Waterbase (2014). Nrs give the nr of observations. All data are in mg (N,P,Si) l^{-1}. Site nrs in Figure 23 are 2, 9 and 20, respectively.

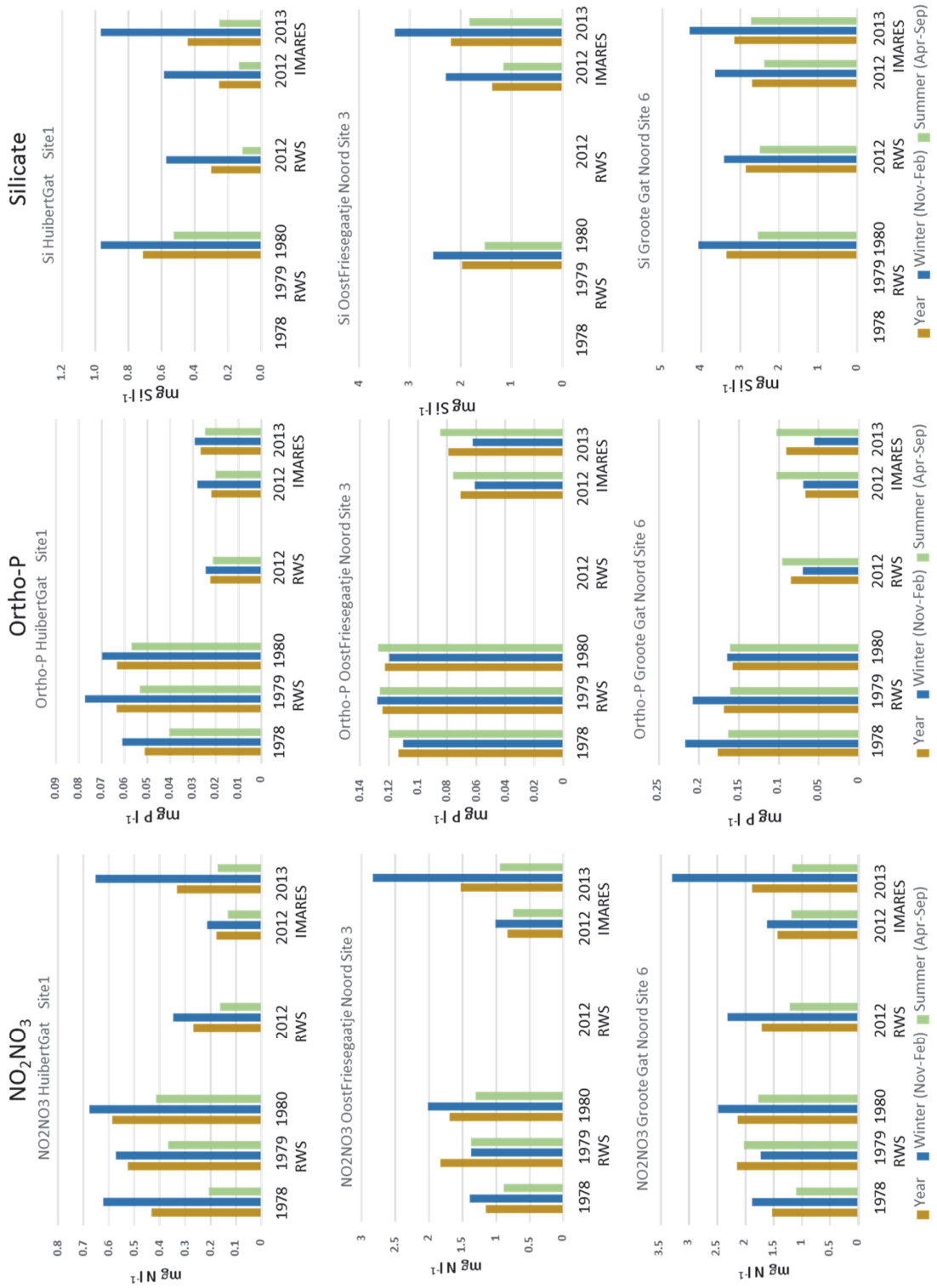

Figure 94 Summary of concentrations of nitrate+nitrite, ortho-phosphate and dissolved silicate as measured by RWS (RWS 2014), and IMARES for sites 1,3 and 6, in 1978-1980, 2012 (RWS) and 2012 & 2013 (IMARES). Year, winter (months 1,2,11,12) and summer (months 4-9) values are shown.

8.4.7 Summary and conclusions

Nutrient concentrations vary considerably between years, and the two years data set obtained in this research shows a different pattern for 2012 and for 2013. Generally:

a) Winter values are always higher than summer values (which is to be expected), although ortho-P concentrations in the inner areas increase rapidly after spring, resulting in summer averages that are higher than winter averages (Figure 94)
b) 2012 winter values are much lower than 2013 winter values
c) All values increase from station 1 to 6, as expected (except nitrite, for which geographical differences are small).

At all stations the same pattern can be observed: first there is a decline in phosphorus and silicate concentrations. In 2012 it looks like that silicate decline is earlier than the one of phosphorus, and in 2012 it is opposite. After spring (at begin summer, month July), phosphate and silicate concentrations increase, while nitrate concentrations drop to low values.

Generally, concentrations of silicate and nitrate do not differ drastically from the average values in previous years. Ammonium concentrations nowadays are considerably lower than in the past, especially in the Dollard area. It is a general picture for the whole Wadden Sea, North Sea coastal zone and also Lake IJssel (Brinkman, 2008; Grunwald et al, 2010). Ortho-phosphate concentrations generally are lower than about 20 years ago. This picture is similar to the western Wadden Sea pattern, but changes are smaller in the Ems-Dollard area (Brinkman, 2008).

8.5 Dissolved inorganic carbon

Dissolved organic carbon (which is almost completely HCO_3^-, and thus, 1 mol inorganic carbon == 1 moleq alkalinity, see section 4.9) is shown as level plot in Figure 95; details are mentioned in Figure 96 and Figure 97.

Summer values normally are lower than winter values, a result of carbon dioxide consumption by phytoplankton, and of higher water temperatures: carbon dioxide solubility decreases with increasing temperature. Dissolved inorganic carbon data were needed because of the ^{14}C-incubation analyses, and thus, these data are a side-product of the primary production measurements.

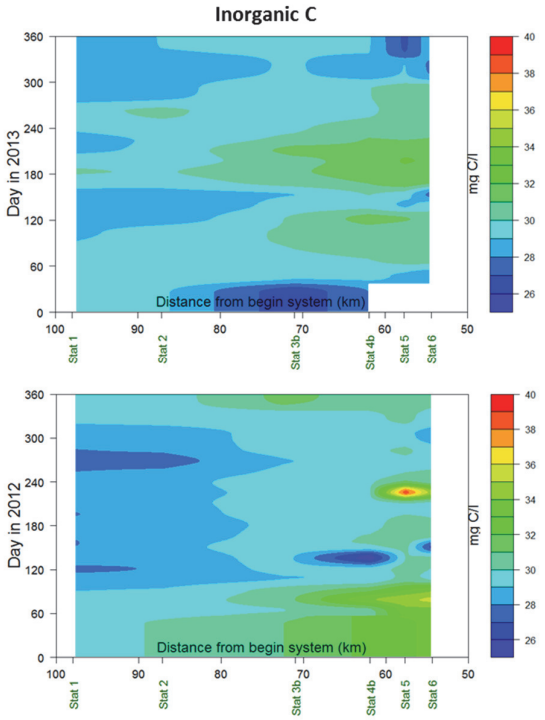

Figure 95 Inorganic carbon content in the water column in the estuary in 2012 (lower) and 2013 (upper). Distances mentioned are from Herbrum (DE). Sampling stations 1-6 mentioned. First values in 2013 might be a bit too low; since there is no connection with the last values for 2012.

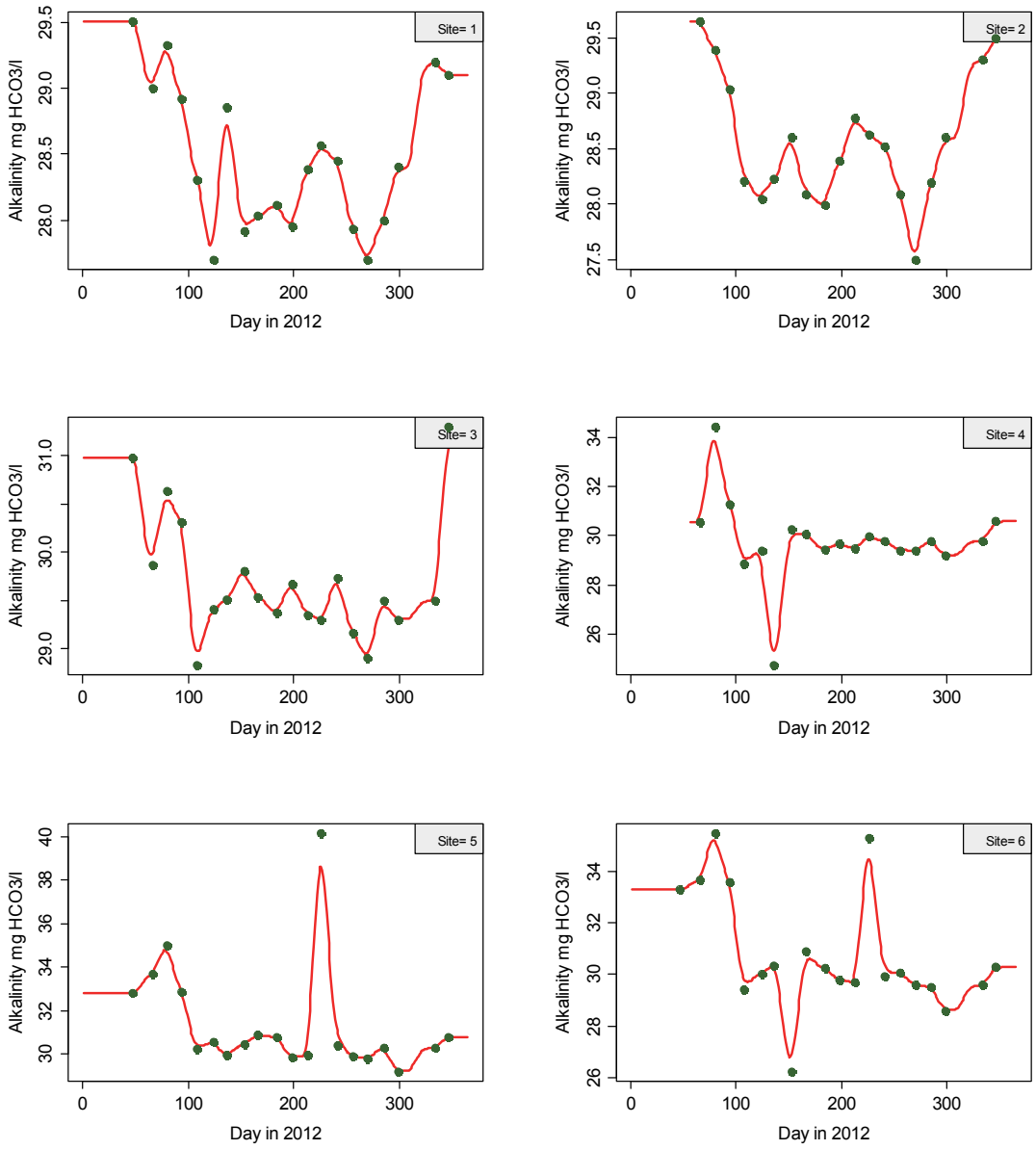

Figure 96 Inorganic carbon dioxide content in the water column at the six station in 2012, measured (dots) and inter/extrapolated (lines), following a moving-average method.

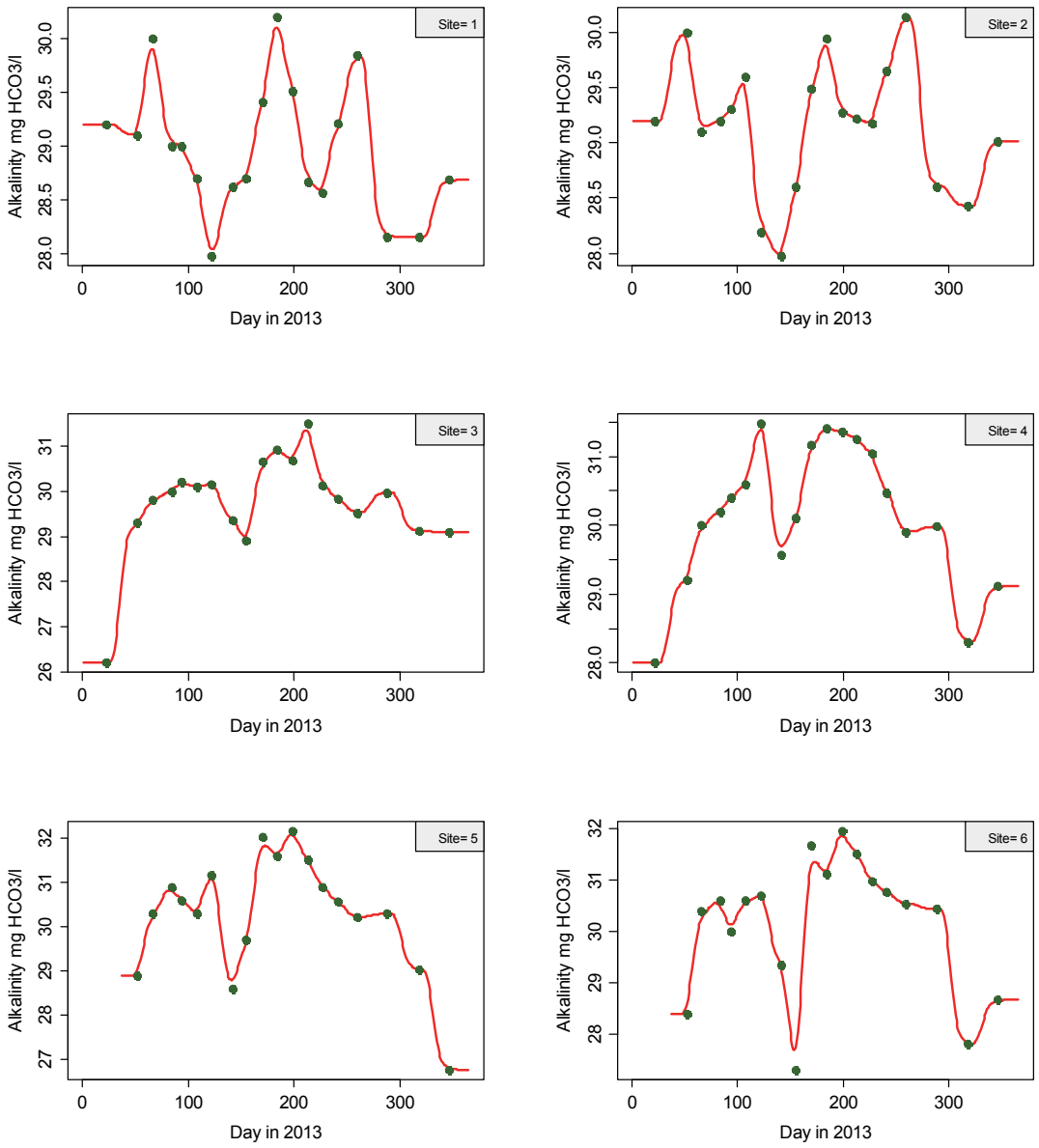

Figure 97 Inorganic carbon dioxide content in the water column at the six station in 2013, measured (dots) and inter/extrapolated (lines), following a moving-average method.

8.6 Oxygen

Oxygen results, as measured by the PocketBox optode, are presented in Figure 98. Mostly, values are around saturation level (==100%), only in summer relatively low values down to about 70% saturation are found. Details are presented in Figure 99 and Figure 100.

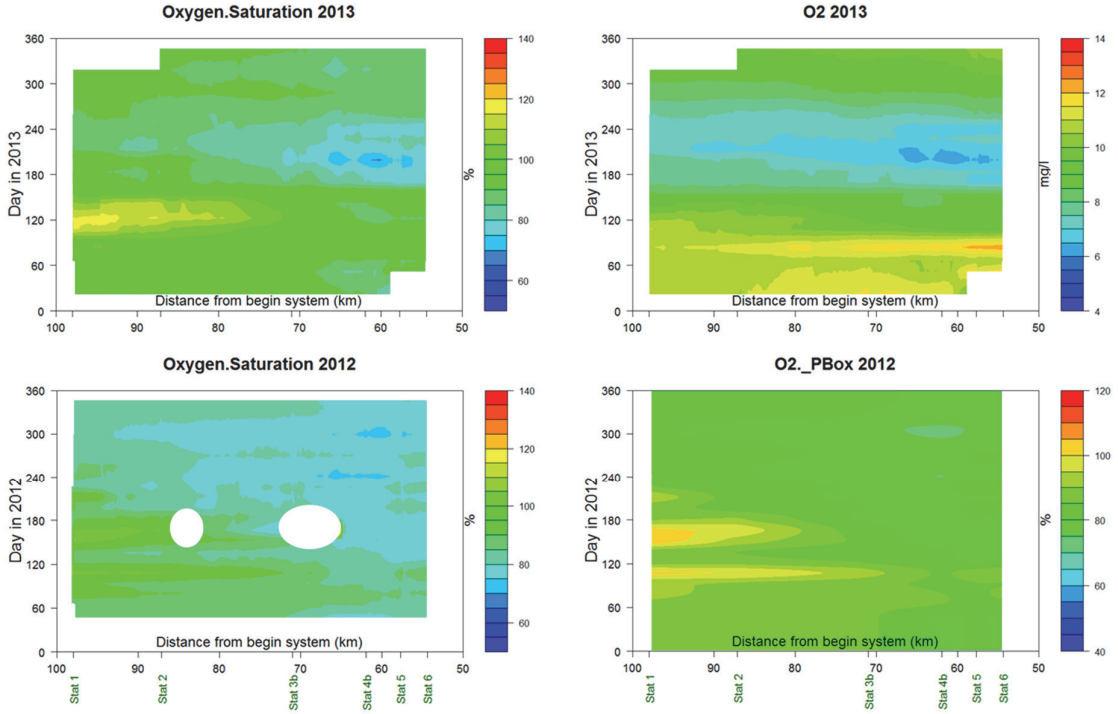

Figure 98 Oxygen concentrations (right, mg O2 l^{-1}) and saturation percentage (left) in the system. Distances mentioned are from Herbrum (DE). Sampling stations 1-6 mentioned. Saturation values in 2012 (lower left) show two gaps due to probe errors.

Historical values (Waterbase, 2014) are summarized in Figure 101. There is one striking difference between nowadays values and those from the period before 1984: values for the Dollard-area then sometimes dropped to values below 3 mg O_2 l^{-1}. Changes in waste water management will definitely have had a major impact on these results; see e.g. Essink (2009). Roughly in 1983, most waste water that was previously sluiced into the Dollard system was directed to waste water treatment plants. Nowadays oxygen deficiencies below 60% saturation value obviously do not occur.

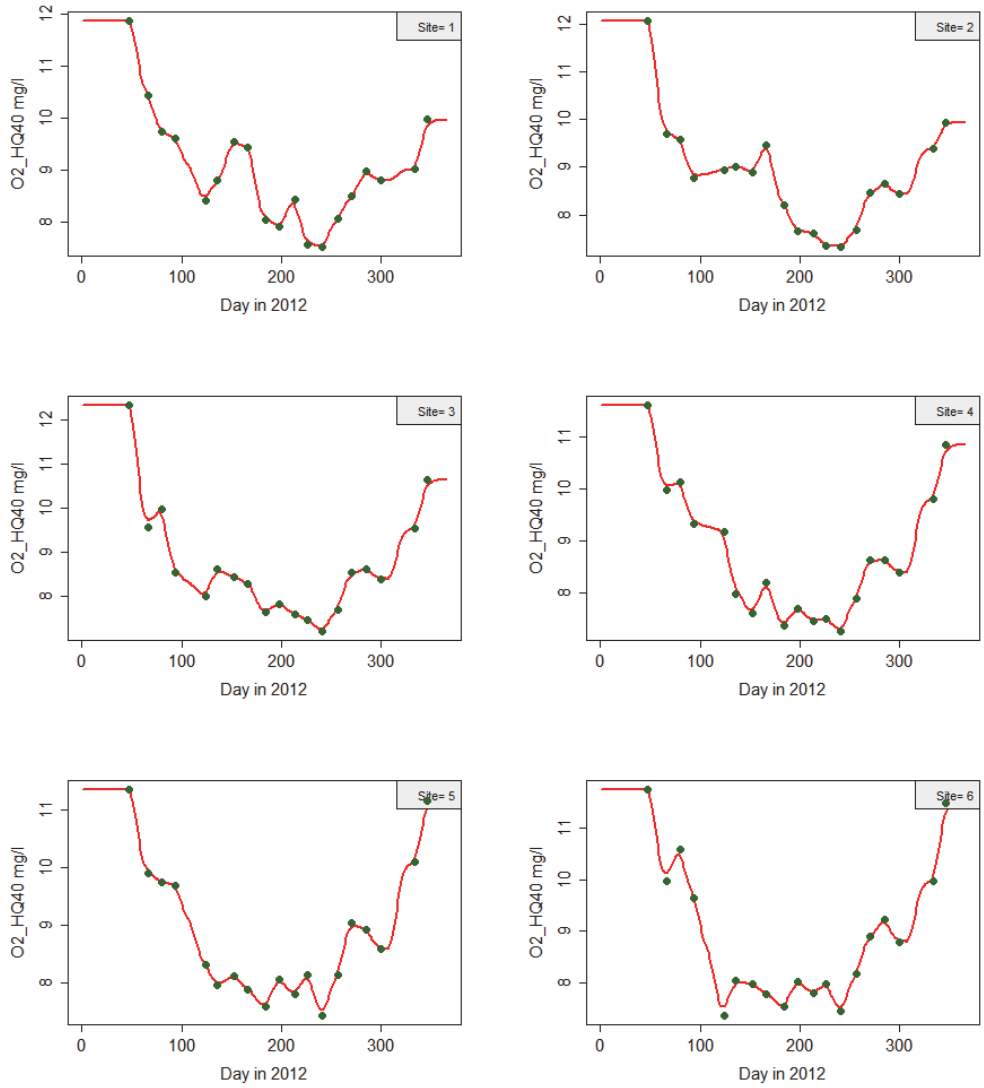

Figure 99 Oxygen content in the water column at the six station in 2012, measured (dots) and inter/extrapolated (lines), following a moving-average method.

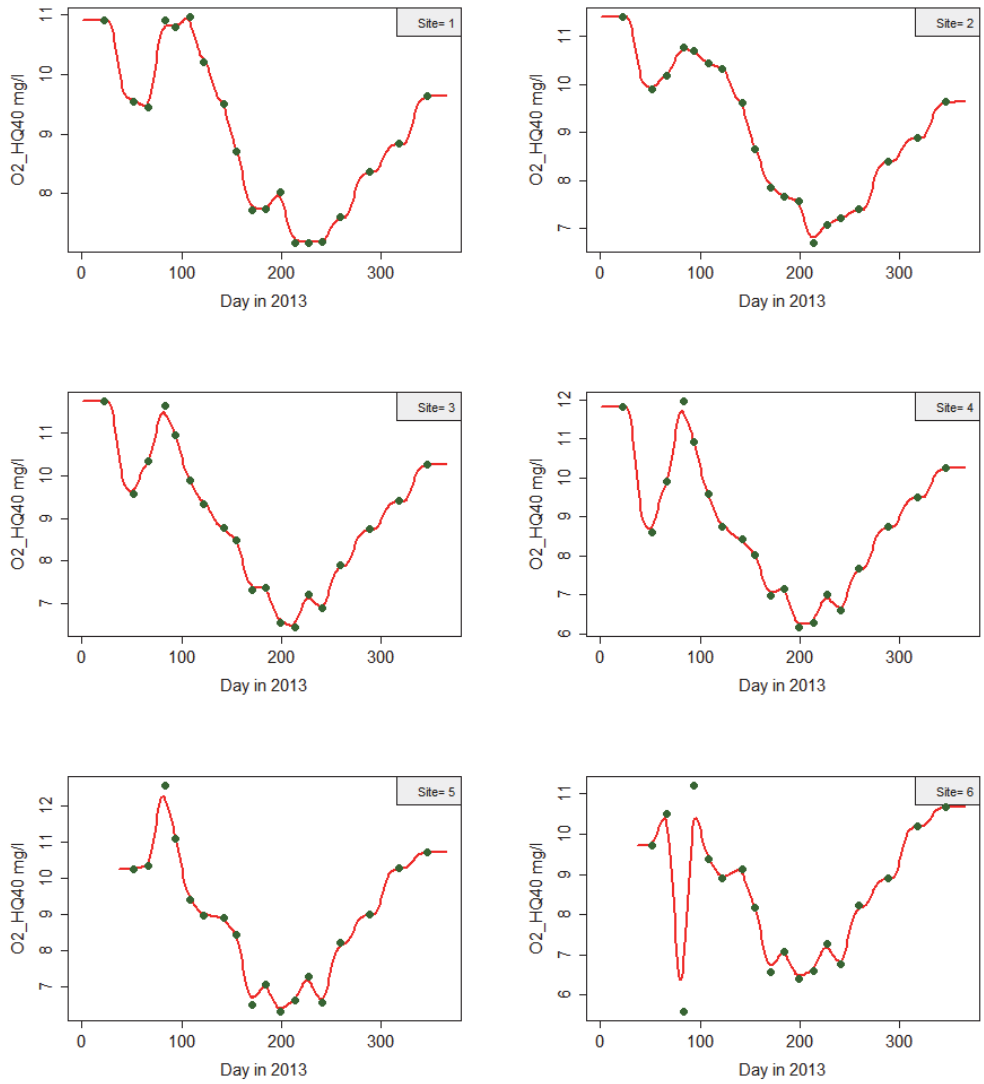

Figure 100 Oxygen content in the water column at the six station in 2013, measured (dots) and inter/extrapolated (lines), following a moving-average method.

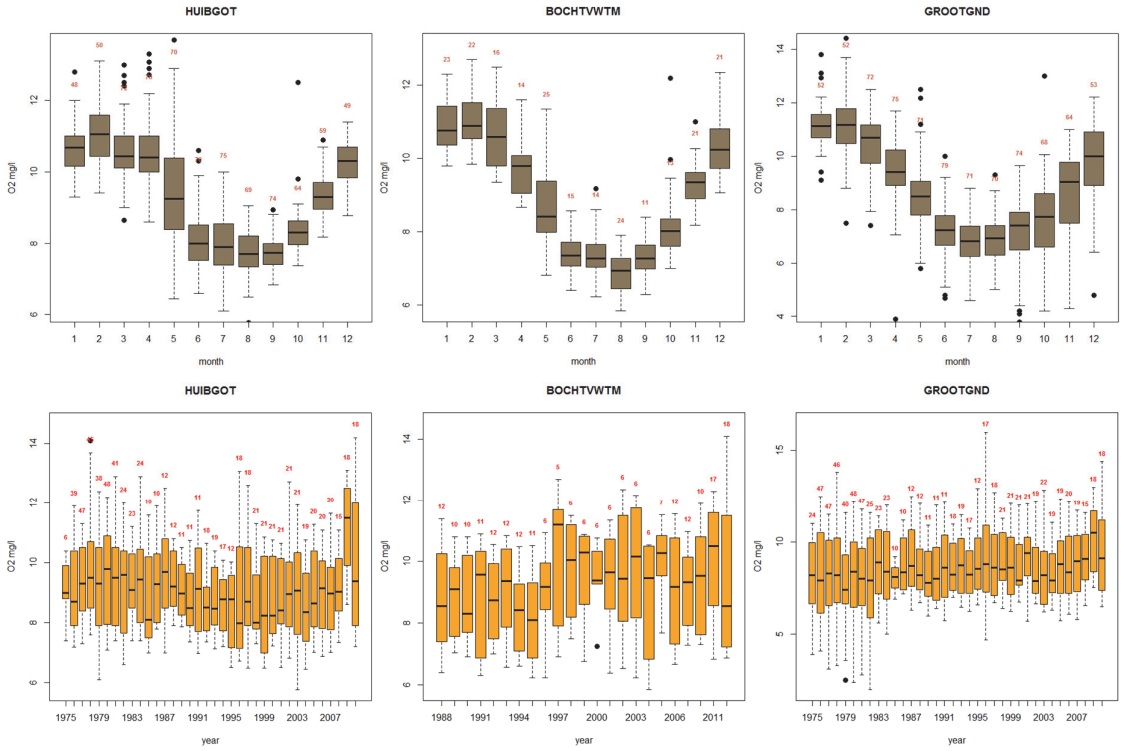

Figure 101 Oxygen in the estuary, monthly (upper) and yearly (lower) averages as boxplots for the period 1975-2011 (Huibert gat Oost, left, site = station 1), 1988-2012 (Bocht van Watum, middle, site = between station 3 & 4), 1975-2011 (Groote Gat Noord, right, site = station 6). Mind the different Y-axis scales. Source: Waterbase (2014). Nrs give the nr of observations. All data are in mg O_2 l^{-1}. Site nrs in Figure 23 are 2, 9 and 20, respectively.

8.7 Suspended matter

8.7.1 Present and previous data

Suspended matter results are presented as average values in Figure 102. In Figure 103Figure 104 and Figure 104 level plots as shown of the measured values, together with estimated values from turbidity data and from C-Star1 attenuation data. Pure measurements are shown in Figure 105 and Figure 106. Monthly monitoring data by RijksWaterstaat (RWS MWTL-data, source: Waterbase, 2104) are plotted in Figure 107 and Figure 108.

First it can be concluded that there are large temporal differences in both years. Winter values usually are higher than summer values, which is expected since wind and waves will strongly affect

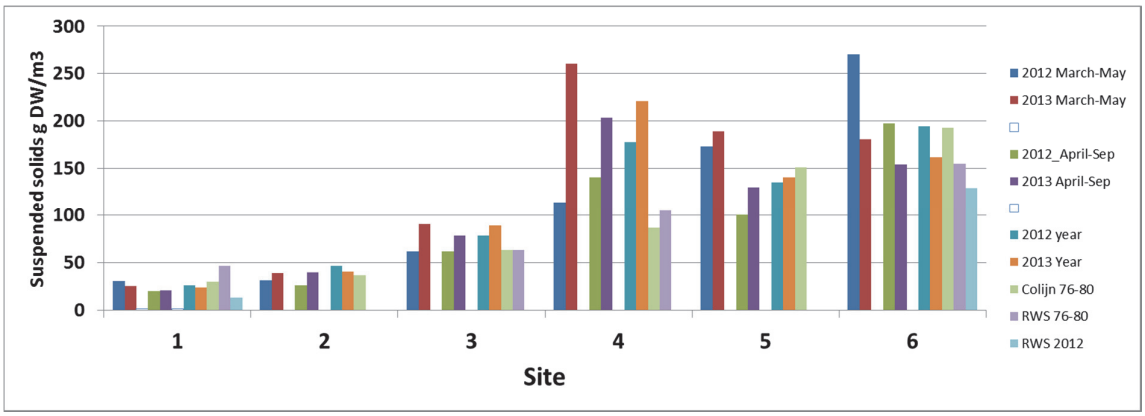

Figure 102 Suspended solids in the estuary. Mean values for the period March-May (MM), April-September (AS) and whole year (Y) for 2012, 2013 and Colijn (1983) results for 1976-1980 (whole period only). RWS monitoring results are included: 2012-data only for the present situation, 1976-1980-data for site 1, 3 and 6, and 1976-1978-data for site 4.

resuspension. This is according the general trend as pictured in Figure 107 and Figure 108. This wind induced behaviour seems to be stronger at site 1 (Huibertgat Oost) than in the Dollard. Possibly, average values in the Dollard already are high, and thus, wind induced variations add less to the absolute values. For more information on silt dynamics see Van Maren et al (2014[a,b]).

Highest values in the Dollard reach up to 700 mg l^{-1}. Values estimated from C-Star1 data have an upper limit of about 150 – 200 mg DW l^{-1}, because of the sensor limit.

From our results, the RWS-dataset and Colijns results (Colijn 1983) a few conclusions can be drawn (not trends, but just differences between the data then and those found now):

Site 1: values found now are slightly lower than Colijns values, and clearly below the 1976-1980 RWS-monitoring values. RWS-2012 values are much lower than IMARES-values.

Site 2: values found now are slightly higher than Colijns values.

Site 3: values now are above the 1976-1980 values of RWS and Colijn, both the latter have the same value.

Site 4: the site with the largest differences found. Values found now are almost twice of the values found in 1976-1980 (both by Colijn and by RWS).

Site 5: values now are almost the same as those found by Colijn.

Site 6: values now are almost the same as those found by Colijn and RWS; present RWS-values are lower than the 1976-1980 values

Some trends can be concluded from the Waterbase data set (Figure 107 and Figure 108) it can be concluded that especially in the middle areas (RWS station Oostfriese Gaatje, nr 13 in Figure 23) suspended solid content has increased with the years (this also was partly the basis for the present research) from 50 to about 120 mg l^{-1} as year average and 60-150 à 200 as higher quartile. In the Dollard area, the trend is not clear: values decrease from the end of the 70's to around 1990, and start to increase again until 2010.

Although RWS- data for site 4 and for the final part of the Ems-river (the shipping channel to the Emden harbour) (Figure 109) only are available until 1986/1987, it is clear that especially there the suspended solid content did increase a lot. This is in agreement with the conclusions based on Figure 102: there where the river Ems enters the estuary, suspended solid content increased a lot since the 1976-1980 period.

8.7.2 Conclusions

Since silt dynamics is one of the core of the whole project, the data presented here add to the data already available, and serve the dynamic models. Conclusions on silt dynamics here would be premature; the reader is referred to the relevant Deltares reports (Vroom et al, 2012; Van Maren et al, 2014[a,b]); only average observed values are relevant here.

Present suspended matter estuary gradients are well in line with results from Rijkswaterstaat, and show a clear increase from the most North Sea site (Huibertgat Oost) to the Dollard site (Groote Gat Noord).

Compared to observations in the period 1976-1980, very clear differences are found at site 4 (Gaatje Bocht Noord) where the Ems river enters the Ems-Dollard: from 1976-1980 to now suspended matter contents almost doubled there from below 100 mg DM l^{-1} to 170 – 220 mg DM l^{-1}. At site 3 (Oostfriese Gaatje) suspended matter has increased since the 1976-1980 period, but to a lesser extend compared to site 4. At Huibertgat, values now are more or less the same as (or a bit lower than) those found by Colijn, and considerably lower than the 1980 RWS-data. In the Dollard area, changes are much smaller, and it is seems that values are more or less the same as those in the Colijn-period.

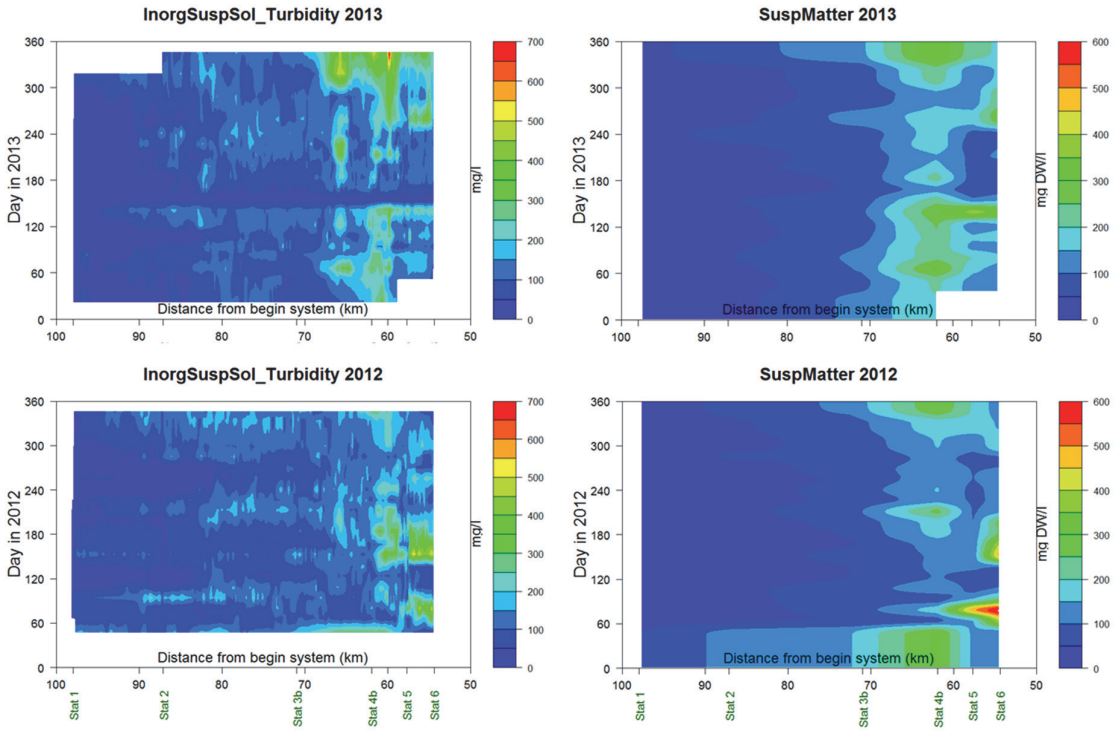

Figure 103 Inorganic suspended solids in the system (1). Upper: 2013, lower: 2012. Right: as measured at the sampling sites. Left: as estimated from pocket Box-turbidity data (see 4.4.7 & 7.10. Mind the different scales. Distance=0 at Herbrum (DE).

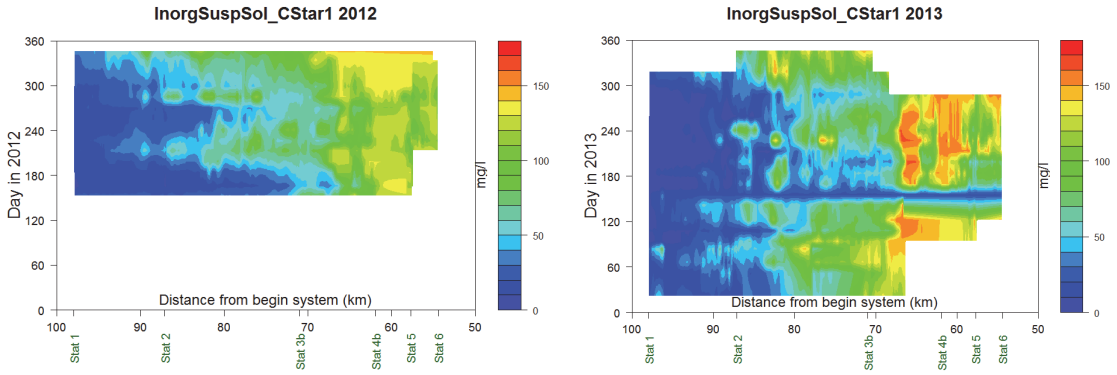

Figure 104 Inorganic suspended solids in the system. Left: 2012, right: 2013. Lower: as estimated from C-Star1 attenuation data (see 4.4.6 & 7.12). Especially C-Star1 –data are missing in the most turbid regions of the system because the sensor reached its upper limit. Mind the different scales. Distance=0 at Herbrum (DE).

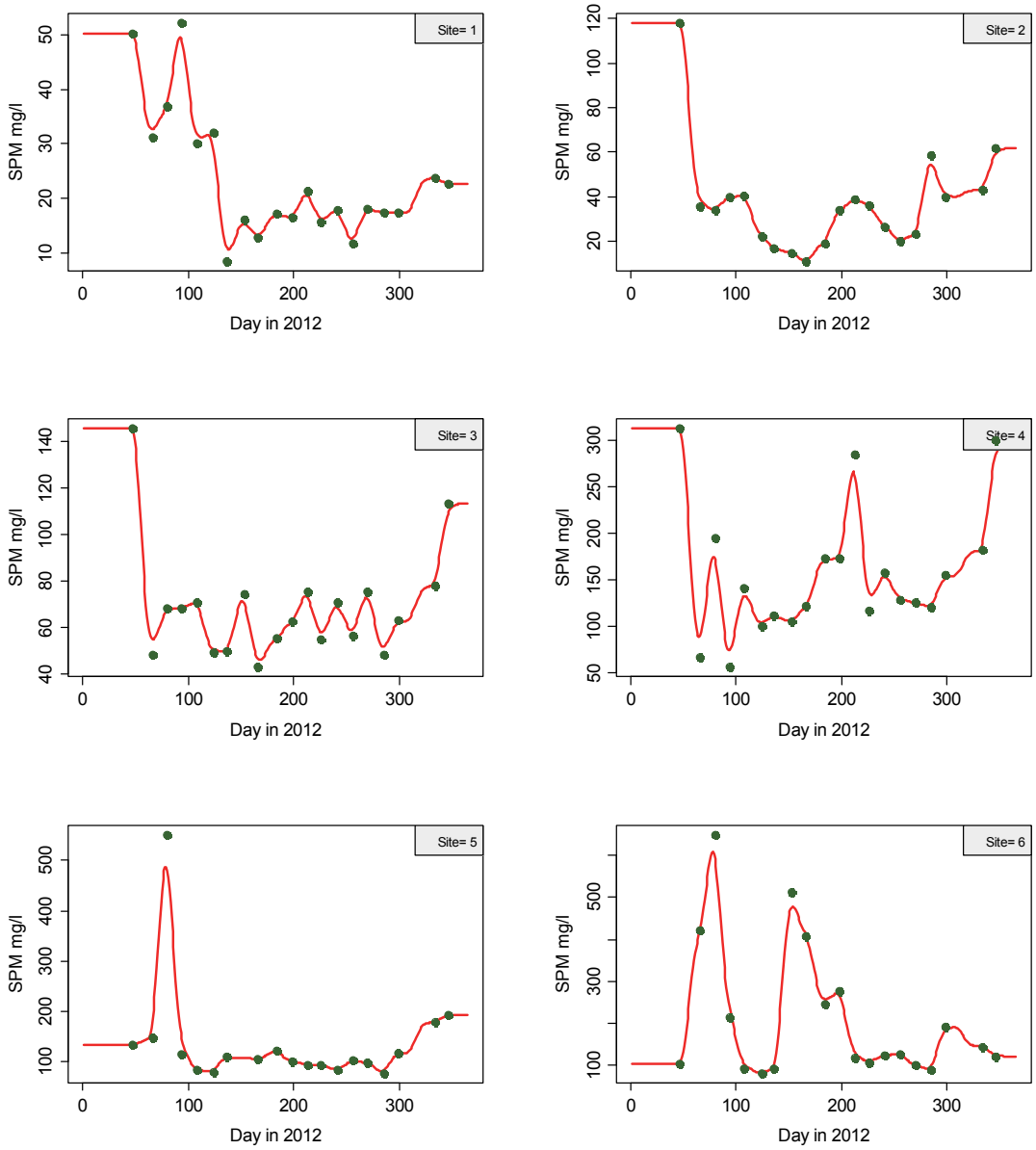

Figure 105 Suspended matter at the six station in 2012, measured (dots) and inter/extrapolated (lines), following a moving average method.

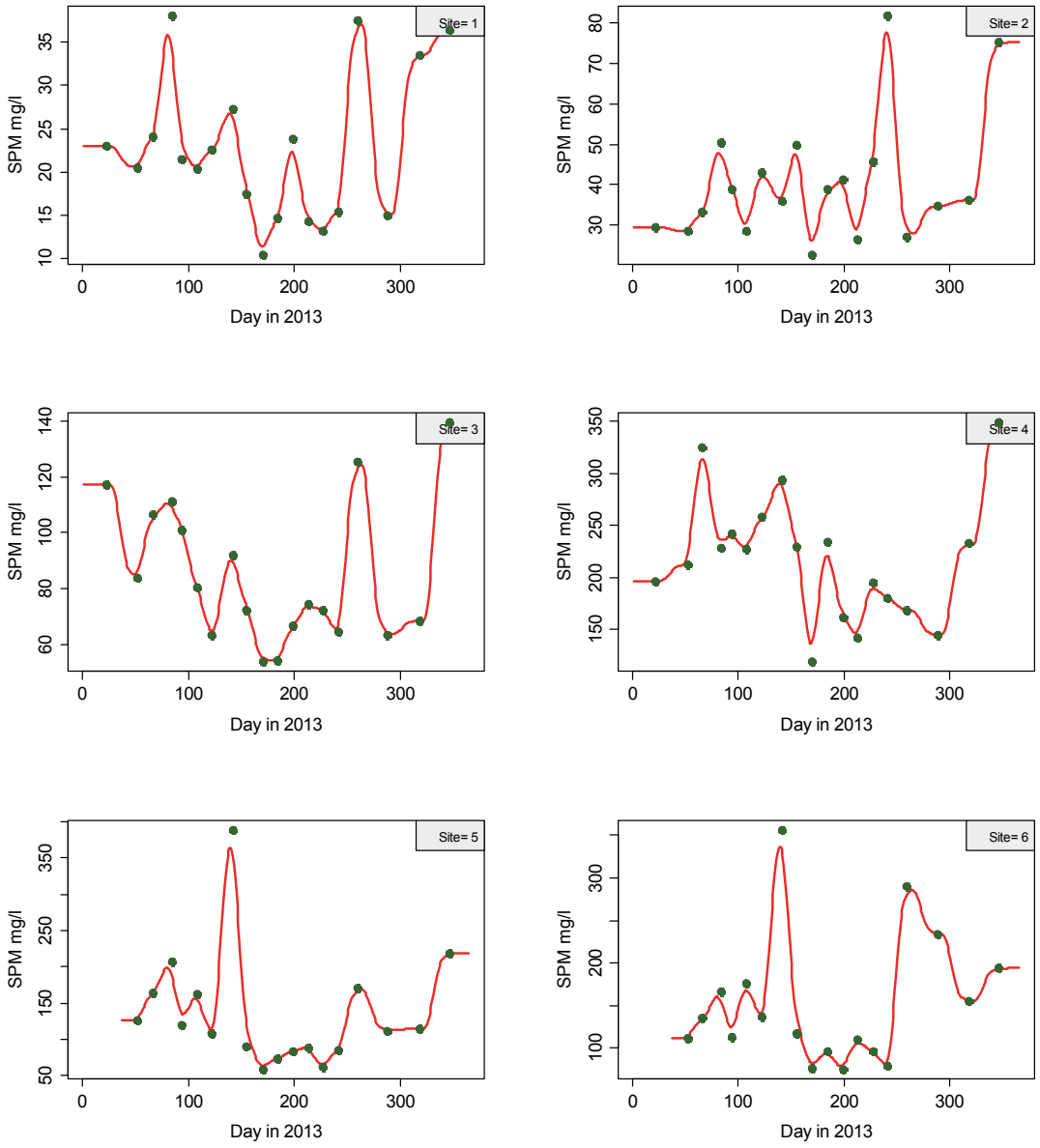

Figure 106 Suspended matter at the six station in 2013, measured (dots) and inter/extrapolated (lines), following a moving average method.

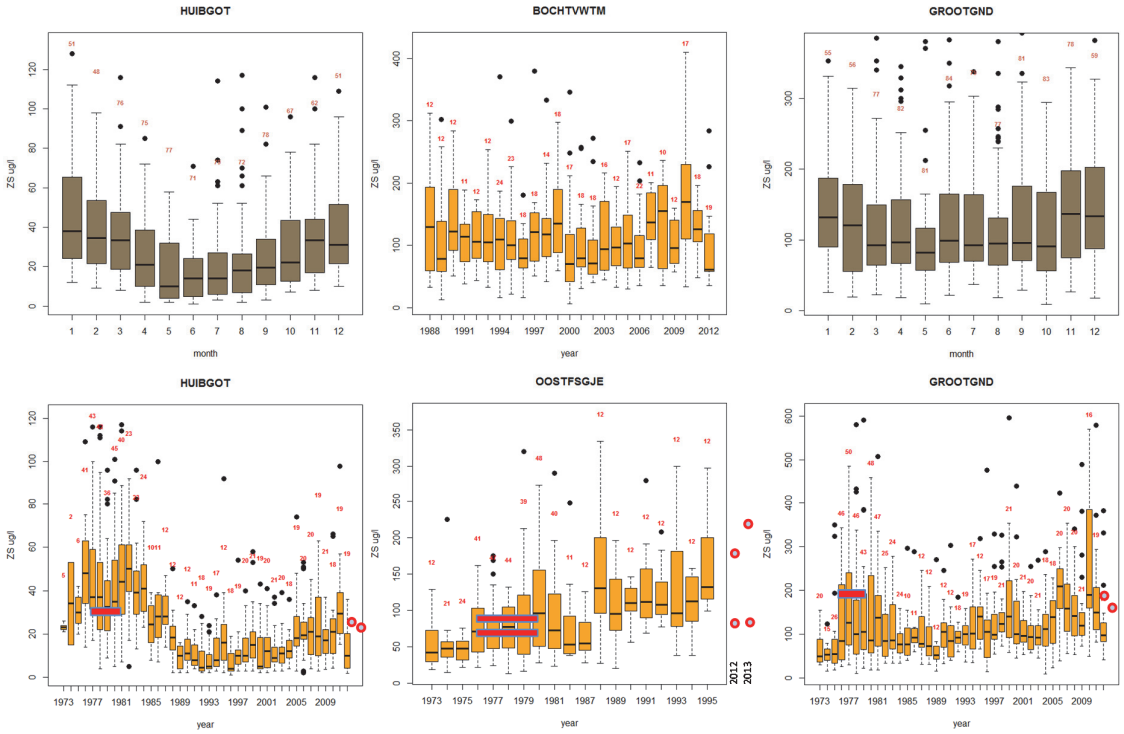

Figure 107 Suspended solids in the estuary, monthly (upper left and upper right) and yearly (lower and upper middle) averages as boxplots for the period 1975-2011 (Huibert Gat Oost, left, site = station 1), 1988-2012 (Bocht van Watum, upper middle, site = west of station 3 & 4), 1973-1995 (OostFriese gaatje, between sites 3 and 4), 1975-2011 (Groote Gat Noord, right, site = station 6). The Bocht van Watum is located in a sedimentation area of the system. Mind the different Y-axis scales. Source: Waterbase (2014). Nrs give the nr of observations. All data are in mg Dry Matter l^{-1}. Site nrs in Figure 23 are 2, 9, 13 and 20, respectively. Data as reported for 1976-1980 by Colijn (1983) as given as bars, averages found in the present research are given as circles (2012 and 2013).

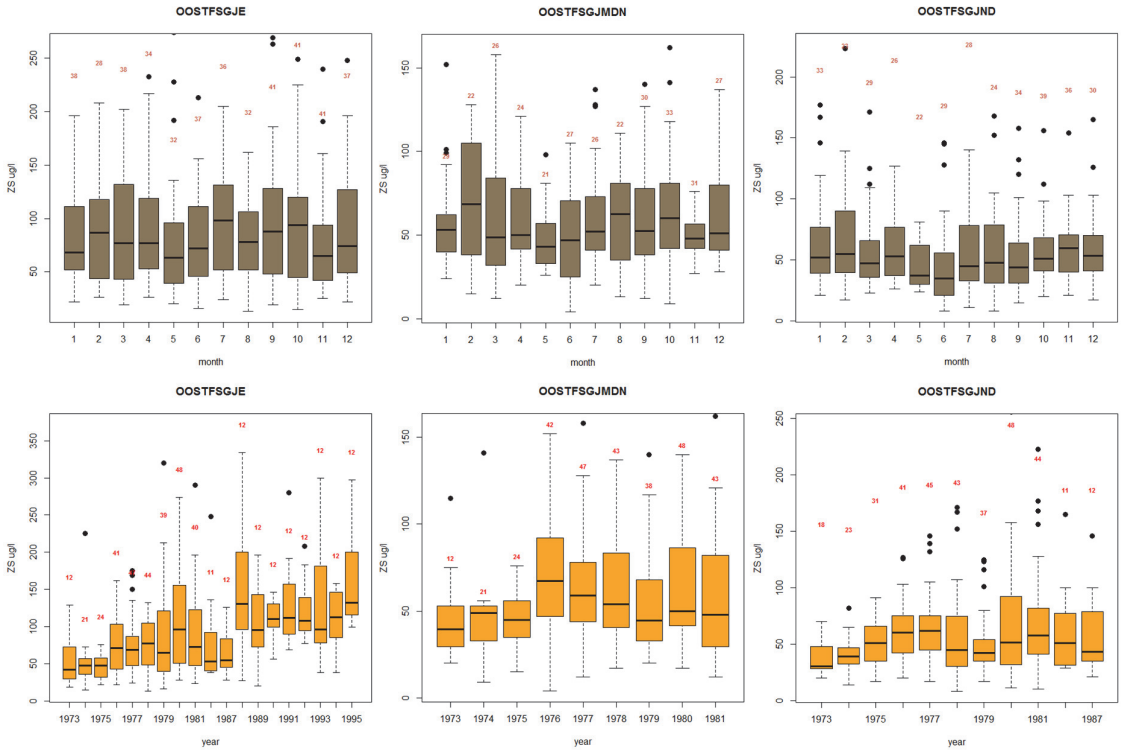

Figure 108 Suspended solids in the estuary, monthly (upper) and yearly (lower) averages as boxplots for the period 1973-1995 (Oost-Friese Gaatje, left), 1973-1981 (Oost-Friese Gaatje Midden, middle), 1975-1987 (Oost-Friese Gaatje Noord, right). Mind the different Y-axis scales. Source: Waterbase (2014). Nrs give the nr of observations. All data are in mg Dry Matter l^{-1}. Position of the left graphs is roughly between sites 3 & 4 with the left graph closest to the Dollard. Exact sites: see Figure 23, numbers are 13, 12 and 14, respectively.

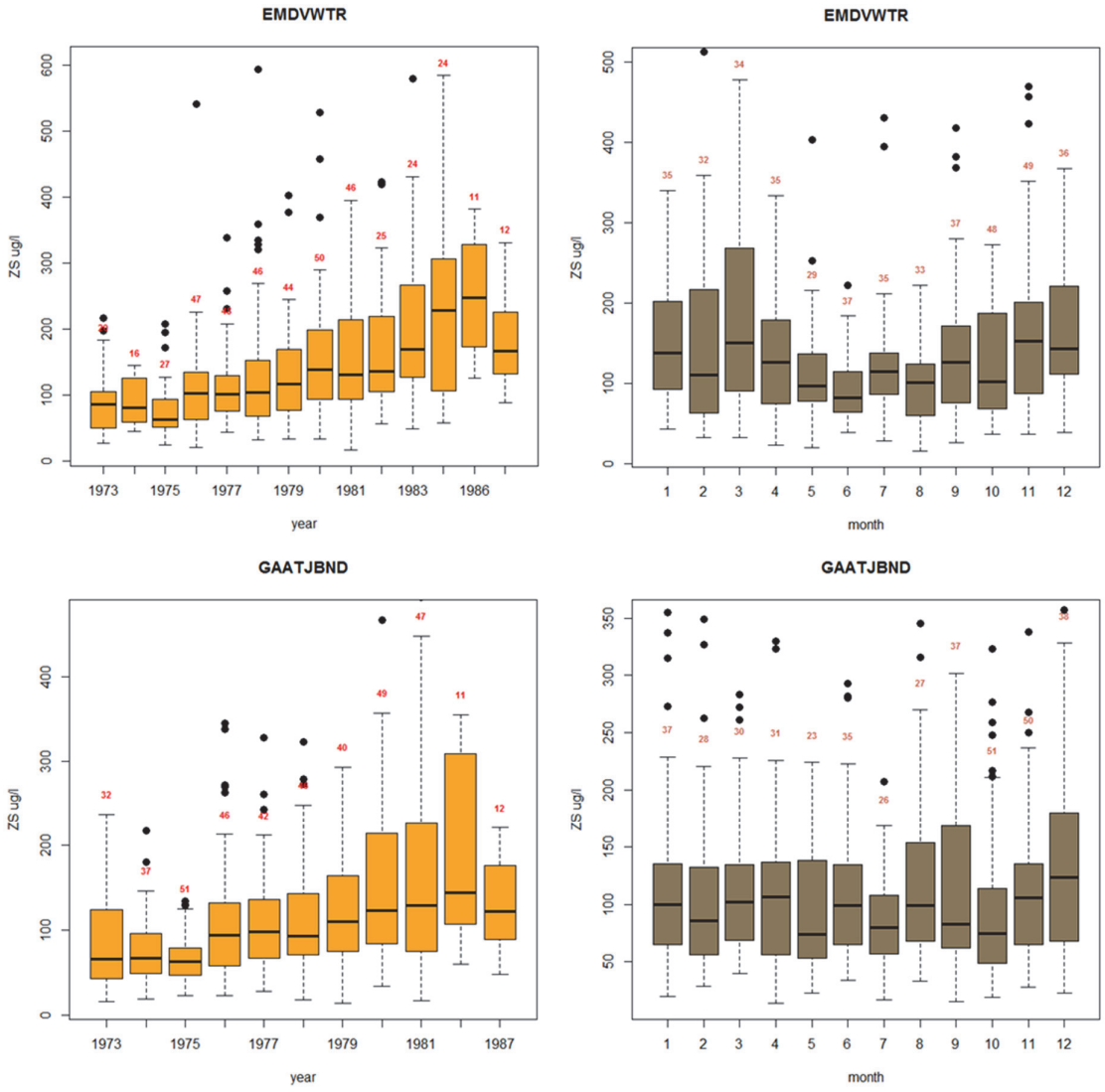

Figure 109 Suspended solids in the estuary, monthly (right) and yearly (left) averages as boxplots for the period 1973-1987 for the last part of the Ems river (upper, Emden channel, site 19 on Figure 23) and there where the Ems has entered the estuary (lower, gaatje Bocht Noord, site 16 on Figure 23). Mind the different Y-axis scales. Source: Waterbase (2014). Nrs give the nr of observations. All data are in mg Dry Matter l^{-1}.

8.8 Pelagic total chlorophyll-a

8.8.1 Introduction

In this section pelagic chlorophyll-a results are presented and compared with other data. It must be remembered that in section 7.13 the different chlorophyll-a analysis techniques were compared. The values produced by the fluorometric analyses are the same as the AOA-chlorophyll-results, and thus both can be considered as true results for the pelagic chlorophyll-a concentrations. However, the fluorometric observations should give total chlorophyll instead of chlorophyll-a alone; it is estimated

that the total chlorophyll values may be about 30%-40% above the fluorometric values reported. It was also concluded that AOA-results are correct; this was based on a comparison with HPLC-results.

In this section 8.8, a comparison with older data is also described. Rijkswaterstaat monthly monitoring data (MWTL, Waterbase, 2014) are based on a variety of methods; several extraction fluids (aceton, ethanol) and detection methods (spectrophotometric, fluorometric) combined with a separation method (HPLC) or not, and depending on the separation, the choice for the absorption wavelength. Flintrop et al (2002) gave an overview. Next, all detection methods use a calibration factor to compute chlorophyll-a values from the response of the analyser (see e.g. the equations in section 4.6), and Flintrop et al (2002) mention a couple of conversion factors that needed correction. Flintrop et al (2002) concluded that data before 1983 had to be corrected with a factor 0.81, which has been implemented in the data nowadays presented in Waterbase (Waterbase, 2104). Next, they suggested another correction factor of 0.81, which nowadays is NOT implemented in Waterbase.

8.8.2 Observations

Chlorophyll-results are shown in Figure 110 - Figure 111 (2012, 2013, values as measured by fluorometry), in Figure 112 (2012, 2013, based on PocketBox-data and the same fluorometry data) and in Figure 113 (based on algal cell volumes). Highest values are found around station 2, with peak levels in spring. Also, these peak levels are most pronounced around station 2; in the inner compartments highest levels (that are much lower than those in the other areas) last almost until the end of summer. Level plots (Figure 112) even better show the rather sharp peak around station 2, which is visible in both years (although much more pronounced in 2013).

Variations within 2012 and 2013 (Figure 117) are different for stations 1-3 and stations 4-6: the first show a distinct spring maximum, while stations 4-6 values stay more or less at similar values from April-August. As a result, year averages in the inner areas are hardly different from those in the outer areas.

8.8.3 AOA-sensors and estimates from algal cell volume

Results shown in Figure 113 illustrate that in many cases there is a good agreement between the AOA-sensor values for chlorophyll-a and those estimated from algal cell volume. However, there is also a number of exceptions; in some cases, AOA-values are much higher than those derived from cell volumes, and the reverse case happens as well:

- at station 2, in the 1st of august 2013 samples a very high dinoflagellate volume was found, completely based on one *Noctiluca scintillans* –cell with a cell volume of 50000000 μm^3 (diameter=0.44 mm). Thus, an exceptional observation that biased the whole estimate for chlorophyll-a. After removal of this *Noctiluca*-observation, 5.1 µg chla l^{-1} remains, which is more or less the same as the AOA-value
- at stations 4 - 6, high values result at day 155 (2013-06-04), whereas AOA-data values stay low. In all cases it is due to high diatom cell volumes, but no irregularities seem to have occurred. In these cases it is not clear what the (most) correct values are.

8.8.4 Comparison with RWS-monthly monitoring data 2012

Monthly monitoring data by Rijkswaterstaat (Waterbase, 2014) (boxplots with medians, upper and lower quartiles, upper and lower boundaries plus outliers: Figure 114; and summer plus yearly averages: Figure 115 and Table 32) show i) a decrease with years in the outer reaches (Huibertgat Oost), and hardly any change in the inner areas.

For 2012, Waterbase (2014) gave low chla concentrations; this is also the case in our 2012-2013 dataset. Values from the present research are close to the Waterbase values. Seen the remarks by Flintrop et al (2002) (see above, section 8.8.1) the Waterbase values presented may still be at the high side. Seen the remarks in section 7.13.6, our data may be at the low side.

8.8.5 Comparison with Colijn data and RWS-Waterbase data for 1976-1980

Colijn-data were extracted from Colijn (1983), and plotted in Figure 117. Colijn used –as we did in the present research- 90% acetone as extraction fluid. Colijn used a spectrophotometric method for chlorophyll-analyses, contrary to the fluorometric method we used. Flintrop et al (2002) stated that an acetone extraction method (sometimes) induces too high chlorophyll-a values as a result of degradation of chlorophylase to chlorophylid, which has the same absorption characteristics as chlorophyll-a. Thus there are enough reasons to consider any comparison with other data with care.

Also, in the first two years (1976 and 1977), Colijn sampled only the second half of the year, and thus he missed the springtime phytoplankton maxima.

Generally spoken, and seen these remarks, the comparison with Colijn's data may lead to the following observations. Colijn found high chlorophyll values in 1979 and 1980. RWS found much lower chla-values in 1980 (Figure 114 and Table 32) than Colijn did; in 1979 these differences are smaller. In the Dollard area, the present chlorophyll-a values are similar to the ones Colijn found and the RWS-data, now and in the past. At station 3-4 (Oostfriese Gaatje) present values are similar to RWS-Waterbase data and to Colijns data, with an exception for 1980 (Colijn) and 1979 (RWS). At station 1 (Huibertgat Oost) values now are considerably lower than in the RWS- and Colijn dataset for the years 1976-1980 (but similar to the RWS-Waterbase data in 2012).

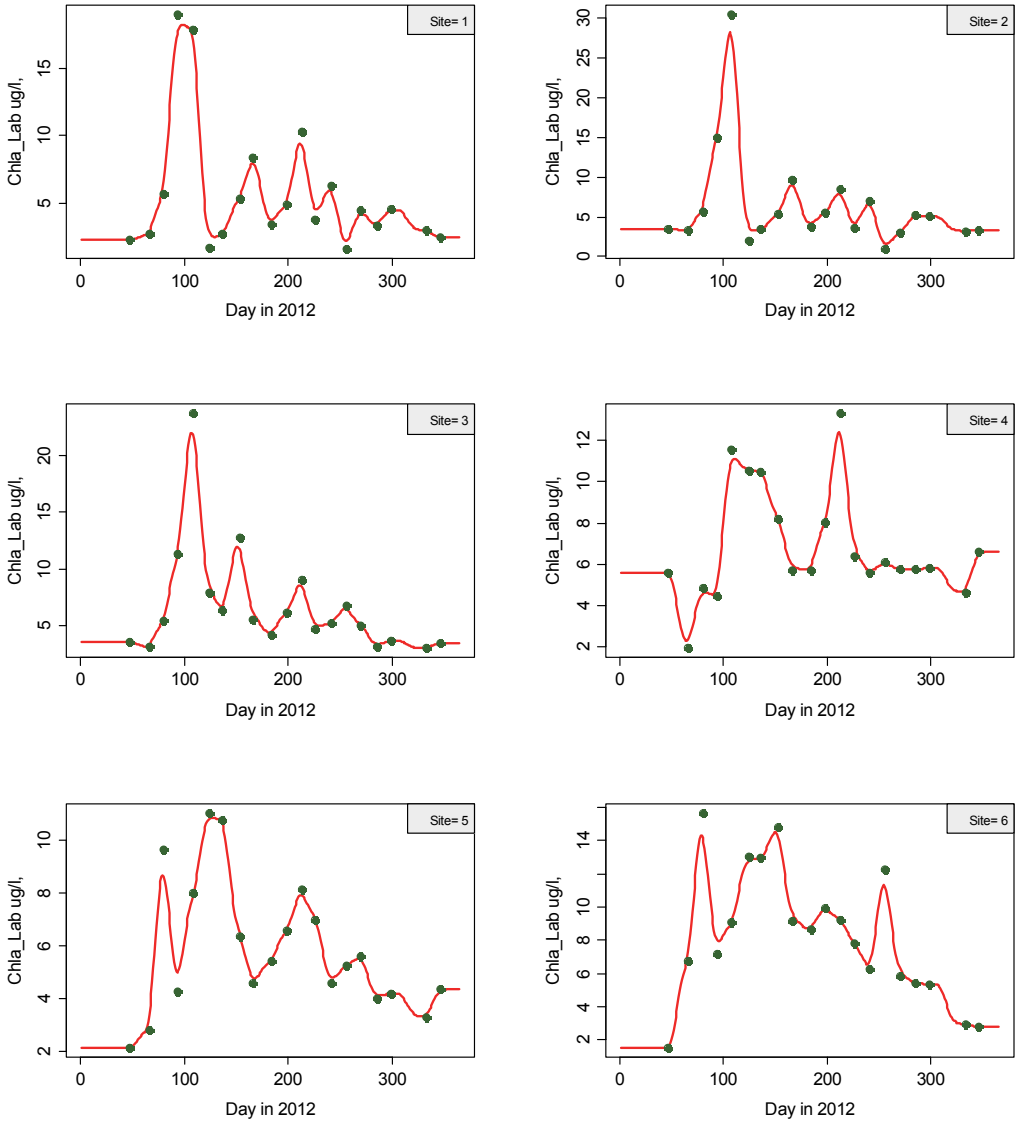

Figure 110 Chlorophyll-a content (after fluorometer analyses) in the water column at the six station in 2012, measured (dots) and inter/extrapolated (lines), following a moving-average method.

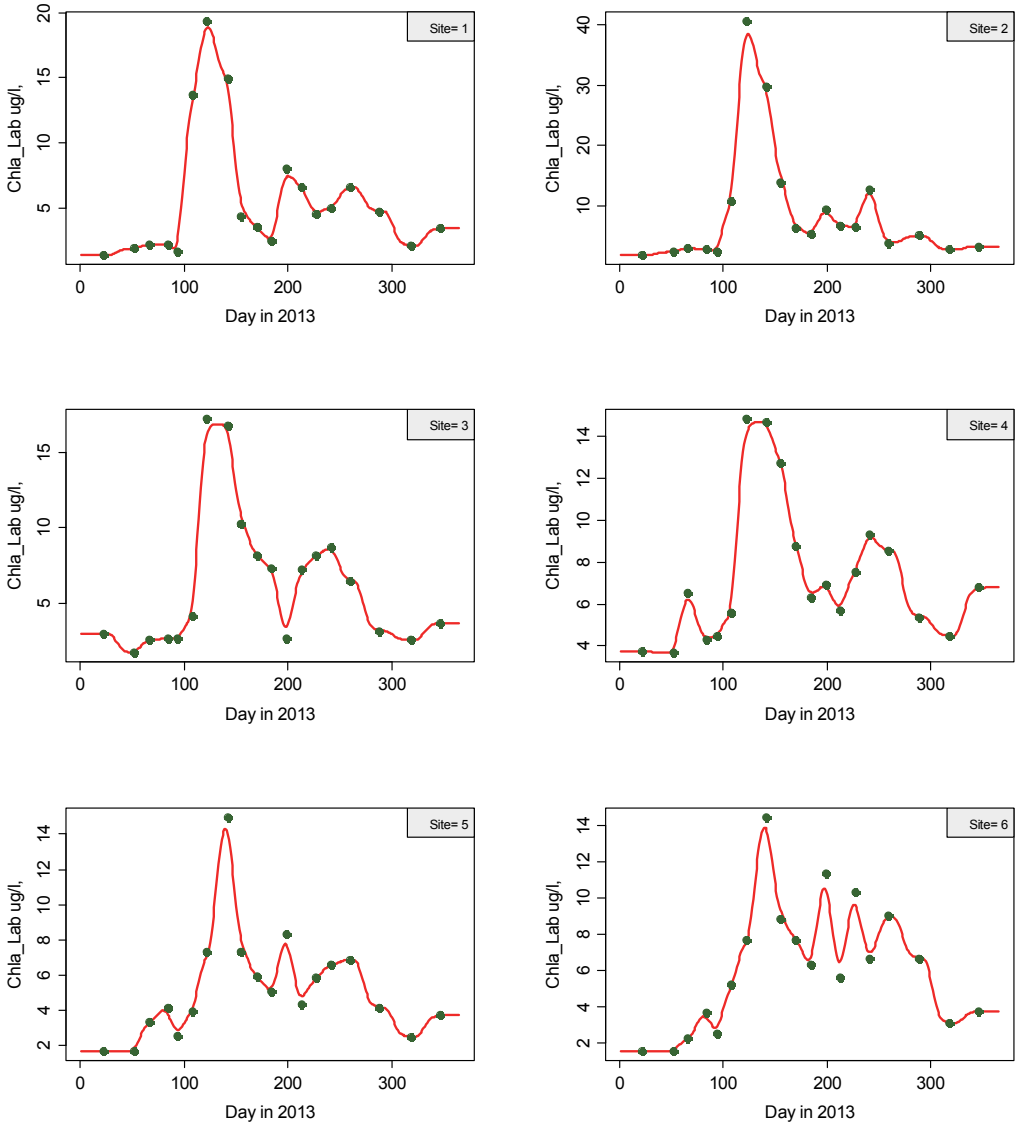

Figure 111 Chlorophyll-a content in the water column at the six station in 2013, measured (dots) and inter/extrapolated (lines), following a moving-average method.

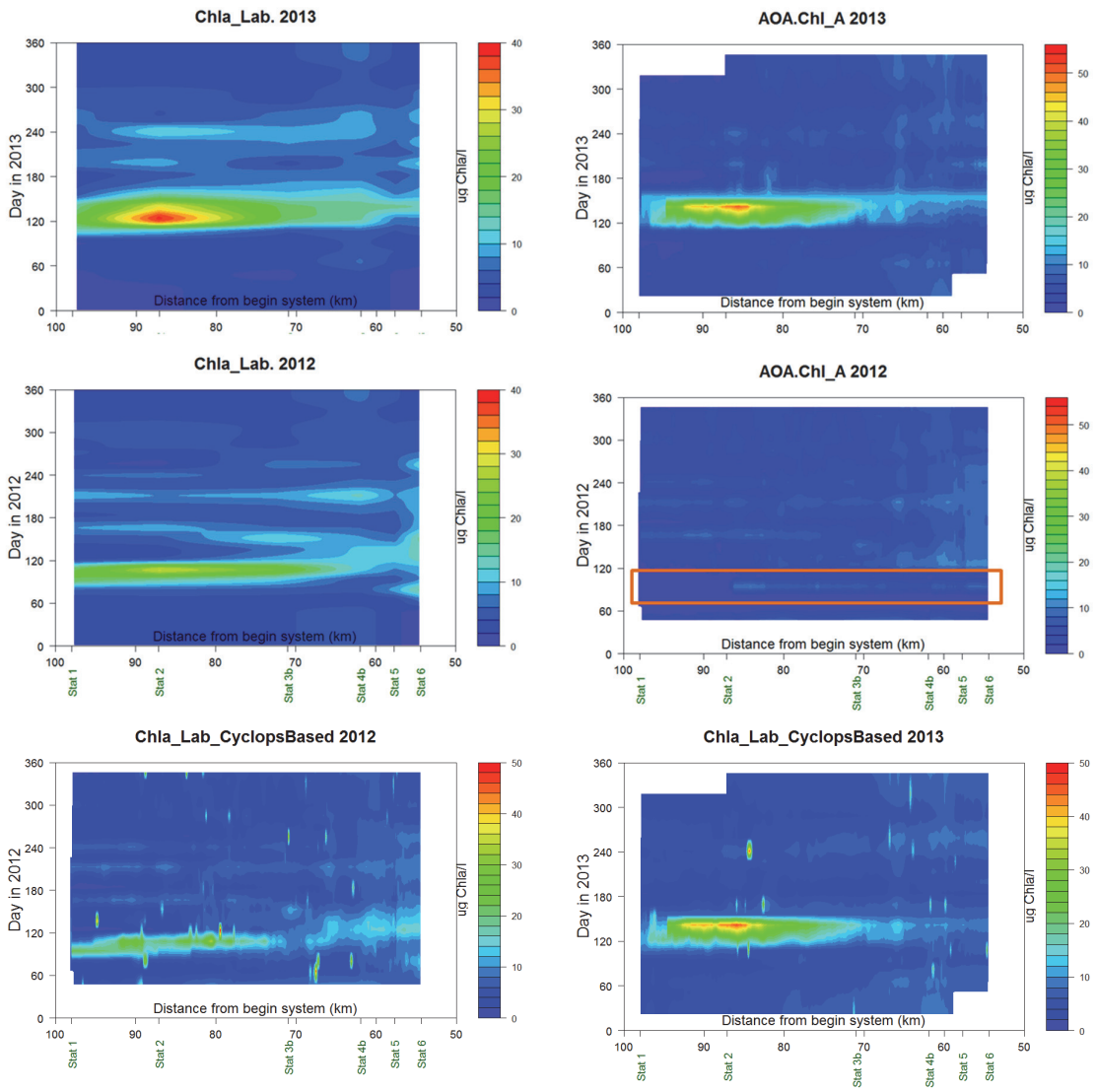

Figure 112 Chlorophyll-level plots. Right upper and middle: chlorophyll-a according to the AOA-sensor results. Mind that the observations during cruises 3-5 are incomplete (within orange rectangle), see section 7.13. Left upper and middle: results from the fluorometer analyses. Lower: Cyclops-chla-results transformed to values compatible with the fluorometer results. Scales are slightly different per set of graphs. See sections 7.12 for further comments on reliability. Distance=0 at Herbrum (DE).

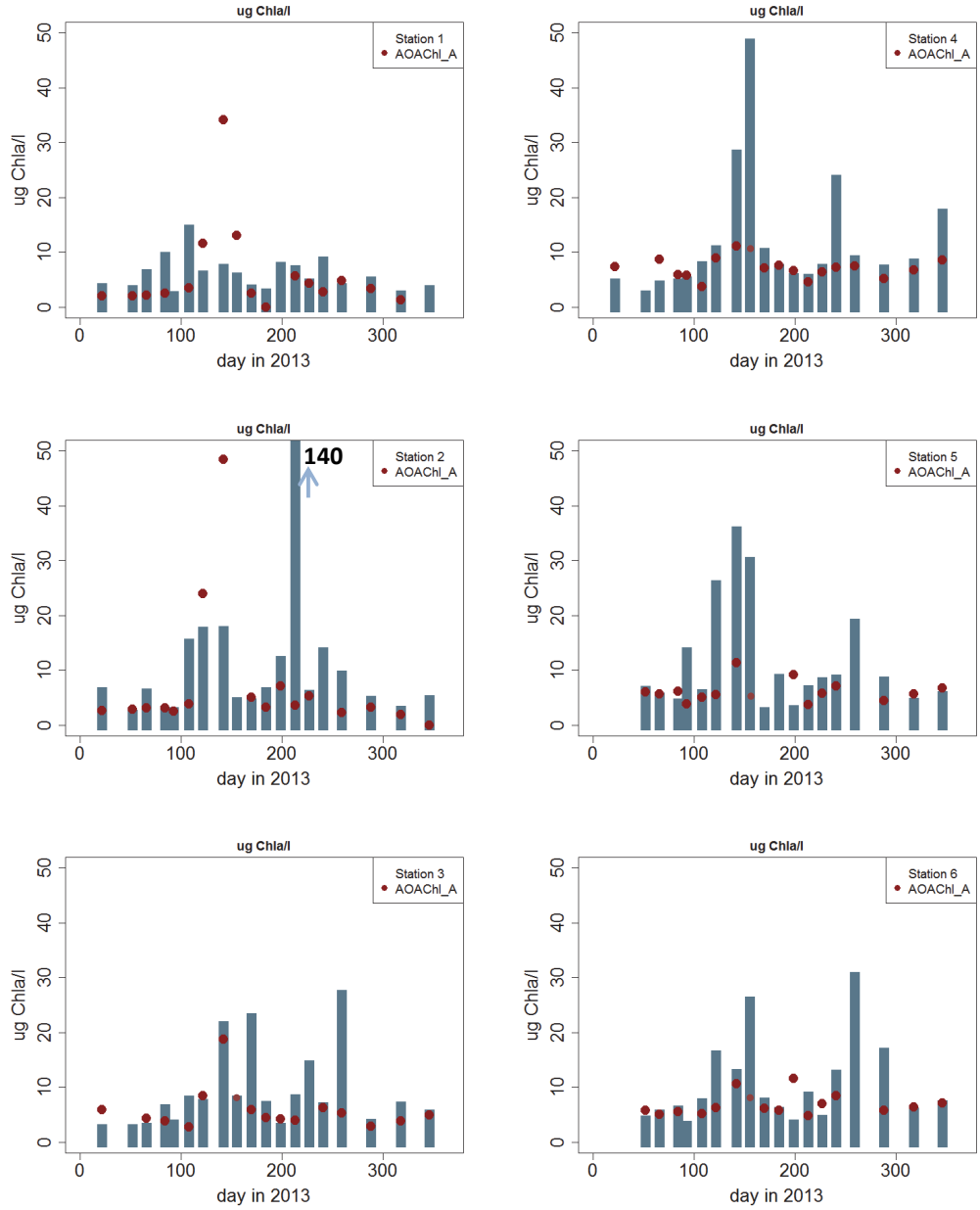

Figure 113 Total chlorophyll-a values as estimated from algal cell volumes (bars) and AOA-results (dots). Y-axis is limited to 50 µg l^{-1}. The exceptional bar value at station 2 is caused by a *Noctiluca scintillans* –observation. After removal of this contribution, 5.1 µg chla l^{-1} remains, which is more or less the same as the AOA-value

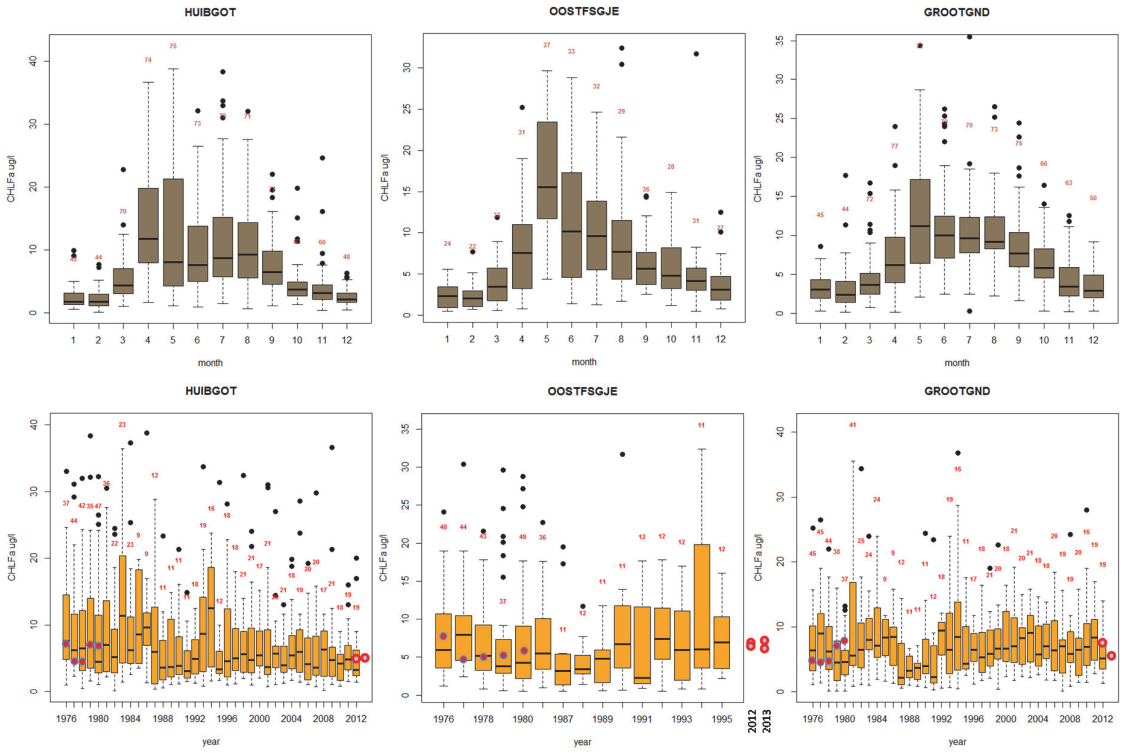

Figure 114 Chlorophyll-a in the estuary, monthly (upper) and yearly (lower) values as boxplots for the period 1975-2011 (Huibert gat Oost, left, site = station 1), 1976-1995 (OostFriese Gaatje, middle, site = between station 3 & 4), 1975-2011 (Groote Gat Noord, right, site = station 6). Mind the different Y-axis scales. Source: Waterbase (2014). Nrs give the nr of observations. All data are in µg chla l^{-1}. Site nrs in Figure 23 are 2, 13 and 20, respectively. Year average data from Colijn (1983) and from the present research are included in the graphs as circles.

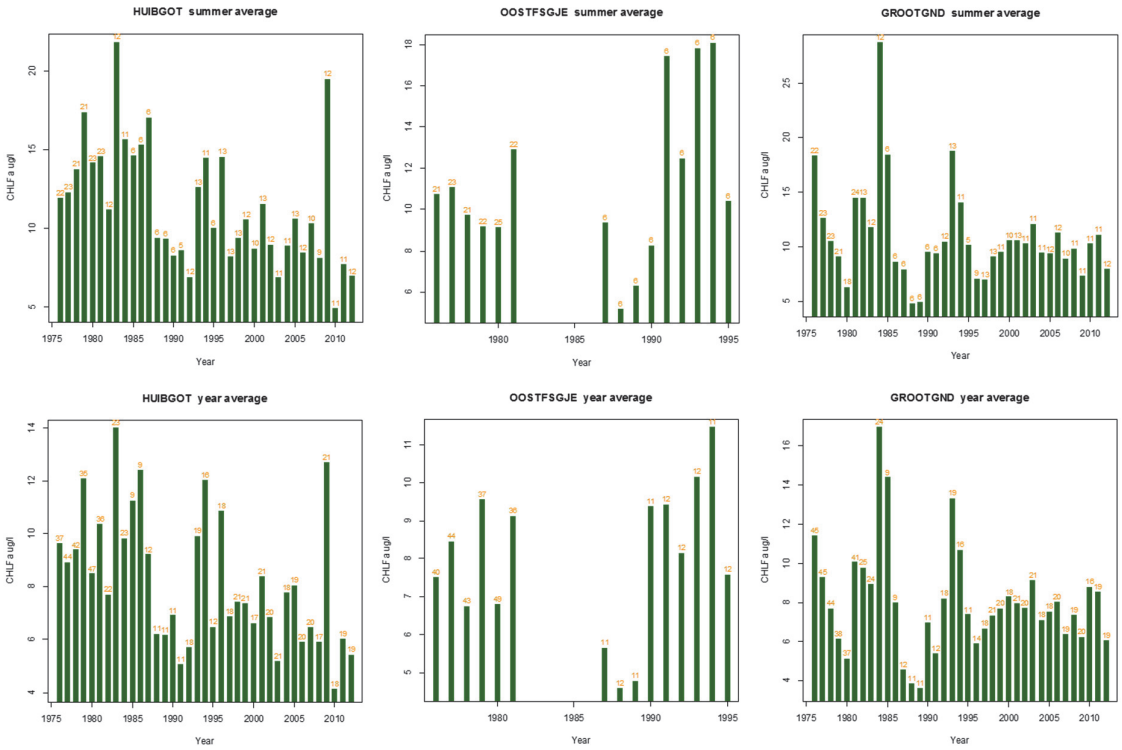

Figure 115 Chlorophyll-a in the estuary, summer (upper) and yearly (lower) averages for the period 1975-2011 (Huibert gat Oost, left, site = station 1), 1976-1995 (OostFriese Gaatje, middle, site = between station 3 & 4), 1975-2011 (Groote Gat Noord, right, site = station 6). Mind the different Y-axis scales. Source: Waterbase (2014). Nrs give the nr of observations. All data are in µg chla l^{-1}. Site nrs in Figure 23 are 2, 13 and 20, respectively. The 1996-RWS-monitoring data for Chlfa contained three extremely large values, which were considered as typo's and were removed from the data set.

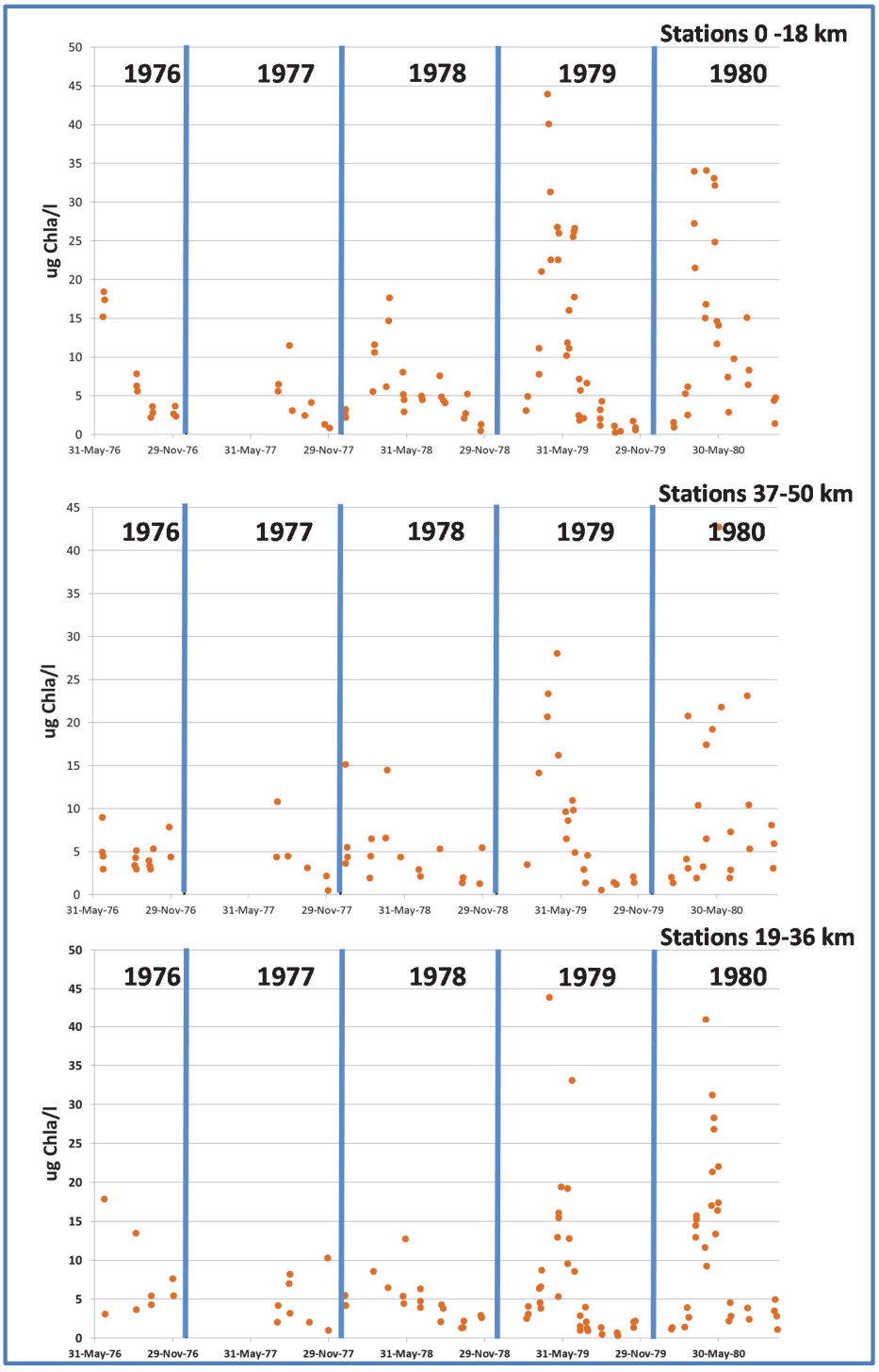

Figure 116 Pelagic chlorophyll-a data in the years 1976-1980, taken from Colijn (1983). Upper: stations 0-18 km (station 1 present). Middle: stations 19-36 km (stations 2-3 present). Lower: stations 37-50 km (stations 4-6 present)

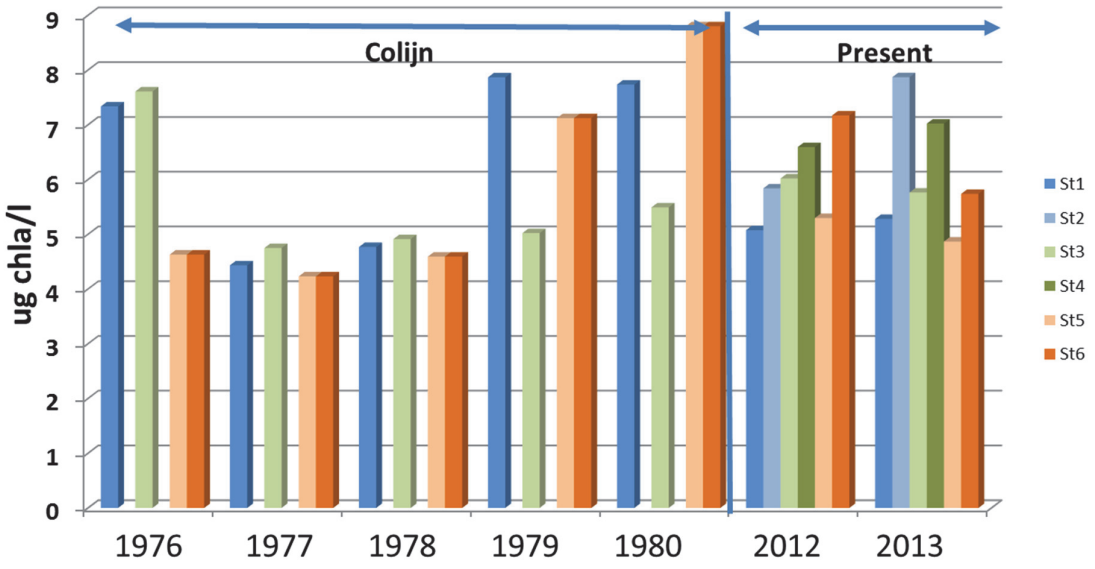

Figure 117 Chlorophyll-averages as found in Colijns research (years 1976-1980) and the present research (2012-2013). Colijn divided the area in three subsections; these values have been assigned to one of the six subsections (=station numbers, St1..St6) we have distinguished in our research. In the years 1976 and 1977 Colijn only sampled in the second half of the year.

Table 32 Year and summer average chlorophyll-data for the Ems-Dollard estuary. In grey: RWS (Waterbase, 2014), in green: Colijn (1983), in light blue: present results.

		Huibertgat Oost			Oostfriese Gaatje			Bocht van Watum			Groote GatNoord		
Year	Source	Avg_ Yr	Avg_ Win	Avg_ Sum	Avg_ Yr	Avg_ Win	Avg_ Sum	Avg_ Yr	Avg_ Win	Avg_ Sum	Avg_ Yr	Avg_ Win	Avg_ Sum
1976	RWS	9.5	7.1	11.7	7.4	4.3	10.6				11.3	5.1	18.1
1976	Colijn	7.3			7.6						4.6		
1977	RWS	8.8	5.0	12.1	8.4	5.2	10.9				9.2	5.5	12.4
1977	Colijn	4.4			4.7						4.2		
1978	RWS	9.3	4.2	13.6	6.7	3.8	9.6				7.6	4.1	10.2
1978	Colijn	5.7			4.6						5.1		
1979	RWS	12.0	3.6	17.2	9.5	13.0	9.0				6.0	2.2	8.8
1979	Colijn	12.4			7.8						8.6		
1980	RWS	8.4	2.5	14.0	6.7	4.4	9.0				5.0	4.2	6.0
1980	Colijn	12.4			10.8						9.5		
2012	RWS	5.3	2.1	6.8				5.3	3.5	6.4	5.9	3.0	7.7
2012	Present	5.1			6.0						7.2		
2013	Present	5.3			5.8						5.7		

8.8.6 Conclusions

Thus, all comparisons with other and older data are somewhat difficult since different methods were used. Yet, we conclude that:

- For most observations: the AOA-results come close to the chlorophyll-a estimates from algae cell volumes
- There is a distinct springtime maximum occurring at stations 1-3.
- It must be concluded from these and older data that, except for this springtime maximum, chlorophyll-a variations are primarily temporal and much less spatial.
- In 1979 and 1980, high chlorophyll-a values were found in the outer areas, present values are considerably lower.
- Present values are similar to the values found by RWS-Waterbase.
- Present values in the inner areas are not very different for those in 1976-1980.

8.9 Phytoplankton organic carbon content and contribution of pelagic and benthic algae

Organic C content, based on phytoplankton cell volumes, is presented in Figure 118. Similar to chlorophyll-a (Figure 113), the large contribution of *Noctiluca scintillans* in August 2013 dominates the picture for station 2. Values are lowest for the two outer stations 1 and 2 where they do not exceed 0.5 (station 1) or 0.7 (station 2) mg C l^{-1} (the *Noctiluca* observation excluded). Values go up a bit at station 3 (1.0 mg C l^{-1}), to maximal 1.5-2 (mg C l^{-1}) at station 4. In both inner stations values decline a bit to about 1.5 (station 5) and 1.2 (station 6) mg C l^{-1}.

Coupled to this picture is the contribution of benthic algae to total phytoplankton presence. Wanink et al (2014) made a distinction between benthic and pelagic algae, showing that benthic algae dominate the water column community, especially in summer (Table 33). Thus, most of the phytoplankton in the inner parts are basically benthic species; and thus wind and resuspension will play an important role for the organic C-data in the samples.

Table 33 (copied from Wanink, 2014): contribution of benthic algae to phytoplankton samples in 2013.

Table 3 Average bio-volume of benthic and planktonic algae in the phytoplankton samples of 2013, and the percentage contribution of benthic algae tot total algal bio-volume.

	Bio volume (mm^3/l)			% Benthic		
Station	**Benthic**	**Plankton**	**Year**	**Summer**	**Winter**	**Year**
Huibertgat	0,79	2,38	0,02	15	39	24
Randzelgat Zuid	1,11	7,08	0,05	18	31	23
Doekegat Zuid	1,53	4,04	0,03	33	31	32
Paapsand Sud	2,44	1,89	0,09	50	44	48
Mond van de Dollard	2,50	1,33	0,06	58	36	52
Groote Gat Noord	2,62	1,43	0,05	56	46	55

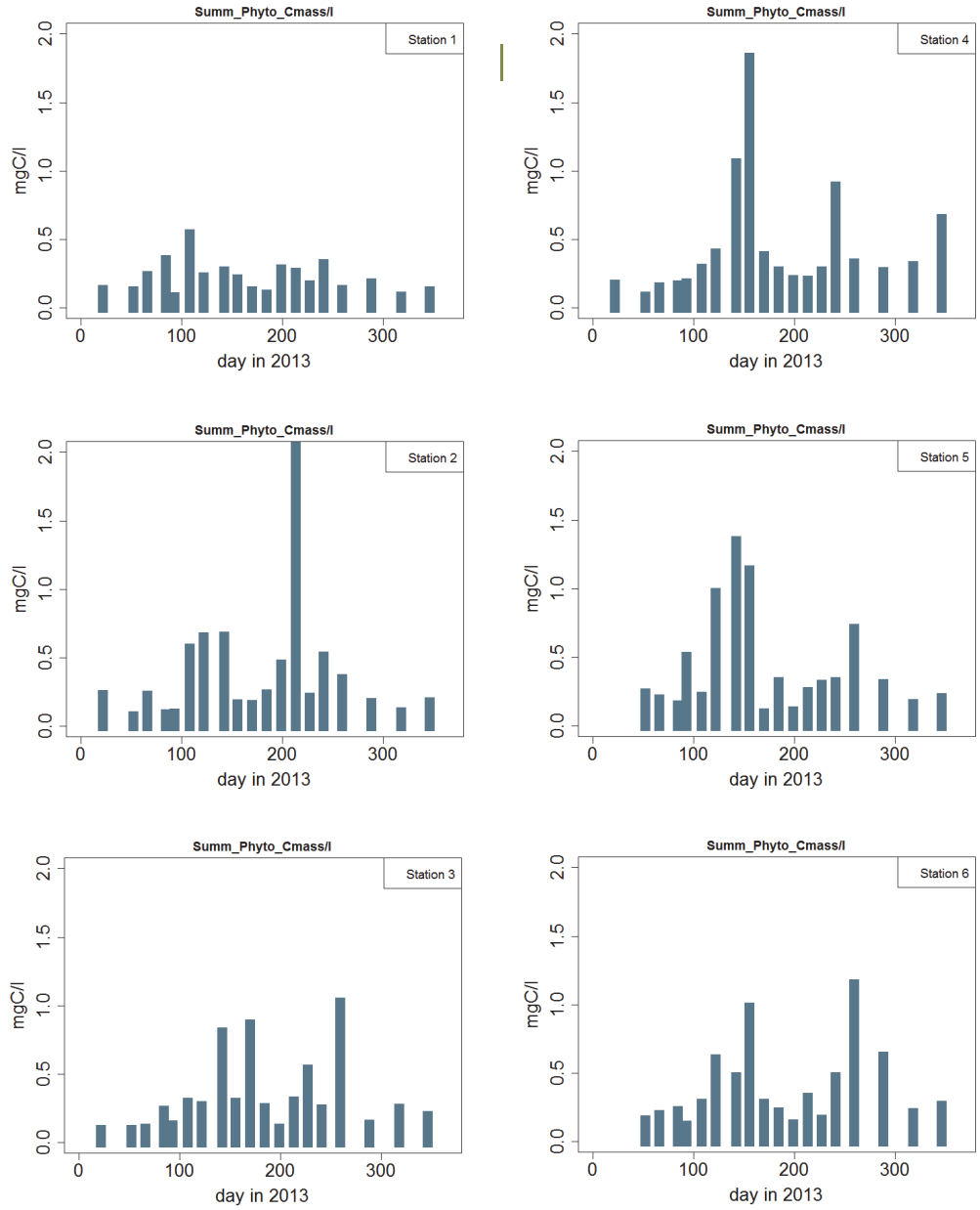

Figure 118 Organic carbon content in 2013 present in all algae together, at each station. Data derived from phytoplankton cell volumes (Koeman & Bijkerk analyses: Wanink et al, 2014) (see also section 4.5.5 in this report). The one extreme value at station 2 at day 213 (August 1st, 2013) is already mentined before, and is the result of one single giant *Noctiluca scintillans* observation.

8.10 Algae groups

8.10.1 Introduction

The AOA-sensors distinguished between cryptophyceae, diatoms, cyanobacteria (blue-greens) and green algae. Koeman & Bijkerk-results distinguish these groups as well, and thus, both results can be compared regarding chlorophyll-a concentrations. In these sections results are presented. There are two complications: Koeman & Bijkerk also distinguished dinoflagellates (that have pigment spectral

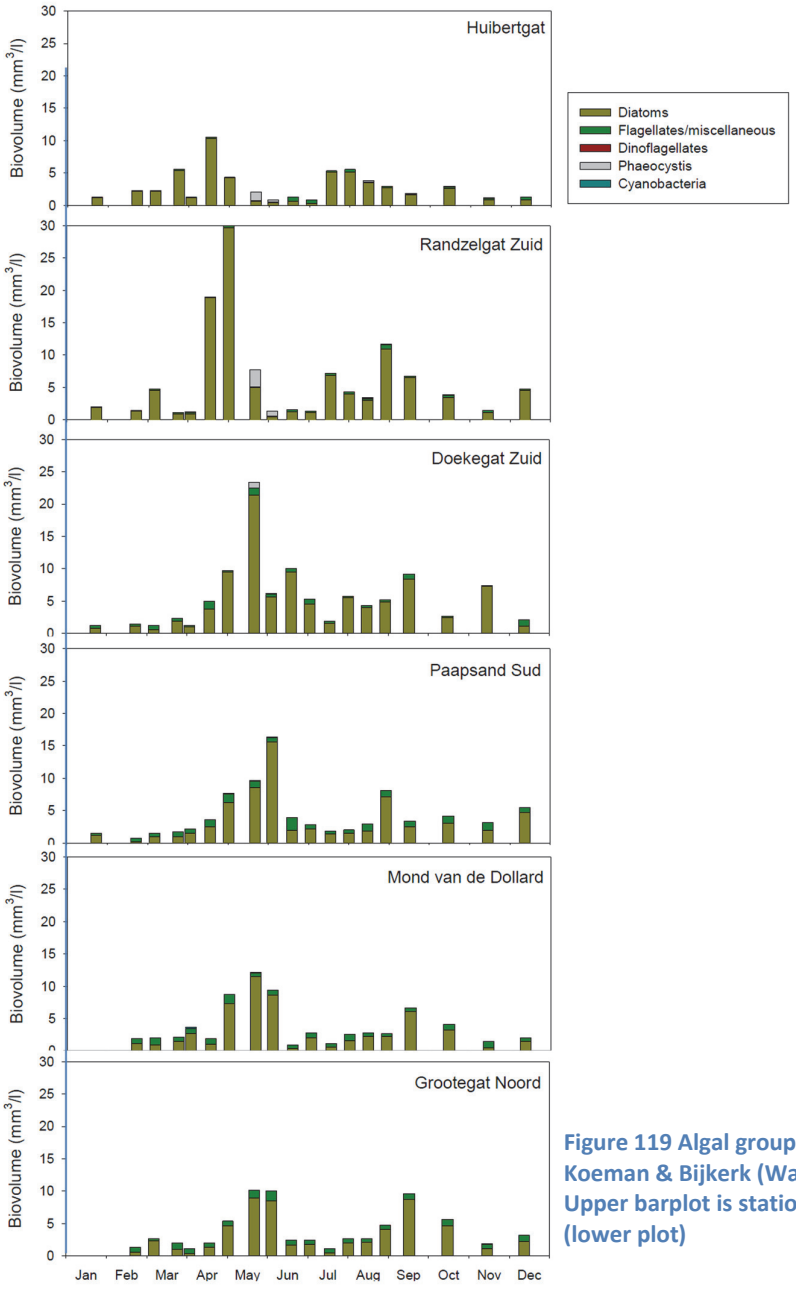

Figure 119 Algal groups identified in 2013 by Koeman & Bijkerk (Wanink et al, 2014, fig 3). Upper barplot is station 1, down to station 6 (lower plot)

Figure 3 Developments in bio-volume per functional group of autotrophic algae during 2013.

characteristics that are very close to those of diatoms), and phaeocystis, that has spectral characteristics similar to green algae.

8.10.2 A short overview of Koeman& Bijkerk-results

Koeman and Bijkerk (Wanink et al, 2014) give a summary of the contribution of main algal groups to total biovolume, this is copied and shown in Figure 119.

From this, it can be seen that diatoms are very dominant in the system. Next to diatoms, green algae appear and only now and then phaeocystis occurs. Blue-greens and dinoflagellates hardly appear in the Koeman & Bijkerk results.

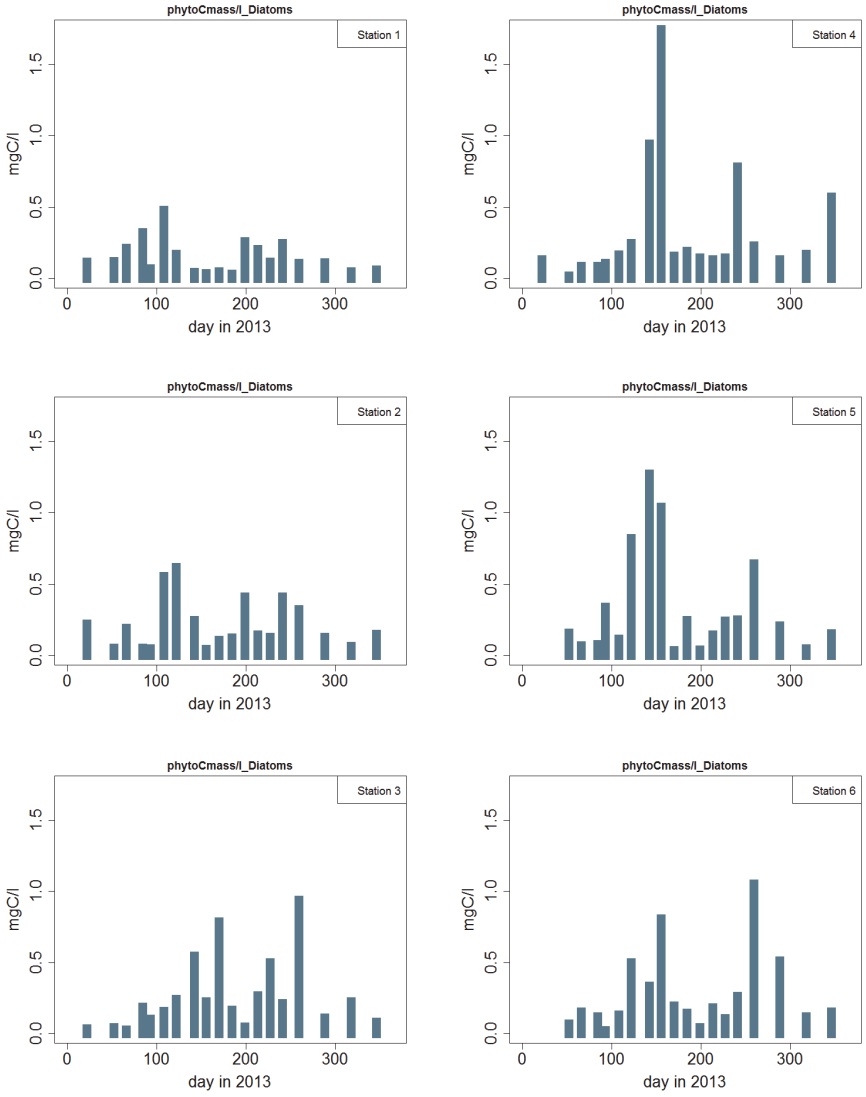

Figure 120 Organic carbon content in 2013 present in diatoms, at each station. Data derived from phytoplankton cell volumes (Koeman & Bijkerk analyses, Wanink et al,

8.10.3 Diatoms

8.10.3.1 Diatom cell volume and organic carbon content

All cell volumes come from the Koeman & Bijkerk analyses; for a full overview see Wanink et al (2014). Organic carbon contents (see section 4.6.5 for method) are presented in Figure 120.

Similar to section 8.9 (and Table 33): most of the diatoms present at the inner stations are benthic species.

8.10.3.2 Diatom chlorophyll-a

According to the AOA-data, diatom peaks are observed between days 110 and 160 (Figure 121), with highest chlorophyll-a values of almost 40 µg chla l^{-1} in 2013. According to the AOA-data, it also is the only bloom in 2013. 2012-values are much lower, and stay below 15 µg chla l^{-1}.

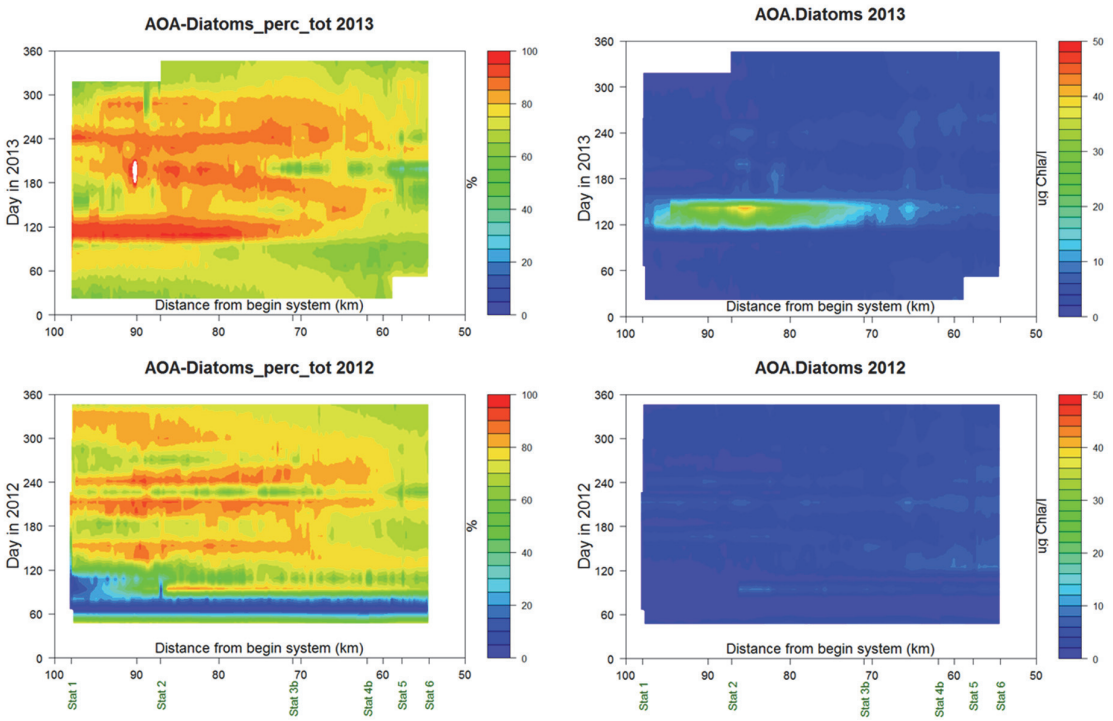

Figure 121 Chlorophyll-a in diatoms, in 2012 (lower) and 2013 (upper), according to the AOA-dataset. Right: absolute values, left: relative contribution of diatoms to total chlorophyll-a. Distance=0 at Herbrum (DE).

Chlorophyll-values as estimated from algae cell volumes are shown in Figure 122, together with AOA-data. Except for a few days, most AOA-data are in agreement with the data estimated from cell volumes. Most of the differences can be observed when the data from the cell volumes are large; only at stations 1 and 2 the opposite occurs in both the May-cruises. The distinct AOA-peak pattern between days 110-160 (Figure 121) is not that clear in the cell volume data; in the latter, high diatom values are much longer present.

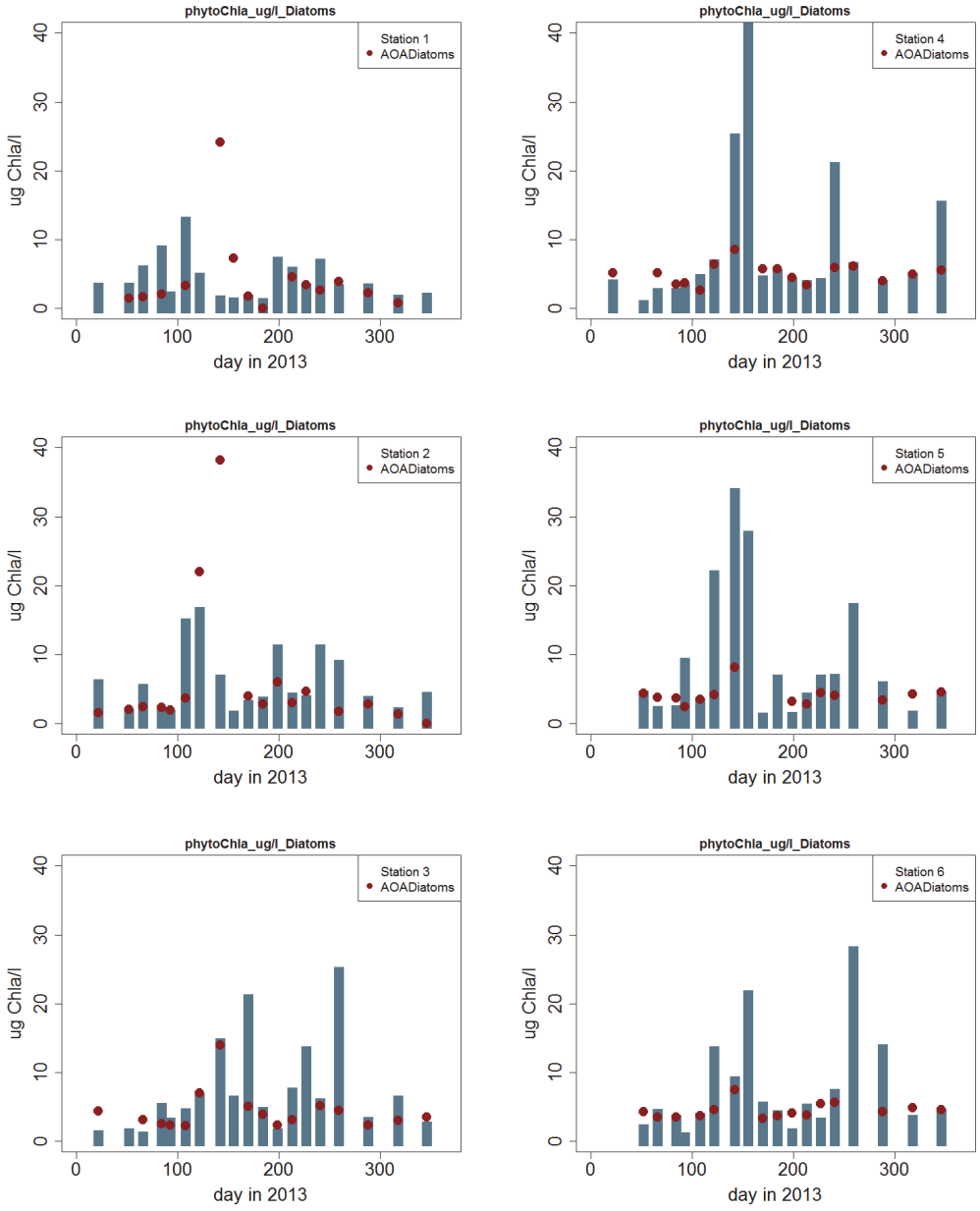

Figure 122 Chlorophyll-content in diatoms, estimated from cell volumes (bars) and as measured by the PocketBox (AOA-data).

In both years, AOA measurements indicate that diatoms make up the majority of phytoplankton (Figure 121, lower graphs), which is in agreement with the cell counts of Wanink et al (2014): 60 to over 90% of the algae biovolume is made up by diatoms.

8.10.4 Cryptophyceae

According to the AOA-data, chlorophyll-a levels for cryptophyceae are much lower than those for diatoms; maximum levels are about 1.0 (2012) to 2.5 (2013) µg chla l^{-1}. Blooms are more spread over the year, and seem to show a bit periodic appearance (Figure 123). Generally, Cryptophyceae contribution to total chlorophyll-a is much less than Diatom contribution.

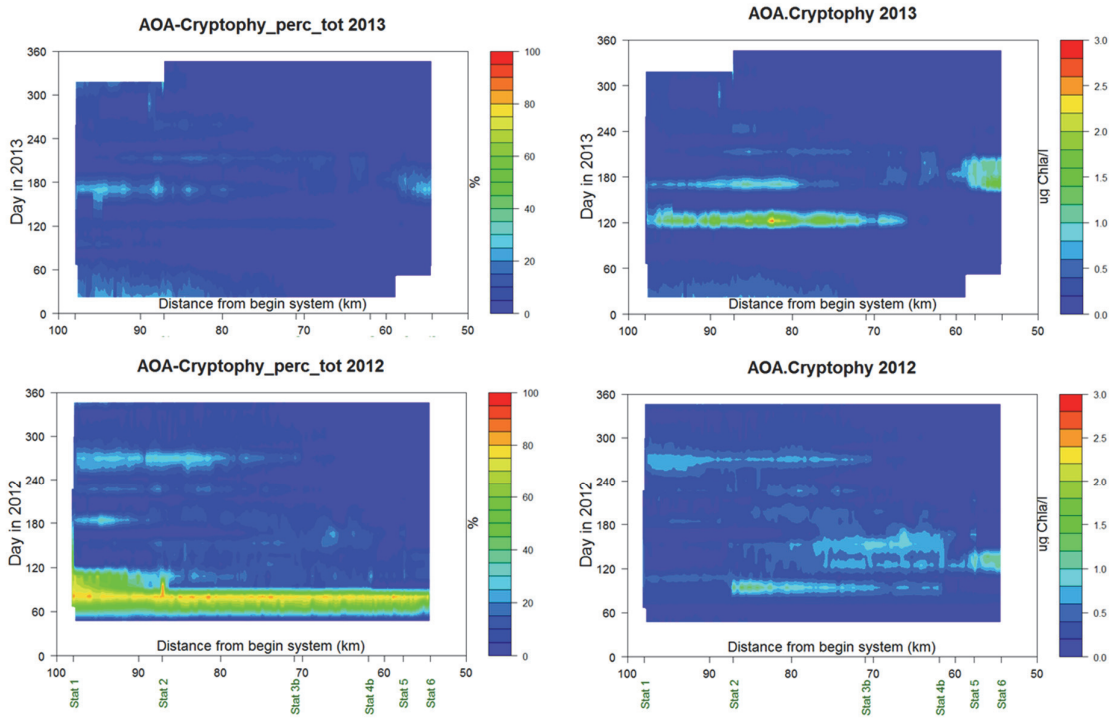

Figure 123 Chlorophyll-a in cryptophyceae, in 2012 (lower) and 2013 (upper), according to the AOA-dataset. Right: absolute values, left: relative contribution to total chlorophyll-a. First relative values in 2012 are not correct since some of the other sensors were offline. Distance=0 at Herbrum (DE).

8.10.5 Green algae

According to the AOA-data, green algae can be abundant during short periods, especially shortly after the peak of the diatom bloom (Figure 124, upper), up to 10 µg chlorophyll-a l^{-1}. Then they can make up more than half of the phytoplankton chlorophyll-a content. For the rest of the year, green algae contributions stay below 20% of total chlorophyll-a.

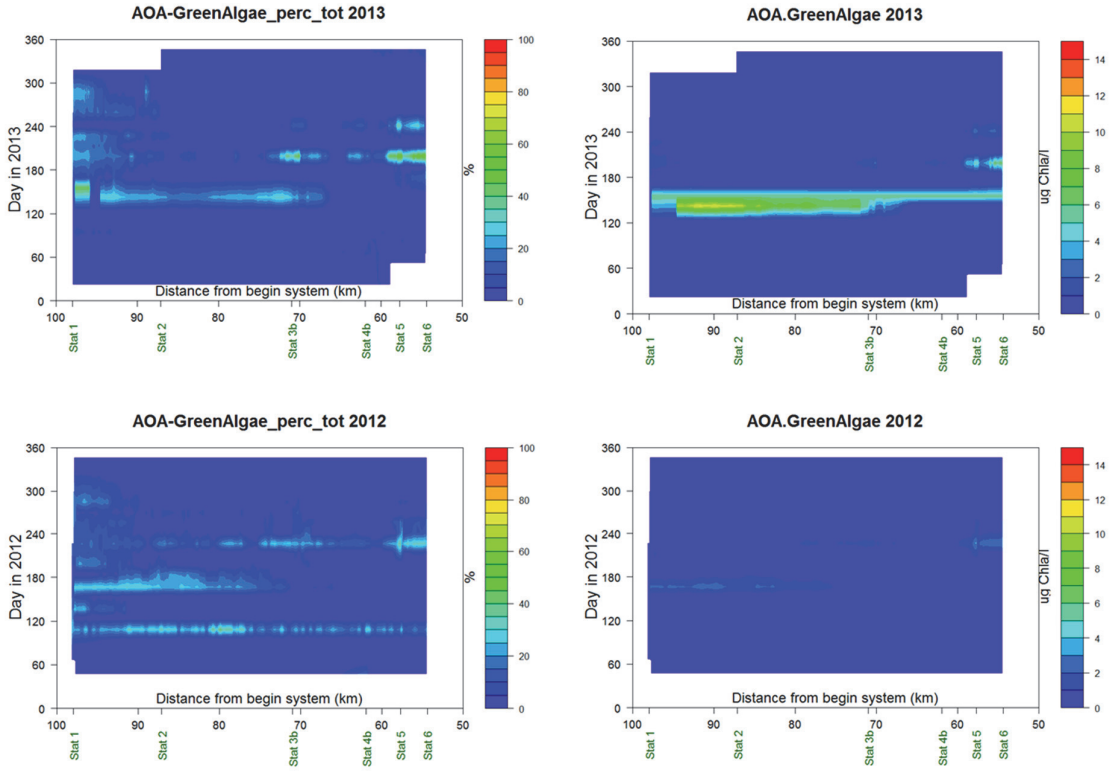

Figure 124 Chlorophyll-a in green algae in 2012 (lower) and 2013 (upper). Right: absolute values, left: relative contribution to total chlorophyll-a. Green algae show an optimum shortly after the diatom bloom (Figure 121). Hardly visible in 2012, values up to almost 12 µg chla l^{-1} in 2013. Distance=0 at Herbrum (DE).

When comparing these AOA-results with the Koeman & Bijkerk-data (Figure 119), it strikes that, according to the latter, green algae contribution seems to be highest in the inner area, and more spread through the year than it appears in the AOA-data. We do not have an explanation for that observation at the moment.

8.10.6 Cyanobacteria (blue-greens), including flow-cytometer results

According to the AOA-data (Figure 125), cyanobacteria appear in periods when diatoms and green algae are less dominant, and also, they appear mainly in the in areas. Chlorophyll-a values reach up to about 3 µg chla l^{-1}; relative contribution to total chlorophyll-a gets up to roughly 30%.

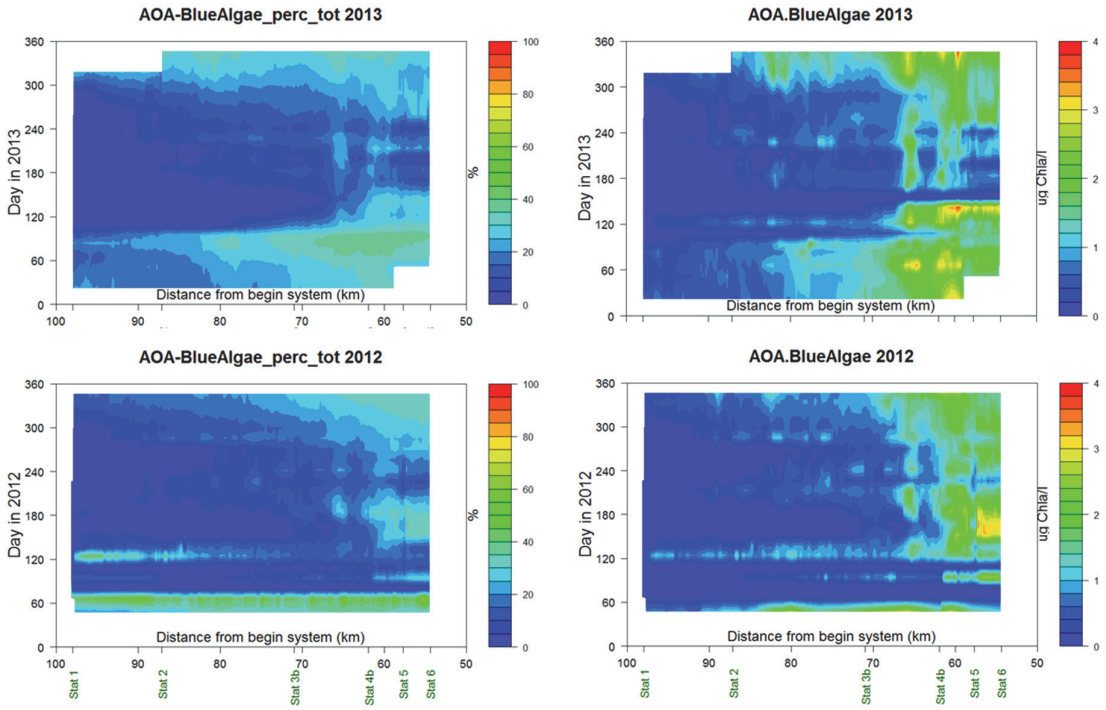

Figure 125 Chlorophyll-a in cyanobacteria (blue-green algae) according to the AOA-measurments. Left: in 2012, right: 2013. Upper: absolute values, lower: relative contribution to total chlorophyll-a. Cyanobacteria show an optimum ouside the period with diatoms and green algae (Figure 121, Figure 124). Cyanobacteria are mostly restricted to the more brackish areas, with values up to about 4 µg chla l^{-1} in 2013 and lowest values in spring (2012) and (early) summer (2013). 2012 cyanobacteria values are only slightly below 2013 values. Distance=0 at Herbrum (DE).

These values are in complete contradiction with the results by Koeman & Bijkerk, who hardly identified cyanobacteria.

The cause of this difference may be the size of the cyanobacteria. Flow-cytometer analyses (FCM), performed during 2012 and part of 2013, revealed mostly cyanobacteria smaller than a few µm; a size that is not common part of the Koeman and Bijkerk analyses results.

These FCM-results were recalculated to cell volumes and from that, chlorophyll-a concentrations were calculated, exactly the same way the Koeman & Bijkerk diatom data were processed (section 4.6.5, eqs 10a-10c). Results are shown in Figure 127 (average values for all stations during the period June 2012 – May 2013) and in (average values per station for the whole period 2012 June-2013 May).

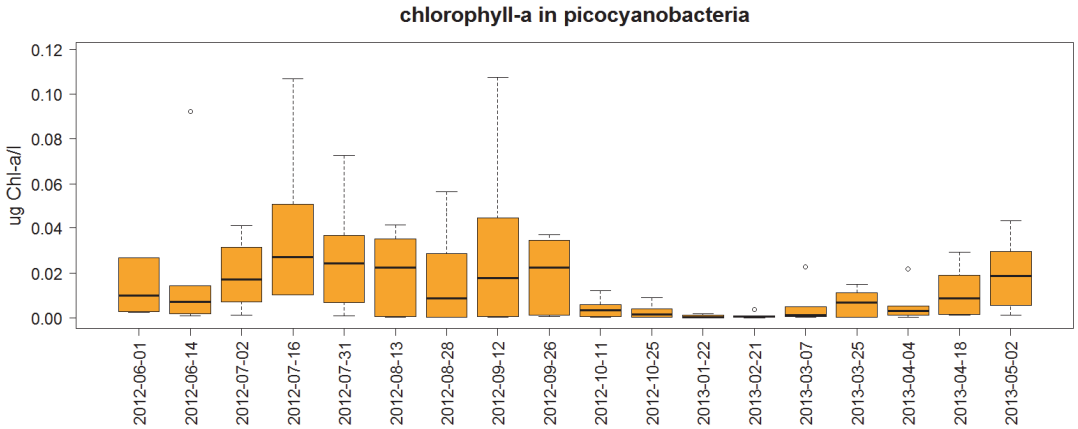

Figure 127 Chlorophyll-a concentrations in pico-cyanobacteria (average size between 0.5 and 4 µm^3). Volumina measured with flow-cytometer, and chlorophyll-a content computed according to section 4.5.5. Values for the whole period 2012 June – 2013 May, averaged for all stations.

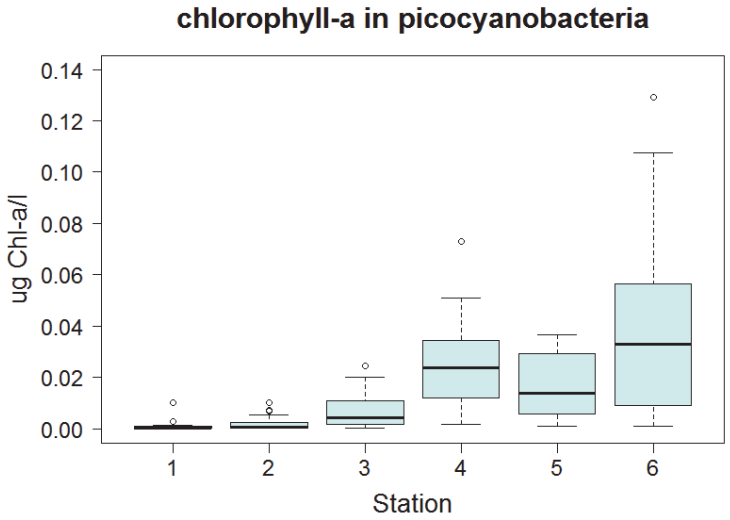

Figure 126 Chlorophyll-a concentrations in pico-cyanobacteria (average size between 0.5 and 4 µm^3). Volumina measured with flow-cytometer, and chlorophyll-a content computed according to section 4.5.5. Values per station, averaged for the whole period 2012 June – 2013 May.

First, the picture from Figure 125 that most cyanobacteria can be found in the inner stations is supported, but that outside the April-May period values are highest is not directly supported. Even more striking is the large difference in absolute values: the results calculated from the FCM-data are much lower than those that follow from the AOA-data. The relationship is sketched in Figure 128. Differences between both are a factor 20 to 50. Up to now we do not have an explanation for this difference.

Remark by the reviewer: she mentions her experience that the AOA also measures non-diatoms in pure diatom cultures. That implies that the factory calibration may not be sufficient.

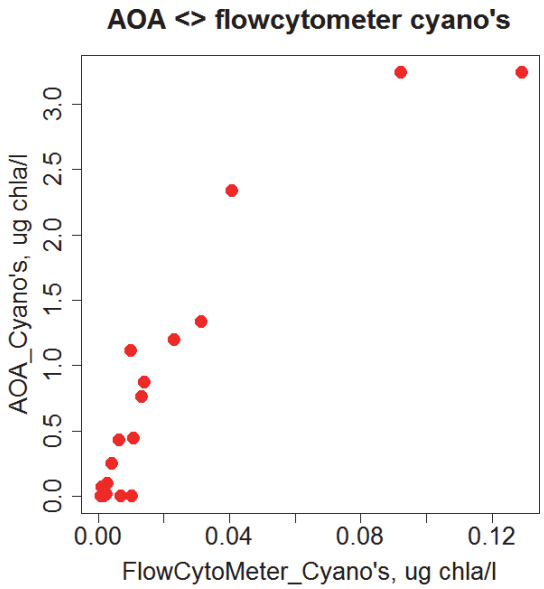

Figure 128 Relationship between cyanobacteria chlorophyll-a as calculated from the flow-cytometer results (X-axis) and as determined by the AOA-sensor (Y-axis).

8.10.7 Colijn 1976-1980 data

Colijn (1983) mentions that in 1979 and 1980 very dense blooms occurred in the whole estuary during spring and early summer (April-July); such a spring maximum was not observed in 1978, partly recorded in 1976 and missed in 1977. Both blooms in 1979 and 1980 were composed of two blooms in succession. In 1980, the first bloom consisted of mainly diatoms in the outer part of the estuary, and the second one of *Phaeocystis pouchetti (*now*: P. globosa)*. The timing of the blooms differed for these two years: in 1979 the diatom bloom peaked at the end of May, and in 1980 at the end of April. Colijn found a comparable shift for *Phaeocystis pouchetti*: in 1979 highest densities were found in July, and in 1980 at the end of May. The duration of the *Phaeocystis*-bloom was short: at the end of July 1979 the bloom had largely disappeared.

8.10.8 Comparison 1979-1980 and 2012-2013

For stations 1-3, chlorophyll-a peaks were observed around day 100 in 2012, and around day 130 in 2013. In the more inner stations (4-6), peaks were less clear, lower and more spread over the whole spring+summer season. As in the Colijn period, these were almost completely composed by diatom species. However, the *Phaeocystis* bloom following this diatom peak was almost completely absent in

2013 (we have no algae counts for 2012). Only at station 1-3 a part of the phytoplankton consisted of *Phaeocystis*, but in absolute terms it did not concern major quantities (see Figure 119).

This has some consequences for the interpretation of the primary production data, since *Phaeocystis* is known to have high maximum specific growth rates, and thus, a large amount of *Phaeocystis* will result in relatively high primary production values.

8.11 Pheophytin

Fluorometer pheophytin results (measured in the lab) are pictured in Figure 129. It was mentioned before (section 7.13.6) that these values probably have resulted from chlorophyll-a degradation between sampling and analysis. Highest values were found in inner system samples.

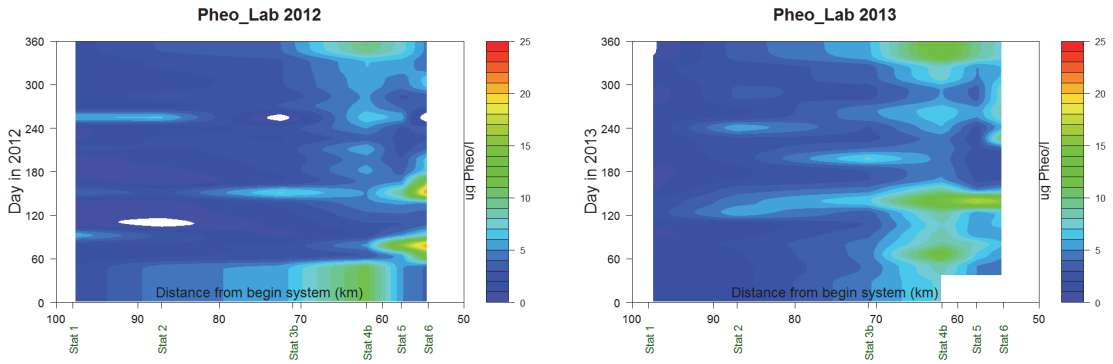

Figure 129 Pheophytin content in the system, as follows from the fluorescence analysis in the lab. Distance=0 at Herbrum (DE).

8.12 Pigment ratios in the samples: chlorophyll-a to total chlorophyll, chlorophyll to carotene and chlorophyll to pheophytin

The HPLC-analyses (only for four sample days in 2013) resulted in concentration values for several pigment types. Pigment ratios are briefly mentioned here.

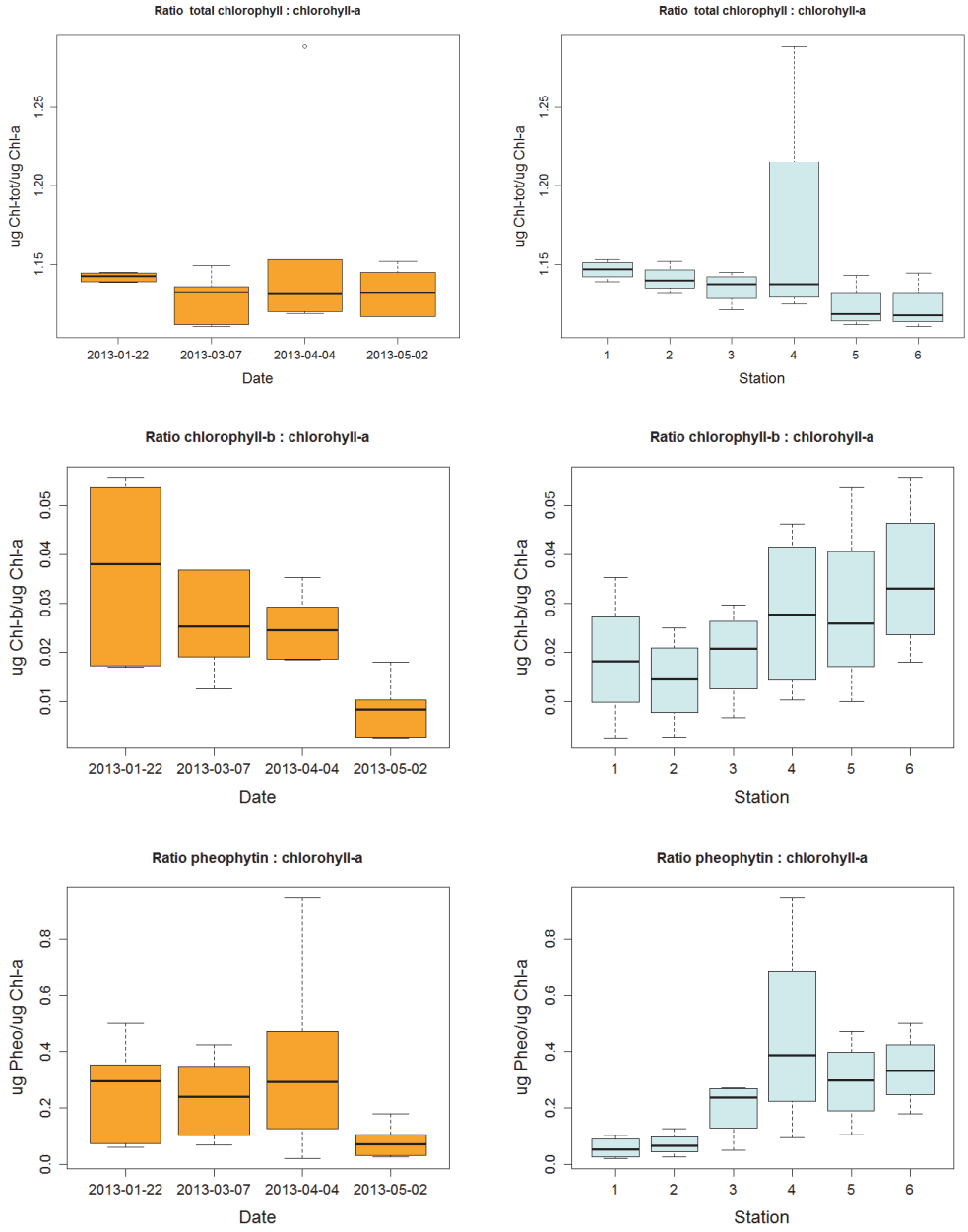

Figure 130 Pigment ratios in the HPLC-samples, as boxplots (1). Left: per sampling date, right per station. Upper: total chlorophyll / chlorophyll-a; middle: chlrophyll-b / chlorophyll-a, lower: pheophytin / chlorophyll-a.

8.12.1 Chlorophyll-a, -b, total chlorophyll and pheophytin

In Figure 130, chlorophyll-a to other pigment –ratios are presented. On the four sampling dates (2013 January – May), total chlorophyll was 1.12 to 1.15 times chlorophyll-a content, with an exception at station 4. Chlorophyll-b was about 4% of chlorophyll-a. Pheophytin found was 5-40% of chlorophyll-a; values that made the DHI-institute mentioning that some chlorophyll-a degradation occurred in the samples.

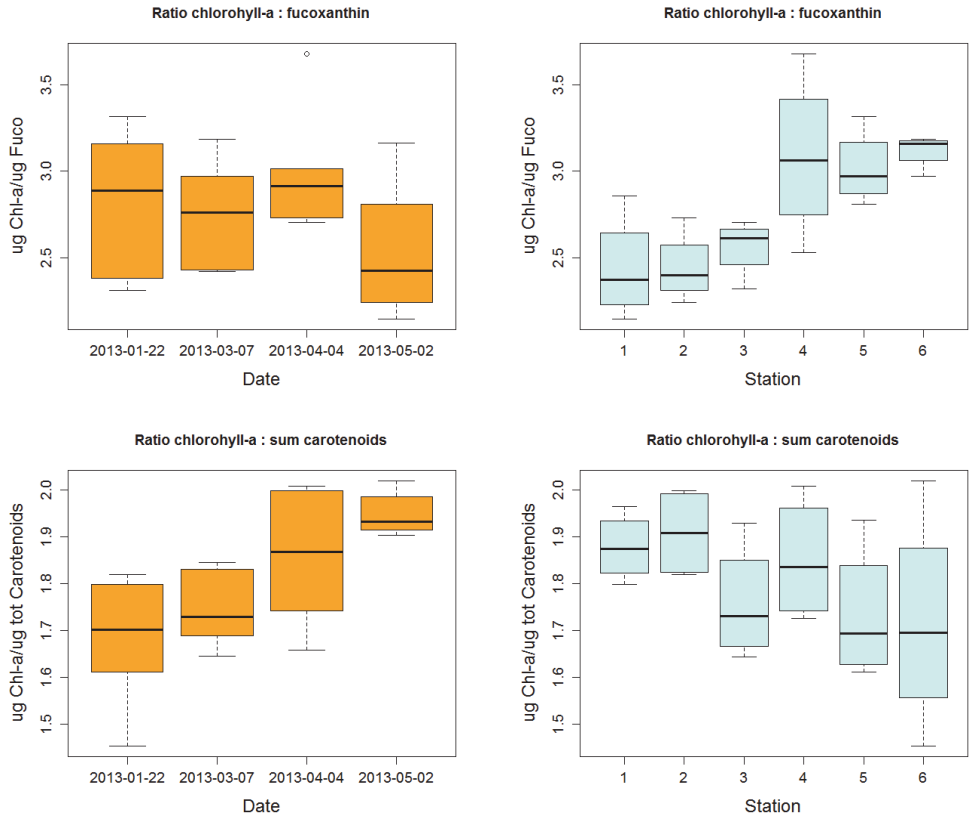

Figure 131 Pigment ratios in the HPLC-samples, as boxplots (2). Left: per sampling date, right per station. Upper: chlorophyll-a / fucoxanthin; lower: chlorophyll-a / sum carotenoids.

8.12.2 Chlorophyll-a and carotenoids

In Figure 131, chlorophyll-a to fucoxanthin and to total carotenoids ratios are presented. Chlorophyll-a is about 2.5 to 3 times the fucoxanthin values; the latter is an indication of diatom presence. Highest ratios are found in the inner stations. The chl-a ratio to total carotenoids is about 1.7 to 2.0; highest values are found in May; values seem to decline a bit for the inner stations.

8.13 Absorption ratios

The idea (section 4.8) was mentioned that the 480 : 665 nm absorption ratio could be a good indication of light limitation for algal growth. A high carotenoid content (and thus high 480 nm absorption) would indicate that light is fully available (and carotenoids needed to protect cells against too much light), whilst at low absorption ratios (low carotenoid content, since light harvesting should be maximal), light limitation might be the case.

In Figure 132, the absorption ratios are shown. Opposite to was expected, lowest values occurred in summer and in deeper system parts (outer areas). It also looks opposite to the diatom distribution (Figure 121), so a second possibility: the absorption ratio reflects diatom presence more than light limitation, must be rejected as well.

Based on these results it must be concluded that this absorption ratio is not a good measurement for light limitation in the system.

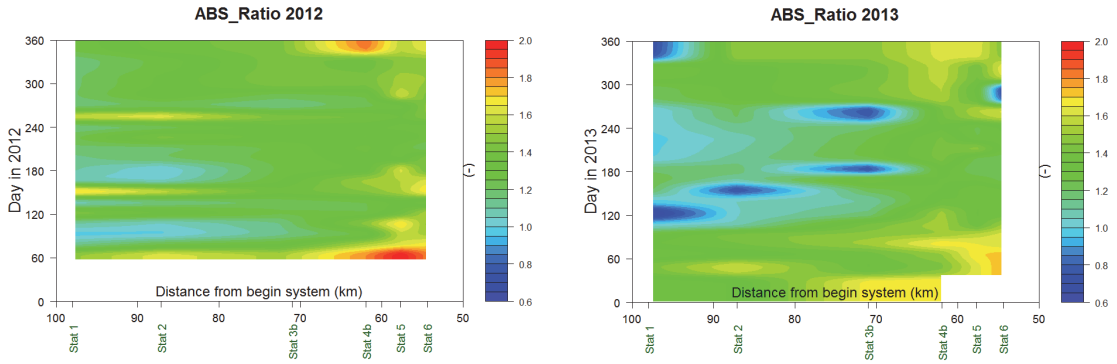

Figure 132 Absorption ratio at 480 nm and 665 nm, corrected for background extinction (section 4.6). Left: 2012, right : 2013. Distance=0 at Herbrum (DE).

8.14 Yellow substances

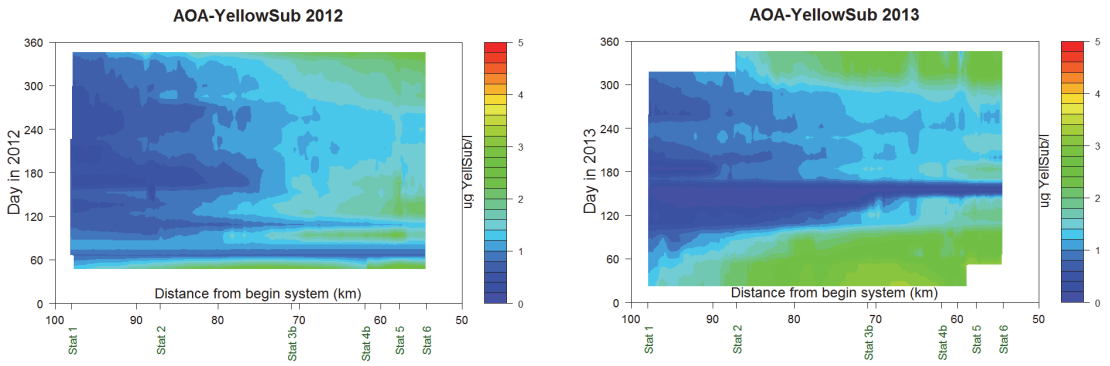

Figure 133 Yellow substances in 2012 (left) and 2013 (right). Values in mg Yellow Substances l^{-1} (not µg as the axis label says). Distance=0 at Herbrum (DE).

Concentrations of yellow substances (merely dissolved organic humic and fulvic acid matter) are highest in the inner estuary parts and lowest in summer. Yellow substance distribution is more or less the inverse of salinity (Figure 78). This is confirmed by a linear regression analysis (Chapter 6), shown in Figure 134, and thus, yellow substance concentration is mainly determined by fresh water input.

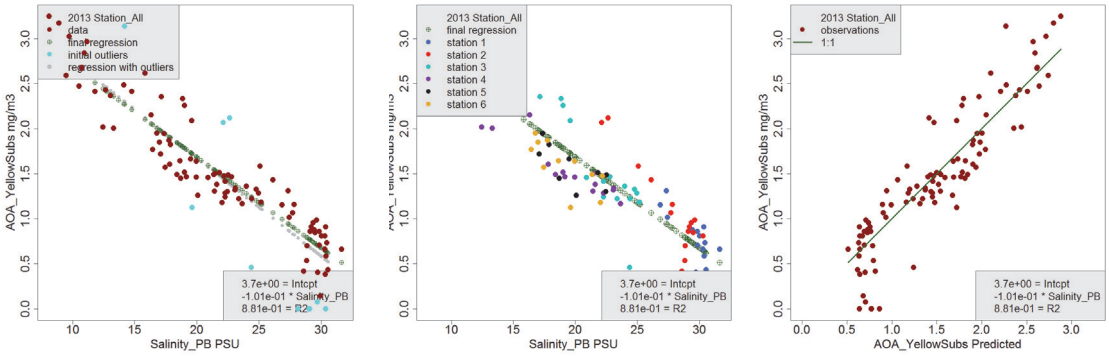

Figure 134 Relationship yellow substances (AOA-data, mg Yellow Substances l^{-1}) and salinity (AOA-data, PSU). 2013 data only. Left: all data, with outliers determined. Middle: same regression as left, but the six monitoring stations are distinguished. Right: Yellow substance predicted with the regression equation, and as measured.

8.15 Coloured organic matter (CDOM)

8.15.1 Data

Concentrations of coloured organic matter are highest in the inner estuary parts and lowest in summer. CDOM distribution is more or less the inverse of salinity (Figure 78). This is confirmed by a linear regression analysis (Chapter 6), shown in Figure 136, and thus, CDOM concentration is mainly determined by fresh water input. Thus, this picture is similar to the one for yellow substances, and both are well correlated (Figure 138).

However, CDOM and Yellow Substances are more or less similar substances, only the monitoring probes differ (Cyclops for CDOM and AOA for Yellow Substance). Since the detection methods are not the same, some difference might be expected, but what is observed now is that the AOA-results is more than twice the Cyclops results. It must be concluded that results have to be seen with caution.

In the RWS monthly monitoring program, dissolved organic carbon is determined as well. Average values at Huibertgat Oost is about 2.5 mg C l^{-1}, and almost 8 mg C l^{-1} at Groote Gat Noord, values that are substantially higher than the CDOM-values.

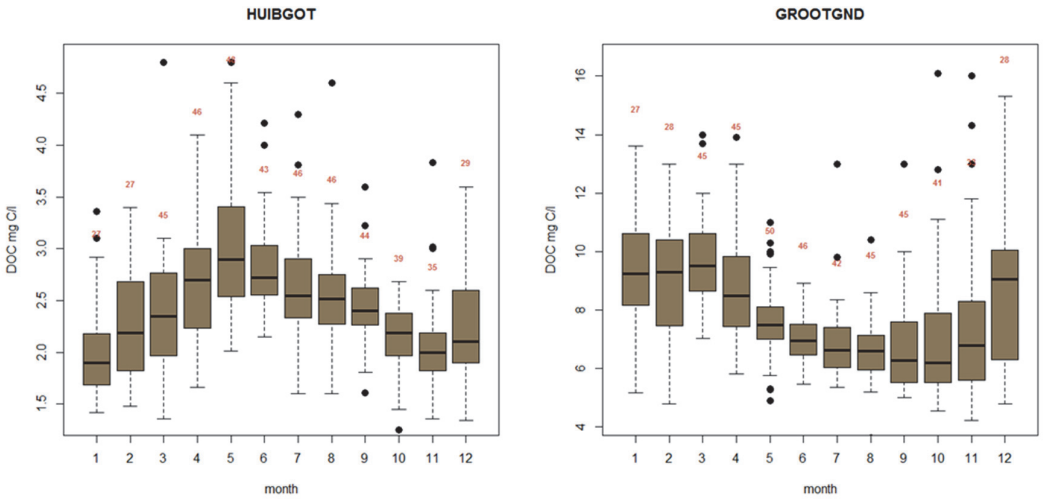

Figure 135 Dissolved organic matter at Huibert Gat Oost (left) and Groote Gat Noord (right). Data from the RWS monthly MWTL-monitoring (RWS, 2014). Averages are about 2.5 and almost 8 mg C l^{-1}.

8.15.2 Conclusions

Further investigation of the data on CDOM, dissolved organic carbon, and Yellow Substances is required to get a better overview of the meaning of these data.

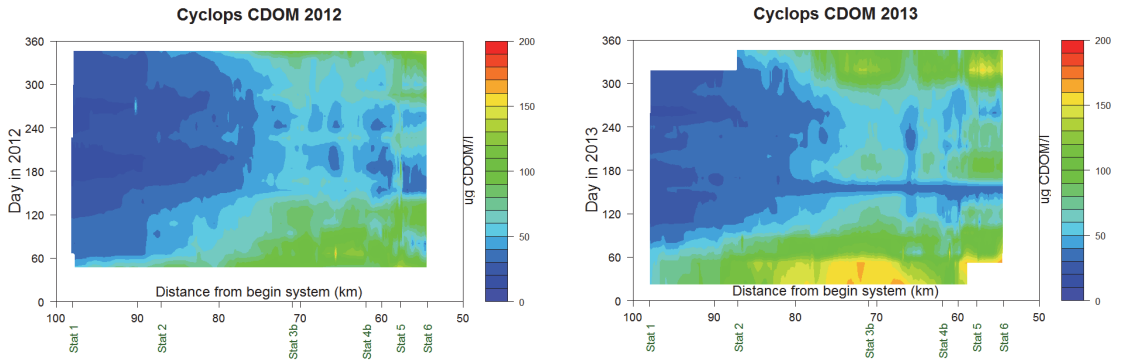

Figure 137 Coloured dissolved organic matter (CDOM, µg l^{-1}), 2012 and 2013. Distance=0 at Herbrum (DE).

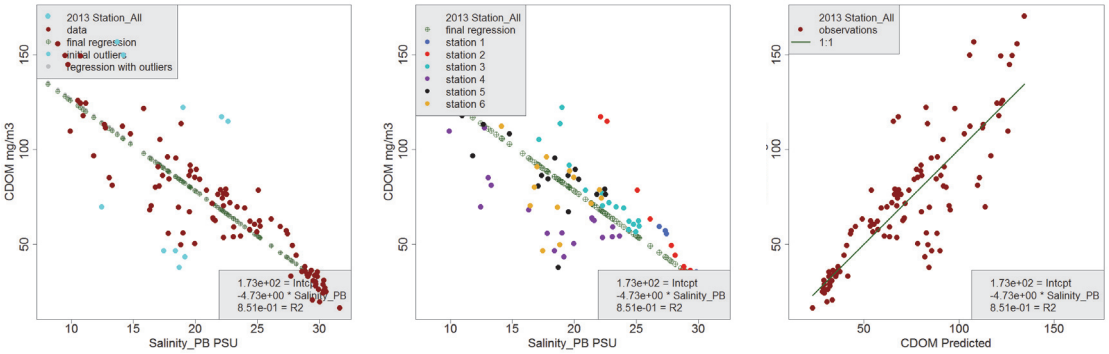

Figure 136 Relationship coloured dissolved organic matter (CDOM, AOA-data, µg l^{-1}) and salinity (AOA-data, PSU). 2013 data only. Left: all data, with outliers determined. Middle: same regression as left, but the six monitoring stations are distinguished. Right: CDOM predicted with the regression equation, and as measured.

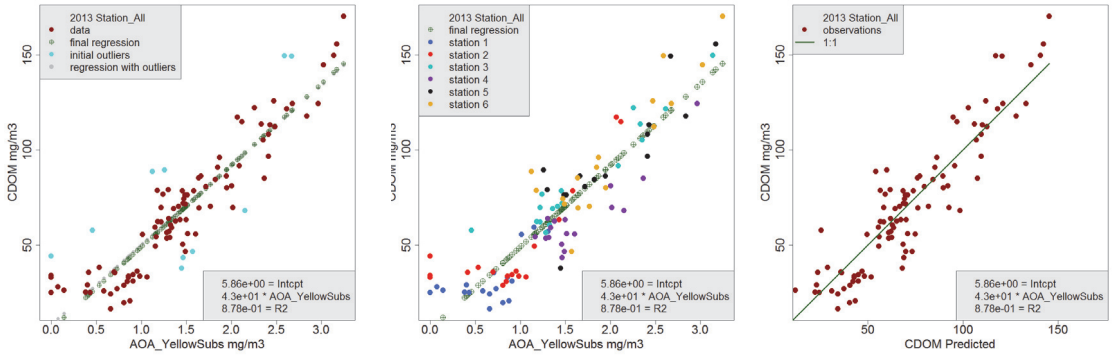

Figure 138 Relationship coloured dissolved organic matter (CDOM, AOA-data, µg l^{-1}) and Yellow substances (AOA-data, mg l^{-1} (not mg m^{-3} as the axis labels say). 2013 data only. Left: all data, with outliers determined. Middle: same regression as left, but the six monitoring stations are distinguished. Right: CDOM predicted with the regression equation, and as measured.

8.16 Benthic chlorophyll-a, after spectrophotometric analyses and validation with Benthotorch results

8.16.1 Spectrophotometric data

Benthic chlorophyll-a values (Figure 139, Figure 141) were needed to translate primary production values from the ^{14}C-incubations to benthic primary production in the field situation. For procedures see sections 4.6.1.3 and 4.6.1.5.

Values found are highest for station 5, and lowest for station 3 and 4.

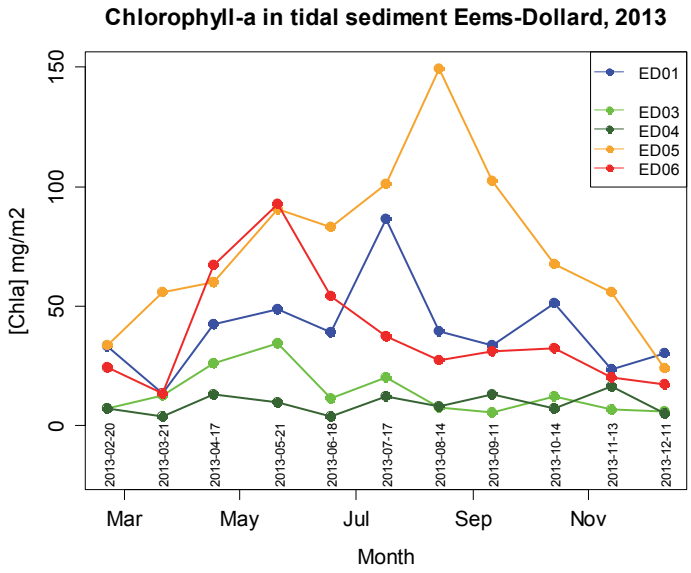

Figure 139 Benthic chlorophyll-a data for the five monitoring sites (site 2 is not mentioned since it was sampled only once).

8.16.2 BenthoTorch data

The average total chlorophyll-a values determined with the BenthoTorch were compared to the values found after spectrophotometric analyses. The correlation for the concentrations measured with the two methods is 28 percent (t=2.13, df=53, p=0.04); with BenthoTorch concentrations being lower than the spectrophotometric results, as was expected (see section 4.6.3). Also, maximum Benthotorch chlorophyll-a values were correlated with the spectrophotometric results. In all cases, Benthotorch values are lower than the spectrophotometric results; a result that is expected since the Benthotorch just 'sees' the upper part of the sediment, and not all the 5 mm's that were extracted and analysed (section 4.6.2).

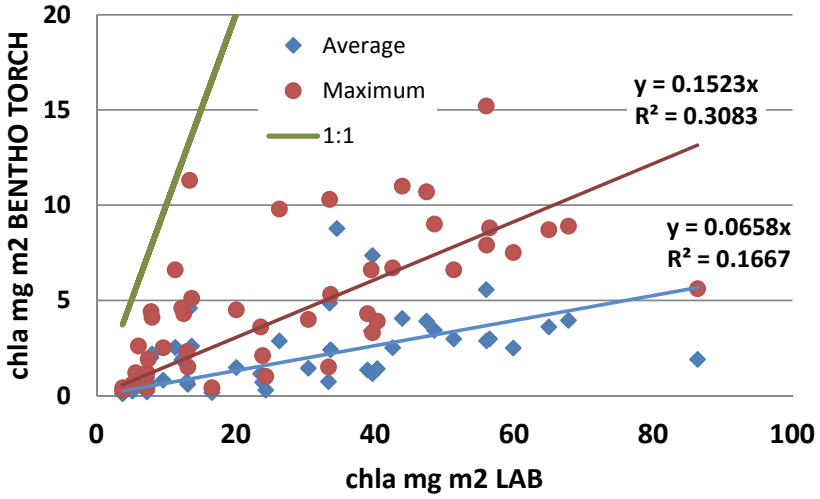

Figure 140 Benthic chlorophyll results after spectrophotometric analyses (X-axis) and after surface analyses with the BenthoTorch. The first method measures total chlorophyll, the Benthotorch just chlorophyll-a. In brown: maximum values obtained with the BenthoTorch, blue: average values for all ten measurements. In green: the 1:1-line. It follows that: lab values = (maximum BenthoTorch)/0.15 and also lab values = (mean BenthoTorch)/0.066.

8.16.3 Discussion

Values found can be compared to the data from De Jonge & Colijn (1994) (Figure 142). Most striking is the large difference between the values De Jonge & Colijn found for stations 3 and 4 (up to about 80 mg m^{-2})), and the present values (with a maximum of about 15 mg m^{-2} for station 4 and 35 mg m^{-2} for station 3). Other values found are mostly below the values of De Jonge and Colijn, but differences are not that large as for these stations 3 and 4.

8.16.4 Conclusions

From the BenthoTorch validation, it must be concluded that the present benthic chlorophyll results are correct. At least, there's no reason to assume that the results largely deviate from was really present in the sediment at the sampling sites.

Thus, it must be concluded that in our samples benthic chlorophyll-a concentrations are lower than the concentrations reported in the seventies (De Jonge and Colijn, 1994).

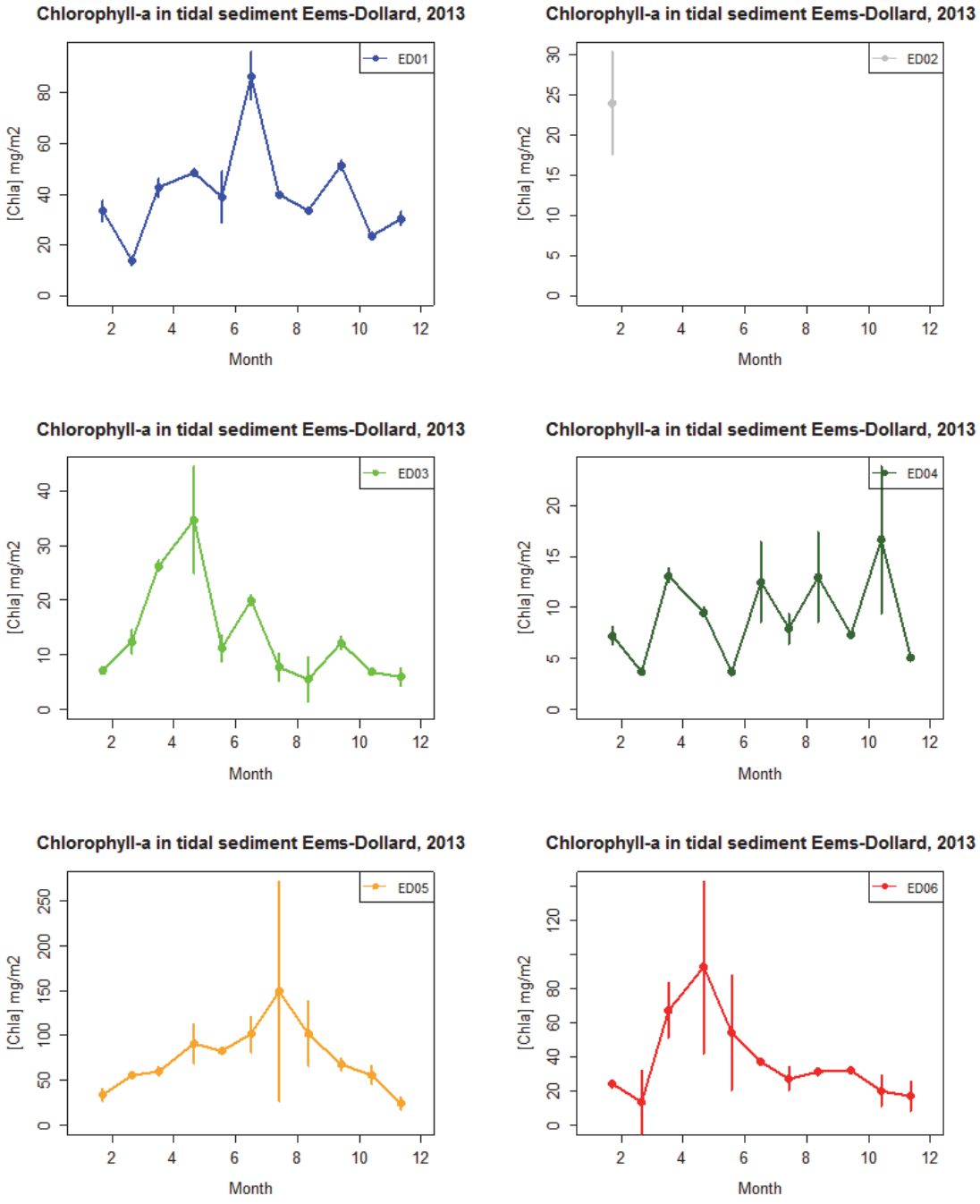

Figure 141 Average benthic chlorophyll-a data for the six monitoring sites (site 2 is only 1 value). Same as previous picture, but now every station at its own extended scale). For all data, n=2.

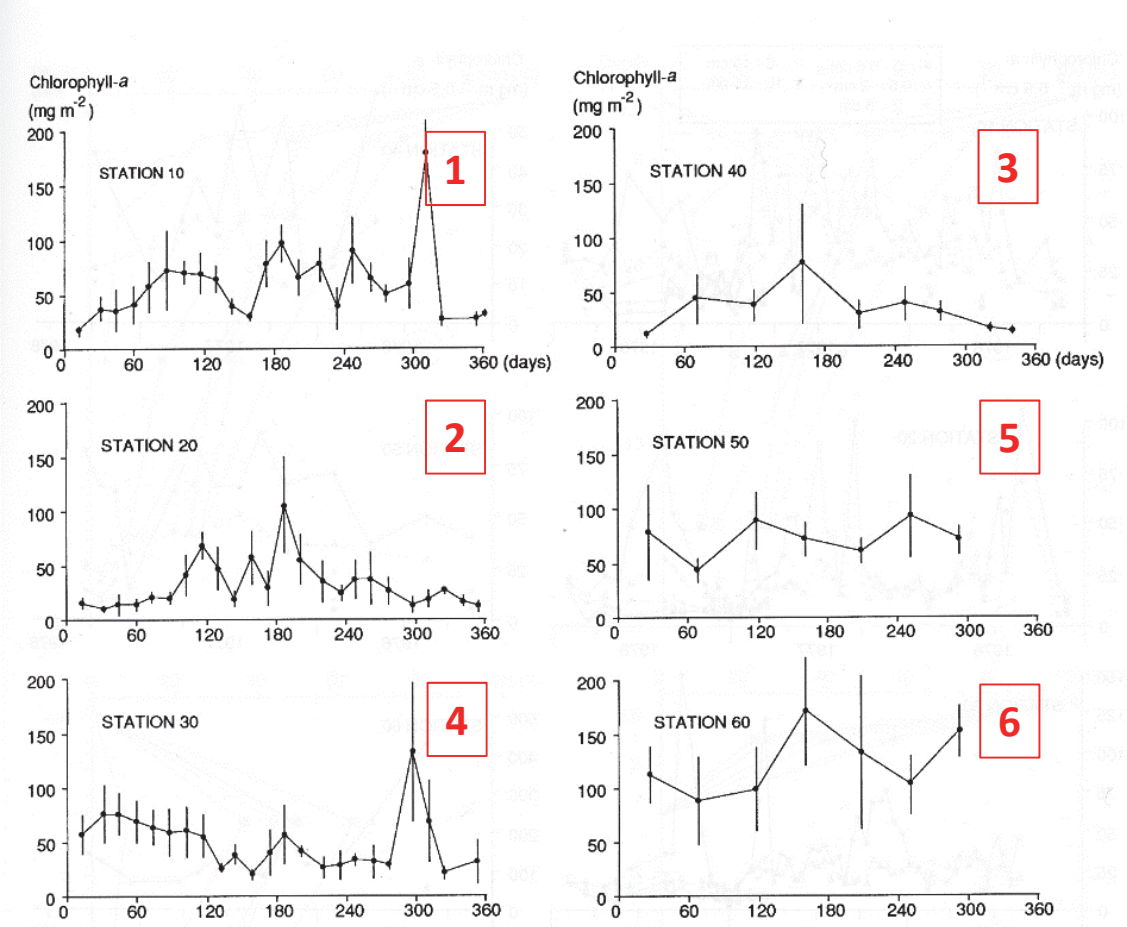

Fig. 4. Plots of the mean chlorophyll-*a* concentrations in the upper 0.5 cm sediment layer of the six main stations in 1977. Bars represent standard deviations.

Figure 142 Chlorophyll-a densities in Eems-Dollard sediments, as determined by De Jonge & Colijn (1994). Figure is a copy from their publication. Present station numbers are mentioned in bold red.

8.17 Extinction coefficients in the water column

Values for the water column light attenuation coefficient k_d (m^{-1}), as determined according to the descriptions in section 4.12, are summarized and interpolated for the whole year in Figure 143 and Figure 144 (2012 and 2013, respectively). K_d values are needed to translate the ^{14}C-incubation results (the PI-curves) to in-situ water column primary production.

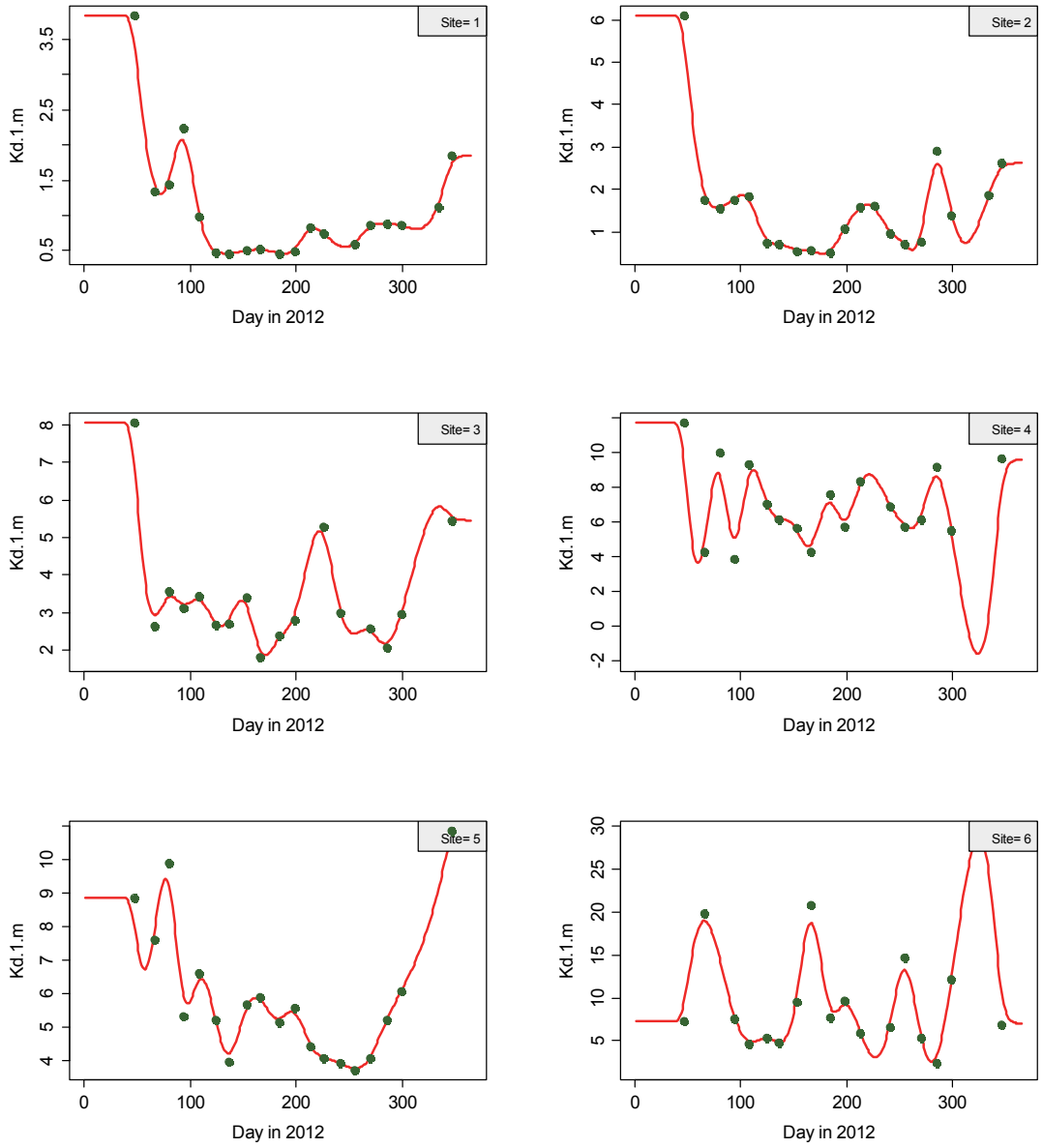

Figure 143 Extinction coefficients at the six stations in 2012, measured (dots) and inter/extrapolated (lines), following a moving average method.

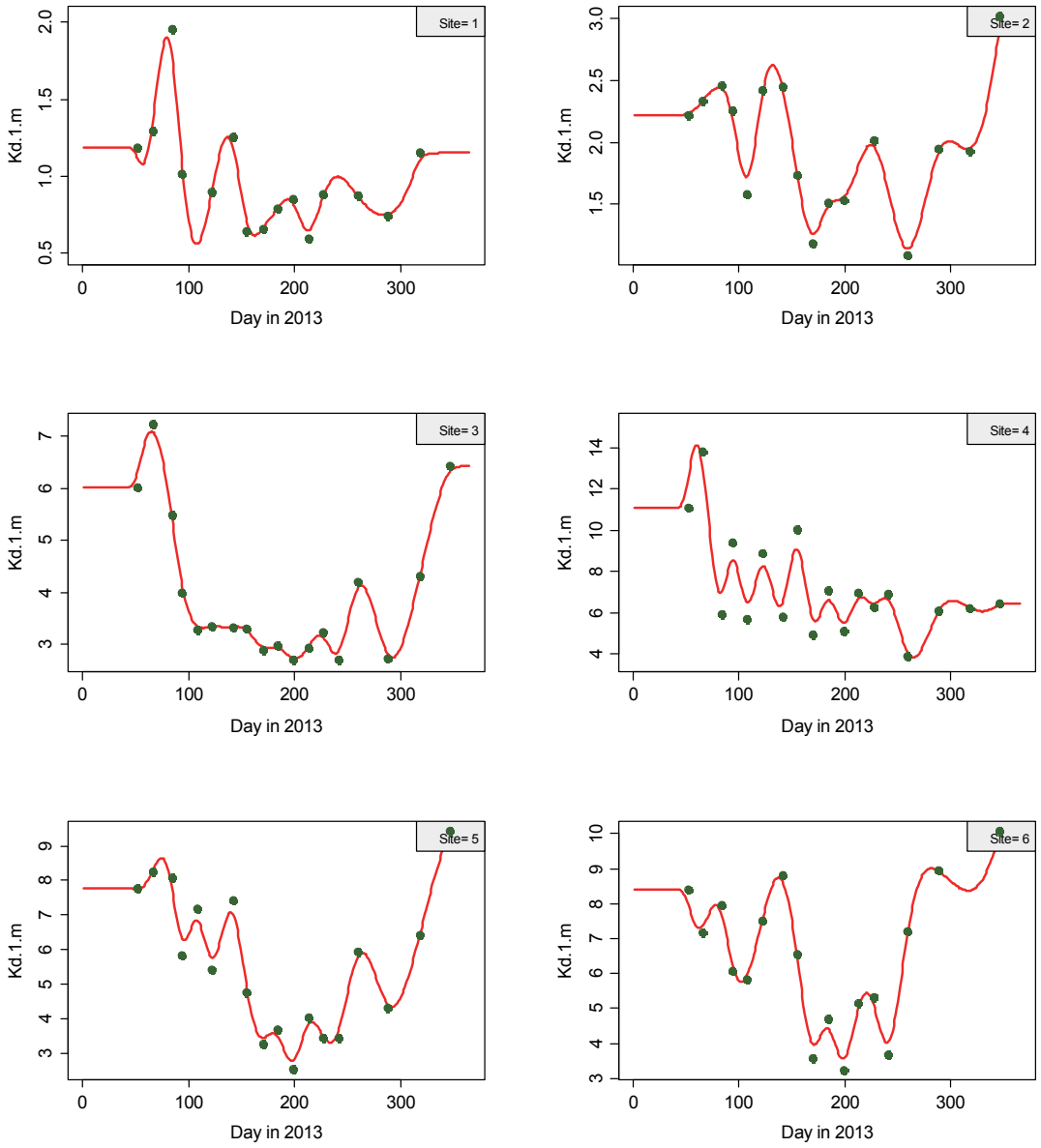

Figure 144 Extinction coefficients at the six stations in 2013, measured (dots) and inter/extrapolated (lines), following a moving average method.

Most striking is the large difference between the two outermost estuary stations 1 and 2 (with k_d values 1.0 - 2.5 m^{-1}) and the three most inner stations 4-6 (with k_d values 3 - 12 m^{-1}). Station 3 shows intermediate values. All data together are summarized in Figure 145.

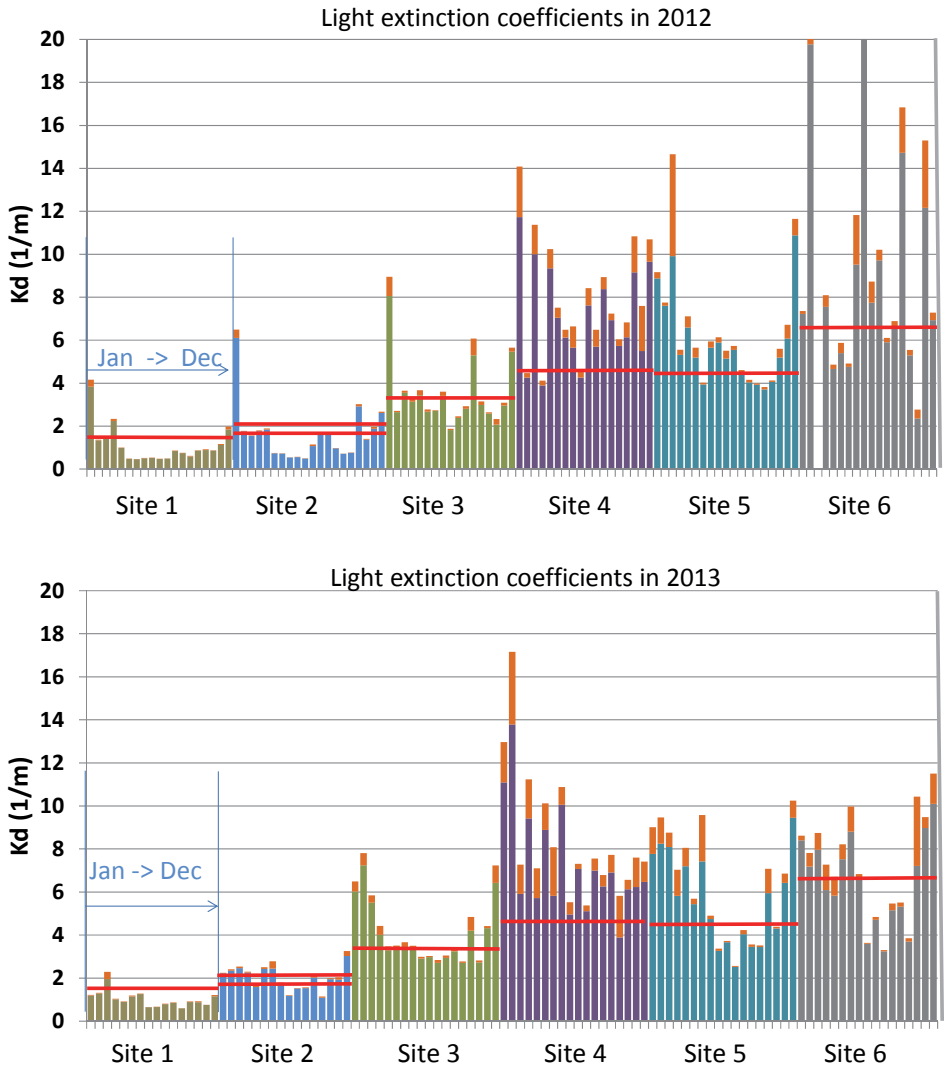

Figure 145 Summary of light extinction coefficients found in the Ems-Dollard area. Upper: 2012, lower: 2013. Data are grouped per station (1->6), and from January (most left per station), to December (most right). Orange bars denote standard deviation of the results (follows from the parameter fit procedure). Red horizontal lines show average values as found by Colijn (1983).

8.17.1 Gradient along the estuary axis

Gradients of the light attenuation coefficient along the estuary axis are shown in Figure 146. A maximum is reached around km 35-40, that is half-way between sites 3 and 4 until site 4 (Figure 21).

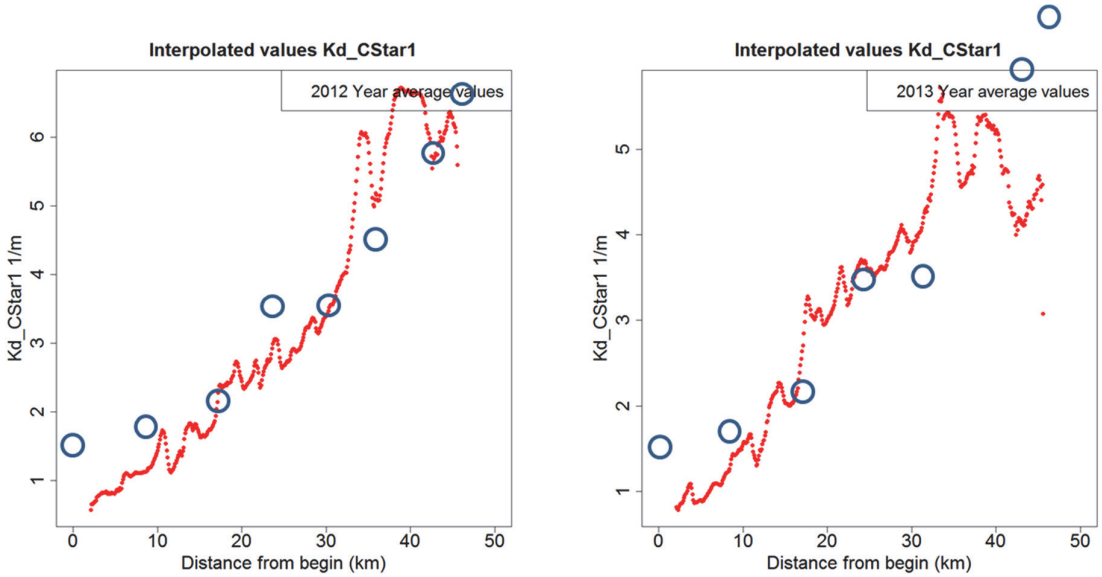

Figure 146 Year-average gradient of the light attenuation coefficient k_d along the estuary axis, based on C-Star1 data (continuous light attenuation monitoring, see sections 7.11 and 8.17 of the full data report (Brinkman, 2014). Circles denote results by Colijn (1983) as average for the years 1976-1980.

Suspended matter is the most important factor determining light attenuation, together with yellow substance; the latter is especially important in the inner areas. Thus, these results are similarly shaped as those for suspended matter (section 8.7).

8.17.2 Comparison with Colijns data

Results reported by Colijn (1983) for the years 1976-1980 are plotted in Figure 145Figure 146. If a structural difference exists, then it is in the outer areas, where Colijn found a larger light attenuation than we did now. This is in agreement with the RWS –data on suspended matter, their monitoring results gave higher values for the end 70's than for the present years (Figure 102).

8.17.3 Conclusions

The light attenuation values we found for the whole estuary (the transect from sea side up to the Dollard) are comparable to those described by Colijn (1983), except for station 1 (North Sea side) where Colijn found higher values. Around the 35 km site (Figure 146) values were higher in 2012 and 2013 compared to the seventies. This is in line with the elevated suspended solid concentrations mentioned in section 8.7.

8.18 Extinction coefficient in the sediment

8.18.1 General

In section 4.14, some literature data on sediment light attenuation were presented.

Now, better values may be obtained based on the relationship found between light attenuation and sediment concentration in the water column (section 7.9, Table 21). Purely based on solids alone (without coloured dissolved matter), k_d = a * [solids]. [solids] in g m^{-3}, k_d in m^{-1}, with a= 0.044 (2012) and 0.037 (2013). As average, a= 0.040 has been taken.

The amount of sediment per unit volume is related to the type of the sediment. Sandy sediment has a low porosity, while silty sediments have a high water content and thus low amount of solids per unit volume. This problem was tackled by using gold data from Lake Veluwe (Brinkman & Van Raaphorst; 1986). Based on those data, a relationship between silt content of the sediment and the sediment porosity was derived. Next, the silt content (with its own attenuation coefficient) and sand content (also with its own attenuation coefficient) is known.

8.18.2 Silt and sand in the sediment

As said (section 4.14), existing data for Lake Veluwe were re-analysed, and used to estimate a relationship between silt content of the sediment and porosity, and thus to estimate the amount of fine silt and sand per m^3 sediment. That offers a possibility to estimate an extinction coefficient in the sediment top layer.

Relevant relationships found were

Thus, it followed from the analyses that

$$\mathrm{H_2O\ (mass\text{-}\%)} = 18.73 + 0.0624 \cdot \mathrm{Fe\ (mg\ g^{-1}ds)} \qquad (29a)$$

and

$$\mathrm{Silt\ (mass\text{-}\%)} = -2.30 + 1.347 \cdot \mathrm{Fe\ (mg\ g^{-1}ds)} \qquad (29b)$$

The relationship between silt and lutum (the mass fraction<2 µm):

$$\mathrm{Silt\ (mass\text{-}\%)} = +0.095 + 1.583 \cdot \mathrm{Lutum\ (mg\ g^{-1}ds)} \qquad (29c)$$

This makes a comparison with the Zwarts' analysis possible: Zwarts (2004) presented a similar relationship

$$\mathrm{Silt\ (mass\text{-}\%)} = +1.478 \cdot \mathrm{Lutum\ (mg\ g^{-1}ds)}$$ (analysed by the "Rijksdienst IJsselmeerpolders") (29d)

and

$$\mathrm{Silt\ (mass\text{-}\%)} = +1.501 \cdot \mathrm{Lutum\ (mg\ g^{-1}ds)}$$ (analysed by the "Instituut voor Bodemvruchtbaarheid" in Haren, Neth) (29f)

Zwarts (2004) notes that the relationship is not strictly linear, and by assuming a third-degree polynomial, the differences between the analyses results (mostly done by different laboratories) disappear. Resuming:

$$Silt\ content\ (<16\ \mu m) = 0.1879 * Silt\ content\ (<63\ \mu m, Malvern) \quad (29g)$$

gives silt (% <16µm) as a function of the available Wadden Sea GeoSea silt data (mass-% <63 µm).

equation (29c) : gives silt-content (mass-% <16µm) as a function of Fe-data (mass-%).

equation (29b) : gives H_2O-content (mass-%) as a function of Fe-data (mass-%).

Finally, a conversion is needed from mass-% H2O to volume-% (or: porosity). This is derived from

$$\text{mass-\% } H_2O = \frac{vol\%\ H2O \cdot \rho_{H2O}}{vol\%\ H2O \cdot \rho_{H2O} + (100 - vol\%\ H2O) \cdot \rho_{sol}} \quad (29h)$$

ρ_{sol} is the specific mass (kg dm^{-3}) of the solids and ρ_{H2O} is the specific mass (kg dm^{-3}) of the water.

After rearranging eq(7), it follows that

$$\text{vol\% H2O} = \frac{100 \cdot mass\%H2O \cdot \rho_{sol}}{100 \cdot \rho_{H2O} + mass\%H2O \cdot \rho_{sol} - mass\%H2O \cdot \rho_{H2O}} \quad (29i)$$

ρ_{H2O} = 1, and ρ_{sol} is taken to be 2.60 (kg dm^{-3}), a value that also follows form the Lake Veluwe analysis.

8.18.3 Kd-values in the sediment

Based on the regression equations above, we now could estimate a K_d-value for the sediments in the Ems-Dollard estuary, whereas specific mass of the solids has been taken as 2.6 (kg dm^{-3}). The results were also compared to the values given by Colijn (1983), and that a possibility to estimate the contribution of sand.

We estimated k_d-values based on the Malvern-data for sediment composition, and on the data found after the Zwarts-transformation. In the "Zwarts"-case, we had to assume that the contribution of sand to the attenuation coefficient is 4000 m^{-1} (g cm^{-3})$^{-1}$ and the one of silt 45000 m^{-1} (g cm^{-3})$^{-1}$. For the "Malvern"-case (silt data used without any conversion, contrary to the "Zwarts"-case), we used 1000 m^{-1} (g cm^{-3})$^{-1}$ for sand and 45000 m^{-1} (g cm^{-3})$^{-1}$ for silt.

Considering k_d values from literature for sandy sediments (e.q MacIntype and Cullen, 1995) and even pure sand (Kuhl et al, 1994) kd for sandy sediments will be between 1 and 4 mm^{-1}, so with 4 mm^{-1} we probably are at the high end of the range, and with 1 mm^{-1} at the lower end.

Table 34 Results of Malvern-sediment composition data (without any conversion), in terms of sediment attenuation coefficients k_d (m^{-1})

Station	Solids g/cm3	Silt g/cm3	Sand g/cm3	Kd silt m^{-1}	Kd sand m^{-1}	kd_all m^{-1}	Kd_min Colijn m^{-1}	Kd_max Colijn m^{-1}	Kd_avg Colijn m^{-1}
1	1.51	0.088	1.43	3949.9	1425.6	5375.5	5470	5600	5535
2	1.51	0.091	1.42	4076.0	1419.1	5495.1	7230	25270	15580
3	1.53	0.076	1.45	3432.4	1452.3	4884.6	9090	9090	9090
4	1.38	0.183	1.20	8256.1	1196.0	9452.1	15480	15480	15480
5	1.05	0.369	0.68	16604.0	676.3	17280.3	5800	5800	5800
6	0.50	0.430	0.07	19366.4	70.1	19436.4	32050	32640	32345

Table 35 Results of sediment composition data (Malvern-data, now converted following the equations of Zwarts), in terms of sediment attenuation coefficients k_d (m^{-1})

Station	Solids g/cm3	Silt g/cm3	Sand g/cm3	Kd silt m^{-1}	Kd sand m^{-1}	kd_all m^{-1}	Kd_min Colijn m^{-1}	Kd_max Colijn m^{-1}	Kd_avg Colijn m^{-1}
1	1.53	0.038	1.5	1707.8	5969.5	7677.4	5470	5600	5535
2	1.51	0.045	1.5	2040.0	5863.1	7903.0	7230	25270	15580
3	1.56	0.026	1.5	1152.7	6145.1	7297.8	9090	9090	9090
4	1.45	0.067	1.4	3008.5	5546.0	8554.5	15480	15480	15480
5	1.15	0.161	1.0	7253.2	3970.4	11223.6	5800	5800	5800
6	0.56	0.224	0.3	10099.8	1328.3	11428.1	32050	32640	32345

All data are given in Table 35, including the values Colijn (1983) estimated from light extinction measurements on sediment suspensions.

8.18.4 Conclusion

It is not possible to come up with well-established values for the sediment attenuation coefficients, this is caused by the fact that no direct measurements were done. Therefore, approximations have to be used, based on

a) sediment composition (based on the Malvern data assessed around 1990, plus a conversion made by Zwarts),

b) estimates for sediment porosity (based on Lake Veluwe data) and

c) as good as possible estimates for the contribution of sand and of silt to the attenuation coefficient, also regarding literature values for k_d. Additionally, old data from Colijn & De Jong are available.

Thus, since there is more than one option for sediment composition and there are old data available for k_d, there will be several results for the computed benthic primary production.

8.19 Vertical profiles of temperature, salinity, turbidity and chlorophyll in the water column at Groote Gat Noord, or: is the water column well mixed?

The question was to what extend the water column in the area was mixed or not. The data obtained in 2013 and 2014 are summarized in Figure 147 and Figure 148. Temperature and conductivity reflect a very well mixed water body with regard to dissolved substances, but solids (pelagic + suspended benthic algae, and silt) show vertical profiles with differences between top and bottom layers that can be substantial. When turbidity profiles are clearly present, chlorophyll-a content also shows a clear vertical profile. Checking the weather conditions: these are listed in Table 36. At the other six dates shown, wind speeds were below 5 m s^{-1}, and thus, conditions then can be regarded as calm.

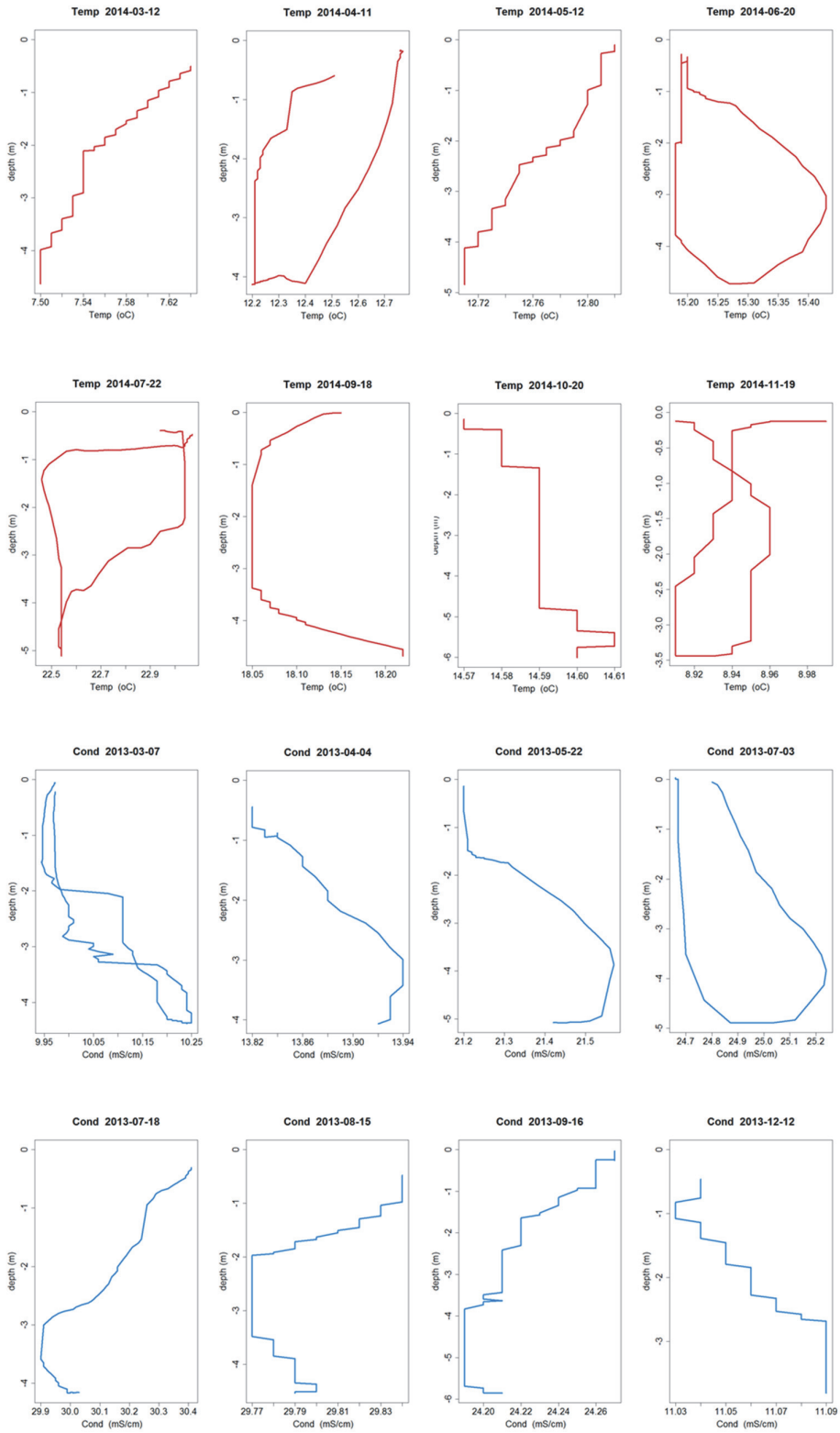

Figure 147 Vertical water column profiles of temperature (upper, in 2014) and conductivity (lower, in 2013) at station Groote Gat Noord. Note that vertical differences are small.

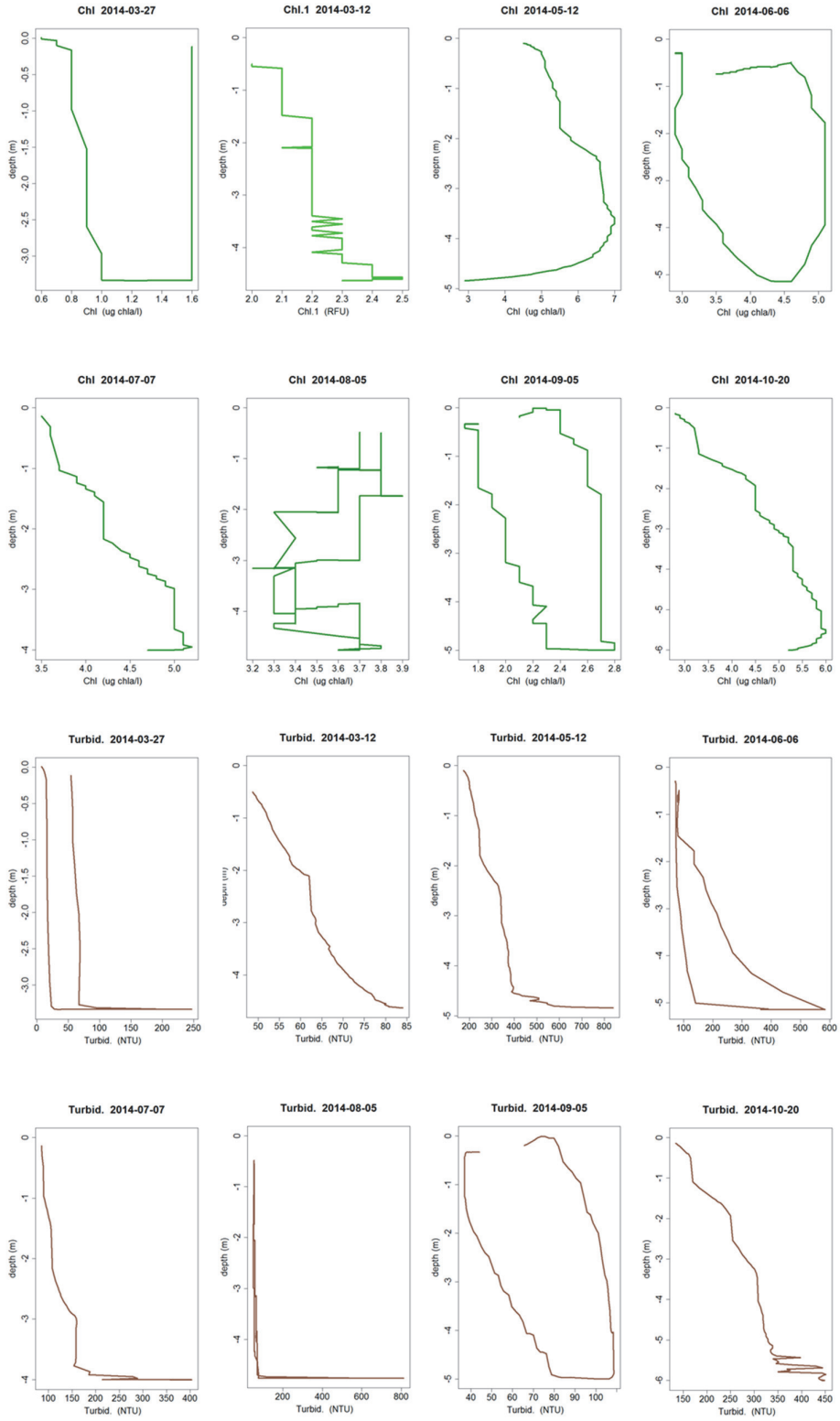

Figure 148 Vertical water column profiles of chlorophyll-a (upper, in 2014, in µg chla l^{-1}) and turbidity (lower, in 2014, in NTU, at same dates as chl-a) at station Groote Gat Noord. Note that vertical differences occur and are larger than those for temperature and conductivity (Figure 147). Note that at 2014-03-12 the fluorescence result is shown since chlorophyll-a data are missing for that day.

Table 36 Daily average wind speeds on the sampling dates shown in Figure 148, plus those on the day before; and maximum speed of each of the 24 1-hour-averages. Beaufort-numbers are mentioned as well. Data from KNMI, 2015)

Date	Avg wind speed	Bft avg	Max 1h avg	Bft of max 1 hr avg
3/9/2014	4.4	3	7	4
3/10/2014	4.3	3	7	4
3/26/2014	3.2	2	6	4
3/27/2014	7	4	10	5
5/11/2014	7.5	4	10	5
5/12/2014	5.2	3	7	4
6/5/2014	5.5	4	7	4
6/6/2014	3.8	3	6	4
7/6/2014	4.7	3	7	4
7/7/2014	3.2	4	5	3
8/4/2014	2.5	4	6	4
8/5/2014	3.3	3	5	3
9/4/2014	4.5	3	7	4
9/5/2014	2.3	2	4	3
10/19/2014	7.7	4	10	5
10/20/2014	6.7	4	9	5

One must conclude that on days with calm weather a vertical gradient for chlorophyll and turbidity occurs. That implies that light attenuation coefficients will increase with increasing depths, and that top water column chlorophyll-a and phytoplankton samples will underestimate the 'real' average concentrations of algae. Consequences for total water column primary production probably are less, because of the low light conditions lower in the water column.

8.20 Conclusions for this chapter: what have we learnt?

8.20.1 Chapter content?

In this chapter, all observations done in the lab, at the monitoring sites and during the cruises are presented. The observations are needed for a comparison with previous years, especially the Colijn years 1976-1980, to feed the subsequent modelling by Deltares, and for the computation of primary production. The latter is the subject of the next two chapters (9: pelagic primary production; 10: benthic primary production).

8.20.2 What went OK?

Temperature (8.2) / Conductivity/salinity (8.3) / Nutrients (8.4) / Dissolved inorganic carbon (8.5) /

Oxygen (8.6) : see chapter 7. Based on the corrections described in chapter 7 reliably data were obtained.

Suspended matter (8.7) : together with the continuous measurements with the C-Star1 and the turbidity instrument, plus the assessment of light attenuation and suspended solid concentrations many data were obtained in the estuary, especially in those areas where suspended solid concentrations were below the upper detection limit of the C-Star1 probe.

Pelagic total chlorophyll-a (8.8) : Based on the findings in chapter 7, reliable chlorophyll data were obtained. However, an uncertainty regarding the best whole trajectory from sample handling to final analyses remains; this impedes a precise comparison with other and older data.

Phytoplankton organic carbon content and contribution of pelagic and benthic algae (8.9) : based on algal counts and volume assessment. A very useful addition to the algae data, and necessary for the data on primary production (next chapter).

Algae groups (8.10) : a combination of AOA-pigment analyses, algae counts and flow-cytometer analyses. To a certain level algae groups could be quantified. So also next section on improvements.

Pheophytin (8.11) : a useful component to analyse, especially since it helps to validate chlorophyll results.

Pigment ratios in the samples: chlorophyll-a total chlorophyll, chlorophyll to carotene and chlorophyll to pheophytin (8.12) : based on HPLC-data. Appeared to be very useful, also when validating chlorophyll-a measurements.

Yellow substances (8.14) / Coloured organic matter (CDOM) (8.15): results gave a good indication that CDOM and yellow Substance have a fresh water origin. See also next section.

Benthic chlorophyll-a, after spectrophotometric analyses (8.16): the benthic chlorophyll-a analyses were subject of discussion; results seemed to be (much) too low. However, after performing a check based on also available BenthoTorch results it could be concluded that the results can be considered as reliable for the samples taken.

Extinction coefficients in the water column (8.17): the data obtained plus the analyses performed are sound.

Extinction coefficient in the sediment (8.18): best possible data were found, despite limited possibilities and with help of data from other systems.

Vertical water column profiles (8.19): under calm weather conditions vertical column profiles exist for solids, not for dissolved substances.

8.20.3 What needs improvement and/or what are main recommendations for future work?

Dissolved inorganic carbon (8.5): for the present situation the method followed is OK. However for investigations in other systems with where high pH-values occur, very precise pH measurements are needed. This was not the case in the Ems-Dollard estuary.

Suspended matter (8.7): for better continuous data assessment, a light attenuation probe with a (very) short light pathway is needed. The 10 cm C-Star1 probe now had an upper detection limit of about 200 mg suspended solids l^{-1}. Although the shortest light path sensor presently available on the market was used now, for a full employability an additional 1 or 2 cm pathway sensor is needed.

Pelagic total chlorophyll-a (8.8) : there is a number of possible uncertainties and choices when determining chlorophyll-a concentrations, starting with sampling, filtering (light/dark), storage (time until freezing at -80 ^{o}C), extraction fluid (acetone, ethanol) and temperature, separation or not (HPLC?), detection method (fluorometry or spectrometry, and if yes, what wave length), and calibration methods. In short: there is a lot to check and may be perform intercalibrations with other labs, and do apply more than one analysis method (we were lucky to have several methods of analyses, so there was a validation possibility).

Absorption ratios (8.13): was meant to distinguish between light or nutrient limited algal growth, but the method appeared not to work. To detect the limiting factor, incubations with several nutrient additions are needed. A second possibility is to apply a bacteria based test as described by Kuipers & Van Noort (2008).

Yellow substances (8.14) / Coloured organic matter (CDOM) (8.15) : both analyses were based on different instruments (AOA respectively Cyclops), but should produce roughly the same results. This was not the case. This needs better calibration.

Benthic chlorophyll-a, after spectrophotometric analyses (8.16): it is recommended to i) test the method better, ii) to analyse sedimentary chlorophyll-a content not only in one slice (5 mm in the present case), but to separate the sediment core into 2 mm slices and analyse chla in each slice and iii) always apply at least two analysis methods (the BenthoTorch data gave us a possibility to validate the laboratory analyses (to a certain extend)).

Microphytobenthos content (and thus benthic chlorophyll values) also depends on grazer activity. It is recommended to pay sufficient attention to the numbers and activity of benthic grazers.

Extinction coefficient in the sediment (8.18): since benthic primary production results are rather sensitive to uncertainties in sediment light attenuation, it would have been better to have separate measurements of the light extinction coefficient of suspended sediments, and if possible, light intensity *in* the sediment.

Vertical profiles (8.19): it is recommended to perform vertical profile measurements at several sites in the research area.

9 Results-3: pelagic primary production

9.1 What is in this chapter

All pelagic primary production results are presented. First (section 9.2) the results of the ^{14}C-incubations are given. In section 9.3, the computation of the gross primary production of the whole system is presented. In section 9.4 the mass specific phytoplankton growth rates are given. A comparison with previous results (Colijn 1983) is presented in section 9.5, and possible causes for differences are discussed in section 9.6. In section 9.7 the effect of a change in turbidity on primary production is discussed. Conclusions are given in section 9.8 and finally, section 9.9 finishes with an overview and recommendations.

9.2 Pelagic primary production parameters

First, results of the ^{14}C-measurements are presented. The Eilers-Peeters formula contains the a,b and c-parameters, in which c is a kind of Monod-parameter, b gives the sensitivity to light and co-determines the PI-maximum, and a expresses importance of light inhibition (and thus also determines the PI-maximum).

The slope of the PI-curve at I=0 is α, which is the inverse of c, and the maximum production (P_{max}, in terms of mg C mg $chla^{-1}$ h^{-1}) can be derived from the a,b and c-values (section 4.12).

Eilers-Peeters a, b and c- values for 2012 are presented in Figure 149 -Figure 151. Values for α in 2012 are shown in Figure 152, and for 2013 in Figure 153. Results for the maximum productivity P_{max} are presented in Figure 154 (2012) and Figure 155 (2013).

The P_{max}- and α-results probably best reflect the PI-characteristics of the algal community. Pmax values roughly range between 2 and 12 mg C mg^{-1} chla h^{-1}, with one exceptional 20 and a few very low values of around 1 mg C mg^{-1} chla h^{-1}.

Typical α-values vary around 0.04 mg C mg^{-1} chla h^{-1} (µE m^{-2} $s^{-1})^{-1}$, with maxima around 0.1. The first measurement in 2012 shows an exceptional 0.8 value, but probably this must be considered as an outlier (although details in the original data do not show abnormalities).

Examination of the P_{max}-results seems to reveal a pattern for a couple of stations. In 2013, all stations show maximum P_{max}-values during the summer season; this is most clear for the four innermost stations. The same pattern also exists in 2012, although it is less clear.

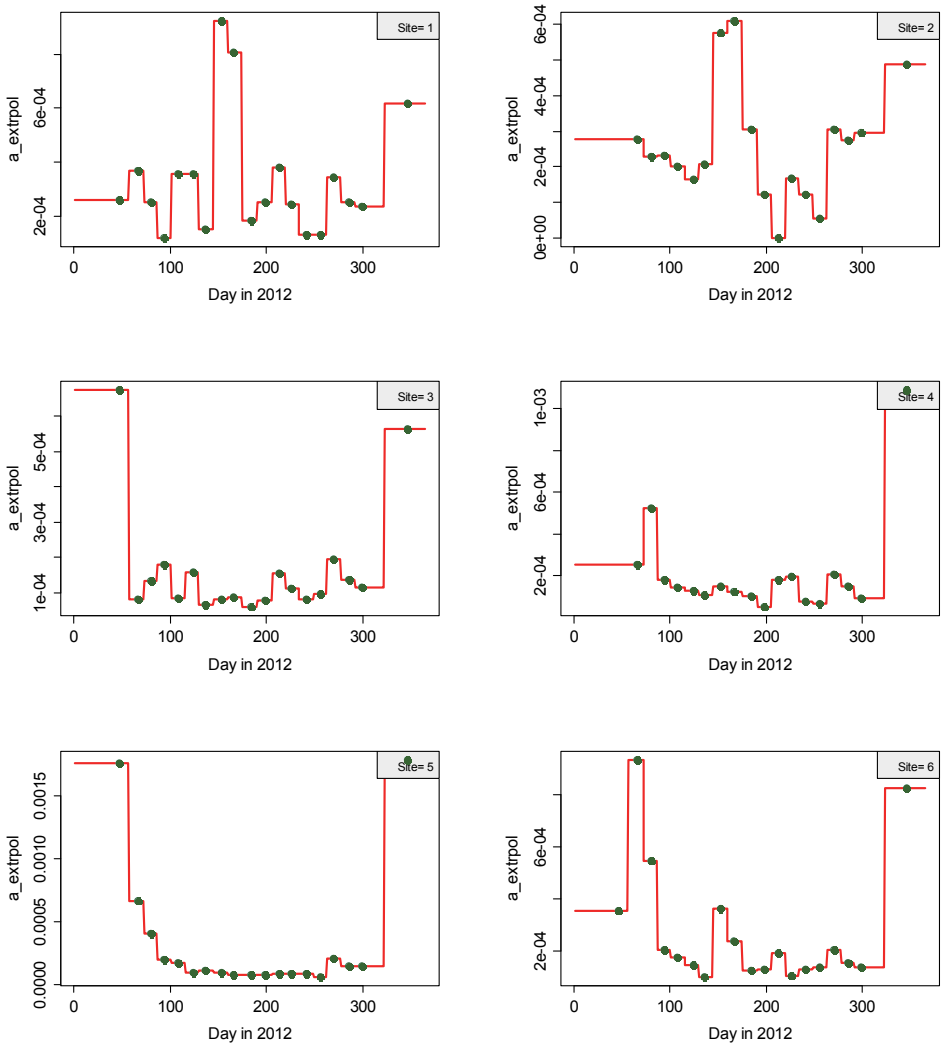

Figure 149 Primary production parameters (a-values) at the six station in 2012, measured (dots) and inter/extrapolated (lines), following a rectangular method.

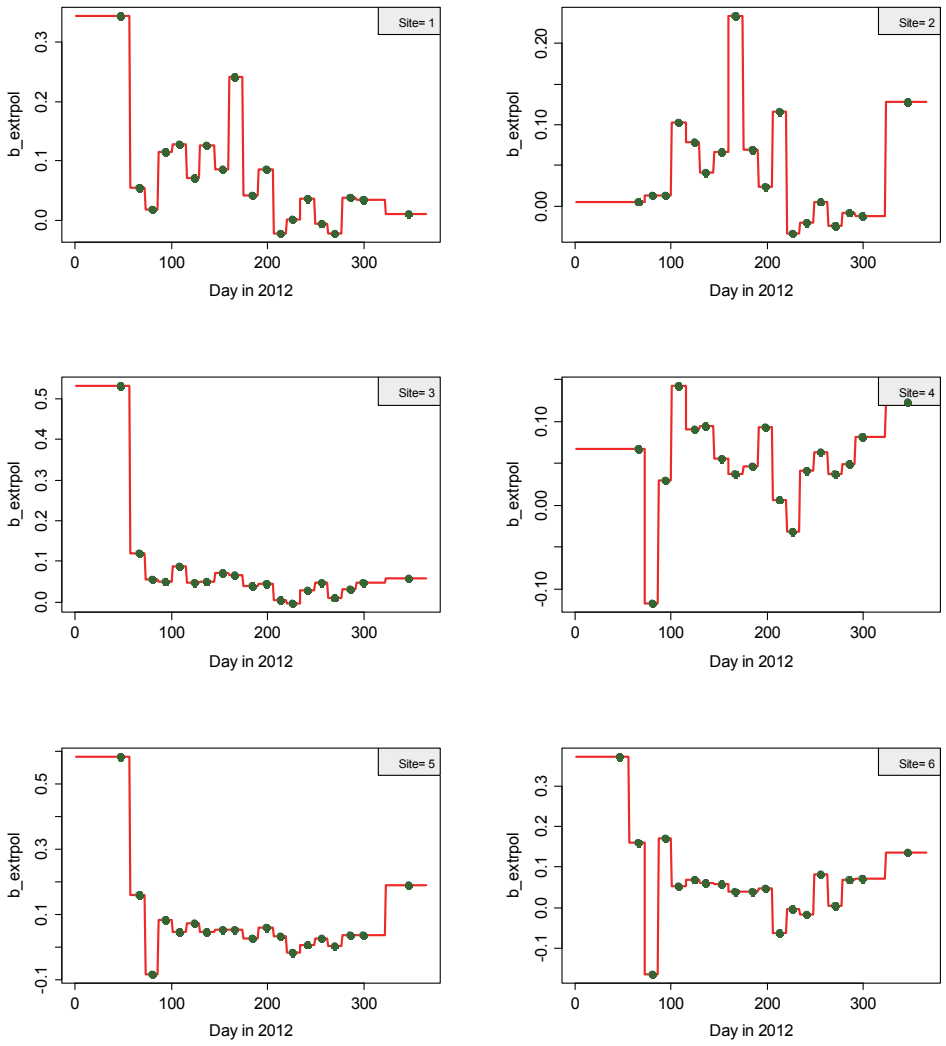

Figure 150 Primary production parameters (b-values) at the six station in 2012, measured (dots) and inter/extrapolated (lines), following a rectangular method.

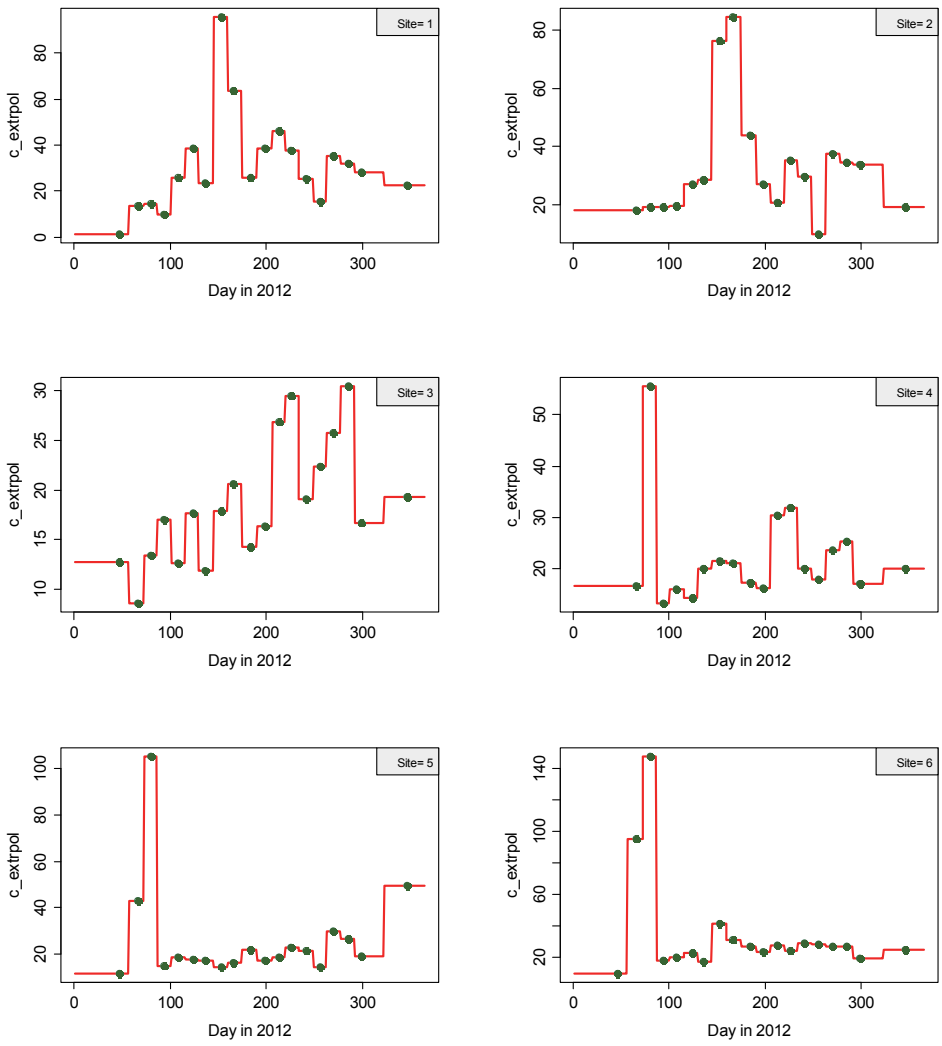

Figure 151 Primary production parameters (c-values) at the six station in 2012, measured (dots) and inter/extrapolated (lines), following a rectangular method

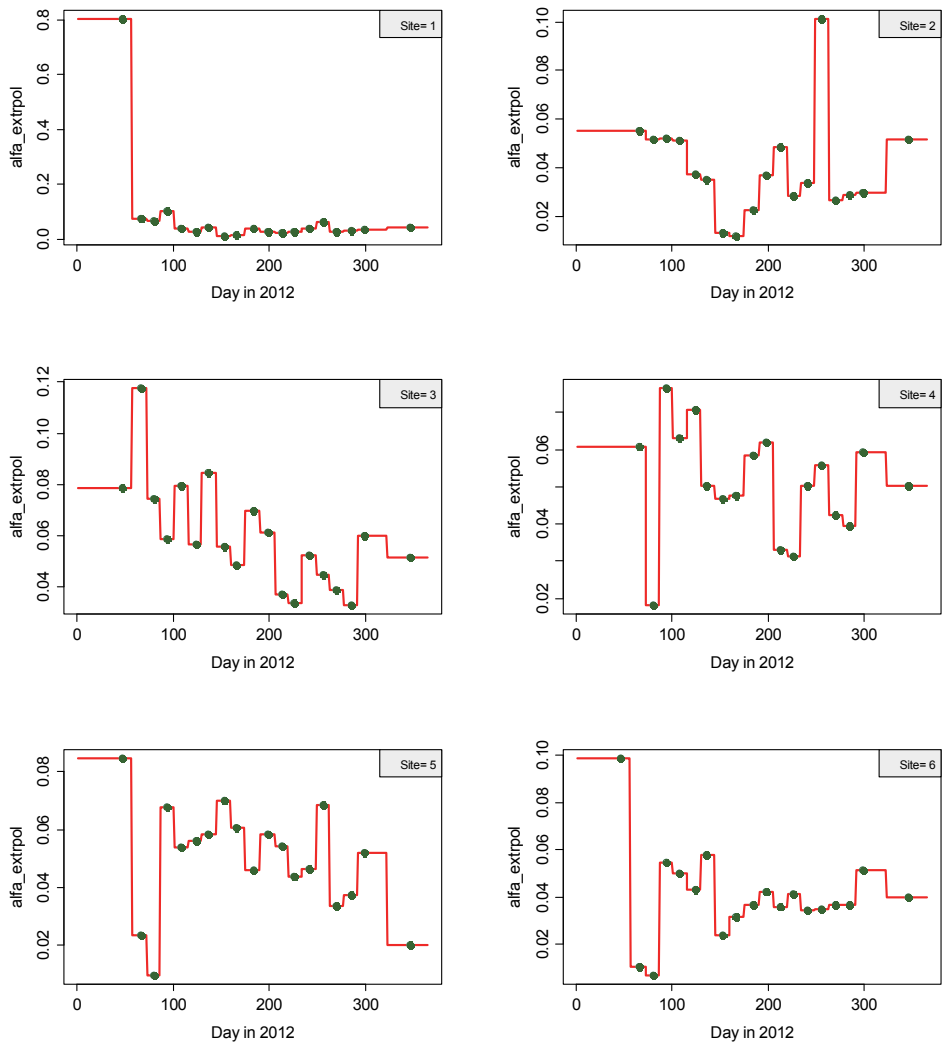

Figure 152 Primary production characteristic (α-values) at the six station in 2012, measured (dots) and inter/extrapolated (lines), following a rectangular method. α denotes the slope of the PI-curve at I=0. Large values imply a high sensitivity to light of primary productivity at low light intensities. Value for station 1 at the first sampling date seems to be an outlier. Unit= mg C mg^{-1} chla h^{-1} (uE m^{-2} s^{-1})$^{-1}$

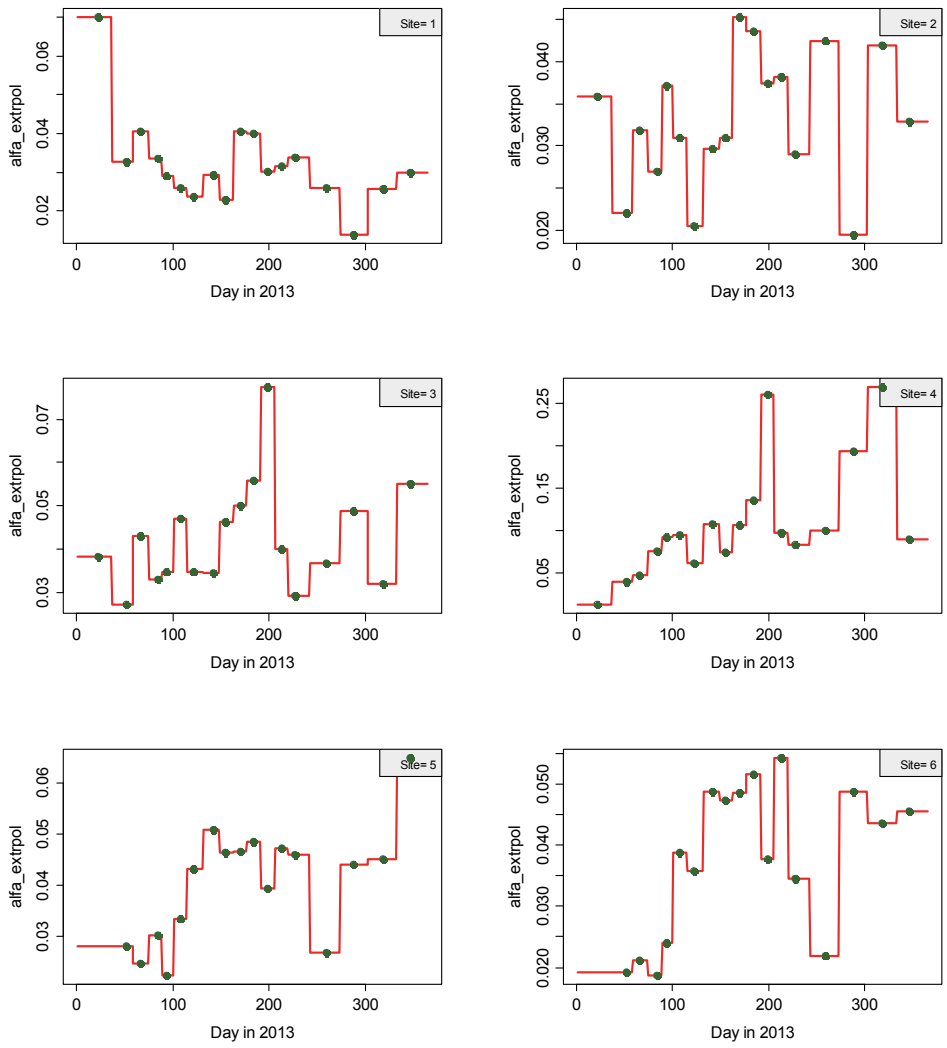

Figure 153 Primary production characteristic (α-values) at the six station in 2013, measured (dots) and inter/extrapolated (lines), following a rectangular method. α denotes the slope of the PI-curve at I=0. Large values imply a high sensitivity to light of primary productivity at low light intensities. Unit= mg C mg^{-1} chla h^{-1} (uE m^{-2} s^{-1})$^{-1}$

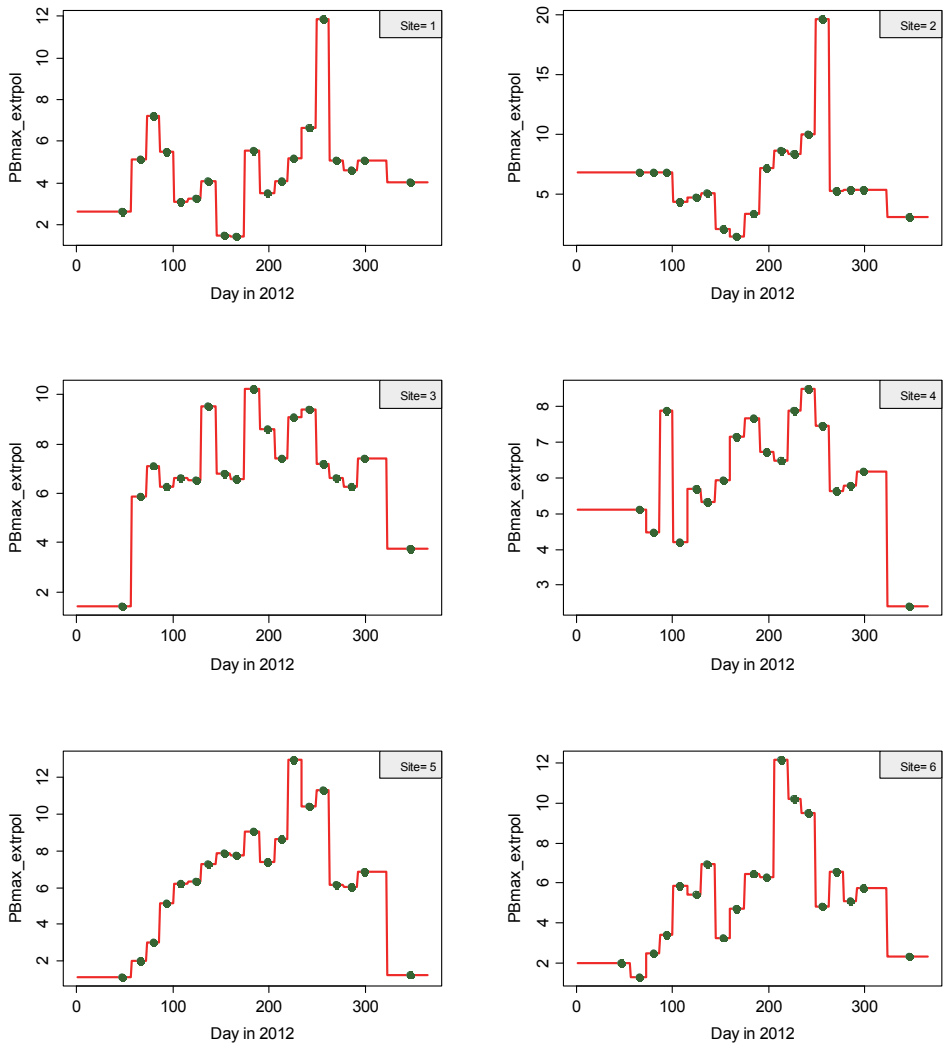

Figure 154 Primary production characteristic (P_{max}-values) at the six station in 2012, measured (dots) and inter/extrapolated (lines), following a rectangular method. P_{max} is as mg C mg^{-1} chla h^{-1}

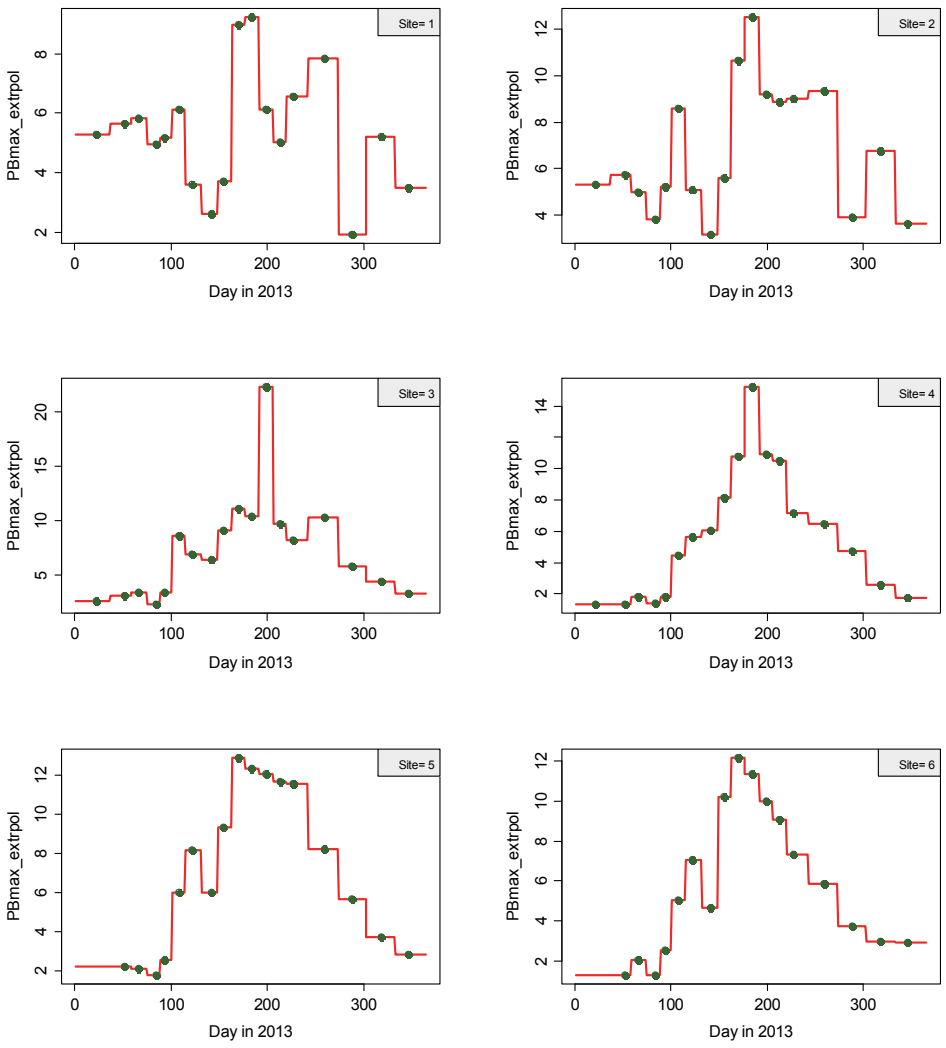

Figure 155 Primary production characteristic (P_{max}-values) at the six station in 2013, measured (dots) and inter/extrapolated (lines), following a rectangular method. P_{max} is as mg C mg^{-1} chla h^{-1}

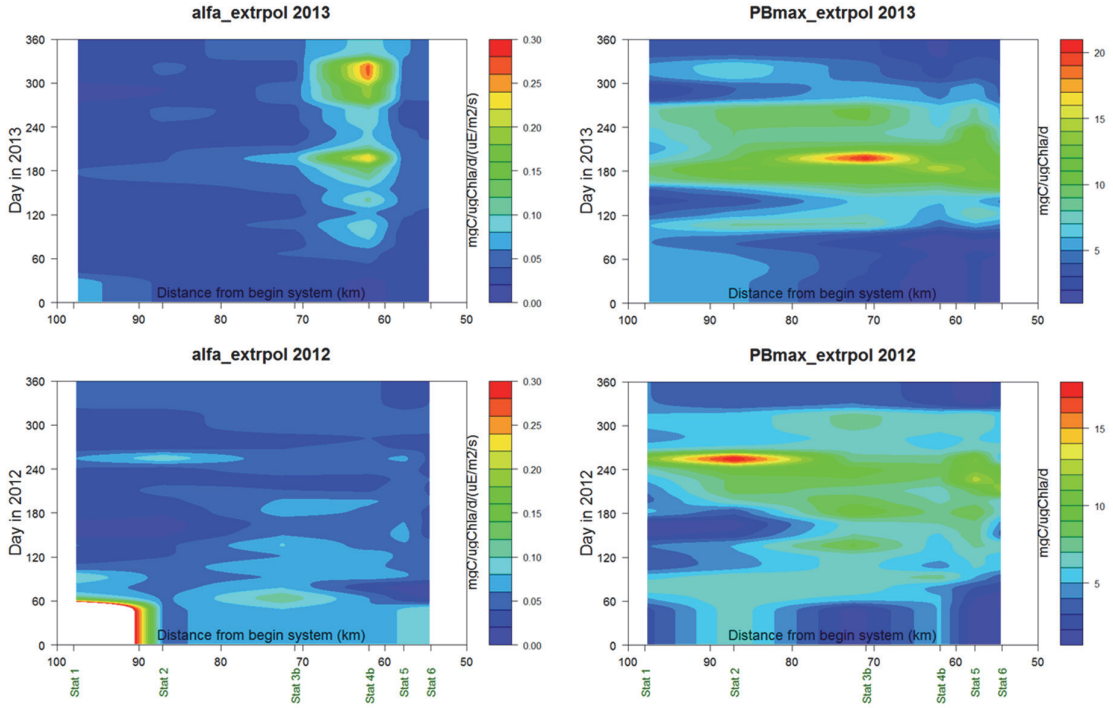

Figure 156 Contour plots for α (the initial slope of the PI-curve) and PBmax (the maximum of the PI-curve == the maximum productivity of the incubated samples mg C (mg Chla l^{-1})$^{-1}$. Upper: 2012, lower: 2013. Distance=0 at Herbrum (DE).

9.3 Pelagic primary production as computed for the field situation

Based on the Eilers-Peeters parameter values mentioned above, the light attenuation coefficients (section 8.18), chlorophyll-a data (section 8.9), local system depths (section 2.6) and the available weather data (section 4.15), water column profiles for light and production rate (in mg C layer^{-1} h^{-1}) are computed (Figure 157 shows an example for day 29 in 2012, field station 1). This was done for each hour in 2012 and 2013, for both parameter interpolation methods (rectangular and moving average). Adding up the production per layer gives the local production per m^2, that hour. Adding up all 24 hours gives the production per m^2 per day.

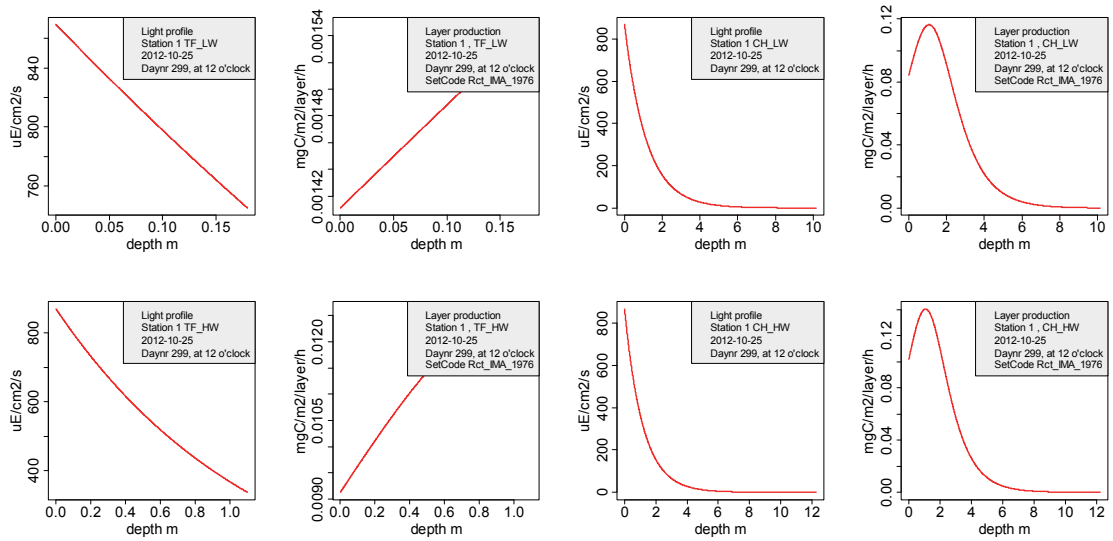

Figure 157 Light profiles and primary production profiles for station 1, day 299 in 2012, on tidal flats (TF) and in channels (CH), at high water (HW) and low water (LW).

Presentation of results comes with a "SetCode", that identify the conditions used: first the interpolation method applied: a rectangular interpolation ("Rect") or on a moving average method ("MovAvg"), than the basis for the light attenuation coefficient: "IMA"= the Kd-data as measured in the water column (the case "Colij"= the data used by Colijn & De Jonge, 1984 was not used at this moment), and finally the year of the weather conditions used:2012 or 2013 for the actual condtions, 1978-1980 for the conditions in the years of the Colijn & De Jonge (1984).

This production pattern is shown in (Figure 158 and Figure 159; for 2012 and 2013 respectively). Summation per year gives the yearly production for each site (Figure 160).

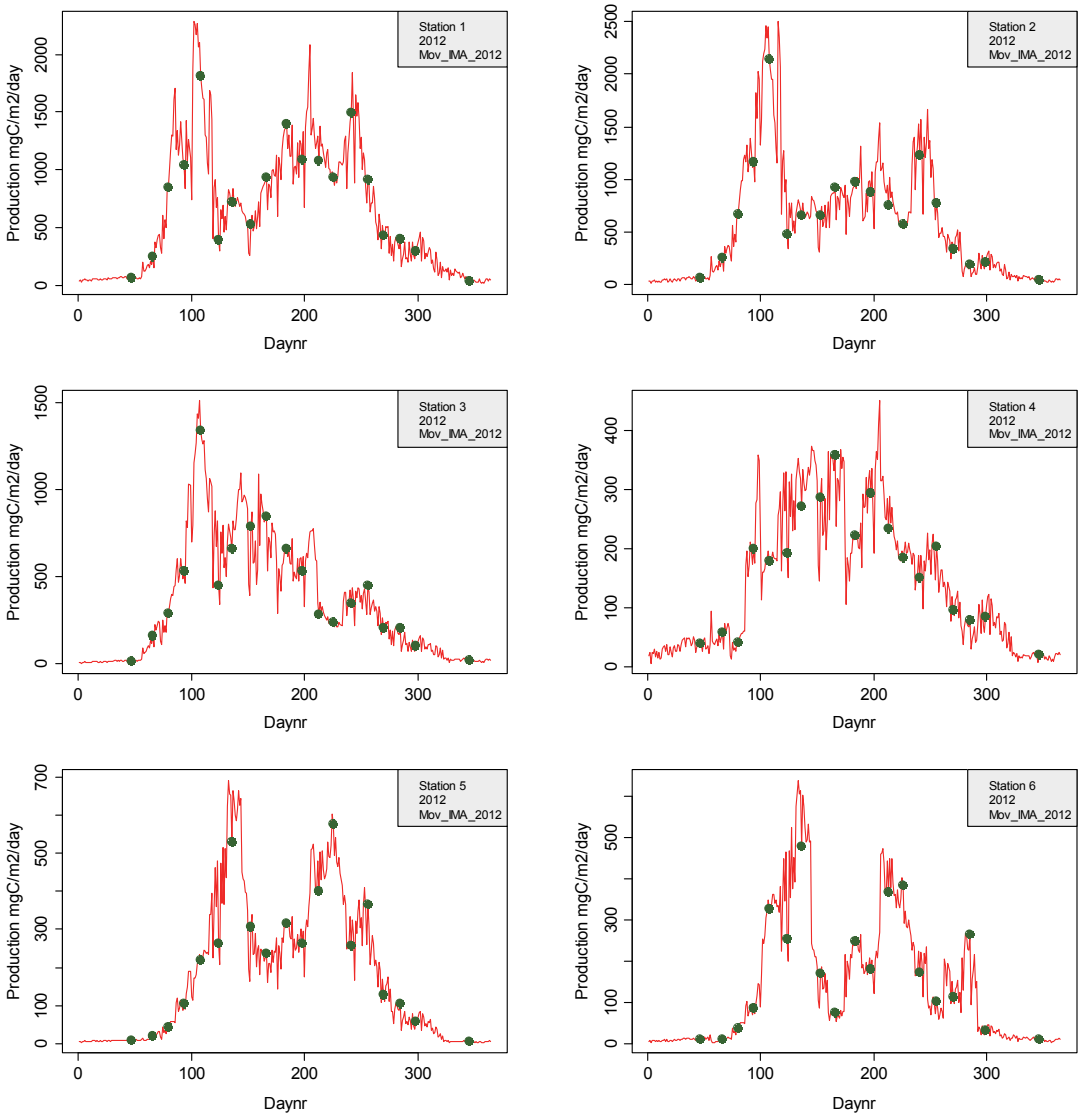

Figure 158 Computed gross primary production (mg C m^{-2} d^{-1}) for all stations in 2012, during high water in channels. Expressed as mgC m^{-2} day^{-1}. Chlorophyll-a, K_d- and Eilers-Peeters values all interpolated following a moving average method. K_d-values used are those from the IMARES-measurements. Dots mark the sampling days.

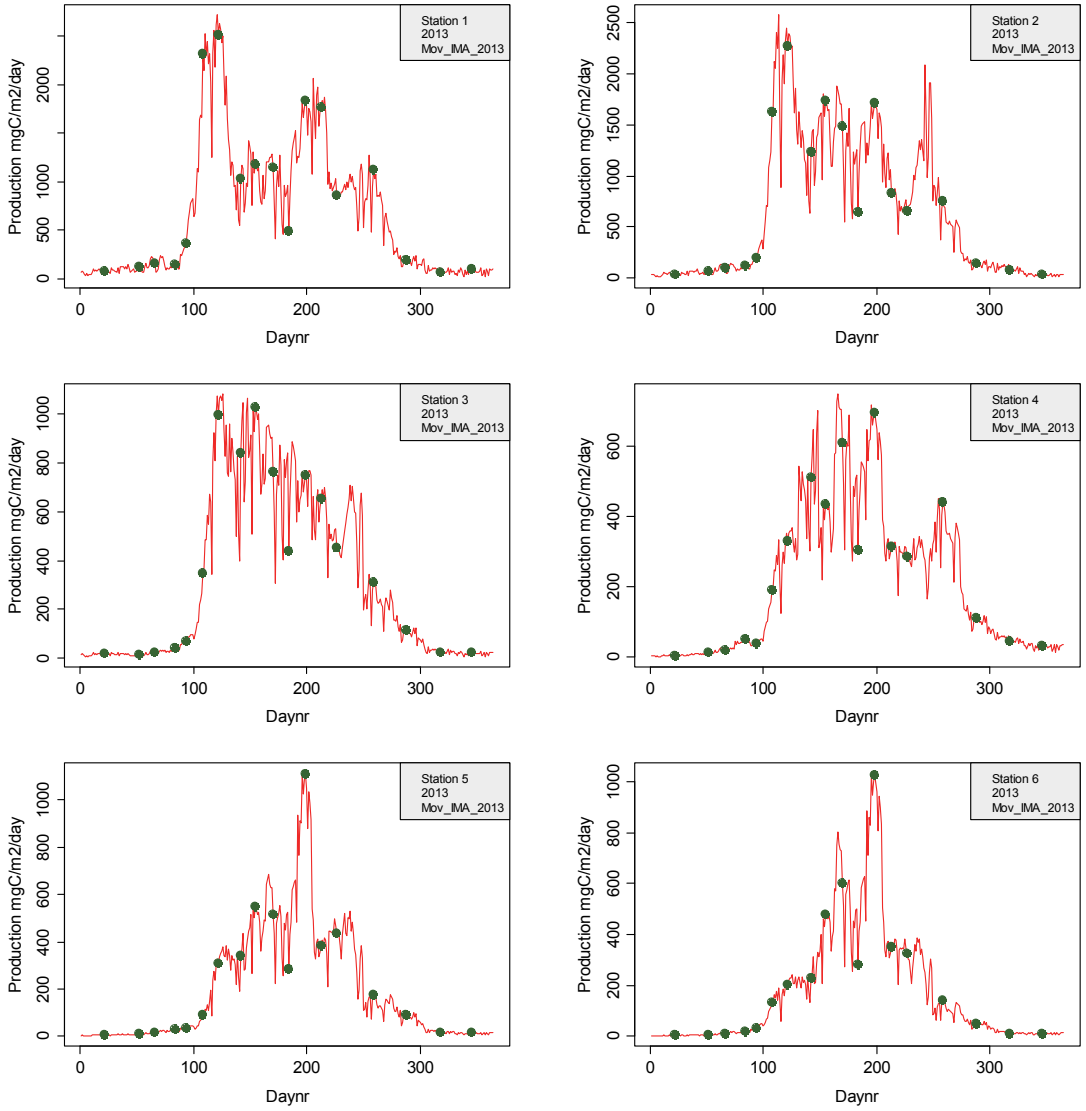

Figure 159 Computed gross primary production (mg C m^{-2} d^{-1}) for all stations in 2013, during high water in channels. Expressed as mgC m^{-2} day^{-1}. Chlorophyll-a, K_d- and Eilers-Peeters values all interpolated following a moving average method. K_d-values used are those from the IMARES-measurements. Dots mark the sampling days.

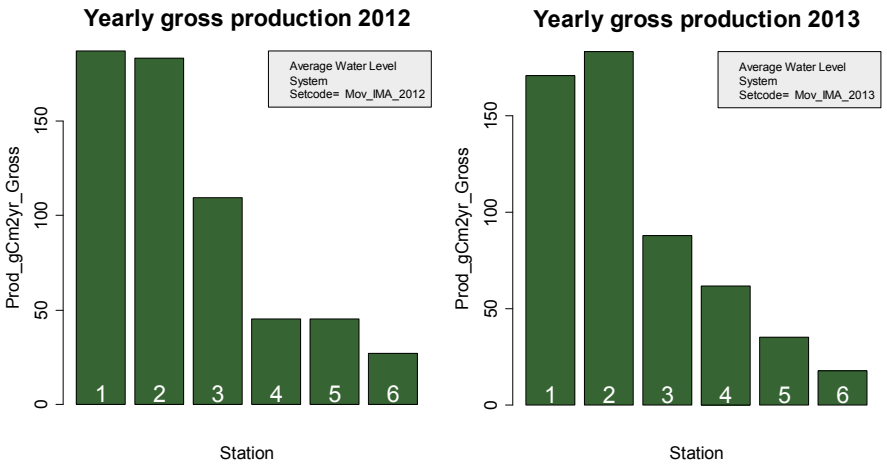

Figure 160 Computed yearly gross production in 2012 and 2013 in each of the six compartments (see Figure 16), expressed as g C m^{-2} y^{-1}.

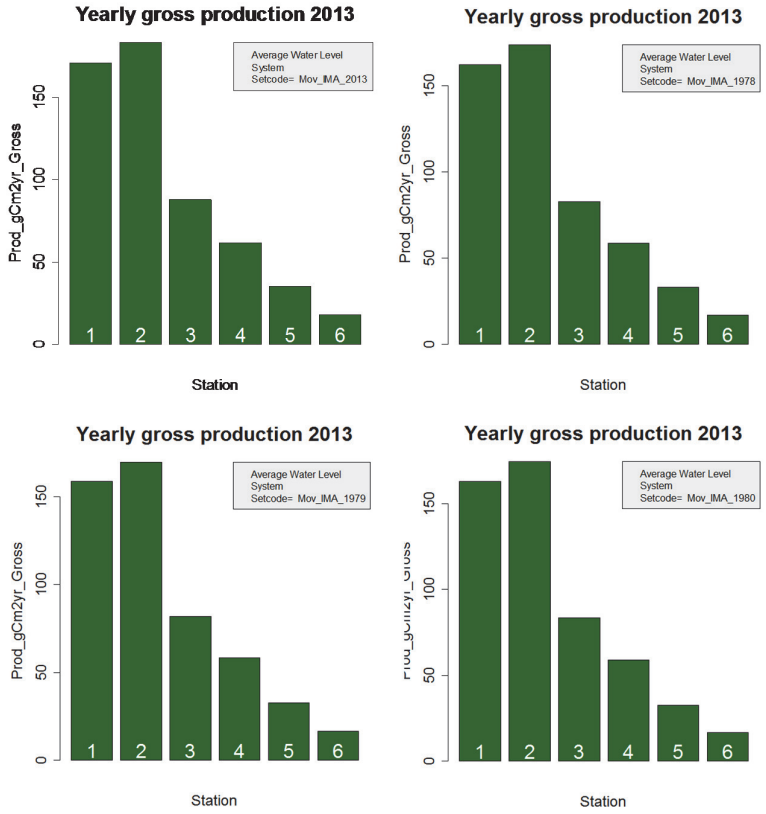

Figure 161 Yearly gross pelagic primary production for the whole system with 2013 parameters. Upper left: weather conditions for 2013; upper right: for 1978; lower left: for 1979 and lower right: for 1980. There are minor differences in absolute values.

Together with the areas for the tidal flats and the channels (Table 6), the average gross production (Figure 160) per compartment can be computed. In Figure 161, also the results of the other computations (both interpolation methods, weather data for the Colijn years 1978-1980 instead those for 2012 and 2013) are summarized.

The total production per compartment is presented in Figure 162. The geographical data (tidal flat and channel areas) are the same as were applied by Colijn(1983). From Figure 162 it is clear that the outer area (compartment 1) contributes the largest part to the overall system production. This is a consequence of the production m^{-2}, and of the size of the area.

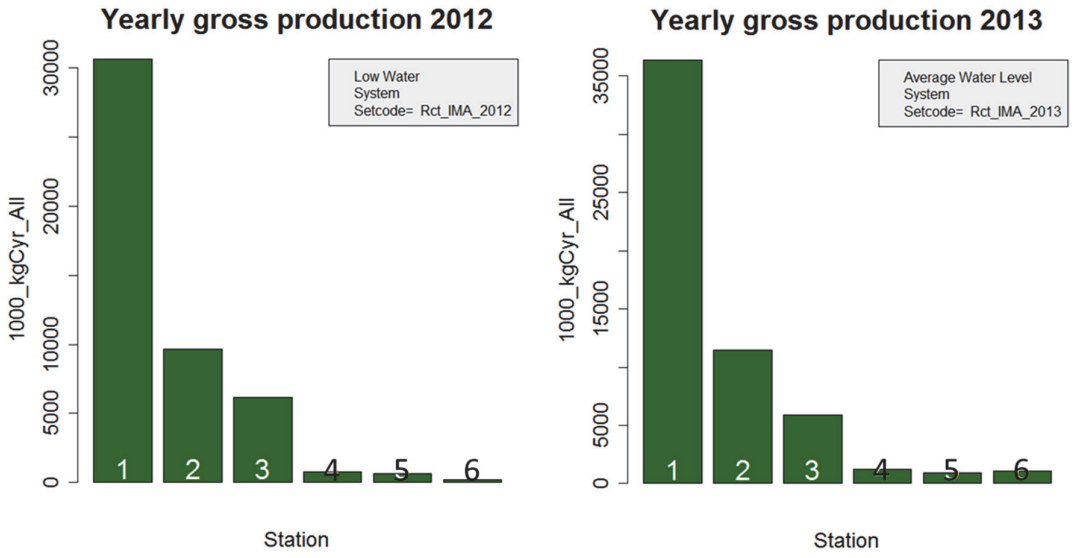

Figure 162 Pelagic contribution of each of the six distinguished compartments to the whole Ems-Dollard estuary.

Total production as average is presented in Figure 163, including results when radiation data from 1978-1980 are applied, instead of those for 2012 and 2013, respectively.

Note that we did not include respiration terms, which also may be more important in the deeper outer area.

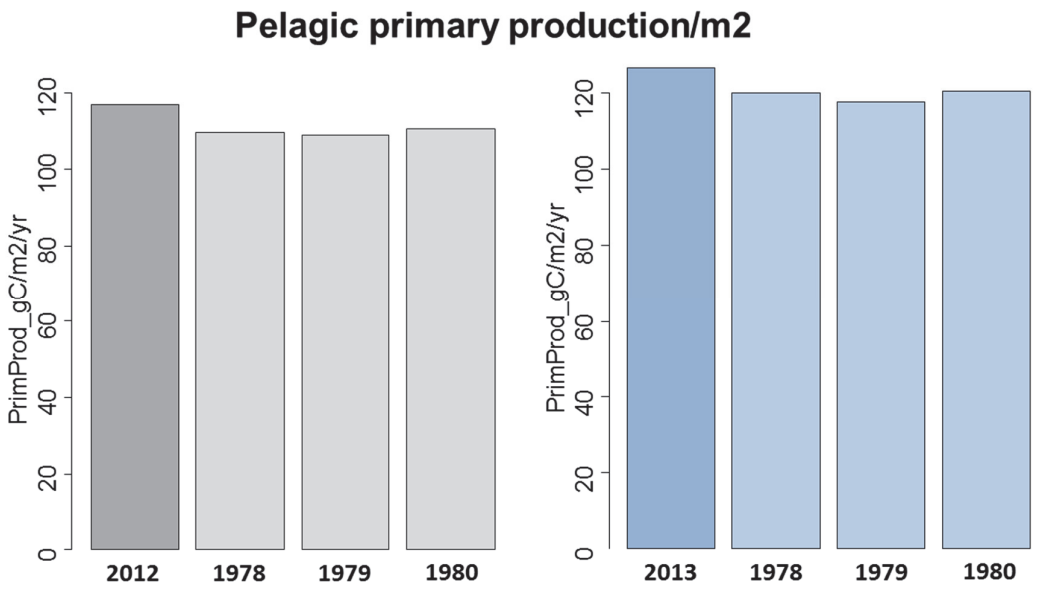

Figure 163 Summary of primary production computations; as average gross primary production (g C m-2 y-1). for the whole Ems-Dollard system. Left: for 2012, right: for 2013. Underlying parameters were interpolated using a rectangular technique. Results based on moving averages are practically the same. Computations for 2012 and 2013 have also been done with weather conditions for the Colijn years 1978-1980 (the three lighter shaded bars).

9.4 Mass specific pelagic productivity

Above, the production at each sampling station plus that for the whole system has been presented. The question now is what the (average) specific phytoplankton growth rate is (or: first order gross ^{14}C uptake rate constant, P_{max_spec}). See also section 4.12.2 for the computation method. A better name for specific phytoplankton growth rate is: first order gross ^{14}C uptake rate constant (d^{-1}). Note that 'uptake' is better than 'growth' since we measured the *uptake* of ^{14}C.

For 2013, we have data –estimated from the bio volumes measured by Koeman and Bijkerk (Wanink et al, 2014)- on organic C in phytoplankton. For 2012, these data are absent, and the only way to come to an estimate is by assuming a fixed ratio between chlorophyll-a and phytoplankton carbon.

For 2012 we used the relationship sketched in Figure 35 to estimate organic-C from chlorophyll-a data (conversion factor then is: 1 mg Chla ≈ 38 mg phytoplankton-C).

For 2013, we have algae C-concentrations from the Koeman & Bijkerk volume data (section 4.8). Next, we have chlorophyll-a data from the Koeman & Bijkerk-data, ánd from the AOA-sensor, ánd from the fluorometer analysis. Thus, there are three results for this specific production. The latter two are assumed to be the most reliable ones, since these are based on measurements; the Koeman & Bijkerk values are based on chlorophyll-estimates. At the other hand, the "KB_Chla" is based on the same data that provide algal C-biomass; a good reason to keep these results included.

Results for 2012 are presented in Figure 164 and for 2013 in Figure 165 and Figure 166 (the same graphs but with adapted scales).

Both the 2012 and 2013 –results are also corrected for temperature, according to the equation by Eppley (1972, eq. 14a,b section 4.12).

In all cases, it should be kept in mind that the chlorophyll-a analyses in the laboratory results probably are about 30% too low (section 7.13.6). This, however, does not affect the specific gross growth rates (or first order gross ^{14}C uptake rate constants) since both the production results as the computed rate constants are based on the same chlorophyll-a data.

9.4.1 2012 mass specific gross uptake rates (or: first order gross ^{14}C uptake rate constant)

The graphs in Figure 164 are an almost similar for stations 1 and 2; stations 3-5 have similar characteristics, and station 6 is an intermediate case. Low specific growth rates at stations 1 and 2 must be related to the low nutrient concentrations at that moment (section 8.4): especially phosphorus. Low nitrate values occur later in the year (after day 200), and thus these seem to be not related to the specific gross growth rates. The relationship with ammonium, having low values around 120, is not clear. The specific growth rates patterns presented here resemble the Pmax-patterns a lot (Figure 154).

The values found for these specific growth rates are high; usual value are around 2-3 (see e.g. Lampert & Sommer, 1993), but it has to be noticed that the phytoplankton C-concentrations were estimated from the chlorophyll-a concentrations; this conversion has a considerable uncertainty (see e.g. Alvarez-Fernandez & Riegman, 2014). Thus, the pattern is more important than the absolute values found.

9.4.2 2013 mass specific gross uptake rates (or: first order gross ^{14}C uptake rate constant)

There are a few striking results. First, there is a considerable difference between the three results.

The far most striking result is that the maximum values found for the specific productivities –or, what a better name is: maximum gross primary production rate coefficients- are far above the usually values of 2-3 (see e.g. Lampert & Sommer, 1993).

When using chlorophyll-a data from the fluorometer analyses, minimum values (temperature corrected) are found between days 100-150, at all stations, except station 3. Here, an extremely high value has been found; to be contributed to a high Pmax (from the ^{14}C-incubation), coupled with a low chlorophyll-a value, and a low phytoplankton-C content (that was derived from the Koeman & Bijkerk data). For stations 1 and 2, this pattern also appears more or less when chlorophyll-a data derived from the cell volumes are applied; the other stations 3-6 do not really show low values. When using AOA-chlorophyll-a data, results show a short period of low values around day 100 (all except station 6) and around day 150 (stations 3-5). As in 2012, this is mostly likely related to low nutrients values. In 2013, low P and Si-values appear after day 120, at the same time also nitrate and ammonium drop

to relatively low values. P and Si show an increase afterwards; P does not have low values anymore after day 180, and Si stays low at stations 1 and 2, but not at the other stations.

Figure 164 Specific maximum productivity (or: first order gross ^{14}C uptake rate constant, P_{max_spec}) of Ems-Dollard phytoplankton in 2012; P_{max} from incubations transformed to field situation, and divided by the concentration of phytoplankton carbon present in the water column. Phytocarbon content was estimated by assuming a phytoplankton C : chlorophyll-a- ratio of 38 (mg C/mg chla). Mind the different Y-axis scales. Red results: corrected for temperature, blue: uncorrected.

Figure 165 Specific maximum productivity (or: first order gross ^{14}C uptake rate constant, P_{max_spec}) of Ems-Dollard phytoplankton in 2013; PB_{max} form incubations transformed to field situation, and divided by the concentration of phytoplankton carbon present in the water column. KB-chla means that for the blue line, chlorophyll-a data have been used that were estimated from the phytoplankton volumina as determined by Koeman & Bijkerk (Wanink et al, 2014); Koeman & Bijkerk did not give any chlorophyll-a data themselves. AOA-Chla means that for the red line, chlorophyll-a data from the AOA-sensor in the PocketBox have been used. Chla-lab means that for the green line, chlorophyll-a data from the fluorometer analyses, done at the same samples that were used for the ^{14}C-incubations, have been used. The latter two are assumed to be (much) more reliable, since it concerns direct chla-measurements instead of estimates from biovolumina.

Figure 166 As Figure 164, now 2013. Specific maximum productivity (or: first order gross ^{14}C uptake rate constant, P_{max_spec}) of Ems-Dollard phytoplankton in 2013; P_{max} from incubations transformed to field situation, and divided by the concentration of phytoplankton carbon present in the water column. Phytocarbon content was estimated by assuming a phytoplankton C : chlorophyll-a- ratio of 38 (mg C/mg chla). Mind the different Y-axis scales. Red results: corrected for temperature, blue: uncorrected.

9.5 Comparison with Colijn (1984)

Pelagic primary production data are mainly available from Colijn (1984). Other sources (Rijkswaterstaat, 1985; Essink & Esselink, 1998) refer to this same source. Also for model tuning (Baretta & Ruardij, 1988) the same data were used. Thus, there is little extra information available.

It has to be noted that the data Colijn presented here concern only the channels, thus not integrated to the whole area (tidal flats, and shallow subtidal areas).

In Figure 167, depth integrated channel primary production for 2012 and 2013 are plotted, together with results from Colijn (1983). Production data are also computed based on the present parameters, and 1978-1980 solar radiation. Relative differences are listed in Table 37.

From Figure 167 it follows that there is only a slight difference between the present results (for 2012 and 2013), and those for 1978. For 1979 and 1980, Colijn found much higher primary production values, especially in the outer areas 1 and 2. Colijn (1983) states that values for 1978 are low because of low chlorophyll-a data in that particular year.

Primary production found in 1978-1980 by Colijn, and the one that would have been found with today's parameters plus 1978-1980 solar radiation data is listed in Table 37. The conclusion then is that primary production conditions in Colijns years (the combination of production parameters and chlorophyll-a content) were better (to much better) than nowadays. This is especially the case for 1979 and 1980; in 1978 conditions were more or less similar.

Average primary production found for the years 1978-1980 by Colijn, and the one found now, for each station, is presented in Figure 168. Differences are largest at station 1, 2 and 4.

It is obvious that the highest production (in terms of gross production) sites can be found in the outer Ems area, whereas the lowest production is found in the Dollard area. Differences between 1979-1980 and now are large, between 1978 and now are minor. Results differ per station, but in all cases production at stations 1 and 2 now is lower than it was in 1979-1980. This is also the case at station 4 and 6 (only 1979 data available), but varies between lower and the same for stations 3 and 5. But, it must also be realised that Colijns results for 1978 are much lower than his own for 1979 and 1980, and are similar to our results. This implies that year-to-year variations are large (a well-known phenomenon) which makes it hard to draw a clear and definitive conclusion.

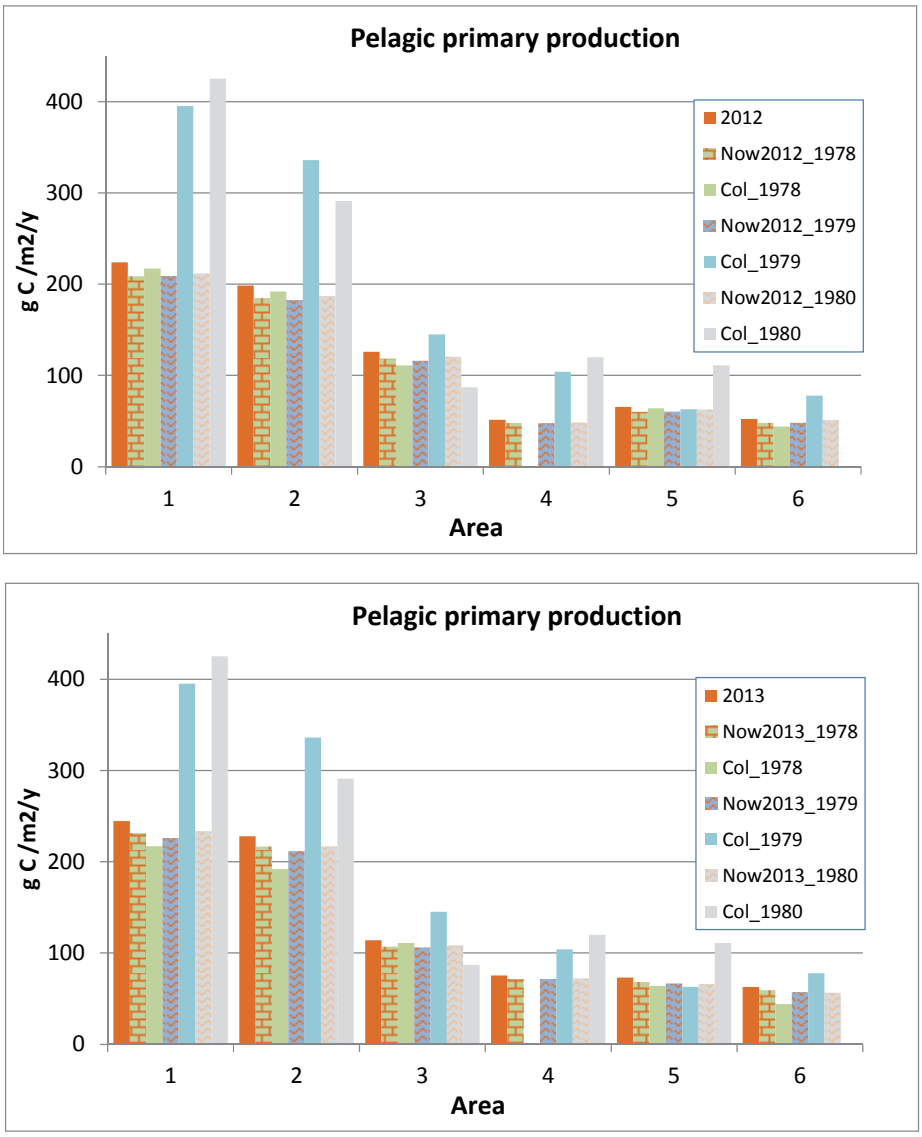

Figure 167 Summary of primary production values for each site: computed for the present situation (2012 (upper) and 2013 (lower), data by Colijn (1983) for the years 1978-1980, and values computed based on the present parameter values, and weather conditions for 1978-1980. See also Table 37. Values are depth integrated productions at each site, thus in the channels.

Table 37 Computed primary production for the channels in the Ems-Dollard area (2012 and 2013, "Now"), data computed with present parameters and weather conditions for 1978-1980 ("Now,weather conditions from.."), and Colijn data (Colijn, 1983). Last three columns give the ratio between the values computed now and those found by Colijn for 1978-1980. Greenish: now=higher, orange/reddish: now=lower/much lower, grey: between 0.9 and 1.1. For comparison between present results and Colijn results, see also Figure 168.

2012	Now, weather conditions from:				Colijn (1983, Chapt IV, table X)			Ratio Now(with 1978-1980 weather)/ Colijn data		
Area	2012	1978	1979	1980	1978	1979	1980	1978	1979	1980
1	224	209	209	212	217	395	425	0.96	0.53	0.50
2	198	185	182	187	192	336	291	0.96	0.54	0.65
3	126	118	116	120	111	145	87	1.06	0.80	1.40
4	51	48	48	49		104	120		0.47	0.40
5	66	60	60	63	64	63	111	0.94	0.96	0.56
6	52	48	48	51	44	78		1.10	0.62	

2013	Now, weather conditions from:				Colijn (1983, Chapt IV, table X)			Ratio Now(with 1978-1980 weather)/ Colijn data		
Area	2013	1978	1979	1980	1978	1979	1980	1978	1979	1980
1	245	231	226	233	217	395	425	1.06	0.57	0.55
2	228	217	212	217	192	336	291	1.12	0.63	0.75
3	114	107	106	108	111	145	87	0.96	0.73	1.25
4	75	72	72	72		104	120		0.69	0.60
5	73	68	67	66	64	63	111	0.94	0.96	0.56
6	63	59	57	57	44	78		1.10	0.62	

2012 g C m^{-2} y^{-1}

Station	PP_now 2012	Colijn 78-'80	Colijn min	Colijn max
1	224	346	425	217
2	198	273	336	192
3	126	114	145	87
4	51	112	120	104
5	66	79	111	63
6	52	61	78	44

2013 g C m^{-2} y^{-1}

Station	PP_now 2013	Colijn 78-'80	Colijn min	Colijn max
1	245	346	425	217
2	128	273	336	192
3	114	114	145	87
4	75	112	120	104
5	73	79	111	63
6	63	61	78	44

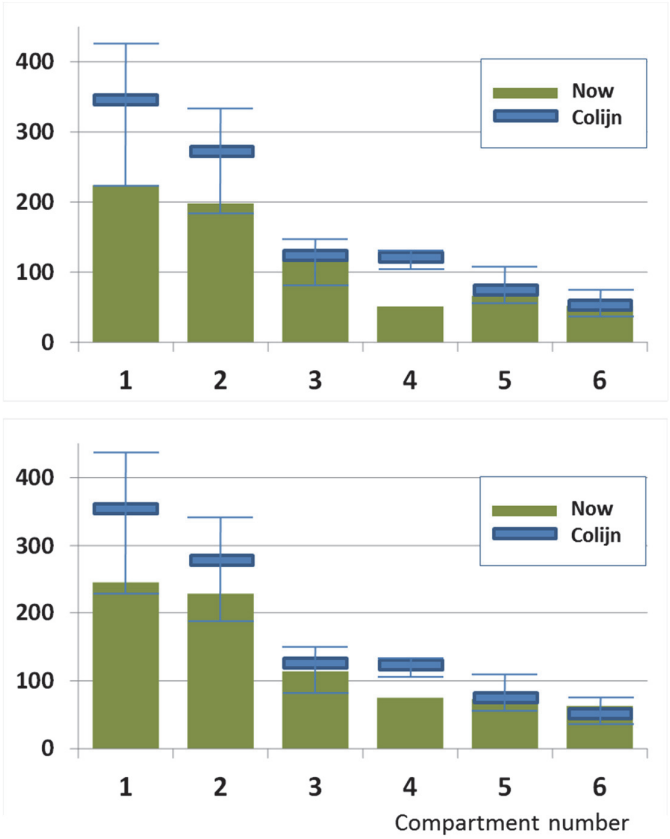

Figure 168 Average water column primary production values for Colijns 1978-1980 research and the present research, for each station (thus: channel values). Colijn results with average, minimum and maximum values.

9.6 Possible causes of the observed differences between the late seventies and present

Next question to be answered is whether changing environmental conditions attribute to the changes seen in the primary production data. Most prominent candidates are temperature, nutrient concentrations, chlorophyll-a content and the water column light climate.

9.6.1 Conditions at station 1 (Huibertgat)

From the Rijkswaterstaat monitoring data series (RWS, 2013), the yearly averaged values at Huibertgat Oost (Figure 23) for dissolved inorganic phosphorus (ortho-P), silicate, chlorophyll-a, temperature, Secchi-depth and suspended solids are presented in Figure 169 and Figure 170. It is

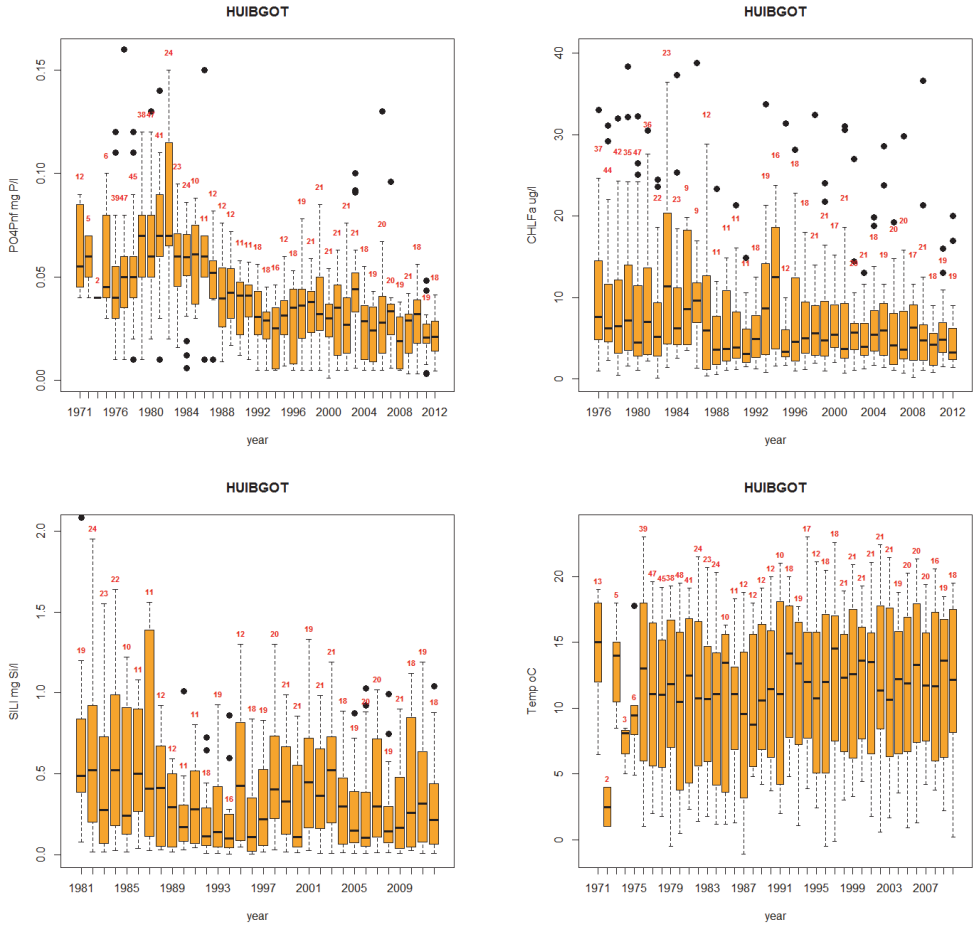

Figure 169 Yearly average values for dissolved ortho-phosphate, silicate, temperature and chlorophyll-a, site HuibertGat Oost. Data from the MWTL-monitoring data series by Rijkswaterstaat (RWS, 2013). Note that the years differ per graph.

clear from these figures that ortho-phosphate concentrations dropped drastically (presently less than half the values of the late seventies). At the same time, chlorophyll-a contents dropped, and also silicate concentrations found now are below those from the late 1970-s. All these three may cause a

decrease of primary production; only the increase in temperature found has an opposite effect. A 10% degree temperature rise also causes an almost 10% increase in primary production; according to the Eppley–equation (1972), mentioned in section 9.4. This approximation is valid as long as temperature differences are not too large.

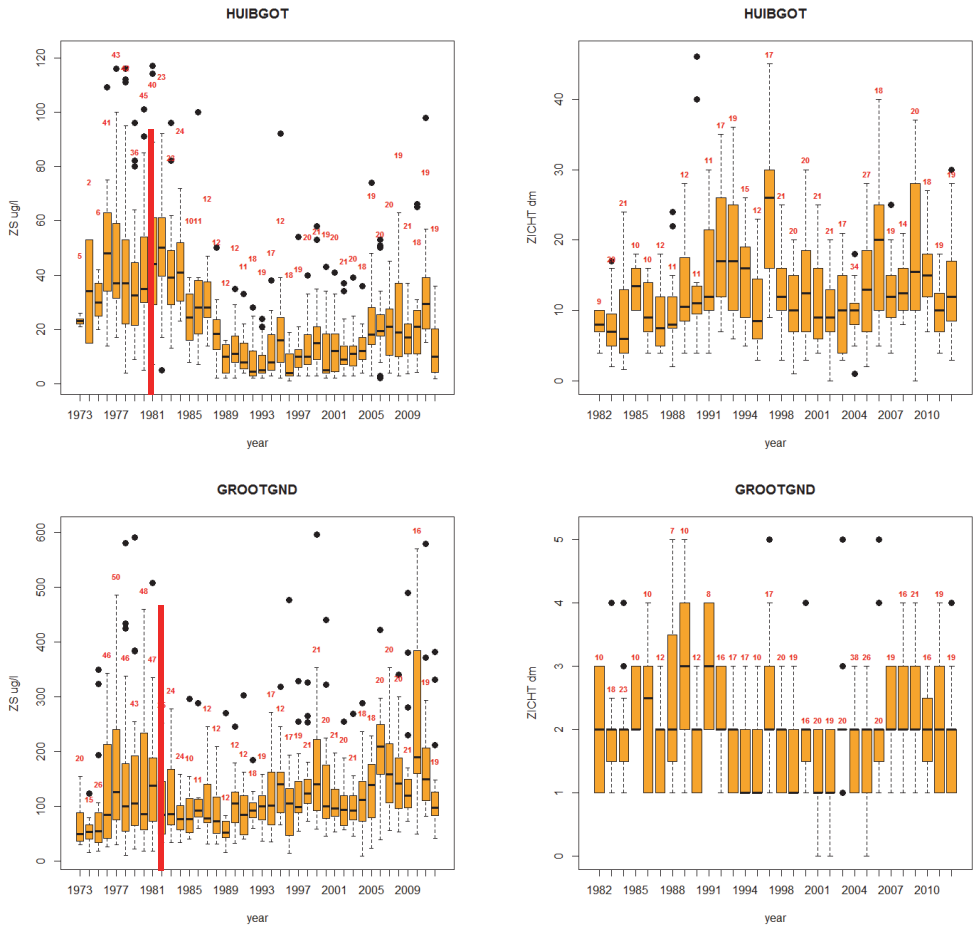

Figure 170 Yearly average values for suspended solids (left) and Secchi-depth (right) at station HuibertGat Oost (upper) and GrooteGat Noord (lower). Data from the MWTL-monitoring data series by Rijkswaterstaat (RWS, 2013). Note that the years differ per graph. Start of right graphs is marked in left graphs by a red line.

According to Figure 170, the water column light climate improved. Present RWS year averages are around 20 mg solids l^{-1}. These values can be compared to the one resented in Figure 105 and Figure 106, these are also in the range 20-25 mg solids l^{-1}.

It must be noted that ortho-phosphate concentrations did *increase* a lot during the Colijn-research, a possible cause for Colijn's observations on increasing chlorophyll-a content of the water; but this is not a very sound conclusion because of the feedbacks that exist in the ecosystem: an increase in nutrient concentration does *not perse* induce an increase in chlorophyll-a content.

9.6.2 Conditions at station 6 (Groote Gat Noord)

From the Rijkswaterstaat monitoring data series (RWS, 2013), the yearly averaged values at Groote Gat Noord (Figure 23) for dissolved inorganic phosphorus (ortho-P), silicate, chlorophyll-a, temperature, Secchi-depth and suspended solids are presented in Figure 170 and Figure 171. It is

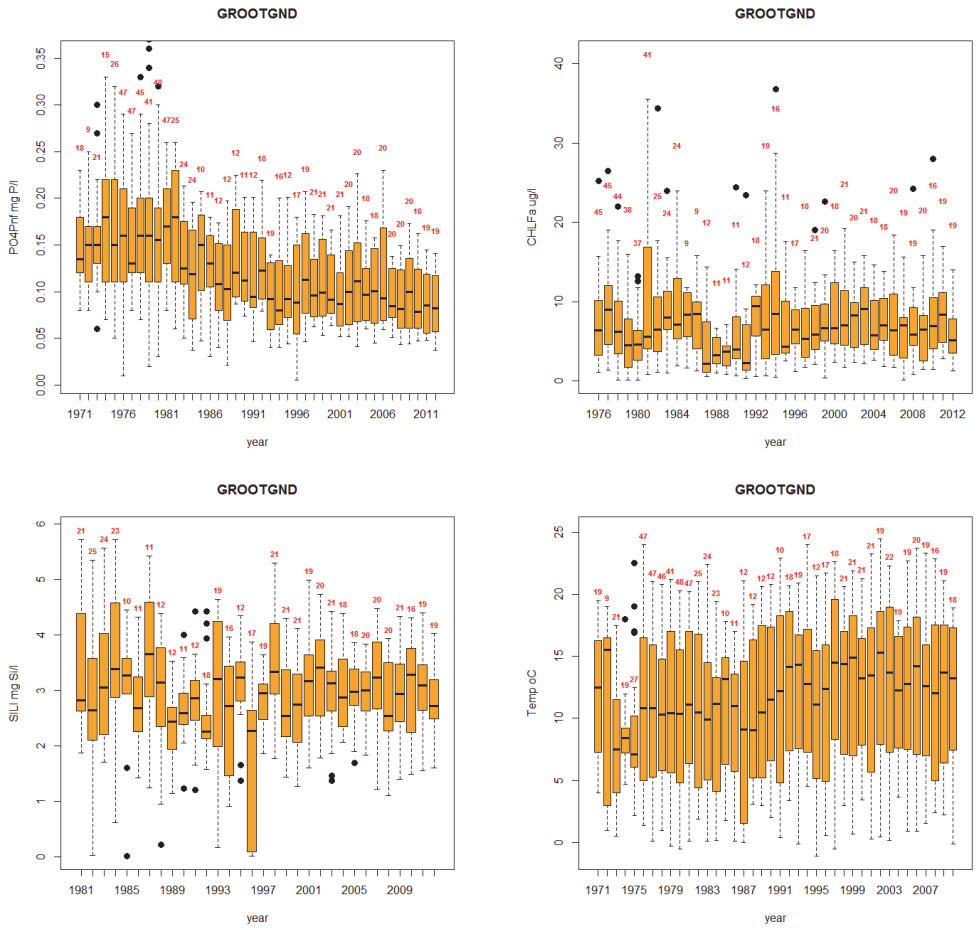

Figure 171 Yearly average values for dissolved ortho-phosphate, silicate, temperature and chlorophyll-a, site Grootegat Noord. Data from the MWTL-monitoring data series by Rijkswaterstaat (RWS, 2013). Note that the years differ per graph.

clear from these figures that ortho-phosphate concentrations steadily decreased, although a bit less pronounced than at Huibertgat Oost. At the same time, chlorophyll-a contents stayed more or less the same, as did the silicate concentration. Our results (see section 8.4) indicate that nutrient effects probably are minor at the most inner stations, and thus, primary production may only be affected by the increase in temperature found. According to Figure 170 suspended matter content increased a lot, and consequently, Secchi-depth decreased (although differences between 2 or 3 dm Secchi-depth are hard to measure). Thus, at Groote Gat Noord, temperature rise may have caused an increase in primary production, and the increased water column attenuation coefficient will have an opposite effect.

Contrary to the situation at Huibertgat (see previous section) no ortho-phosphate increase was observed from 1978-1980. The differences Colijn observed in primary production at that site probably cannot be assigned to a changed phosphate-concentration.

9.6.3 A possible effect of nitrate

In the previous section, effects of phosphate and silicate on the primary production results was discussed. Nitrate may have an effect as well. But, however nitrate concentrations dropped in the outer areas Figure 172, changes are less prominent as the drop in phosphate concentrations; a picture that can be seen everywhere in the Wadden Sea (Brinkman, 2008). In the inner areas, nitrate +nitrite contents staid (more or less) the same or even increased a bit. It is less likely that nitrate is seriously limiting phytoplankton growth rates. The only period that this might be the case is the

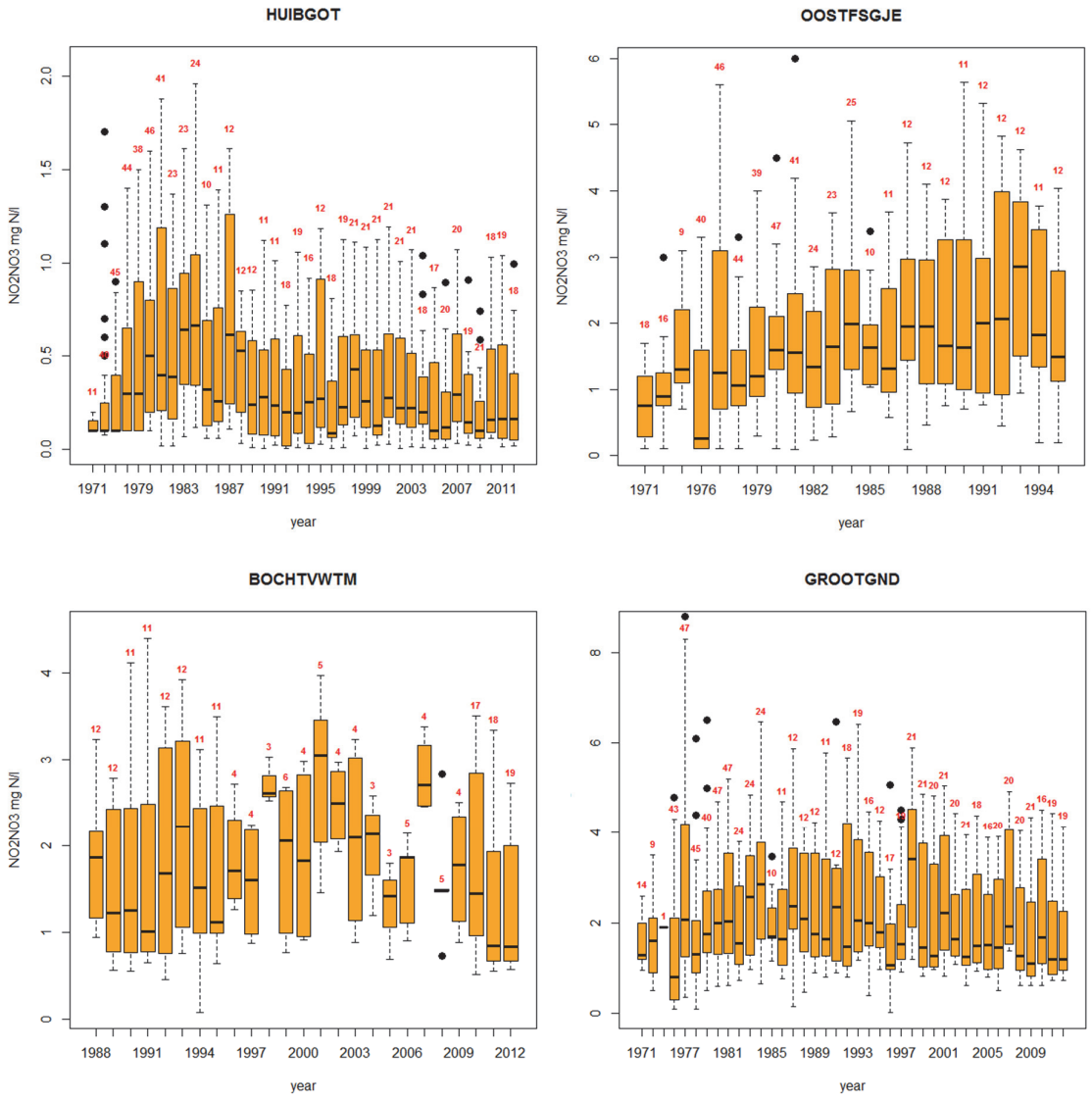

Figure 172 Yearly average nitrate concentrations in the Ems-Dollard estuary. Data in mg (NO_3+NO_2)-N l-1. Data source: Waterbase (2014).

period July-August at stations 1 and 2. Then there is a short moment that *and* nitrate concentrations are low (see also Figure 90) *and* the temperature corrected specific growth rate is low (Figure 166). However, this stays at the level of *possible* limitations; we did not do experiments that can confirm this.

Looking back at the end of the seventies, it is striking that in those days nitrate concentrations increased a lot between 1978 and 1980, in the Dollard area, Oostfriese Gaatje and Huibertgat Oost (station 6, 3/4 and 1). It might well have been that in those days nitrate was a more important candidate for limiting phytoplankton growth rates than phosphate; a situation that has changed later on. There have been many discussions and papers have been written on this subject, without a clear result, see e.g. De Jonge & Essink (1991,1992).

9.7 Effect of changing water column light attenuation coefficient

The effect of a changing light attenuation coefficient K_d in the water column was tested by simply repeating all field production computations, but assuming a 60% and a 140% value of K_d.

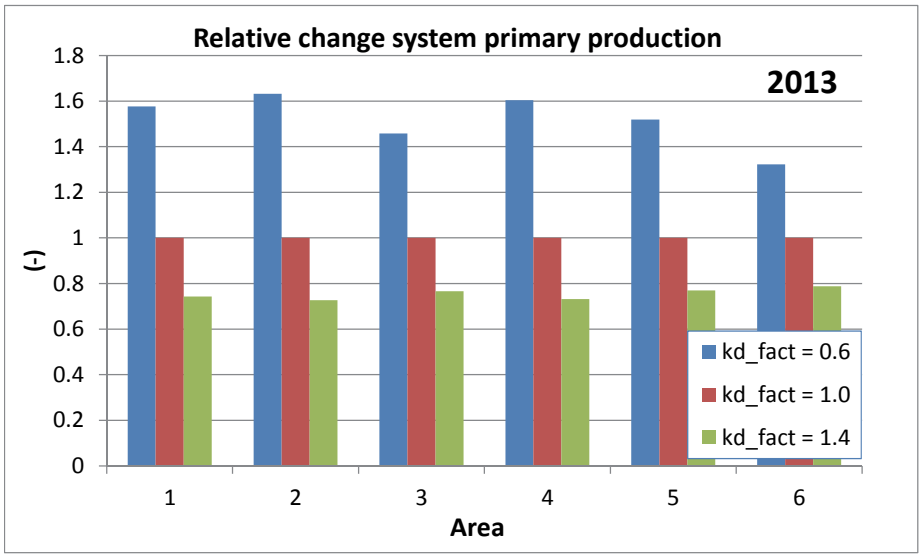

Figure 173 Effect of a changing light attenuation coefficient. 2013 data only.

Results are shown in Figure 173, for 2013 only. It is clear that effects are largest in the outer areas, but differences between the areas are not very large. In the inner areas, where light penetration in the water column is low, effects are smallest.

It must be kept in mind that the role of nutrients is not incorporated in this graph. If nutrients are limiting e.g. in springtime, a changing underwater light climate will have much less effect than presented in Figure 173.

9.8 Conclusions

It is obvious that primary production in the Ems-Dollard area as measured in 2012 and 2013 was considerably lower than in 1979 and 1980, and about the same as it was in 1978. It is also clear that in the outer area (stations 1 & 2) absolute differences are largest. In the inner areas, absolute differences are much smaller and it also differs per site. It also must be concluded that year-to-year differences may be large, a well-known phenomenon in ecosystems. De Jonge & Essink (1991,1992) already stressed the importance of river discharges for primary production. They mentioned yearly discharges of the Ems river, but it should also be realised that the timing of the river runoff may be important: a large discharge in winter has a different effect than a large late springtime discharge.

There are three possible explanations left for the differences found in the outer areas:

i: lower chlorophyll-a content in the water column at site 1 compared to 1979-1980

ii: decreasing nutrient availability in the outer areas seems to be the most likely explanation for the lower primary production found there, since in 2012 and 2013 light attenuation was less than in the 1978-1980 period. A detailed data study is needed to come closer to the quantitative effect nutrient supply; a part of it can be done with modelling, including monthly or even weekly river runoff data for the Ems river and the Dutch Westerwoldse Aa.

iii: major occurrence of *Phaeocystis pouchetii* (now: *P. globosa*) as highly productive alga in 1979-1980, opposite to 2013 when *Phaeocystis* did occur but not dominantly (see section 8.10). This may also be an effect of a lower eutrophication status.

At station 4, lower present production can be explained by the increased turbidity.

9.9 Conclusions for this chapter: what have we learnt?

9.9.1 Chapter content?

The pelagic primary production as computed for the Ems-Dollard estuary for the years 2012 and 2013 is presented. Also a comparison with results from Colijn (1983) is made, and possible reasons for observed differences are discussed. Effects of a changing turbidity were presented.

9.9.2 What went OK?

Computation of the water column primary production at each sampling site and each sampling day was well possible because of the available primary productivity parameters, the light attenuation coefficient and weather conditions. Extrapolation to a whole system primary production was possible because morphological data were available, as were hourly weather data.

The use of weather data from 1978-1980 made it possible to compute primary productions based on the present primary productivity parameters and the meteorological conditions in the period Colijn did his research.

9.9.3 What needs improvement and what are main recommendations for future work?

The research now (equal to Colijns research) lacks information on the effect of nutrients. This makes

it hard to identify the reasons for observed differences. Also, temperature effects have not been investigated, not now nor by Colijn; a second suggestion to pay attention to in future.

Last but not least: model studies are required that include directly the effect of changing river runoff, nutrient discharges and feedback mechanisms that exist in the Ems-Dollard ecosystem (as in any ecosystem) like the presence of grazers in the system.

10 Results-4: benthic primary production

10.1 What is in this chapter?

All benthic primary production results are presented. First (section 10.2) the results of the ^{14}C-incubations are given. In section 10.3, the computation of the gross primary production of separate sites is outlined, and in 10.4 benthic primary production for the whole system is presented including a comparison with previous results (Colijn & De Jonge, 1984). In section 10.5, mass specific phytoplankton growth rates are given. Section 10.6 is a discussion and finally, in section 10.7 contains remarks (what have we learnt), and some recommendations are given.

10.2 Benthic primary production parameters

First, results of the ^{14}C-measurements are presented. The Eilers-Peeters formula contains the a,b and c-parameters, in which c governs the slope of the PI-curve at low light intensities, b gives the sensitivity to light, and a expresses importance of light inhibition (section 4.12): Figure 174 - Figure 176.

The slope of the PI-curve at I=0 is α (mg C (mg Chla)$^{-1}$ h^{-1} (µE cm^{-2} s^{-1})$^{-1}$) (Figure 177), which is the inverse of the c-parameter (Figure 176). P_{max}-values (Figure 178) range around 4, with maxima up to 8 à 10 (mg C mg^{-1} chla h^{-1}). P_{max}-values in summer are higher than winter values, especially in the innermost stations, but some low values also occur (Figure 178).

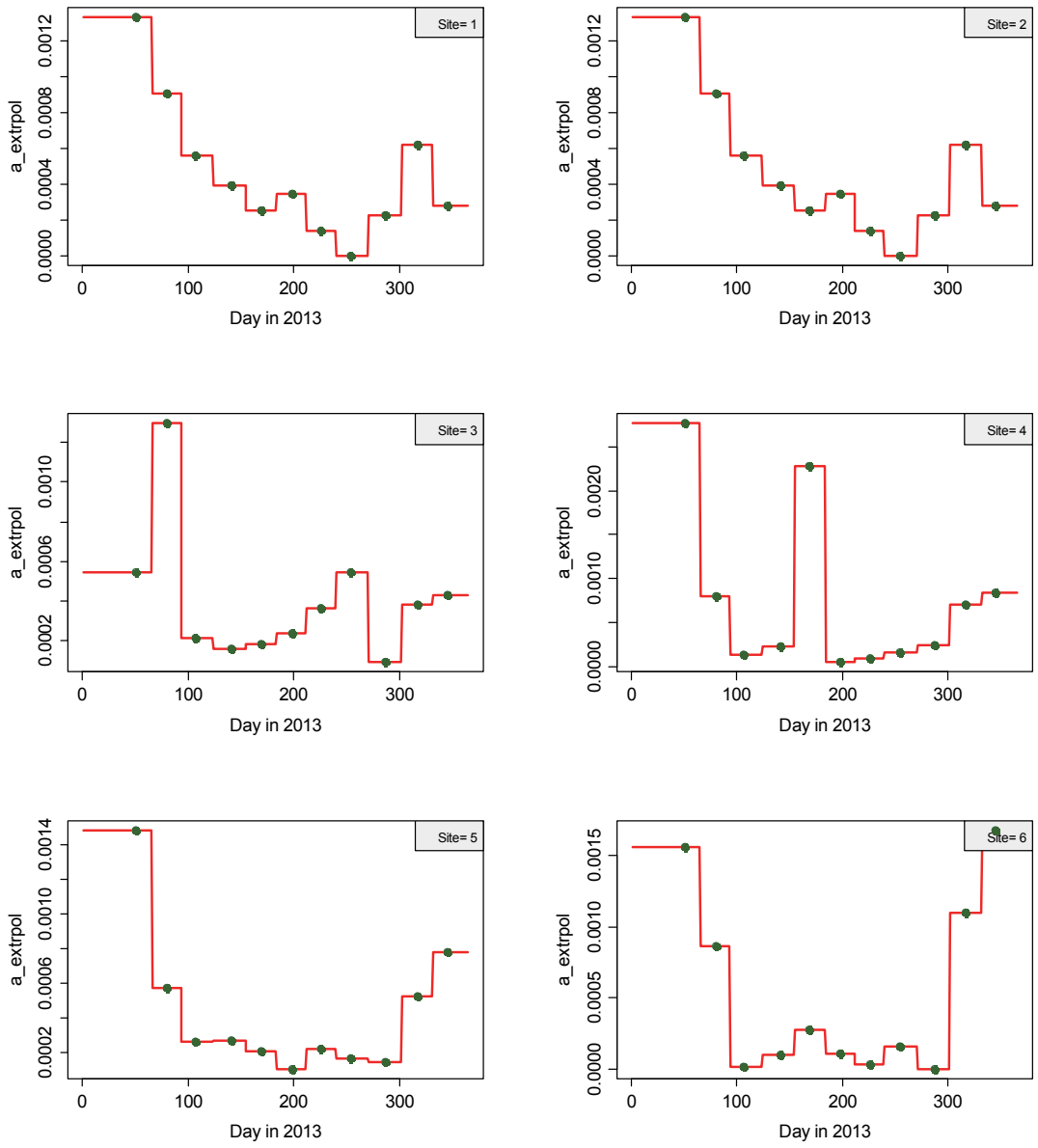

Figure 174 Benthic primary production Eilers-Peeters parameter a (determines photoinhibition), year 2013. The larger the value, the more sensitive phytobenthos is to high light intensities (in a negative way).

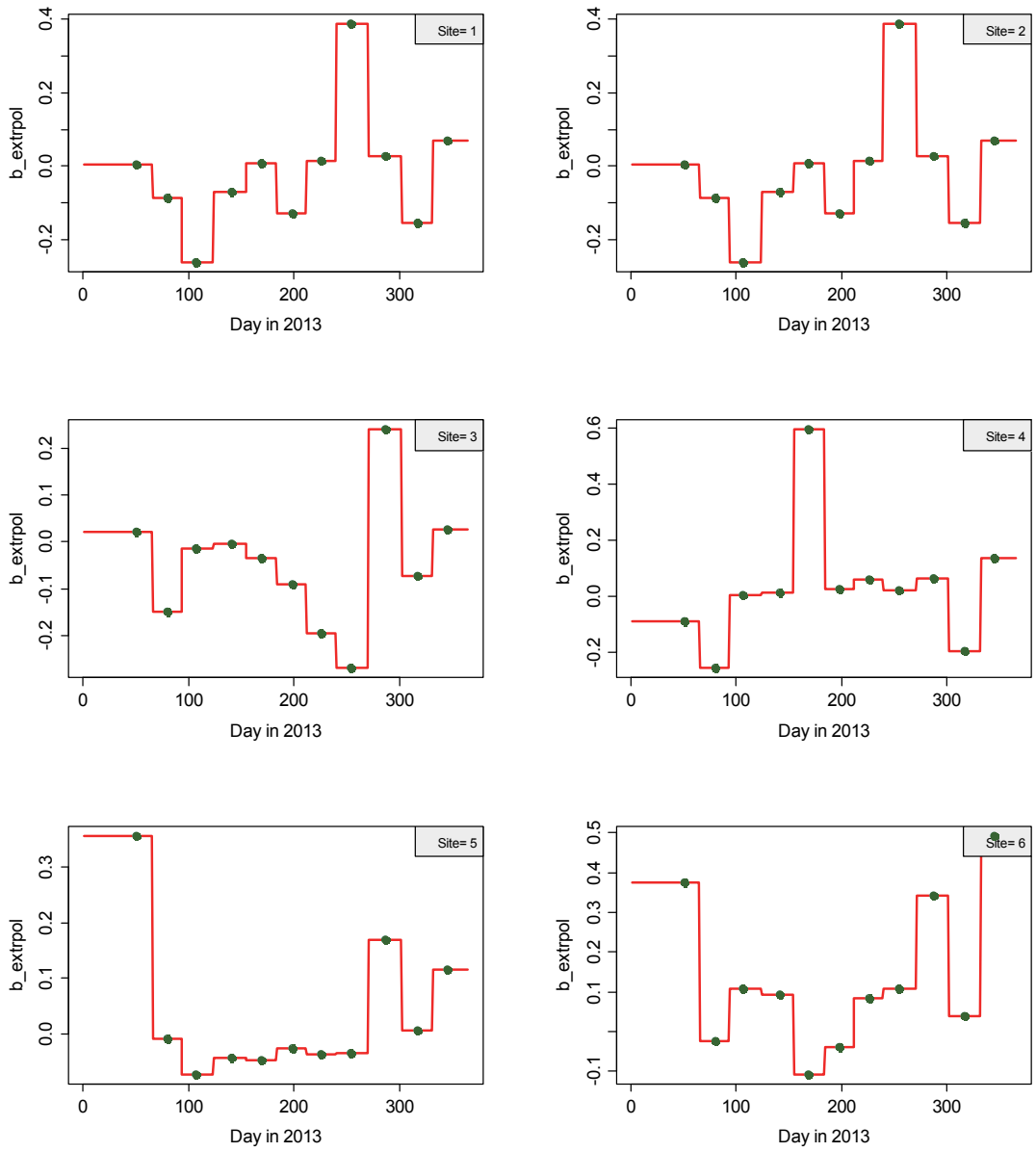

Figure 175 Benthic primary production Eilers-Peeters parameter b (determines a decreasing production per amount of photons), year 2013. The larger the value, the more production increase is negatively affected by light intensity (tends to saturation).

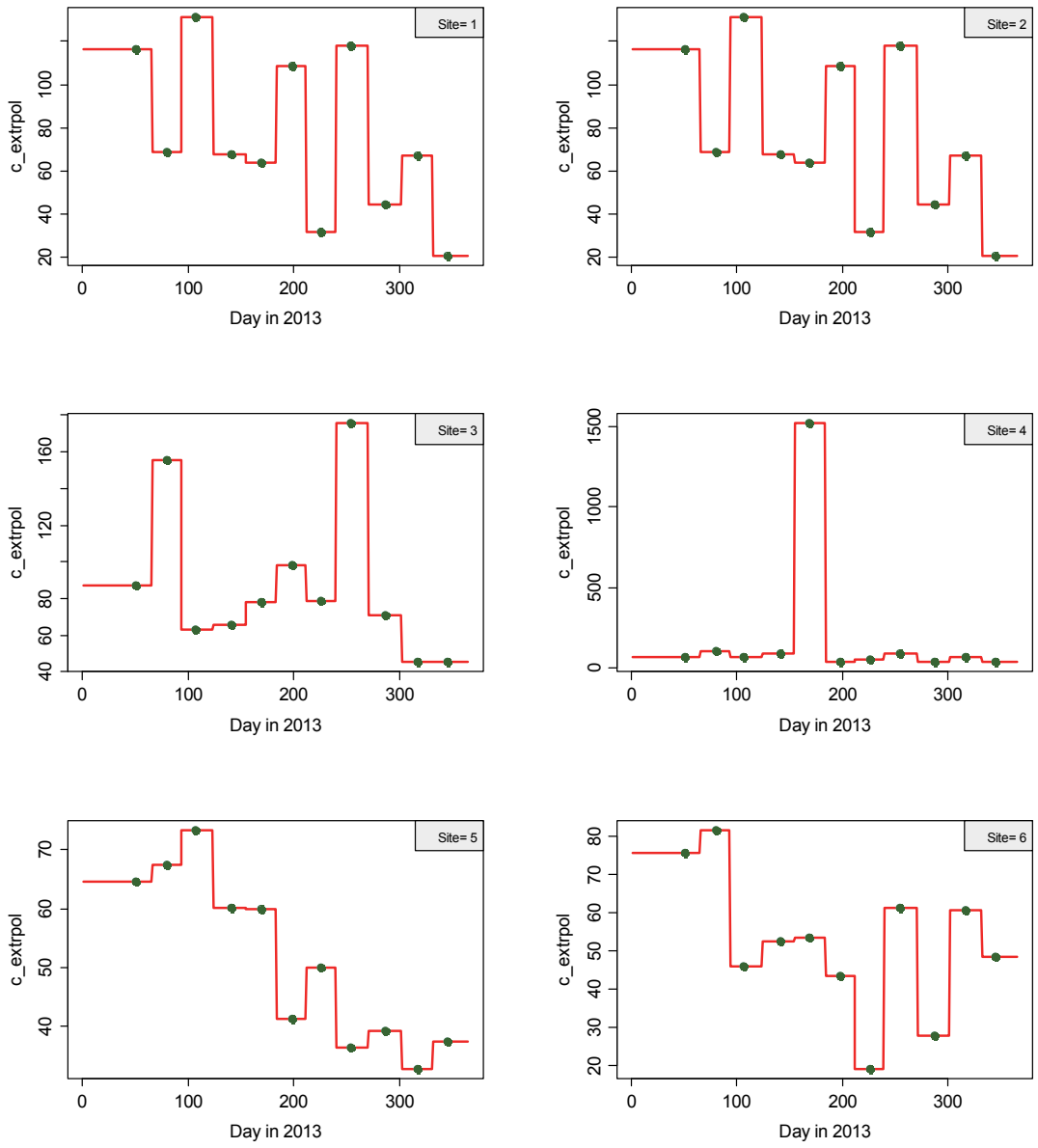

Figure 176 Benthic primary production Eilers-Peeters parameter c (determines the sensitivity of benthic primary productivity for light at low light intensities), year 2013. The smaller the value, the more algal production increases with increasing light intensity at low light intensities.

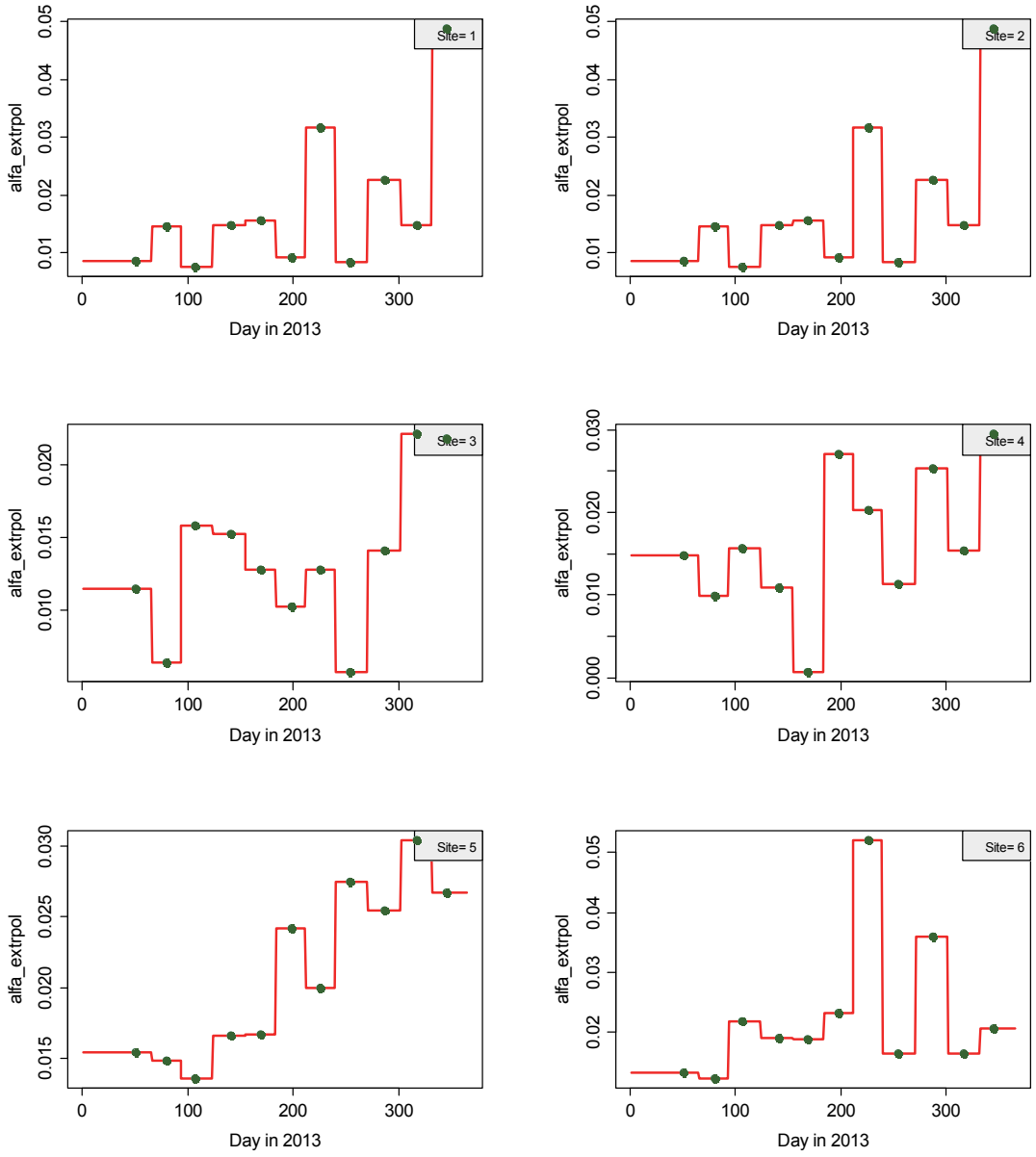

Figure 177 Slope of the PI-curve at zero light intensity. Is the reverse of the Eilers-Peeters c-parameter. Unit= mg C mg^{-1} chla h^{-1} (uE m^{-2} s^{-1})$^{-1}$

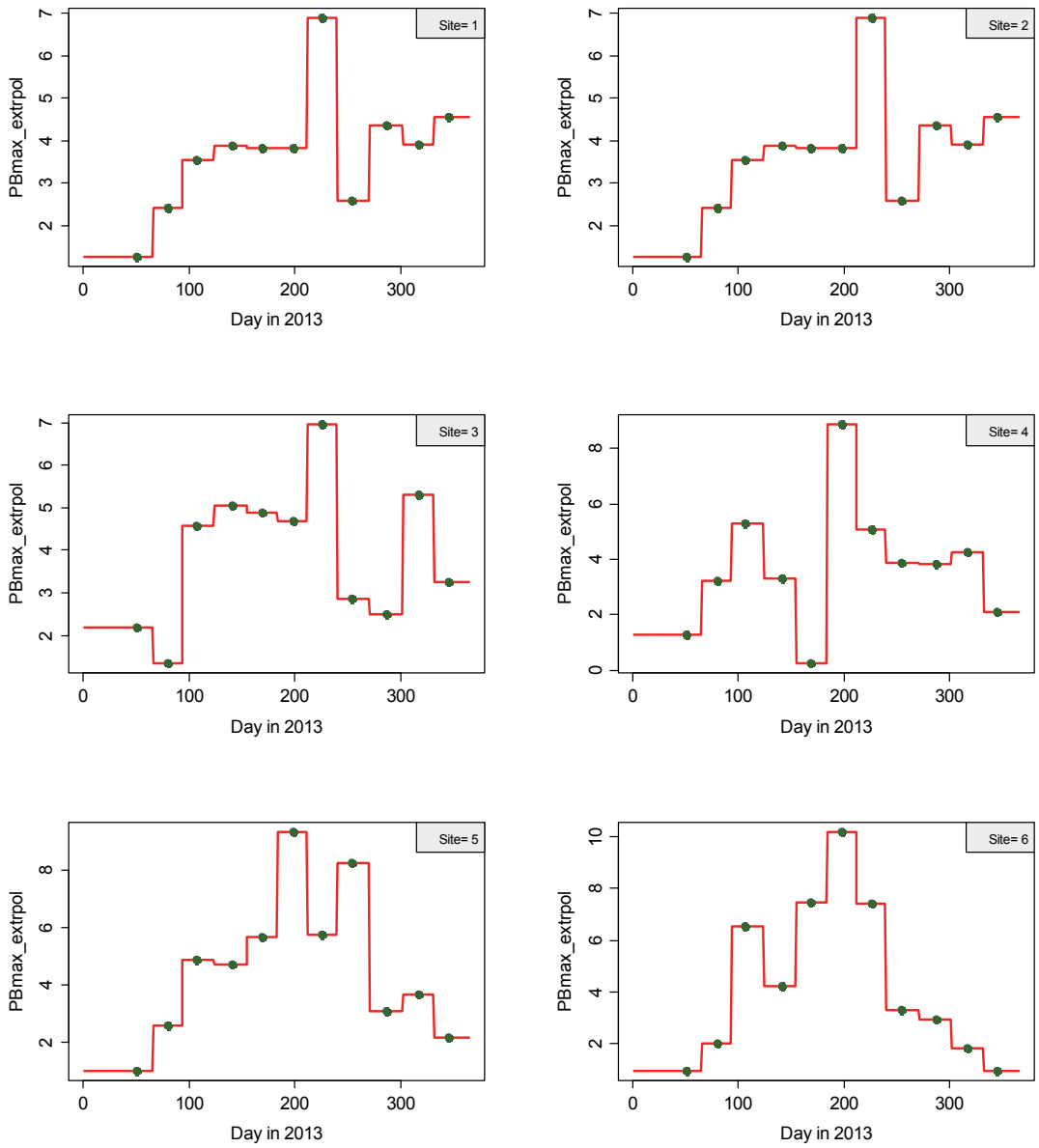

Figure 178 Maximum phytobenthos primary productivity, computed from the Eilers-Peeters parameters a, b and c, year 2013. Unit mg C mg^{-1} chla h^{-1}.

10.3 Benthic primary production as computed for the field situation

10.3.1 Problems encountered

Above, the productivity per unit of chlorophyll-a mass is given, as a function of light intensity. The chlorophyll-a content of the sediment is known as well (amount per unit of volume, see sections 3.7.3 and 4.6.1.5), and thus, the productivity related to radiation intensity in the sediment is known.

An estimate for the benthic primary production in the system now can be computed from the Eilers-Peeters parameters (Figure 174 - Figure 176), weather conditions, an estimate for the sediment light attenuation (section 8.18) , and the interpolation of benthic chlorophyll content (Figure 141).

First: there was some, but not a major difference in results regarding the possible options as mentioned in section 8.18 (different options for sediment composition, weather conditions = solar radiation, type of interpolation). So, these options will not be discussed further here.

Yet, another, and much more important problem was encountered. First computations, using the results for the sediment extinction coefficients, and assuming an equal distribution of chlorophyll-a in the sediment (based on the 0.5 cm chlorophyll-analyses) produced such low benthic primary production values that these were considered unusable.

10.3.2 Variations examined

Next, a few other possibilities were examined. First, it was assumed that the assumption of equal distribution with depth was not realistic, which also follows from data from De Jonge & Colijn (1994), and De Boer (2000). An exponential function was applied to describe the decrease of chlorophyll-a content with depth z (cm) of chlorophyll-a:

$$Chla_z = Chla_0 * \exp(-k_c z) \qquad \text{(mg chla dm}^{-3}\text{ sediment)}$$

with k_c (cm^{-1}) as distribution coefficient. For the De Jonge and Colijn (1994)-data, k_c = 0.7 à 1.0 cm^{-1}, For the data given by De Boer (2000) k_c was smaller, and ranged around 0.2 -0.25 cm^{-1}. See also his tables 10 & 11.

Applying such a distribution resulted in a bit higher primary production values, but differences were minor.

Next, the possibility of benthic migration towards the best possible light condition was taken into account. Du et al (2010) mention a study by Hopkins (1963) who observed that benthic diatoms were capable to migrate from 1 mm depth to the surface with 1.5 hour. Du et al (2010) found that this movement was triggered by light; e.g. such a migration was absent during night. They also found that in sandy areas migration could be faster than in silty areas.

Thus, the next idea tested here was the assumption that benthic diatoms can move to that region where light climate is optimal. This implies that in case light saturation occurs, upper diatoms can move downward to better conditions and diatoms from deeper in the sediment can move upward. This is illustrated in Figure 179.

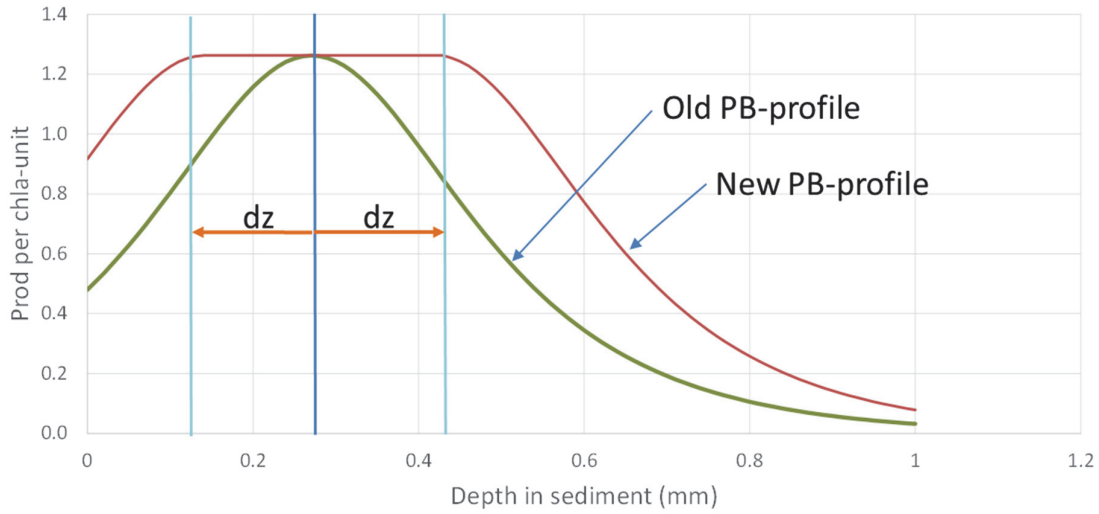

Figure 179 Benthic primary production profile in the sediment, a hypothetical situation. The green line represents the situation if phytobenthos is not motile at all, and benthic light climate determines the production rate (with a light saturation effect above 0.3 mm depth amd thus decreasing productivity for small depths). In case benthic diatoms are capable of migrating to better conditions, say effectively dz mm within the light period the production rate with depth is described by the brown line. A much larger part of the phytobenthos reaches the depth with optimum light conditions, but also algae that do not reach the optimum region have improved their light conditions.

Presentation of results comes with two setcodes. SetCode1 identifies the conditions used: first the sediment composition (based on the RWS-"Sedimentatlas" (RIKZ,1998) or the same data but elaborated after Zwarts, 2004: "Malvern"or "Zwarts"), than: or based on a rectangular interpolation ("Rect") or on a moving average method ("MovAvg"), than the basis for the light attenuation coefficient ("IMA"= the present data as derived from the suspended solid and Kd-measurements in the water column, or "Colij"= the data used by Colijn & De Jonge, 1984) (seeTable 34 and Table 35), and finally the year of the weather conditions used: 2013 for the actual condtions, 1976-1978 for the conditions in the years of the Colijn & De Jonge (1984).

SetCode2 gives the choices for the distribution of light in de sediment and for the mobility of diatoms in the sediment. Ext10 /05 says that the light attenuation coefficient in the sediment is 1 or 0.5 times the original value.

Hmov= the distance in 0.1 mm that diatoms can move towards the optimum light conditions. NO_mov means that their mobility is zero.

Textbox 1 Explanation of codes that identify the benthic primary production computations.

1	Light ext*1.0 Chla Linear	Normal light extinction, chla linear distribution
2	Light ext*1.0 Chlexp no mov	Normal light extinction, chla exponential distribution
3	Light ext*1.0 Chla exp mov 0.1 mm	Normal light extinction, chla exponential distribution, 0.1 mm diatom movement assumed
4	Light ext*1.0 Chla exp mov 0.4 mm	Normal light extinction, chla exponential distribution, 0.4 mm diatom movement assumed
5	Light ext*1.0 Chla exp mov 1.0 mm	Normal light extinction, chla exponential distribution, 1.0 mm diatom movement assumed
6	Light ext*1.0 Chla Linear	Light extinction *0,5, chla linear distribution
7	Light ext*1.0 Chlexp no mov	Light extinction *0,5, chla exponential distribution
8	Light ext*1.0 Chla exp mov 0.1 mm	Light extinction *0,5, chla exponential distribution, 0.1 mm diatom movement assumed
9	Light ext*1.0 Chla exp mov 0.4 mm	Light extinction *0,5, chla exponential distribution, 0.4 mm diatom movement assumed
10	Light ext*1.0 Chla exp mov 1.0 mm	Light extinction *0,5, chla exponential distribution, 2.0 mm diatom movement assumed

Textbox 2 Overview of options discussed in this chapter.

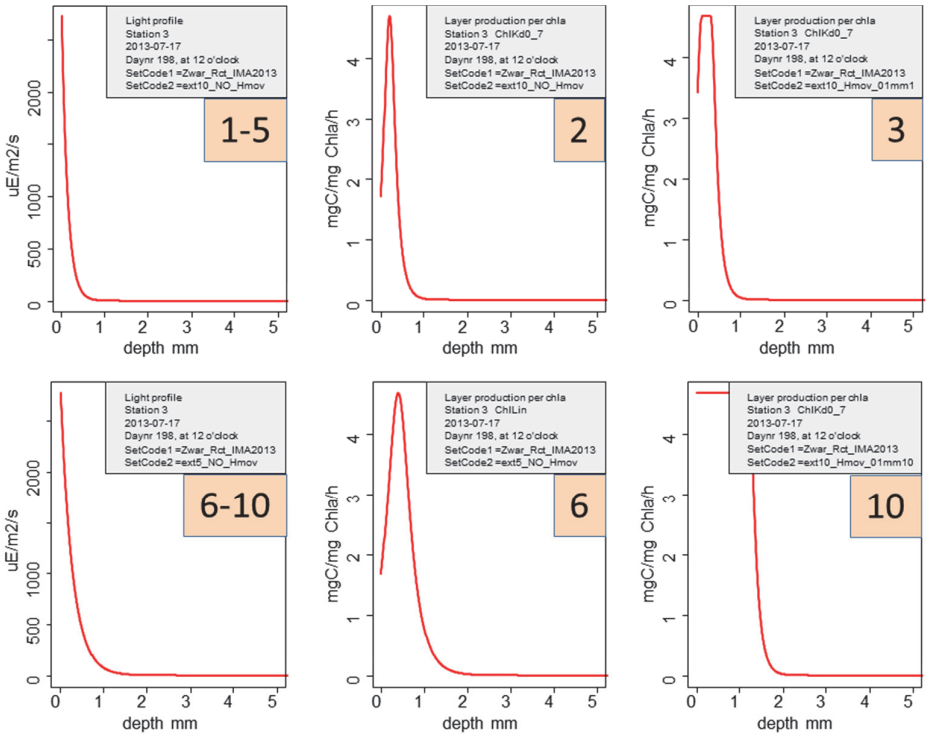

Figure 180 Some benthic primary production results. Station 3, day 198. A and D: light profile in the sediment, 1-5 with 'normal' light extinction coefficient, 6-10 with 0.5 that value (improving light penetration). 2,3,6,10: profiles of production (mg C mg^{-1} chla h^{-1}). 2: exponential chla-profile (k_c=0.7 cm^{-1}), no movement of diatoms. 3: as 2, but diatoms move 0.1 mm towards the optimum light condition. 5: light as 6-10, chla is linearly distributed. 10: as 6, but diatoms can move 1 mm towards the optimal light conditions. These numbers are those from Textbox 2.

10.3.3 Station results

Some results, for one station and for several options are presented in Figure 180. When diatoms are assumed to move towards the best light conditions, they can increase their production substantially. Because of the high light attenuation coefficient (4 mm^{-1} and up), a small displacement already has a large effect on their production. Most results come with a couple of codes that identify the conditions of the computation. These codes are explained in Textbox 1 and Textbox 2.

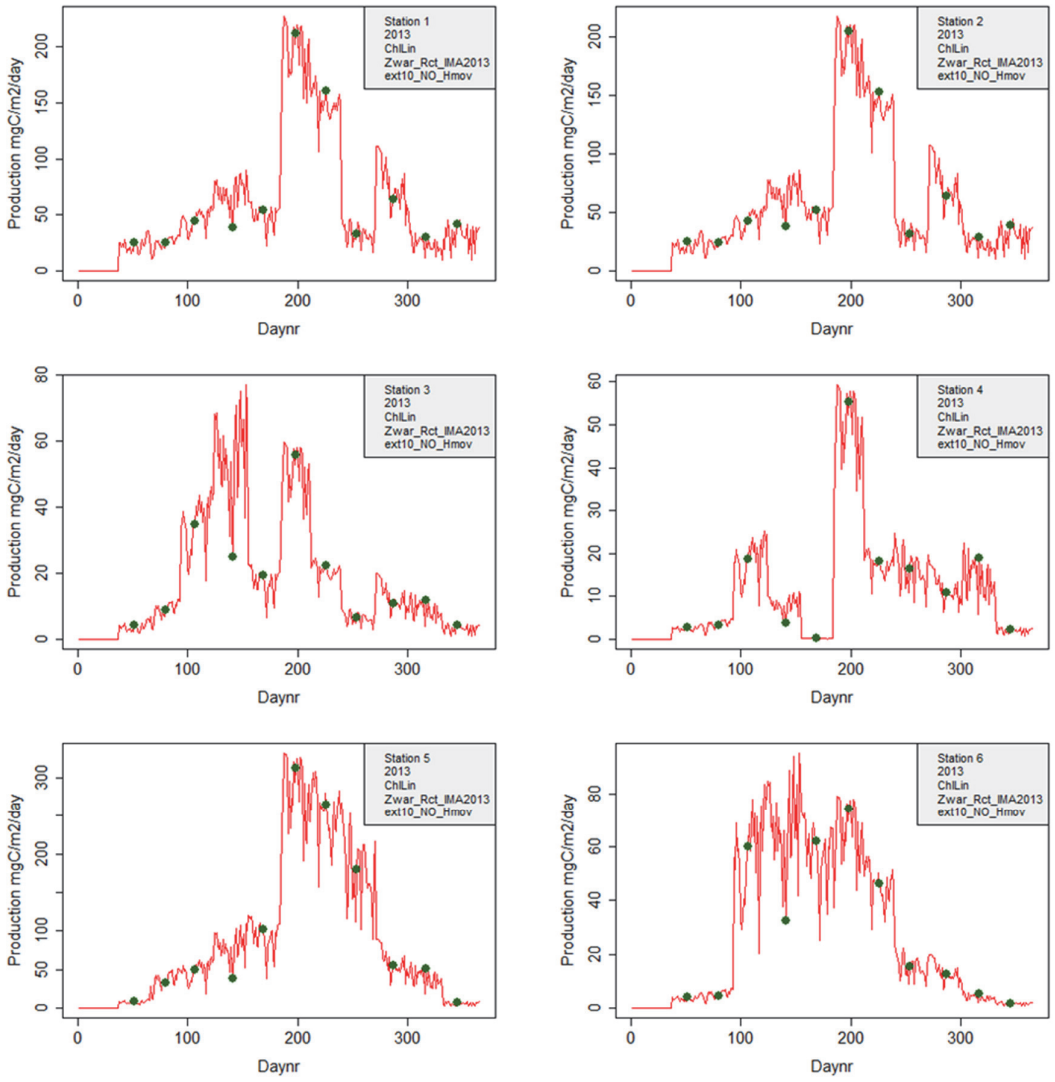

Figure 181 Benthic primary production computed with a linear distribution of chlorophyll-a in the sediment, the standard light attenuation coefficients and no movement of diatoms assumed (thus option 1 from Textbox 2). Radiation data for 2013.

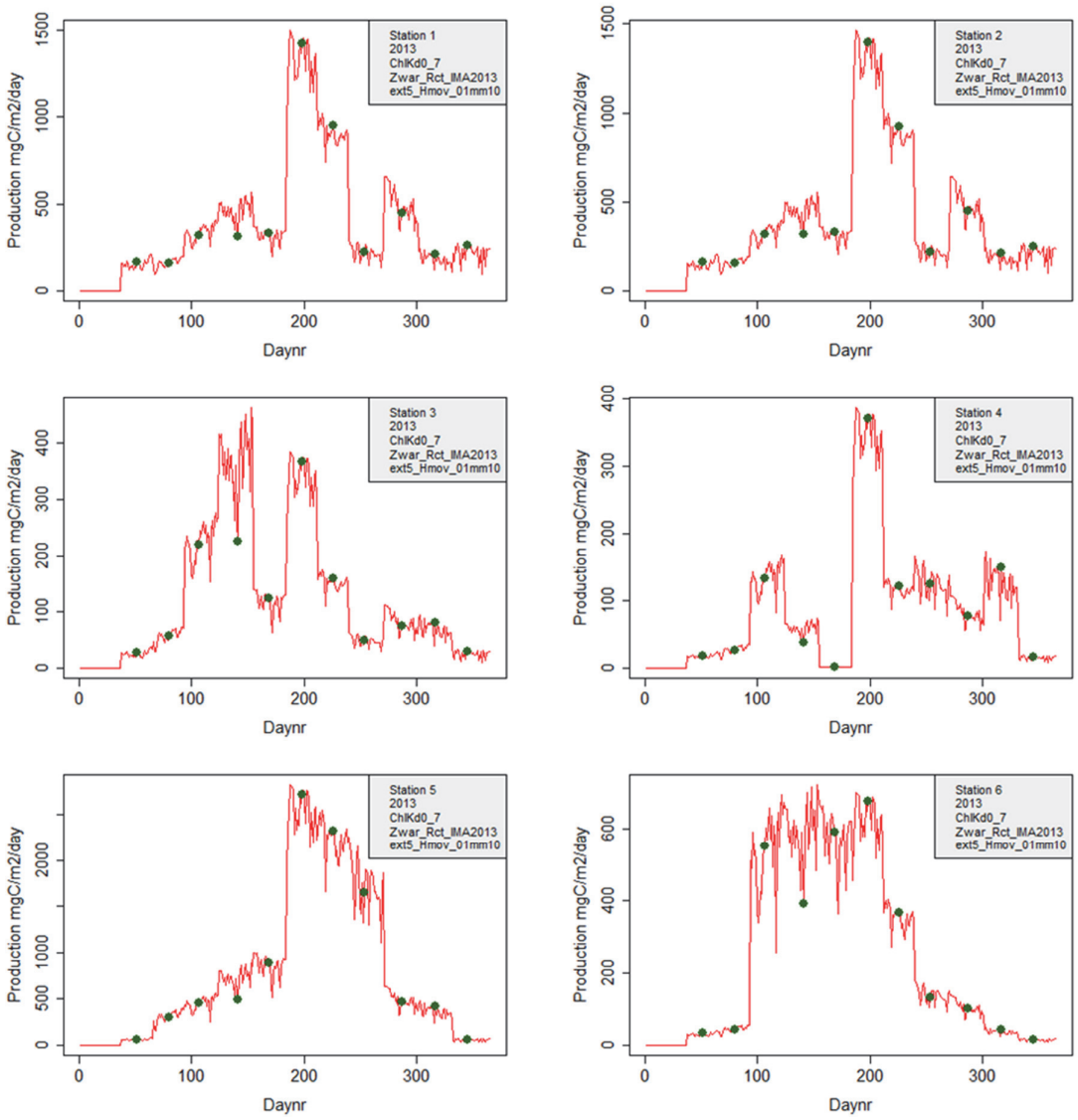

Figure 182 Benthic primary production computed with an exponential distribution of chlorophyll-a in the sediment (k_c = 0.7 cm^{-1}), light attenuation coefficients that are 50% of their standard values (see Table 35) and assumed that diatoms can move 1 mm towards the optimal light conditions (thus option 10 from Textbox 2). Radiation data for 2013.

Two examples of benthic primary production results are shown in Figure 181 and Figure 182, for each station and for each day in 2013. The results illustrate the large differences depending on the choices for the conditions. The values as presented in Figure 181 and Figure 182 are summed for each station, and presented (including those for the other possibilities mentioned in Textbox 2 (except one)) and shown in Figure 183.

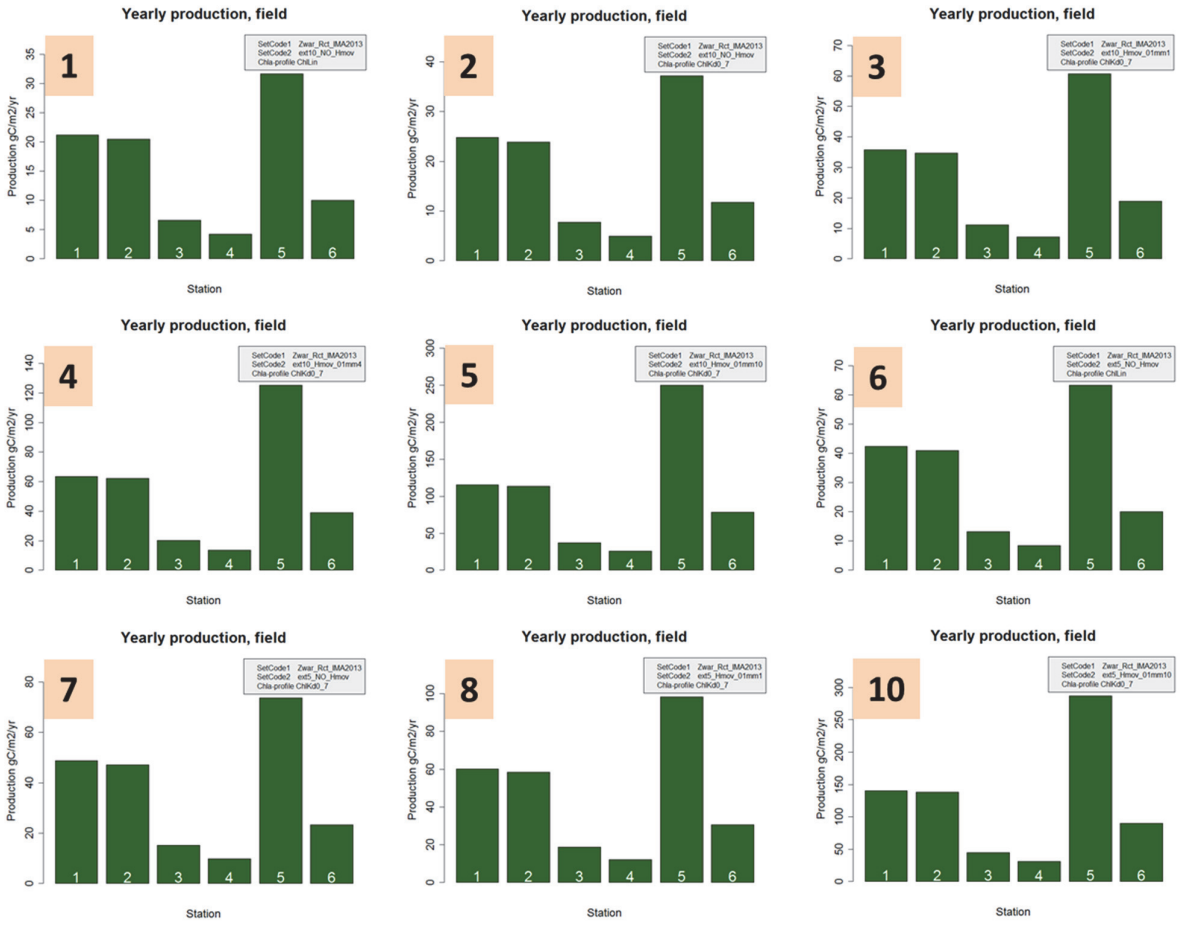

Figure 183 Benthic primary production at each station computed for the several possible light attenuation coefficients and phytobenthos movements as described in Textbox 2, only option 9 is not shown. Radiation data for 2013. For meaning of additional codes, see Textbox 1. Note that the difference between station 1 and 2 is a result of slightly different solar radiation and different sediment characteristics; all production parameters have been copied from station 1.

The pattern is the same for all options, the absolute values differ a lot, from 30 g C m^{-2} y^{-1} as highest value for option 1 (light attenuation coefficient as listed in Table 35, and microphytobenthos cannot move to better light conditions) to almost 300 g C m^{-2} y^{-1} for option 10 (light attenuation coefficient is half the one listed in Table 35, and microphytobenthos can effectively move to better light conditions over 1 mm distance). Station 5 shows the highest production, a result of the higher chlorophyll-a content found here (Figure 139 and section 8.16). This is also the explanation for all differences: at stations 3 and 4 we found lowest chlorophyll-a content, and intermediate values at stations 1 and 6.

10.3.4 System results

The results from Figure 183 are integrated over the whole system, and presented in Figure 184, of course showing the same large difference between minimum and maximum computed values: 10 – 80 g C m^{-2} y^{-1}, when regarding the whole day including the period when tidal flats are submerged, and 18-130 g C m^{-2} y^{-1} if only the period when flats are dry is taken into account. Such a large difference between lowest and highest values makes it hard to conclude what the benthic primary production was in the system in 2013.

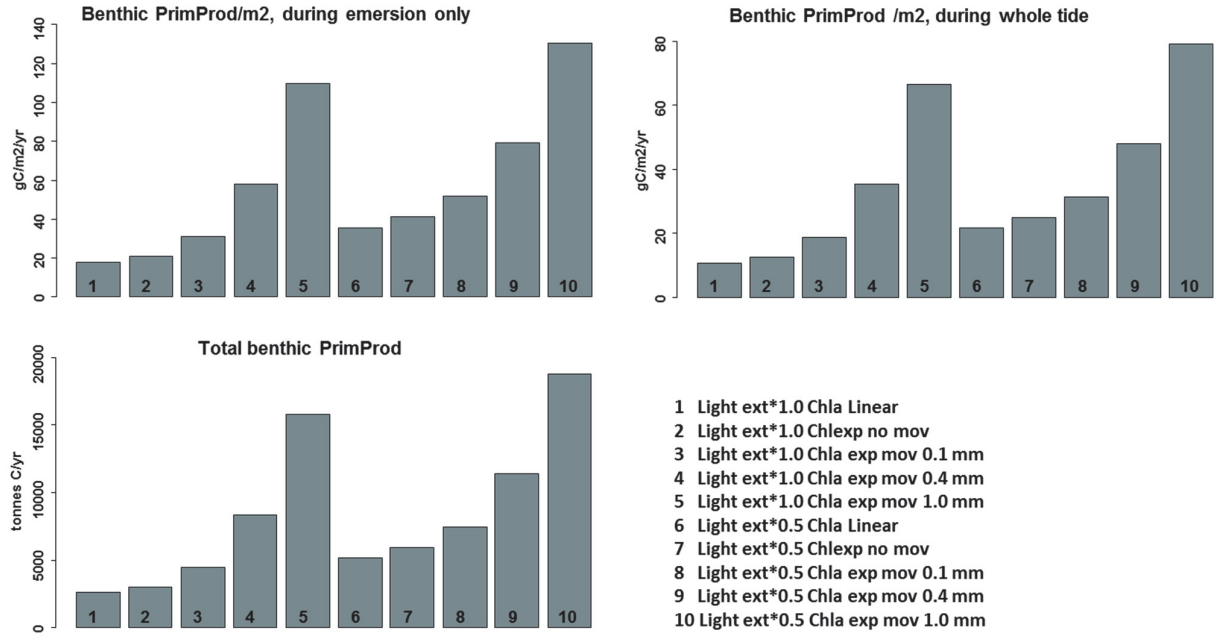

Figure 184 Benthic primary production in the Ems-Dollard estuary as computed for the possible light attenuation coefficients and phytobenthos movements (the 10 options mentioned here, same as Textbox 2). Radiation data for 2013. Upper left: production during emersion only, during the whole day (including night). Upper right: due to flooding, production is only possible during a part of the day, the real contribution of the tidal flats to system primary production is lower than that. Lower left: whole system benthic primary production.

10.4 Benthic primary production: system overview

Above it was explained

- how the Eilers-Peeters parameters were obtained, and how they are extrapolated to the whole year (sections 4.11, 4.12 & 10.2),
- how the chlorophyll-a content in the ^{14}C was analysed (sections 4.6.4)
- how the chlorophyll-a content of the sediment at the five sites was measured (sections 4.6.2 & 8.16)
- how the incident radiation is obtained from the KNMI-data (section 4.15)
- how the light penetration in the sediment is computed (sections 4.14 & 8.18).The global radiation values were increased because of the backscattering (upwelling light) in the sediment top layer; this upwelling factor differed per site: 1.8 for sites 1 and 2, 1.4 for sites 3 and 4, and 1.2 for sites 5 and 6.
- How different phytobenthos motility was included in the computations.

Thus:

a) the ^{14}C-incubation provides the PI-curve (a,b, and c-parameters). These are extrapolated to the whole year
b) the fluorometric analysis provides the chla content of the ^{14}C-samples
c) the spectrophotometric chla analysis gives the chla content in the sediment (Figure 139 Figure 142). These are extrapolated to the whole year. Also, one of the options computed is that an exponential distribution of chlorophyll-a with depth is assumed.
d) (b) and (c) together give the possibility to convert the ^{14}C-incubation results to the field situation
e) the global radiation data (KNMI) give the energy influx at the sediment top-layer
f) the estimates for the light attenuation give the light intensity at each depth in the sediment (section 8.18).
g) an assumption is applied on the vertical migration of microphytobenthos towards optimal light conditions in the sediment (section 10.3).
h) with (e) - (h) the primary production at each depth is computed. This is done for 2000 layers of 0.01 mm (from 0.. 20 mm).
i) summed it gives the hourly benthic production (mg C m^{-2} h^{-1}) at each moment, and thus the daily production can be calculated, assuming 100% emersion (Figure 181 & Figure 182).
j) from GIS-information, average emersion times for each site can be obtained (Table 6)
k) each site is assumed to be representative for a certain area (compartment). These compartments were taken from Colijn (1984), see Figure 14, and Table 6.
l) finally, benthic primary productions are computed for each compartment, and thus, for the whole Ems-Dollard area.

Results for these steps are presented above. These computations were repeated with other sediment composition estimates (Malvern-sediment data: Table 34, sediment data converted according to Zwarts: Table 35), weather conditions (present, and those from 1976-1978), light attenuation characteristics (present estimates and those by De Jonge and Colijn (1984), see Table 34 & Table 35) and interpolations method (rectangular or moving average). These variations hardly changed the picture above, and are not presented separately here.

10.5 How realistic are the values? Evaluation

The question now is what the value is of the above results. The range of calculated primary productions is almost one order of magnitude, and is based on different assumptions for the light attenuation coefficient in the sediment and the position of the benthic diatoms with respect to the light conditions in the sediment.

10.5.1 Light attenuation in the sediment top layer

The values for k_d we used here, and were listed in Table 34 and Table 35 (values used: k_{d_avg}), were based on our own estimate of effects of silt (measured in the water column) and an estimated contribution of sand (merely based on literature values), the sediment composition ánd a comparison with the estimates of Colijn & De Jonge (1983) plus other literature values. It was concluded that our estimates are within the ranges mentioned in literature, and possibly a bit on the high end of the rages mentioned. The latter was a good reason to compute benthic primary production with a 50% light attenuation coefficient as well.

10.5.2 Chlorophyll-a content of the sediment

The results a linearly related to the amount of chlorophyll-a detected in the sediment (section 8.16); the values found here are, with one exception (station 5) at the lower end of normally reported ranges. The procedure followed here to analyse the chlorophyll-a content, including the qualitative validation with the BenthoTorch-data (section 8.16.2) gave no reason to doubt these values. Nevertheless, De Jonge & Colijn (1994) argue that there are large differences with respect to the position in the tidal zone: the higher up in the tidal zone, the higher also phytobenthic biomass. They give average values of 4-12 gC m^{-2} from -50 to +100 cm NAP, with a C/Chla-ratio of 60 (as a rough average of the values mentioned in the same paper) it gives 60 – 200 mg chla m^{-2} (the range of individual chla-values is much larger: mean annual values range from 28.6 – 247 mg chla m^{-2}). Thus, it is to be expected that the primary production values computed here will be lower than those found by Colijn & De Jonge (1983).

10.5.3 Production rates per unit chlorophyll-a

PB_{max}-values found here range between 2 and almost 10 mg C (mg chla)$^{-1}$ h^{-1}, and are a bit lower than those found for the pelagic phytoplankton (chapter 9). Wolfstein & Hartig (1998) measured a maximum value of almost 2 on the Keitum Watt (Sylt, Germany) with the ^{14}C-incubation method, and up to 4 mg C (mg chla)$^{-1}$ h^{-1} based on oxygen production during incubation. MacIntyre and Cullen (1996) found 8-10 mg C (mg chla)$^{-1}$ h^{-1} as maximum value in the Corpu Christi Bay (SE Texas, USA), with highest values at highest temperature. Such values are also presented by Dube (2012) in his master thesis on remote sensing methods, with values of 3 at 5 ^{o}C to 10 mg C (mg chla)$^{-1}$ h^{-1} at 25 ^{o}C.

10.5.4 Positioning of microphytobenthos in the sediment

A part of the benthic diatoms (the epipelic diatoms) can actively choose their position in the sediment, and thus find the optimal light conditions. De Jonge (1980) mentions that almost all benthic algae belong to this type. Migration distances found in literature are about 0.6 to 1 mm h^{-1} (see e.g. Consalvey et al,

2004). Thus we might conclude that from the computed options (10.3.4) the ones with a 1 mm migration assumption are more likely than those with 0.1 mm or even without migration.

10.5.5 Conclusions

We conclude that

i) Chlorophyll-a data found in the sediment are typical for the samples sites
ii) Lower or higher in the tidal zone chlorophyll-a values may be lower cq higher
iii) Production rates per unit of chlorophyll-a is well in line with literature results
iv) The assumption that microphytobenthos can migrate over a 1 mm distance to the optimum light conditions seems to be realistic
v) The computed light attenuation values are in line with those reported in literature. The case we also computed with a 50% lower attenuation coefficient probably is at the optimistic side.

Nevertheless, since we did not measure primary production *in situ*, but computed it needing one estimate (on k_d) and one assumption (on the distribution of microphytobenthos with respect to light conditions) it is hard to draw strict conclusions on benthic primary production in 2013. Most likely, it ranges between 70 and 140 g C m^{-2} y^{-1} for the period only when flats are dry, and 40-80 g C m^{-2} y^{-1} as whole year contribution to overall primary production of the system.

10.6 Mass specific pelagic production

Similar to pelagic specific production rates, benthic specific production rates (P_{max_spec}) were computed. Or again: the better name is first order gross ^{14}C uptake rate constant (d^{-1}). Since microphytobenthos carbon content is unknown, this is estimated based on a 1:38 chlorophyll-a : C ratio (section 4.6.5). Results are presented in Figure 185. Temperature corrected values (using the Eppley-equation, Eppley, 1972, see section 4.12.2) are shown as well. Pelagic temperatures as sampled by the PocketBox were used. These observations mostly occurred one day after the benthic sampling (see Table 10 and Table 12).

At all stations, a maximum of the temperature corrected values can be observed in spring, but this is not very distinct. Very low values are not observed, except for station 4, at mid-June 2013. The value is a combination of a high chlorophyll-value and low ^{14}C-uptake. Consequently, characteristics that may indicate dependence on low nutrient concentrations are lacking. Not-temperature corrected values reach higher levels, with maxima in summer.

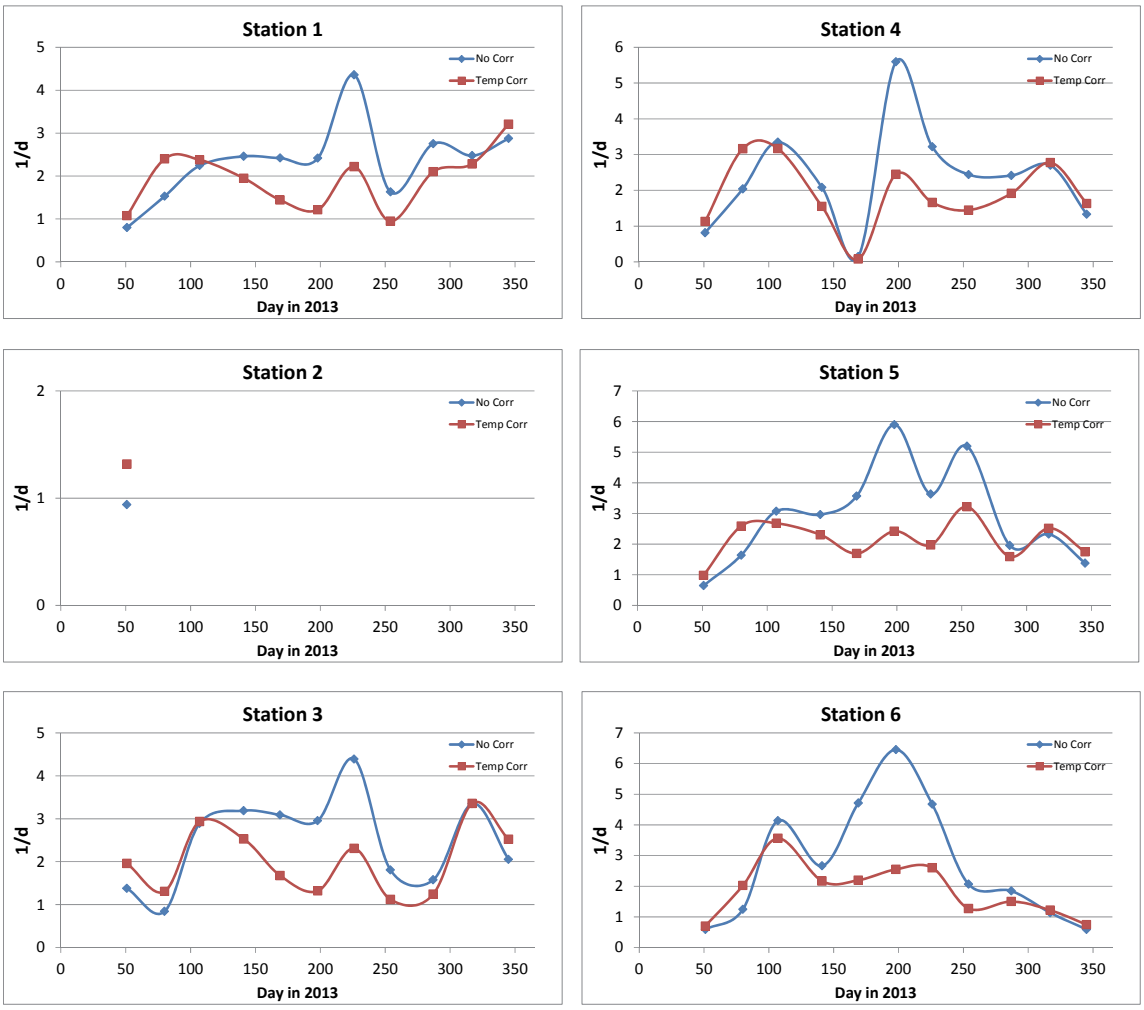

Figure 185 Specific maximum productivity of Ems-Dollard phytobenthos in 2013; P_{max_spec} from incubations transformed to field situation, and divided by the concentration of phytoplankton carbon present in the samples. Phytocarbon content was estimated by assuming a phytoplankton C : chlorophyll-a- ratio of 38 (mg C/mg chla). Mind the different Y-axis scales. Red results: corrected for temperature, blue: uncorrected.

10.7 Discussion

Benthic primary production values (Figure 183) of stations 1 and 5 show much higher values than 3, 4 and 6. Station 2 is almost similar to station 1 because the station 1 parameters were used here. From Figure 185 it follows that these differences cannot be attributed to very different microphytobenthos characteristics, but mostly to differences in local microphytobenthos biomass densities (mg chl-a m^{-2}). These differences have already been mentioned in section 8.16 (Figure 139 - Figure 142); there is no information what caused these differences. In chapter 8 we already mentioned the possible effect of grazing, which is not investigated. Kamermans (1992) gave examples of Baltic Tellins that may locally deplete microphytobenthos presence.

Effects of nutrient limitation seem to be absent, since there no close-to-zero P_{max}-value in 2013 (Figure 185). This is also what may be expected, generally, since benthic algae have access to benthic nutrient resources and nutrient limitation is not very common. This also what results of benthic modelling that include microphytobenthos indicate (unpublished results of the IMARES- EcoWasp ecosystem model, Brinkman).

Absolute values for the P_{max_spec} depend on the assumed C:Chla mass ratio (here taken as 38). De Jonge (1980) analysed this ratio during three years and found average yearly ratios of 40.3 – 61.4 (years 1976-1978), locally varying between 10 and 154. If the ratio of 38 would be doubled, the values of P_{max_spec} (specific gross productivity) would be half the values given in Figure 185. Taking another ratio would not change the benthic primary production in the field as presented in Figure 180 - Figure 184. References cited by De Jonge (1980) give an even wider range of values; higher C:Chla ratios especially occur under N-limitation (chlorophyll-a needs nitrogen as part of the molecule). De Jonge (1980) also mentions the difficulty to distinguish between vital microphytobenthos cells and detritus, and states that thus all C:Chla-ratios stay best estimates.

Benthic primary production values computed for 2013 show a wide range, a result of the estimates for the light attenuation coefficient and assumptions for the microphytobenthos motility. The most likely values of 40-80 g C m^{-2} y^{-1} contribution to overall system production is well in line with the global range of 50-200 g C m^{-2} y^{-1}, mentioned by Colijn & De Jonge (1983).

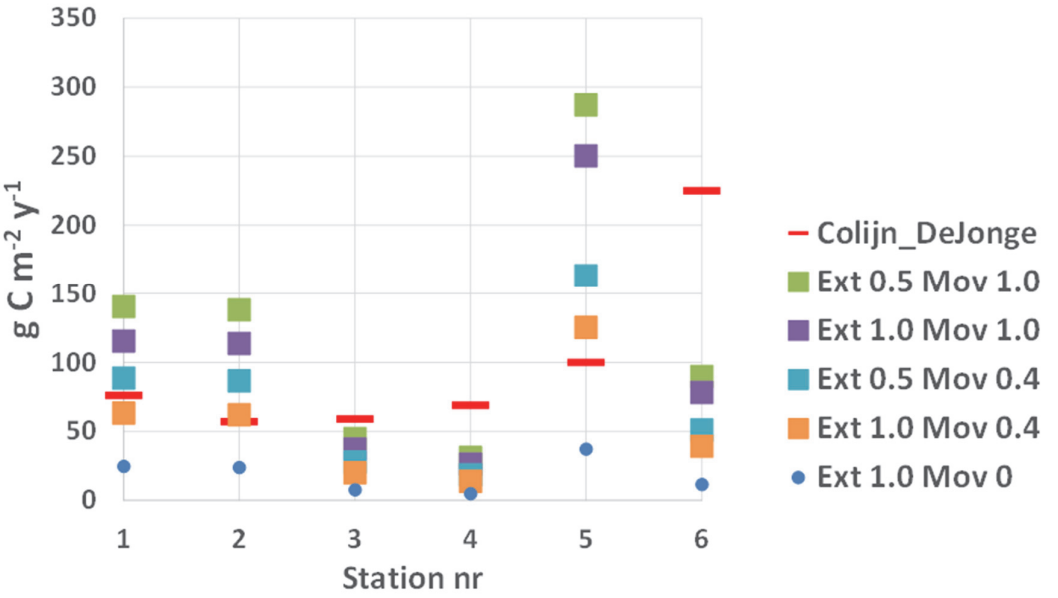

Figure 186 Benthic primary production at the several stations, during emersion, for 4 different options (from Textbox 2) abd compared to results by Colijn & De Jonge (1983).

System average benthic primary production can be computed from the data by Colijn & De Jonge (1983), which gives 93 g C m^{-2} y^{-1}, including the submersion period. That is 7-8 times the present lowest values (standard k_d, no microphytobenthos motility), and roughly the same as our 'most likely' values. Unfortunately, this gives reason not to draw any conclusions on differences between phytobenthic primary production nowadays and in 1980.

10.8 Conclusions for this chapter: what have we learnt?

10.8.1 Chapter content?

We outlined here the benthic primary production as computed for the Ems-Dollard estuary for the year 2013. Also a comparison with results from Colijn & De Jonge (1984) were made, and possible reasons for observed differences discussed.

10.8.2 What went OK?

Measuring primary production parameters and productivity per unit of chlorophyll-a was reliable.

The use of weather data from 1978-1980 made it possible to compute primary productions based on the present primary productivity parameters and the meteorological conditions in the period Colijn did his research.

10.8.3 What needs improvement and what are main recommendations for future work?

Assessment of benthic primary production had two major difficulties: estimation of the light attenuations coefficient and the assumption of microphytobenthos motility.

Integration over the whole system, and the whole year was well possible since morphological data and weather data were well available.

A weak point of *any* temporal extrapolation and interpolation is that the time constant for microphytobenthos is small, and thus, changes can be large between –and in between- two sampling dates. Also, spatial variations can be large, and thus –without being able to quantify this- the uncertainty in the final result is considerable.

Chlorophyll-a contents of the sediment differed a lot with the values found by Colijn & De Jonge (1983), and also by De Boer (2000), but with one exception for station 5. There, this resulted in high benthic primary production values, a major reason for the final whole system result.

What we do not know is *why* most chlorophyll-a densities are much lower than they were in 1976-1978 and 1992-1999. It is known from De Boer (2000) that also in the ’90-s large differences occurred, and that might be the case now. It is also known that grazers may largely affect phytobenthic abundance, but data on zoobenthos abundance fail completely. And finally, there are differences from low to high in the tidal zone. Thus, main recommendations are:

- Be sure that microphytobenthos is know well; use more than one analysis method
- Use more than one method to determine benthic primary production. If a comparison with other results is at stake, be sure to use also to same method
- Pay attention to the benthic light attenuation
- Pay attention to zoobenthic abundance and grazing activity
- Determine benthic chlorophyll-a content not only in one sediment slice, but find the depth profile.
- Consider to measure a chla-profile from low to high in the tidal zone

11 Final considerations and conclusions

11.1 General

Now we come to the final part: answering the main questions asked at the beginning of the research (see section 1.4). These questions will be answered in the next sections, including a short elucidation if appropriate.

11.2 Question: What is the pelagic primary production (PP) at present and what are differences between now and the late seventies?

11.2.1 Information

Pelagic production was determined after ^{14}C-incubations at six stations and during 40 cruises in 2012 and 2013. Most important results from the incubation measurements concern the maximum productivity per unit of chlorophyll-a (P_{max}) and the first order gross ^{14}C uptake rate constant (P_{max_spec}).

Incubation results were translated to the field based on actual weather conditions and measurements of the water column light attenuation coefficient.

11.2.2 Incubation results

Current pelagic primary production characteristics are presented in chapter 9. The first order gross ^{14}C uptake rate constant (or: mass specific ^{14}C uptake rate), corrected for temperature effects, reaches values up to 4 d^{-1} in 2012, and up to about 6 d^{-1} in 2013. Much higher results occur, but it should be questioned whether these have to be contributed to the chlorophyll-a values used.

11.2.3 Total primary production

Primary production values computed for the channels in 2012 and 2013 are of the same order as for 1978, but much lower (almost half) than those measured in 1979 and 1980. Largest absolute differences are found at the two outer stations (1 and 2), where present results are 60% of the values in 1979-1980. Relative differences in the inner stations are of the same order. Maximum relative differences is about a factor 2.

System average primary production values found for in 2012 and 2013 are 120 and 125 g C m^{-2} y^{-1}, respectively; this is including the tidal area and taking into account the emersion time of the tidal flats. This value is about 70-75 % of the values found by Colijn (1983) (system wide average of 164 g C m^{-2} y^{-1}).

11.3 Question: What is the benthic PP at present, and what are differences between now and the late seventies?

11.3.1 Information

Benthic production was determined after ^{14}C-incubations at five stations and during 11 cruises in 2013 (of which one had to be cancelled). Most important results from the incubation measurements concern the maximum productivity per unit of chlorophyll-a (P_{max}) and the first order gross ^{14}C uptake rate constant (P_{max_spec}).

Incubation concerned the sediment top 0.2 cm layer, field chlorophyll-a determinations concerned the sediment top 0.5 cm layer.

Incubation results were translated to the field based on actual weather conditions, measurements of benthic chlorophyll-a content, estimates for the sediment light attenuation coefficient and assumptions for microphytobenthos motility and thus movement to optimal light conditions.

11.3.2 Incubation results

Current benthic primary production characteristics are presented in chapter 10. The estimated maximum first order gross ^{14}C uptake rate constant, corrected for temperature effects and based on a C/Chla-ratio of 38, reaches values up to 3-4 d^{-1} in 2013.

11.3.3 Total primary production

For yearly benthic primary production, including the submersion period of the tidal flats, a lowest value of 11-14 g C m^{-2} y^{-1} is computed; the light attenuation coefficient is taken as estimated and microphytobenthos motility is excluded. A highest value of 40-80 was computed; for half the attenuation coefficient values and microphytobenthos moving 1 mm towards the optimum light condition.

If the emersion period only is considered, these primary production values are 16-23 g C m^{-2} y^{-1} and 70-140 g C m^{-2} y^{-1}, respectively. In case of a sufficiently large motility, the result is not very sensitive to the choice of the attenuation coefficient.

The lower primary production values computed for 2013 are much lower than the ones found for 1976-1978 by Colijn & De Jonge (1984); the higher ones are roughly the same. They found an average value of about 93 g C m^{-2} y^{-2} on tidal flats, including the submersion period. Differences between stations are large, which can mainly be attributed to differences in sediment chlorophyll-a content.

11.4 Question: what is the impact of suspended matter (SPM) on pelagic and benthic PP?

11.4.1 Information

It was tested what the effect is of an increased or decreased light attenuation coefficient on primary production (section 9.6, Figure 173).

11.4.2 Difference in primary production

For the most inner station, a 50 % change in light attenuation (which is near a 50% change of the suspended solid content of the water column) results in a 25% change in primary production. For the outermost station, a similar change results in a 35-40% change in primary production. These estimates did not take nutrient limitation effects into account. The two outer stations suffer from nutrient deficiency in (late) spring; a drop in the light attenuation coefficient during that period in time does not necessarily imply an increase in primary production. Thus, the figures mentioned here for the outer stations are too optimistic: changes will be much smaller. Better answers have to be provided after ecosystem modelling exercises.

11.4.3 Timing of the start of phytoplankton seasonal growth

It has not been investigated what the effect is a change in light attenuation on the start of the phytoplankton growing season. However, it can be argued that, especially at the beginning of the phytoplankton growing season, light is the most important limiting component, more than temperature and nutrients. Especially then, changing light conditions will have their largest effect on algal biomass development. The more turbid, the lower the algal growth rates are, and thus, nutrient demands. Consequently, if nutrient limitation becomes relevant, this moment will be reached (a bit) later in the year with increasing turbidity (and vice versa).

11.5 Question: are there factors, other than SPM, that have affected the water column irradiances in the last decades?

11.5.1 Information

The relationship between the light attenuation coefficient (k_d) and several dissolved and dispersed components was investigated (sections 7.9, 7.10).

11.5.2 Results

Next to suspended solids, also coloured organic carbon (CDOM) and yellow substances contribute to the light attenuation. This is especially the case in the more inner stations, where high concentrations of suspended solids occur, and also (relatively) high concentrations of yellow substances and CDOM are found. Without CDOM/Yellow Substance taken into account, the proportionality coefficient between the light attenuation coefficient and suspended solids is 0.044; with CDOM it gets 0.032 (and 0.024 for CDOM), with Yellow Substances it gets 0.026 (and 0.023 for Yellow Substances). Units for suspended solid constant: m^{-1} $(mg\ l^{-1})^{-1}$; for CDOM and Yellow

Substance: m^{-1} ($\mu g\ l^{-1})^{-1}$). Both CDOM and Yellow Substances are closely and inversely related to salinity, which raises the conclusion that both are mainly imported to the system; and thus, fresh water input (also) affects water column transparency trough this CDOM/Yellow Substance import.

11.5.3 The relationship between Kd and suspended matter now and in the late seventies

The relationship found here between K_d and suspended matter (K_d=0.044*[suspended solids]) is almost the same as found by Colijn (1982) (K_d=0.43+0.05*[suspended solids]).

11.6 Question: to what extent is primary production by planktonic or benthic algae limited by nutrients or light?

11.6.1 Information

The information is based on the estimations for the first order gross ^{14}C uptake rate constant (P_{max_spec}), coupled to nutrient concentrations and light climate. It was intended to use the absorption ratio (pigment absorption ratio at 480 and 665 nm) to distinguish between nutrient and light limitation, but it appeared to be not a good quantitative measure.

11.6.2 Pelagic primary production

Pelagic primary production in both outer stations (1 and 2) is likely limited by low phosphorus and silicate concentrations in spring. Nitrate concentrations do not seem to have an impact. Effects of ammonium were not clear. The three most inner stations (4 - 6) most likely did not suffer from nutrient deficiency; the situation for station 3 is not (always) clear.

11.6.3 Benthic primary production

There was no indication that nutrients play an important production limiting role for microphytobenthos.

11.6.4 Effect of changing nutrient concentrations since the late seventies

Primary production in both outer stations found in this research was about 10-20% below the 1978-values, and almost half of the 1979-1980 values. This could not be attributed to weather conditions: applying 1978-1980 weather conditions to the present setting revealed roughly the same results. Since light attenuation presently was less (conditions improved) compared to 1979-1980, this could not be a reason. Nutrients limitation is a possible cause: concentrations, especially of ortho-phosphate, dropped a lot since the late seventies (down to about 50%) and this could be a major reason for lowering primary production in the outer areas. It can hardly be a reason for a changing primary production at the inner stations; the increased turbidity is the most plausible cause for the changes there (see section 9.6). A second possibility is the low contribution nowadays of highly productive *Phaeocystis*, which also is considered a result of declining eutrophication.

Although it seems likely that pelagic primary production in both outer stations (1 and 2) is limited by low phosphorus and silicate concentrations in spring, we could not prove this with the data from this

research. Nitrate concentrations do not seem to have an impact nowadays. Based on the observed nutrient concentrations, the three most inner stations (4 - 6) very likely did not suffer from nutrient deficiency; the situation for station 3 is not clear.

11.6.5 Possible reasons not considered

It must be noted that in any ecosystem there exist a lot of feedbacks; these have not been considered in this study. A most important one, also stressed in ecosystem modelling studies like the one by Brinkman (2013), is grazing by shellfish (and/or other organisms). Grazers on the one hand depend on food availability, but will also affect food concentration. Therefore, conclusions on increasing or decreasing primary production –and secondary production- are especially meaningful if such feedback mechanisms are fully accounted for.

11.7 Question: are there geographical variations and/or temporal variations in the limitation of the growth of algae within the estuary?

11.7.1 Information

The answer is based on the nutrient and suspended matter concentrations measured.

11.7.2 Temporal variations in limitations

Nutrient limitations are most obvious at both outer stations at the end of spring, begin summer. At the inner stations, nutrient limitation is not likely at all.

Light limitation occurs in the whole estuary, but at the outer stations it mostly exist at the beginning of the phytoplankton growing season, and in late summer. At the inner stations, light limitation occurs throughout the year.

11.8 Question: is there a substantial contribution of microphytobenthos to the water column algae?

11.8.1 Information

Based on phytoplankton analyses on a species level a distinction between pelagic and benthic algae could be made (section 8.10).

11.8.2 Contribution of microphytobenthos to pelagic algae

At the outer stations, benthic algae make of 15% (summer)-40% (winter) of the pelagic algae volumes; in the inner area these fractions are around 50%. These data were found for 2013. So it can be concluded that especially in the inner area phytobenthos contributes substantially to the algal biomass of the water column.

11.9 Recommendations

Based on the present research, recommendations are listed. Note that the methods and procedure chosen were also limited by the financial possibilities. Partly, the recommendations concern extension of the measurements, and thus have budget implications.

1: the fluorometric analysis (and subsequent computation) of chlorophyll-a and pheophytin. The method was calibrated against chlorophyll-a standard solutions, but not against pheophytin standards. The algorithm used is rather sensitive to errors: an error in the pheophytin measurements directly affects the chlorophyll-a result. It is recommended to use pheophytin standard as well.

2: the carotenoid:chlorophyll adsorption ratio was supposed to give information whether phytoplankton growth was nutrient or light limited. Afterwards it appeared that it had been better to test this method better; the results now can hardly be interpreted the way they were meant to. To detect the limiting factor, incubations with several nutrient additions are needed. A second possibility is to apply a bacteria based test as described by Kuipers & Van Noort (2008).

3: measuring benthic primary production is difficult; it would have been better to apply and the present method, and the one used by Colijn. Next to that, there are other methods to assess benthic primary production, and such methods need to be considered as well; not instead of, but additional to the present method.

4: the continuous measurement of light attenuation (C-Star1 & 2) was successful, but in the most turbid areas even the shortest light pathway sensor available (C-Star1) appeared to be too long. An even shorter sensor (2-3 cm) is needed to cover the most turbid areas.

5: the PocketBox was equipped with two sensors that measured Coloured Dissolved Organic Matter: the Cyclops CDOM-sensor and the AOA-Yellow Substance sensor. They both should gave similar results, but they did not. It is necessary to calibrate both sensors against the same standards.

6: flow cytometer analyses appear promising, but need much more time to come to reliable results; combination with algae cell counts probably is needed.

7: despite the observation that the pelagic primary production incubations went OK, it is advised to include other methods as check, such as an oxygen optode detection and/or chlorophyll activity detection with a pulse-amplitude modulation method (PAM).

8: computation of benthic primary production is rather sensitive to the estimated light penetration in (and attenuation of) the sediment top layer and to benthic diatom motility. More attention is to be paid to assess these sediment top layer characteristics.

9: to find out whether light or nutrient are phytoplankton growth limiting, incubations with different nutrient additions could have been performed. A second possibility is after the bacteria activity tests following Kuipers & Van Noort (2008).

10: Dissolved inorganic carbon. For the present situation the method followed is OK. However for investigations in other systems with where high pH-values occur, very precise pH measurements are needed. This was not the case in the Ems-Dollard estuary.

11: Benthic chlorophyll-a, after spectrophotometric analyses. It is recommended to i) test the method better, ii) to analyse sedimentary chlorophyll-a content not only in one slice (5 mm in the present case), but to separate the sediment core into 2 mm slices and analyse chla in each slice and iii) always apply at least two analysis methods (the BenthoTorch data gave us a possibility to validate the laboratory analyses (to a certain extend)).

Microphytobenthos content (and thus benthic chlorophyll values) also depends on grazer activity. It is recommended to pay sufficient attention to the numbers and activity of benthic grazers.

12: Model studies are required that include directly the effect of changing river runoff, nutrient discharges and feedback mechanisms that exist in the Ems-Dollard ecosystem (as in any ecosystem) like the presence of grazers in the system.

13: A weak point of *any* temporal extrapolation and interpolation is that the time constant for microphytobenthos is small, and thus, changes can be large between –and in between- two sampling dates. Also, spatial variations can be large, and thus, the uncertainty in the final result is considerable. Although we cannot quantify it. These considerations make it hard when a comparison with Colijn & De Jonge (1984) has to be made. We know now that the large differences observed mainly are a result of different chlorophyll-a densities between now and 1976-1978. What we do not know is *why* these chlorophyll-a densities are much lower than they were in 1976- 1978 and 1992-1999. It is known from De Boer (2000) that also in the ’90-s large differences occurred, and that might be the case now. It is also known that grazers may largely affect phytobenthic abundance, but data on zoobenthos abundance fail completely. Thus, main recommendations are:

- Be sure that microphytobenthos is know well; use more than one analysis method
- Use more than one method to determine benthic primary production. If a comparison with other results is at stake, be sure to use also to same method
- Pay attention to the benthic light attenuation
- Pay attention to zoobenthic abundance and grazing activity
- Determine benthic chlorophyll-a not only in one sediment slice, but find the depth profile.
- Sample trajects from high to low sites in the tidal zones

14: In this research, at each site one sample was taken. Mostly from the PocketBox water, so it is not a sample at one particular site, but a suggestion is to sampling a track. Then, a more representative water sample for a certain area is obtained.

12 References

Admiraal W. 1984. The ecology of estuarine sediment-inhabiting diatoms. In: F.E. Round & D.J. Chapman (eds.), Progress in Phycological Research, Vol.3, pp. 269-322, Biopress, Bristol.

Admiraal W & Peletier H. 1980. Distribution of diatom species on an estuarine mudflat and experimental analyses of the selective effect of stress. J Exp Mar Biol Ecol 46.157-175.

Admiraal W, Peletier H & Zomer H, 1982. Observations and experiments on the population dynamics of epipellic diatoms from an estuarine mudflat. Estuar Coast Shelf Sci 14:471-487.

Admiraal W, Peletier H & Brouwer T, 1984. The seasonal succession patterns of diatom species on an intertidal mudflat: an experimental analysis. Oikos 42:30-40.

Armitage AR & Fong P. 2004, Upward cascading effects of nutrients: shifts in a benthic microalgal community and a negative herbivore response, Oecologia, 139, 560-567

Azam F, Fenchel T, Field JG, Gray JS, Meyer-Reil LA & Thingstad F . 1983. The Ecological Role of Water-Column Microbes in the Sea. Mar. Ecol.Progr. Ser. 10(3): 257-263.

Baillie PW & Welsh BL, 1980. The effect of tidal resuspension on the distribution of intertidal epipelic algae in an estuary. Estuarine Coastal Mar. Sci., 10: 165 -180.

Baretta J & Ruardij P. 1988. Tidal flat estuaries. Springer Verlag. Berlin.353 pp.

Baretta JW & Malschaert JFP. 1988. Distribution and abundance of the zooplankton of the Ems estuary (North Sea). Neth. J. Sea Res. 22 (1), 69-81

Bates DM & Chambers JM. 1992 *Nonlinear models.* Chapter 10 of *Statistical Models in S* eds Chambers JM and Hastie TJ, Wadsworth & Brooks/Cole.

Billerbeck M, Roy H, Bosselmann K, Huettel M . 2007, Benthic photosynthesis in submerged Wadden Sea intertidal flats, Estuary Coastal Shelf Science, 71, 704-716

Bissinger JE, Montagnes DJS, Sharples J & Atkinson D. 2008. Predicting marine phytoplankton maximum growth rates from temperature: Improving on the Eppley curve using quantile regression. Limnol. Oceanogr. 53(2): 487-493

Blanchard GF, Guarine JM, Orvain F & Sauriau P. 2001, Dynamic behaviour of benthic microalgal biomass in intertidal mudflats, Journal of Exp. Mar. Biol. Ecol., 264, 85-100

Blanchard GF, Simon-Bouhet B & Guarini J-M. 2002 Properties of the dynamics of intertidal microphytobenthic biomass. J Mar Biol Ass UK 82:4077/1-2.

BOEDE, 1985. Biological research Ems-Dollard estuary. Rijkswaterstaat Communications no. 40/1985, The Hague. 182 pp.

Brinkman AG. & Van Raaphorst W, 1986. De fosfaathuishouding in het Veluwemeer. PhD thesis, Twente Univ. Technology. 700 pp.

Brinkman AG. 2008. Nutriënt- en chlorofylgehaltes in het westelijke en oostelijke deel van de Nederlandse Waddenzee; waarden en trends tussen 1980 en 2005 en mogelijke oorzaken daarvan.

Brinkman AG. 2013. Modelling the effects of mussel seed collectors on the Wadden Sea ecosystem. Wageningen, IMARES Report number C061/13. 160pp

Broecker WS. 1974. Chemical Oceanography. Harcourt Brace Jovanovich Inc. 214 pp.

Brunet C, Brylinski JM & Lemoine Y. 1993. In situ variations of the xanthophylls diatoxanthin and didinaxanthin: photoadaptation and relationships with a hydrodynamical system in the eastern English Channel. Mar. Ecol. Progr. Ser. 102: 69-77

Cadee GC & Hegeman J. 1974. Primary production of benthic microflora living on tidal flats in the Dutch Wadden Sea, Neth. Journal of Sea Research, 8(2-3), 260-291

Cadée GC. 1976. Sediment reworking by Arenicola marina on tidal flats in the Dutch Wadden Sea, Netherlands Journal of Sea Research, 10, 440-460

Cahoon LB. 1999. The role of benthic marine microalgae in neritic ecosystems, Oceanography Marine Biology; Annual rev. 37, 47-86

Cahoon LB & Safi KA. 2002. Distribution and biomass of benthic microalgae in Manukau Harbour, New Zealand, New Zealand Journal of Marine and Freshwater research, vol. 36, 258-266

Chambers JM. 1992 Linear models. Chapter 4 of Statistical Models in S eds J. M. Chambers and T. J. Hastie, Wadsworth & Brooks/Cole.

Cibic T, Blasutto O, Burba N & Umani SF. 2008. Microphytobenthic primary production as C-14 uptake in sublittoral sediments of the Gulf of Trieste (northern Adriatic Sea): Methodoogical aspects and data analyses, Estuar. Coast. Shelf Science, 77, 113-122

Cloern JE. 2001. Our evolving conceptual model of the coastal eutrophication problem, Mar. Ecol. Progr. Ser, 210, 223-253

Colijn F. 1983 Primary production in the Ems-Dollard estuary. Ph. D. Thesis, Groningen, The Netherlands, 123 pp.

Colijn F & Dijkema KS. 1981. Species Composition of Benthic Diatoms and Distribution of Chlorophyll a on an Intertidal Flat in the Dutch Wadden. Marine Ecology Progress Series, 4, 9-21.

Colijn F & De Jonge VN. 1984. Primary production of microphytobenthos in the Ems-Dollard Estuary. Marine Ecology Progress Series, 14, 185-196. doi: 10.3354/meps014185.

Colijn F, Admiraal W, Baretta JW & Ruardij P. 1987. Primary Production in a Turbid Estuary, the Ems-Dollard Fieldand Model Studies. Continental Shelf Research 7(11-12): 1405-1409.

Consalvey M, Paterson DM & Underwood GJC (2004), The ups and downs of life in a benthic biofilm: migration of benthic diatoms, Diatom Research, 19 (2), 181-202 DOI: 10.1080/0269249X.2004

Darley WM 1977. Biochemical composition. In D Werner, ed: The biology of diatoms. Botanical Monographs Vol 13, 198-223. Blackwell Scient. Publ. Oxford.

De Boer WF, 2000. Ontwikkeling van de biomassa van het microfytobenthos in het Eems-Dollard estuarium in de periode 1992-1999. Koeman en Bijkerk bv, Rapportnr 2000-31.

De Jonge VN, 1980. Fluctuation in the organic carbon to chlorophyll-a ratios for estuarine benthic diatom populations. Mar. Ecol. Prog, Ser. 2: 345-353

De Jonge VN, 1985. The occurrence of 'epipsammic' diatom populations: a result of interaction between physical sorting of sediment and certain properties of diatom species. Estuarine Coastal Shelf Sci., 21: 607-622.

De Jonge VN & Essink K, 1991. Long-term changes in nutrient loads and primary and secondary production in the Dutch Wadden Sea. In: M. Elliott & J.P. Ducrotoy (eds.). Estuaries and coasts: spatial and temporal intercomparisons, Olsen & Olsen International Symposium Series, 307-316.

De Jonge VN & Essink K, 1992. Lange-termijnveranderingen in nutriëntenbelasting en daarmee gepaard gaande primaire en secundaire productie in de Nederlandse Waddenzee. RWS-rapport DGW-92.002

De Jonge VN. 1992. Physical processes and dynamics of microphytobenthos in the Ems estuary (The Netherlands). PhD. Thesis, University of Groningen, 176 pp.

De Jonge VN and Van Beusekom JEE. 1992. Contribution of resuspended microphytobenthos to total phytoplankton in the Ems estuary and its possible role for grazers, Netherlands Journal of Sea Research, 30, 91-105

De Jonge VN & Colijn F. 1994. Dynamics of microphytobenthos biomass in the Ems estuary. Mar.Ecol. Prog. Ser. 104: 185-196

De Jonge VN , 1995a. Wind driven tidal and annual gross transports of mud and microphytobenthos in the Ems estuary, and its importance for the ecosystem. In: K.R. Dyer & C.F. D'Elia, eds.) Changes in fluxes in estuaries, 29-40.

De Jonge VN, 1995b. The Ems Estuary. A case study, 81-107. In: A.J.McComb (ed.) Eutrophic Shallow Estuaries and Lagoons, CRC-Series, CRC Press. 240 pp.

De Jonge VN & Van Beusekom JEE, 1995. Wind and tide induced resuspension of sediment and microphytobenthos from tidal flats in the Ems estuary. Limnol. Oceanogr. 40: 766-778.

De Jonge VN , 2000. Importance of temporal and spatial scales in applying biological and physical process knowledge in coastal management, an example for the Ems estuary. Continental Shell Research 20: 1655-1686.

De Jonge VN and De Jong DJ. 2002. Global impact of inter-annual variation in water discharge as a driving factor in dredging and spoil disposal in the river Rhine system and of turbidity in the Wadden Sea, Estuarine, Coastal and Shelf Science, 55, 969-991

De Jonge VN and Brauer VS. 2006. The Ems Estuary: Changes in functioning and structure of a system under pressure. Report RUG 7032007; 99 pp.

De Jonge VN, De Boer WF, De Jong DJ & Brauer VS. 2012. Long-term mean annual microphytobenthos chlorophyll a variation correlates with air temperature. Mar Ecol Progr Ser 468: 43-56

De Wolf P, et al., 1979. Samenvattingen van de voordrachten over de biologie van het Eems Dollard estuarium gehouden op de informatiedag BOEDE. 46 pp.

Du GY, Oak JH, Li H & Chung IK. 2010. Effect of light and sediment grain size on the vertical migration of benthis diatoms. Algae 25(3) 133-140.

Dube T. 2012. Primary productivity of intertidal mudflats in the Wadden Sea: a remote sensing method. University of Twente, Master thesis, 55pp.

Eppley RW. 1972. Temperature and phytoplankton growth in the sea. Fish. Bull. 70: 1063–1085

Essink K & Esselink P. 1998. Het Eems-Dollard estuarium: interacties tussen menselijke beïnvloeding en natuurlijke dynamiek. Rijkswaterstaat, rapport RIKZ-98.020.

Essink K. 2009. Stormvloed 1509. Geschiedenis van de Dollard. Lezing Stichting Verdronken Geschiedenis op het Ubbo Emmius Gymnasium Leer (Ost-Friesland).

Flintrop P, Prins H & Ruiter H. 2002. Het is groen en verandert- meer dan vijfentwintig jaar chlorofylanalyses – RWS-RIZA Werkdocument 2002.148X

Fofonoff NP & Millard RC Jr. 1983. Algorithms for computation of fundamental properties of seawater. UNESCO technical papaers in marine science 44. 53pp.

Glud RN, Kühl M, Wenzhöfer F & Rysegaard S. 2002. Benthic diatoms of a high Arctic Fjord (Young Sound, NE Greenland): importance of ecosystem primary production, Marine Ecology Progress Series, 238, 15-29

Golterman HL, 1975. Physiological limnology. Elsevier Scien. Publ. Comp. 489 pp.

Gould DG & Gallagher ED. 1990. Field measurement of specific growth rate, biomass and primary production of benthic diatoms of Savin Hill Cove, Boston. Limnol. Oceanogr. *35*: 1757-1770

Grunwald M, Dellwig O, Kohlmeier C, Kowalski N, Beck M, Thomas H. Badewien Th H, Kotzur S, Liebezeit G & Brumsack H-J. 2010. Nutrient dynamics in a back barrier tidal basin of the Southern North Sea:Time-series, model simulations, and budget estimates. Journal of Sea Research 64 199-212

Harrison SJ. 1985. Heat exchanges in muddy intertidal sediments, Chichester Harbour, West Sussex, England, Estuary, Coastal and Shelf Science, 20, 477-490

Havaux M & Niyogi KK. 1999. The violaxanthin cycle protects plants from photooxidative damage by more than one mechanism. Proc. Natl. Acad. Sci USA. 96: 8762-8767 (Plant Biology)

Hoek, C. van den, W. Admiraal, F. Colijn & V.N. de Jonge, 1979. The role of algae and seagrasses in the ecosystem of the Wadden Sea: A review, p. 9-118. In: W.J. Wolff (ed.) Flora and vegetation of the Wadden Sea, Stichting Veth tot steun aan waddenonderzoek, Leiden.

Holm-Hansen O, CJ Lorenzen, RW Holms &JDH Strickland. 1965. Fluorometric Determination of Chlorophyll. J. Cons.perm.int Explor. Mer. 30: 3-15.

Hopkins JT. 1963. A study of the diatoms of the Ouse estuary, Sussex (I). The movement of mudflat diatoms in response to some chemical and physical changes. J. Mar. Biol. Assoc. U.K. 43: 653-663

Hoppenrath M, Elbrachter M & Drebes G. 2009. Marine phytoplankton. Kleine Senckenberg-Reihe 49. Schweizerbart'sche Verlagsbuchhandlung, 264 pp.

Ichimi K, Tada K & Montani S. 2008. Simple estimation of penetration rate of light in intertidal sediments. Journal of Oceanography (64): 399-404

Jak RG & R Riegman. 2012. Primary Production Measurements Ems-Dollard Interim Report 2012 (Final Concept Report IMARES)

Jesus, B., V. Brotas, M. Marani & D.M. Paterso. 2005. Spatial dynamics of microphytobenthos by PAM fluorescence, Estuarine, Coastal and Shelf Science, 65(1), 30.42

Kamermans, P. 1992. Growth limitation in intertidal bivalves of the Dutch Wadden Sea. PhD-thesis Univ Groningen, 135 pp.

Kirk JTO. 1994. Light and photosynthesis in aquatic ecosystems. Cambridge Univ. Press. 2nd ed. 509 pp.

KNMI, 2015. Royal Netherlands Meteorological Institute. Hourly meteorological data.

Kromkamp JC, Barranguet C & Peene J. 1998. Determination of microphytobenthos PSII quantum efficiency and photosynthetic activity by means of variable chlorophyll, Marine Ecology Progress Series, 162, 45-55

Kromkamp JC & Forster RM. 2006. Developments in microphutobenthos primary productivity studies, in: Kromkamp JC, De Brouwer JFC, Blachard GF, Forster R, Creach V, editors, Functioning of Microphytobenthos in Estuaries, Amsterdam, Royal Netherlands Academy of Arts and Sciences, pp. 9-30.

Kühl M, Lass C & Jørgenson BB. 1994. Light penetration and light intensity in sandy marine sediments measured with irradiance and sclara irradiance fiber-optic microprobes. Mar Ecol Progr Ser 105: 139-148

Kuipers BR & Van Noort GJ. 2008. Towards a natural Wadden Sea? J Sea Res. 60: 44-53

Lake SJ & Brush MJ (2011), The contribution of microphytobenthos to total productivity in upper Narragansett Bay, Rhode Island, Estuarine, Coastal and Shelf Science, 95, 289-297

Lampert W & Sommer U. 1993. Limnoökologie. Georg Thieme Verlag Stuttgart. 439 pp.

Larson F & Sundback K. 2008. Role of microphytobenthos in recovery of functions in a shallow-water sediment system after hypoxic events, Mar. ecol. Prog. Ser., 357, 1.16

Lingeman-Kosmerchock, M.. 1978. The contents of nitrogen, phosphorus, and silicon in phytoplankton cells. Delft Hydraulics Laboratory & Amsterdam University, limnological laboratory Rep. R 1310

Loebl M, Colijn F, Van Beusekom JEE, Baretta-Bekker JG, Lancelot Chr, Philippart CJM, Rousseau V, Wiltshire KH. 2009. "Recent patterns in potential phytoplankton limitation along the Northwest European continental coast." Journal of Sea Research **61**(1-2): 34-43.

Lorenzen CJ. 1967. Determination of chlorophyll and pheo-pigments: spectrophotometric equations. Limnol. Oceanogr. 12: 343-346.

MacIntyre HL & Cullen JJ. 1995. Fine-scale vertical resolution of chlorophyll and photosynthetic parameters in shallow-water benthos. Mar Ecol Prog Ser. 122: 227-237

McGlathery KJ, Sundback K & Fong P. 2013. Estuarine benthic algae, in: estuarine ecology, 2nd edition, J.W. Day, B.C. Crump, W.M. Kemp and A. Yánez-Arancibia, Wiley-Blackwell

MacIntyre HL, Geider RJ and Miller DC. 1996. Microphytobenthos: the ecological role of the “secret garden” of unvegetated, shallow-water marine habitats. 1. Distribution, abundance and primary production, Estuaries, 19, 186-201

Malkin SY, Kromkamp JC & Herman PM (in prep.) Primary production in the Oosterschelde: an analysis of historical data, size distribution and effect of grazing pressure.

Merckelbach LM & Eysink WD, 2001. Trendanalyse zwevend stof in Eems estuarium in relatie tot aanslibbing haven Delfzijl. WL Delft hydrolics.

Miller DC, Geider RJ & MacIntyre HL. 1996. Microphytobenthos: The ecological Role of the ‘Secret garden’of unvegetated, shallow-water marine habitats, Estuaries, vol. 19 (No2A), 202-212

Morris EP & Kromkamp JC. 2003. Influence of temperature on the relationship between oxygen- and fluorescence-based estimates of photosynthetic parameters in a marine benthic diatom (Cylindrotheca closterium, European Journal of Phycology, 38, 133-142

Orvain F, Le Hir P, Sauriau P-G & Lefebre S. 2012. Modelling the effects of macrofauna on sediment transport and bed elevation: application over a cross-shore mudflat profile and model validation, Estuarine, Coastal and Shelf Science, 108, 64-75

Peletier H. 1996. Long-term changes ion intertidal estuarine diatom assemblages related to reduced input of organic waste. Mar Ecol Prog Ser 137:265-271.

Philippart CJM, Beukema JJ, Cadée GC, Dekker R, Goedhart PW,Van Iperen JM. 2007. Impacts of Nutrient Reduction on Coastal Communities. Ecosystems DOI: 10.1007/s10021-006-9006-7

R Core Team, 2013. R: A language and environment for statistical computing. R Foundation for Statistical Computing, Vienna, Austria. ISBN 3-900051-07-0, URL http://www.R-project.org/.

Rasmussen MB, Hendriksen K and Jensen A. 1983. Possible causes of temporal fluctuations in primary production of microphytobenthos in the Danish Wadden Sea, Marine Biology, 73, 109-114

Riegman R, Colijn F, Malschaert JFP, Kloosterhuis HT & Cadée GC. 1990. Assessment of Growth-Rate Limiting Nutrients in the North-Sea by the Use of Nutrient-Uptake Kinetics. Neth.J. Sea Res. 26: 53-60.

Riegman R & F Colijn. 1991. Evaluation of measurements and calculation of primary production in the Dogger Bank area (North Sea) in summer 1988. Mar. Ecol. Prog. Ser. 69: 125-132.

Riegman R, Kuipers BR, Noordeloos AM & Witte HJ. 1993. Size-differential control of phytoplankton and the structure of plankton communities. Neth. J. Sea Res. 31 (3): 255-265

Riegman R & Rowe A. 1994. Nutritional-Status and Pigment Composition of Phytoplankton during Spring and Summer Phaeocystis Blooms in Dutch Coastal Waters (Marsdiep-Area). Neth. J. Sea Res. 32: 13-21.

Riegman R, Flameling IA &, Noordeloos AAM. 1998. "Size-fractionated uptake of ammonium, nitrate and urea and phytoplankton growth in the North Sea during spring 1994." Marine Ecology-Progress Series **173**: 85-94.

RIKZ. 1998. Sedimentatlas Waddenzee. Ministry of Transport, Public Works and Water Management/National Institute for Coastal and Marine Management (RIKZ), Haren (CD ROM)

Riley GA. 1957. Phytoplankton in the North Central Sargasso Sea, 1950-1952. Limnol. Oceanogr. 2: 252-270.

RWS. 2013. http://www.rijkswaterstaat.nl

Saburova, M.A. and I.G. Polikarpov. 2003. Diatom activity within soft sediments: behavioural and physiological processes, Marine Ecological Progress Series, 251, 189-207

Spilmont N, Seuront L, Meziane T & Welsh DT. 2011. There’s more to the picture than meets the eye: Sampling microphytobenthos in a heterogenous environment, Estuarine, Coastal and Shelf Science, 95, 470-476

Spiteri C, Riegman R, Winterwerp H, Brinkman B, Stolte W, Jak R & Van Maren B. 2011. Mud dynamics in the Eems-Dollard, research phase 1. Literature review mud and primary production. Report Deltares, IMARES. Project 1204891-000.

Sundback K & McGlathery K. 2005. Interactions between benthic macroalgal and microalgal mats, In: Kristensen E, Haese RR & Kostka JE (eds), Interactions between macro- and microorganisms in marine sediments, AGU series: Coastal and Estuarine Studies, vol. 60, 7-29

Stal LJ. 2010. Microphytobenthos as a biogeomorphological force in intertidal sediment stabilization, Eco. Eng. Journal, Vol. 36, 236-245

Stutes AL, Cebrian J & Corcoran AA. 2006. Effects of nutrient enrichment and shading on sediment primary production and metabolism in eutrophic estuaries, Marine ecology progress series, 312, 29-43

Toming K, Arst H, Paavel P, Laas A & Nõges T. 2009. Spatial and temporal variations in coloured dissolved organic matter in large and shallow Estonian waterbodies Boreal Environment Research 14: 959-970

Underwood GJC & Kromkamp J. 1999. Primary production by phytoplankton and microphytobenthos in estuaries, Adv. Ecol. Res, 29, 93-153

Van Beusekom JEE & De Jonge VN. 1998. "Retention of phosphorus and nitrogen in the Ems estuary." Estuaries **21** (4A): 527-539.

Van der Wal D, Van Kessel Th, Eleveld MA & Vanlede J. 2010. Spatial heterogeneity in estuarine mud dynamics, ocean dynamics, 60, 519-533

Van der Werff A. 1960. Die Diatomeen des Dollart-Emsgebietes. Verh. Kon. Ned. Geol. Mijnbouwk. Gen., Geol. Ser. 19: 153-201.

Van Maren B, Riegman R, Stolte W, Brinkman B, Spiteri C & Jak J. 2011. Mud dynamics in the Eems-Dollard, research phase 1. Working plan phase 2 and 3. Report Deltares, IMARES. Project 1204891-000.

Van Maren B, Vroom J, Sittoni L, Van Kessel Th, Cronin K & Arentz L. 2014a. Mud dynamics in the Eems-Dollard, phase 2 Setup sediment transport models. Deltares Report 2014.

Van Maren B, Stolte W, Sittoni L, Vroom J, & Arentz L. 2014b. Mud dynamics in the Ems Estuary, phase 2 Model analysis, final report. Deltares Report 2014

Verity PG, Robertson CY, Tronzo CR, Andrews MG, Nelson JR & Sieracki ME. 1992. Relationship between cell volume and the carbon and nitrogen content of marine photosynthetic nanoplankton. Limnol, Oceanogr. 37: 1434-1446

Vroom J, Van den Boogaard H & Van Maren B. 2012. Mud dynamics in the Ems-Dollard, research phase 2. Analysing existing data. Deltares report 1205711-001

Wanink JH, Bijker R & Brochard CJE. 2014. Phytoplankton of the Ems-Dollard estuary 2013. Koeman en Bijkerk BV. Report 2014-015.

Waterbase (2014). http://live.waterbase.nl/waterbase_wns.cfm?taal=nl

Werner D. 1971. Der Entwicklungscyclus mit Sezualphase bei der marinen Ditaomee Coscinodiscus asteromphalus. II. Oberflächenabhängige Differenzierung während der vegetativen Zellverkleinerung. Arch. Mikrobiol. 80: 115-133

Wickliff JL & Aronoff S. 1963. Degradation of chlorophyll-a to pheophytin a, pheophorbide a, and pyrroporphin XV for tracer studies.

Williams WD. 1986. Conductivity and Salinity of Australian Salt Lakes. Aust.I.Mar. Freshw. Res. 37: 177-82.

Wolff WJ (ed.) Flora and vegetation of the Wadden Sea, Stichting Veth tot steun aan waddenonderzoek, Leiden.

Wooster WS, Lee AJ & Dietrich G. 1969. Redefinition of salinity. Int. Mar. Sci., 7(1): 4-5.

Wright SW & Jeffery SW. 1987. Fucozanthin pigment markers of marine phytoplankton analysed by HPLC and HPTLC. Mar. Ecol. Progr. Ser. 38: 259-266. Analytical biochemistry 6: 39-46

Zwarts L. 2004. Bodemgesteldheid en mechanische kokkelvisserij in de Waddenzee. RIZA Lelystad. Rapport RIZA/2004.028

Addendum 1: Primary production equations

A1.1 Eilers_Peeters equation (Eilers & Peeters, 1981)

The Eilers-Peeters equation is:

$$PB = \frac{I}{aI^2+bI+c} \quad \text{(A1)}$$

PB here is the specific productivity at the actual radiance I, (mg C (mg Chla)$^{-1}$ h^{-1})

1/c is the initial slope of the line (mg C (mg Chla)$^{-1}$ h^{-1} (W m^{-2})$^{-1}$)

This can be checked by

$$\frac{dPB}{dI} = \frac{1}{aI^2+bI+c} + \frac{I(-2aI-b)}{(aI^2+bI+c)^2} \quad \text{(A2)}$$

or, to put it in one term

$$\frac{dPB}{dI} = \frac{aI^2+bI+c-2aI^2-bI}{(aI^2+bI+c)^2} = \frac{-aI^2+c}{(aI^2+bI+c)^2} \quad \text{(A3)}$$

At I=0, it follows that dPB/dI= c/c^2 = 1/c.

From the first measurements (at low light intensities), a slope can be computed, and this is equal to 1/c; this gives the initial estimate for c.

The maximum PB-value is reached at I_m, where d(PB)/dI = 0,

and thus,

$$\frac{dPB}{dI} = \frac{-aI_m{}^2+c}{(aI_m{}^2+bI_m+c)^2} = 0 \quad \text{(A4)}$$

and thus,

$$-aI_m{}^2 + c = 0 \rightarrow \quad I_m{}^2 = \frac{c}{a} \rightarrow \quad I_m = \sqrt{\frac{c}{a}} \quad \text{(A5)}$$

From this, it follows that a first guess for a= c/I_m^2.

And an initial estimate for b finally follows from the value of PB_{max}, with a= c/I^2_{PBmax} substituted, and it follows that

$$b = \frac{1}{PB_{max}} - aI_m - \frac{c}{I_m} \rightarrow b = \frac{1}{PB_{max}} - \frac{c.I_m}{I_m{}^2} - \frac{c}{I_m} \rightarrow b = \frac{1}{PB_{max}} - \frac{2c}{I_m} \quad \text{(A6)}$$

And PB_{max} follows from

$$PB_{max} = \frac{\sqrt{\frac{c}{a}}}{a\frac{c}{a}+b\sqrt{\frac{c}{a}}+c} = \frac{\sqrt{\frac{c}{a}}}{2c+b\sqrt{\frac{c}{a}}} = \frac{1}{2\sqrt{ac}+b} \quad \text{(g C g}^{-1}\text{ Chla h}^{-1}\text{)} \quad \text{(A7)}$$

A common problem for this equation –with an optimum- is that the data *have* to include very high light intensities (sufficiently above I_m), otherwise the parameter estimation routine will fail to produce correct results.

A1.2 PBmax and α

Colijn (1983) also mentions PB_{max} and α as photosynthetic parameters. PB_{max} is explained above, α is nothing else than the slope at zero light intensity (I=0), thus α=1/c (from the Eilers-Peeters equation).

Units: PB_{max}: g C g^{-1} Chla h^{-1}, α: g C g^{-1} Chla h^{-1} (µE $m^{-2}s^{-1})^{-1}$

A1.3 Case: there is no maximum

If a maximum is not reached, the estimation of a is not really possible. In that case, a is set to 0, and equation (A1) turns into a simple Monod-equation and only the two parameters b and c have to be found. The initial slope stays the same (1/c), and PB_{max} from eq(A7) becomes: PB_{max}= 1/b.

A1.4 Minimizing with respect to a, b and c.

The non-linear parameter estimation routine NLS (from R) minimises the sum-of-squares SumSQ:

$$SumSQ = \sum_1^M (Obs_i - Pred_i)^2 \qquad \text{(A8)}$$

This implies that at the end, d(SumSQ)/da = d(SumSQ)/db = d(SumSQ)/dc =0.

A1.5 Connection to a Monod-equation

Results from the Eilers-Peeters parameter estimation session can be used to provide Monod-parameters as well.

If the PI-relationship is assumed to follow a Monod-equation, this relationship is written as

$$Prod = P_{max} \frac{I}{I+M} \qquad \text{(mg C } m^{-2} \text{ (0.1 mm)}^{-1} \text{ } h^{-1} \text{)} \qquad \text{(A9)}$$

The Monod-parameter is the value of the light intensity ($I_{0.5}$) where 50% of the maximum production is reached.

Thus,

$$\frac{I_{0.5}}{I_{0.5}+M} = \frac{Prod}{P_{max}} = 0.5 \qquad \text{(A10)}$$

Written conform the Eilers-Peeters-equation:

$$\frac{I_{0.5}}{a{I_{0.5}}^2 + \mathrm{b}I_{0.5} + \mathrm{c}} = 0.5 \cdot P_{max} \qquad \text{(A11)}$$

or

$$I_{0.5} = 0.5 \cdot P_{max} \left(a{I_{0.5}}^2 + \mathrm{bI}_{0.5} + \mathrm{c}\right) \quad \text{(A12)}$$

With

m = 0.5 P_{max} a

n = 0.5 P_{max} b -1

p = 0.5 P_{max} c

it becomes

$$m{I_{0.5}}^2 + nI_{0.5} + p = 0 \quad \text{(A13)}$$

And thus, it simply follows that the light intensity $I_{0.5}$ where P = 0.5 P_{max}

$$I_{0.5} = \frac{-n+\gamma\sqrt{n^2-4mp}}{2m} \;,\; \gamma = \pm 1 \quad \text{(uE m}^{-2}\text{ s}^{-1}\text{)} \quad \text{(A14)}$$

$I_{0.5}$ must be positive, and < I_m from eq(A4). In that case, γ the above equation should be -1. This is not directly clear from the equation, but it is simply checked.

In case there is no maximum value for the production (a=0), the equation is simplified to

$$I_m = \frac{0.5c}{1-0.5b} \quad \text{(uE m}^{-2}\text{ s}^{-1}\text{)} \quad \text{(A15)}$$

The Monod-term M is the same as the value for I_m.

A1.6 Connection to a Smith-equation

Results from the Eilers-Peeters parameter estimation session can be used to provide Smith-parameters as well.

If the PI-relationship is assumed to follow a Smith-equation, this relationship is written as

$$Prod = P_{max} \frac{\frac{I}{I_k}}{\sqrt{1+(\frac{I}{I_k})^2}} = P_{max} \frac{I}{\sqrt{I_k^2+I^2}} \quad \text{(mg C m}^{-2}\text{ (0.1 mm)}^{-1}\text{ h}^{-1}\text{)} \quad \text{(A16)}$$

The equation has two unknown parameters: the maximum productivity P_{max} (mg C m^{-2} (0.1 mm)$^{-1}$ h^{-1}) and the Smith-parameter Ik (uE cm^{-2} s^{-1}). It is easy to see that at large I, Prod=P_{max}, and at small I Prod = P_{max}/I_k*I. Thus, the slope at I=0 is P_{max}/I_k.

The Eilers-Peeters analysis gives P_{max}, ánd the slope at I=0: it equals 1/c. Thus,

$$I_k = Pmax \cdot c \quad \text{(A17)}$$

And thus, for and the Monod-equation ánd the Smith-equation, the wanted parameter-values are the same. The difference can be found in the behaviour of the function at higher light intensities.

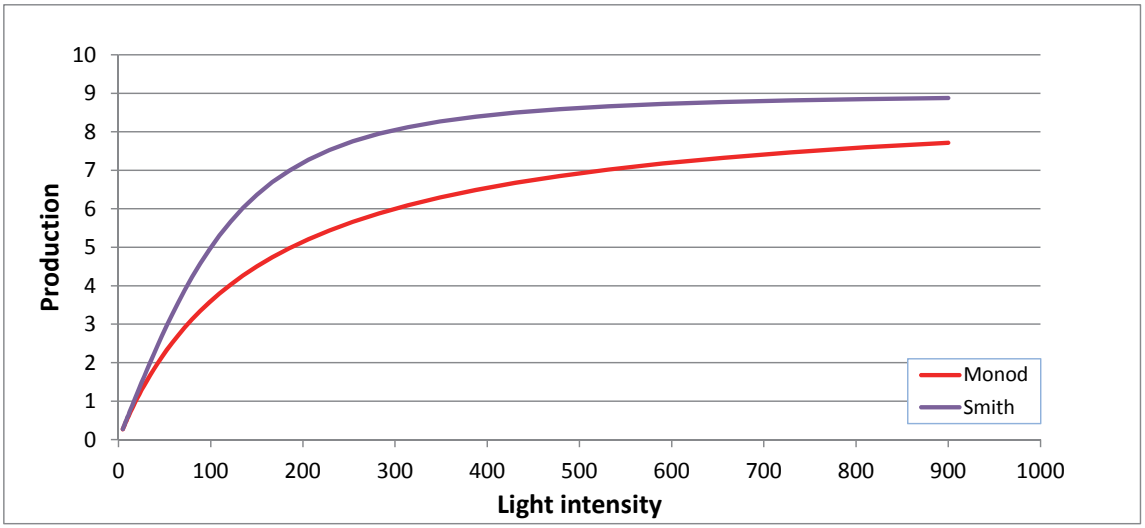

Figure 187 Differences between a Monod-approximation of the PI-curve and a Smith-approximation. In both cases, the parameters are the same (Pmax=9, Ik=M=150).

In Figure 187 it can be seen that a Smith-equation approaches the maximum value much faster than a Monod-equation does.

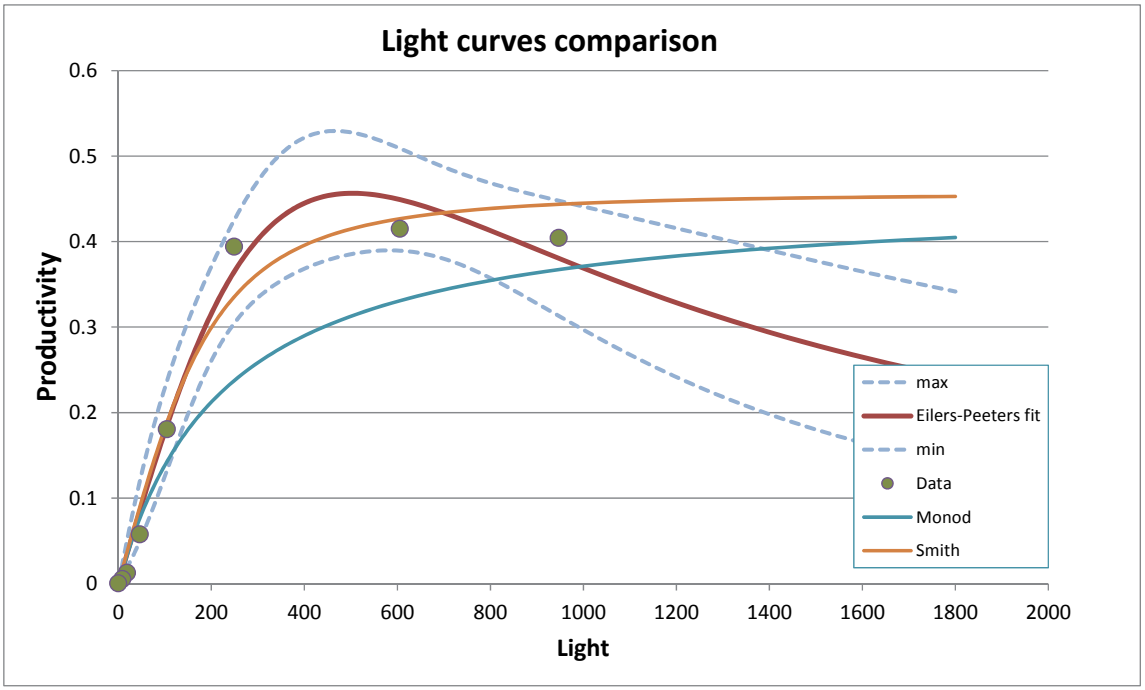

Figure 188 Light curves for benthic station1006, day 171 (2013-06-20). Data plus Eilers-Peeters fit, including the 95% confidence lines of the fit; and the Monod- and Smith-curves as they follow from the parameters derived from the Eilers-Peeters fit.

From this it has to be concluded that a separate parameter estimation for a Monod-approach, using the same observations, would result in different parameter values for P_{max} and M then when derived from the Eilers-Peeters parameters as sketched above.

For one situation the resulting Monod- and Smith-curves are sketched in Figure 188. The graph clearly shows that –in this case- the Monod-approach will give serious deviations from the measurements.

A2. HPLC-analyses WQI

HPLC_analyses were performed by the DHI/ Water Quality Institute in Denmark.

ilac-MRA DANAK
TEST Reg.nr. 0026

DHI

Agern Allé 5
DK-2970 Hørsholm
Denmark

Tel: +45 4516 9200
Fax: +45 4516 9292
E-mail: lsc@dhigroup.com
Web: www.dhigroup.com

Ref: lsc
Init: lsc

Date: 15-10-2013

IMARES - Ecosystems Department
P.O. Box 167
1790 AD Den Burg, Texel
The Netherlands

Att.: Hans Verdaat

Result of pigment analyses: Test report no. DAN/2013/035 from DHI: pigment analysis of 24 filter samples received in dry ice 18 September 2013.

Method:
The filters were transferred to vials with 6.00 mL 95% acetone with internal standard (vitamin E). The samples were mixed on a vortex mixer, sonicated on ice, extracted at 4°C for 20 h, and mixed again. The samples were then filtered through 0.2 µm Teflon syringe filter into HPLC vials, and placed in the cooling rack of the HPLC. 357 µl buffer and 143 µl extract were injected on the HPLC (Shimadzu LC-10A HPLC system with LC Solution software) using a pre-treatment program to mix in the loop before injection. The HPLC method used was the HPL method (Van Heukelem & Thomas, 2005. *In* Hooker et al., 2005, NASA Technical Memorandum). Internal method No.: SF No.: 30/852:02.

Results:
The pigment concentrations (µg/L) in each sample are shown in the table on page 2. α-carotene co-elutes partly with β-carotene and chlorophyll *c*1 co-elutes partly with chlorophyll *c*2, but the pigments were separated using the software of the HPLC. Chlorophyll c_1 was calculated by the response factor of chlorophyll c_2 (no standard for this pigment). The samples were somehow affected by degradation, since the concentrations of pheophytin *a* and pheophorbide *a* were higher than usually seen for water samples.

The limit of quantitation is approx. 0.002 µg/L. The uncertainty of the method is <1.0 %. The results will be stored on DHI. Please do not hesitate to contact us if you have any questions to the analyses, the method and the results.

Yours sincerely
DHI

Louise Schlüter, M.Sc., Ph.D.

Merete Allerup, Lab.Tech..

Test results relate only to the item(s) tested. *The test report may only be reproduced in extract, if the laboratory has approved the extract.*	Date: 15 October 2013 Report No.: DAN-2013-035 Page 1 of 2

A3. Marine phytobentos, a short literature overview

Contribution by Mascha Dedert

A3.1 Introduction

Microphytobenthos consists of unicellular algae and cyanobacteria that live on the upper few millimetres of illuminated sediment surfaces in coastal areas, such as estuaries. Generally, microphytobenthos is dominated by diatoms, followed in abundance by cyanobacteria, euglenoids, chlorophycean and dinophycean species (Cahoon, 1999). The estimations of primary productivity by MPB in estuaries vary from 27 to 234gC m-2/y (Underwood and Kromkamp, 1999). In comparison, phytoplankton primary productivity is calculated to vary from 7 to 875 27 to 234gC m-2/y. Despite the fact that estuarine microphytobenthos (MPB) can contribute up to 50% of the total estuarine carbon budgets (Underwood and Kromkamp, 1999), scientific research has predominantly focused on the pelagic phytoplankton. However, in recent years, it has become clear that the impact of microphytobenthos on ecosystem functioning is profound, covering aspects such as nutrient cycling (Underwood and Kromkamp, 1999), food web dynamics (Gould & Gallagher, 1990), and sediment stabilisation (Stal, 2010).

Microphytobenthos abundance and productivity is controlled by a range of conditions, varying from strong gradients in physical, fluid, sediment, chemical, and biological properties (Miller et al., 1996). As a means of mitigating the potential impact of damaging environmental conditions, benthic diatoms apply a migratory strategy. The main drivers of migration through the sedimentary column are light and tidal phases (Figure 1; Consalvey et al., 2004). In addition, migratory movement within the biofilm seems to provide the cells with an additional mechanism to prevent damage to the cell's functions through e.g. overexposure to potentially damaging light levels, high temperatures, desiccation and grazing, and has also been proposed as a means to avoid nutrient and/or CO2 limitation (Consalvey et al., 2004). Such strategies are thought to explain why photo inhibition rarely occurs in intact microphytobenthic biofilms (Rasmussen et al., 1983).

Estuarine ecosystems provide optimal conditions for the growth of benthic microalgae, given the high levels of irradiance reaching the bottoms and overall high availability of nutrients in such environments (Cahoon and Safi, 2002). MPB is a significant source of organic matter and thus an important contributor to the food web. The quantification of their role in carbon and nutrient cycling will add to understanding how this group of benthic producers affect their surrounding environment and ecology.

A3.2 Controls on biomass and productivity

Intertidal zones, such as estuaries, undergo large variations in environmental conditions. For example, tidal changes, erosion, exposure and submersion, will all affect the productivity and

biomass of MPB and result in differences in spatial and temporal distribution. MPB shows large

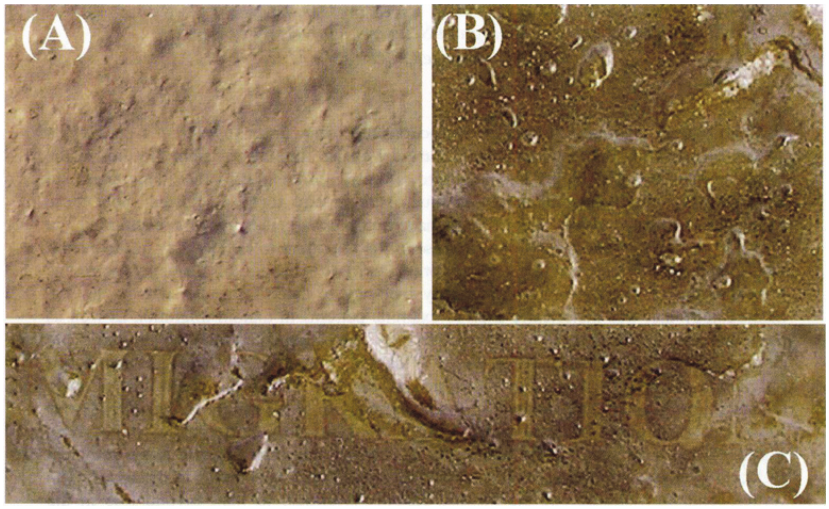

Fig. A3.1 Migration of benthic diatoms (source: Consalvey et al. 2004)

variations in biomass throughout year, with the highest biomass present in the summer and lowest amounts of biomass formed during the winter months (Van der Wal et al., 2010). Apart from these parameters, other bottom-up controls that mainly drive seasonal differences in MPB biomass cover temperature (Colijn and De Jonge, 1984), wind intensity and tidal currents. The sediment characteristics (i.e. grain size) is the main factor controlling the spatial distribution of MPB biomass. For example, the diatom assemblage composition appears to differ between different sediment types, resulting in variations in MPB biomass (Orvain et al., 2012). In addition to these physical factors, biological controls, notably grazing, function as a top-down control on MPB biomass (Blancard et al., 2001).

A3.3 Light

As for all other primary producers, microphytobenthos needs light for their photosynthesis process, using wavelengths covering the 400-700nm spectrum, which is known as the photosynthetic active radiation (PAR). Light is attenuated exponentially with depth depending on the attenuation coefficient, thus light available to MPB is tightly linked to the bathymetry of the system. The coefficient is affected by factors, for example, the amount of suspended particulate matter (SPM) in the waters or density of phytoplankton cells. Eutrophication can affect the light availability on the bottom through stimulating phytoplankton growth that attenuate light higher up in the water column. As a result, photosynthesis in benthic primary producers can be depressed. Another important process that decreases light availability at the bottom is the concentration suspended particulate matter (SPM) in the water column. Anthropogenic activities such as dredging (de Jonge & de Jonge (2002) can lead to increases of SPM as well as tidal currents that result in erosion of the upper bottom layers.

The Ems-Dollard waters are known for its high nutrient loads that can promote dense phytoplankton blooms. In addition to the attenuation of light intensity in the water column by these blooms, SPM is present in high concentrations in the Ems-Dollard, further reducing the amount of light reaching the bottom. As benthic primary production is largely controlled by nutrient concentrations and light intensity, any fluctuations in both parameters will result in changes in the productivity of microphytobenthos.

Overall, MPB has the ability to adapt to changes in light availability. Particularly, benthic diatoms seem to be able to adjust well and can survive periods of time with only a few percent of incident light (Larson and Sundback, 2008). In addition to migrating vertically, they can regulate their photosynthesis to prevalent light intensities (Glud et al., 2002). Light availability decreases to a few % within the upper few millimetres. This sharp decrease in light availability results a biofilm made up of layers of different benthic primary producers with each their own light intensity requirements; a top layer formed by diatoms, followed by cyanobacteria and finally by photosynthetic purple sulphur cyanobacteria (McGlathery et al., 2013).

A3.4 Nutrient availability

Benthic microalgae can acquire their nutrients from the overlaying water or from the sediments. Nutrient input into the ecosystem can take place from external sources, such as atmospheric deposition and transport via rivers, or made available in the ecosystem through nutrient recycling.

Studies on the effects of eutrophication on microphytobenthos have shown that under high nutrient conditions, the primary limiting factor in productivity of microphytobenthos is light (Stutes et al. 2006). On the whole, nutrient concentrations are considered not to be a limiting factor for MPB productivity (Underwood and Kromkamp, 1999). However, nutrient limitation in MPB is linked to sediment composition, and can occur in sandy sediments although under sufficient advective transport the nutrient availability can support a high MPB productivity (Billerbeck at al., 2007). Microphytobenthos assemblage composition can be affected by nutrient availability, with high nutrient concentrations resulting in increased abundances of cyanobacteria and purple sulphur bacteria, whereas low nutrient availability promotes high diatom abundance (Armitage and Fong, 2004).

The temperature of the sediments and CO2 availability to the cells can be of importance to the benthic primary production. Particularly, in a biofilm with a high density of cells, CO2 may be limiting to the primary production (Jesus et al., 2005). The surface sediment temperature can vary by 10°C within a few hours (Harrison 1985) and is thought to affect the photosynthetic rates of MPB (Morris and Kromkamp, 2003).

Determining the productivity of MPB is complicated as various factors are of influence, such as photosynthesis, nutrient availability and sediment optics. Also, estuaries and coastal regions show a large variability in space and time, making good measurements of MPB productivity complicated. Furthermore, aspects such as vertical migration and differences between the various MPB species that make up the assemblages should preferably be taken into account.

A3.5 Methods of measuring productivity

Photosynthesis by MPB takes place in a thin layer of the sediment that is penetrated by light. The rates of photosynthesis in this layer are controlled by sharp gradients in various factors, such as light, temperature and nutrient availability. However, abundance patterns are more diffuse due to active migration (Cadee & Hegeman, 1974) or hydrodynamical processes and bioturbation (Cadee, 1976), and stretch up to several centimetres in muddy sediments and up to 8 centimetres in sandy sediments (Saburova & Polikarpov, 2003). Vertical migration allows MPB to control their nutrient uptake and avoid limitation.

For determining the potential impact of benthic primary producers on the ecological conditions in estuaries and coastal regions, several methods can be applied to measure MPB primary production. In general, productivity can be measured by analysis of chlorophyll content of the cells in the upper sediment layer as an indication of biomass, and ^{14}C assimilation measurements (MacIntyre et al., 1996). For these analyses, the MPB present in upper 2mm of 5 sediment cores is isolated and either analysed for chla content or photosynthetic parameters are determined through incubation with a known concentration of ^{14}C-labeled bicarbonate. A relatively new method using variable fluorescence techniques provides a non-intrusive means of measuring photosynthetic activity (Kromkamp et al., 1998). However, each of these methods has disadvantages. For example, processing the sediment cores for analysis destroys the natural gradient (Cibic et al, 2008). In case of the variable fluorescence method, no methodological consensus is lacking. Another point of critic is the fact that these methods do not take into account the variations in species composition or long-term changes therein. Furthermore, migration of microphytobenthos is largely overlooked whereas for modelling studies a homogenous distribution of biomass with depth is assumed (Spilmont et al., 2011).

Considering the different factors affecting the distribution of MPB on and within the sediment, a sampling strategy that takes these factors into account and focuses on obtaining representative samples is vital for a correct measurement of biomass and production. Spilmont et al. (2011) calculated that conventional methods of sampling can result in an error of about 40%, in case of insufficient sampling density. In order to minimise a sampling error, the number of sampling is best based on the heterogeneity of the MPB distribution in the sampling area. Furthermore, MPB starts to migrate downward into the sediment about 30 to 60 minutes before the tide returns (Kromkamp and Forster, 2006). Not taking this process into account during sampling will create an additional bias.

A3.6 Ecological impact

Coastal waters have long been under influence of high nutrient loads that have stimulated primary productivity in the water column. As a result, attenuation of light by phytoplankton in the water column has hampered benthic primary production. Since several decades, the problems with eutrophication are decreasing due to more stringent regulation. A potential effect of this decrease is

a decline in phytoplankton biomass is an increased light availability at the sediment surface and concomitant an increased productivity by MPB (Lake and Brush, 2011). In addition, these authors note that if nutrients have accumulated in the sediments, MPB productivity may benefit from high nutrient concentrations that they can retain in the sediment as MPB can function as a sediment cap. By the formation of EPS, diatoms bind sediment particles which prevent sediments from becoming eroded or suspended. Through this mechanism, sediment stabilisation may also further increase, thereby decreasing turbidity caused by tidal currents.

Furthermore, under light conditions, the influence of benthic microalgae on nutrient fluxes between sediment and overlying waters is often expressed as lower fluxes, or no flux at all (Sundback and McGlathery, 2005), which will impact pelagic primary producers. Consequently, organisms higher in the foodweb could be affected. Nonetheless, up to half of the food resource of filter feeders can consist of resuspended benthic microalgae (De Jonge and Van Beusekom, 1992), and may compensate for a decreased primary productivity by phytoplankton.

A3. Quality Assurance

IMARES utilises an ISO 9001:2008 certified quality management system (certificate number: 124296-2012-AQ-NLD-RvA). This certificate is valid until 15 December 2015. The organisation has been certified since 27 February 2001. The certification was issued by DNV Certification B.V. Furthermore, the chemical laboratory of the Fish Division has NEN-EN-ISO/IEC 17025:2005 accreditation for test laboratories with number L097. This accreditation is valid until 1th of April 2017 and was first issued on 27 March 1997. Accreditation was granted by the Council for Accreditation.

A4. Justification

Report C160/14

Project Number: 4306119901

The scientific quality of this report has been peer reviewed by a colleague scientist and the head of the department of IMARES.

Approved: Dr Pauline Kamermans

Senior researcher aquaculture

Signature: 

Date: 2015-07-02

Approved: Drs Jakob Asjes

Head Ecosystems Department

Signature: 

Date: 2015-07-02